# TECHNICAL AMENABILITY STUDY OF LABORATORY-SCALE SENSOR-BASED ORE SORTING ON A MISSISSIPPI VALLEY TYPE LEAD-ZINC ORE

by

Yan Tong

B.A., University of Science and Technology, Beijing, 2009

A THESIS SUBMITTED IN PARTIAL FULFILLMENT OF
THE REQUIREMENTS FOR THE DEGREE OF

MASTER OF APPLIED SCIENCE

in

THE FACULTY OF GRADUATE STUDIES

(Mining Engineering)

THE UNIVERSITY OF BRITISH COLUMBIA

(Vancouver)

October, 2012

©Yan Tong, 2012

## Abstract

Automatic sensor-based sorting is a clean preconcentration technique that can be used to separate valuable ore rock from waste rock based on the difference of the detected physical properties. This research evaluated the amenabilities of a Mississippi Valley type lead-zinc ore sample from Pend Oreille Mine to X-ray Fluorescence Sorting, X-ray Transmission Sorting, Optical Sorting and Microwave-Infrared Sorting using laboratory-scale bench-top sensing systems. A methodology for laboratory-scale quick evaluation of the amenability of an ore sample to automatic sensor-based sorting using bench-top sensor systems was generated as reference for future study.

The preliminary testwork results showed that the two X-ray methods exhibited the best sorting results. About 37.7%~52.8% of the feed mass could be rejected as waste while above 95% of the lead and zinc was recovered in the product. The sorting feed (-37.5+26.5 mm) could be upgraded by a factor of 1.5~2. The optical sorting method seemed not as effective as the X-ray methods. Only 18.8% of the sorting test feed (-37.5+26.5 mm) was rejected to maintain above 95% metal recovery in the product. The test feed was upgraded by a factor of 1.2. Microwave-Infrared sorting results demonstrated that carbonate gangue mineral does not heat when exposed to microwave heating, while lead-zinc bearing sulfide does. Factors such as particle size, heating time and quantity of particles being heated at a time would influence microwave heating of rocks. Sorting feed of -19+13.2 mm presented the best segregation results after 10s of microwave heating. Above 95% of lead and zinc was recovered in a mass yield of 70% to the product. The test feed was upgraded by a factor of 1.4.

The preconcentrate of X-ray Fluorescence sorting had a bond work index 12% smaller than that of the feed ore. The overall metal (lead and zinc) recoveries and grades in the flotation products were also improved after XRF sorting. The costs of both the grinding and the flotation reagent could also be reduced due to the reduction of the feed mass by rejecting the dolomitic gangue minerals up to 50%.

# Table of Contents

Abstract ..... ii

Table of Contents ..... iii

List of Tables ..... vii

List of Figures ..... viii

List of Abbreviations ..... xi

Acknowledgements ..... xii

CHAPTER 1 INTRODUCTION ..... 1

1.1 Automatic Sensor-Based Ore Sorting ..... 1

1.2 Objectives ..... 2

1.3 Mine and Mineralogy ..... 2

1.4 Methodology ..... 3

CHAPTER 2 LITERATURE REVIEW ..... 4

2.1 Automatic Sensor-Based Sorting ..... 4

2.2 X-Ray Fluorescence Sorting Technology ..... 8

2.2.1 X-Ray Fluorescence (XRF) Technology and XRF Analyzer ..... 8

*2.2.1.1 XRF basic theory* ..... 8

*2.2.1.2 XRF analyzer* ..... 9

2.2.2 The XRF Sorter and Its Application ..... 10

2.3 X-Ray Transmission Sorting Technology ..... 14

2.3.1 X-Ray Transmission Theory ..... 14

2.3.2 DE-XRT Sorting Principles ..... 14

2.3.3 DE-XRT Sorter ..... 17

2.3.4 Dual-Energy X-Ray Transmission Sorting Applications ..... 19

2.3.5 Summary ..... 20

2.4 Optical Sorting Technology ..... 21

2.4.1 Optical Sorting ..... 21
2.4.2 The Color Ore Sorter and Its Applications in the Metal Mining Industry ..... 22
*2.4.2.1 Color ore sorter* ..... 22
*2.4.2.2 Applications of color ore sorting in the metal mining industry* ..... 24
2.4.3 Summary ..... 25
2.5 Microwave-Infrared Sorting Technology ..... 26
2.5.1 Microwaves and Heating Rates of Minerals ..... 26
2.5.2 Microwave Heating and Its Potential for Sorting ..... 27
2.6 Summary ..... 30
CHAPTER 3 SORTING TEST PROGRAM ..... 31
3.1 Sample Preparation ..... 31
3.2 X-Ray Fluorescence Sorting Test ..... 32
3.2.1 Materials ..... 32
3.2.2 Equipment ..... 32
3.2.3 Experimental Procedures ..... 33
3.2.4 Results and Discussions ..... 33
*3.2.4.1 Sortability of this ore using the Innov.X XRF analyzer* ..... 33
*3.2.4.2 Grade-Recovery relationship* ..... 36
*3.2.4.3 Summary of XRF sorting results* ..... 39
3.3 X-Ray Transmission Sorting Test ..... 41
3.3.1. Equipment ..... 41
3.3.2. Experimental Procedures ..... 42
*3.3.2.1 Sample preparation* ..... 42
*3.3.2.2 Image capture* ..... 42
*3.3.2.3 Sample assay* ..... 42
*3.3.2.4 Image processing and data extraction* ..... 42
*3.3.2.5 DE-XRT Sorting criterion determination* ..... 45

3.3.3 Results and Discussion ..... 46
*3.3.3.1 Simplified image analysis by GIMP* ..... 46
*3.3.3.2 Image analysis by PACT software* ..... 49
*3.3.3.3 Comparison of sorting results by two image analyzing methods* ..... 51
3.4 Optical Sorting Test ..... 53
3.4.1 Ore Characterization ..... 53
3.4.2 Sample Preparation ..... 53
3.4.3 Equipment ..... 54
*3.4.3.1 Hardware* ..... 54
*3.4.3.2 Software* ..... 54
3.4.4 Color Sorting Potential Study ..... 55
3.4.5 Image Capture ..... 56
3.4.6 Data Analysis ..... 57
*3.4.6.1 Generation of characteristic color data for waste rock and mineralized ore* ..... 57
*3.4.6.2 Rejecting criteria determination* ..... 61
3.4.7 Sorting Results ..... 66
3.4.8 Laboratory-Scale Color Ore Sorting Amenability Study Flowsheet Design ..... 68
3.5 Microwave-Infrared Sorting Test ..... 69
3.5.1 Experimental Procedures ..... 69
*3.5.1.1 Equipment* ..... 69
*3.5.1.2 Testing procedures* ..... 69
3.5.2 Results and Discussion ..... 73
*3.5.2.1 Factors influencing microwave heating of lead-zinc sulfide ore* ..... 73
*3.5.2.2 Distinguishability of waste rock from lead-zinc sulfide ore* ..... 82
*3.5.2.3 Sorting results summary* ..... 87
3.6 Ore Sorting Test Summary ..... 90

CHAPTER 4 SORTING IMPACT EVALUATION ..... 93
4.1 Experimental Procedures ..... 94
4.1.1 X-Ray Diffraction Analysis ..... 94
4.1.2 Grinding Energy Consumption Test ..... 94
4.1.3 Flotation Test ..... 95
4.2 Results and Discussion ..... 97
4.2.1 X-Ray Diffraction Analysis ..... 97
4.2.2 Grinding Energy Savings ..... 98
4.2.3 Flotation Test Results ..... 98
CHAPTER 5 CONCLUSIONS AND RECOMMENDATIONS ..... 101
5.1 Conclusions ..... 101
5.1.1 Conclusions from the XRF Sorting Test ..... 101
5.1.2 Conclusions from the XRT Sorting Test ..... 102
5.1.3 Conclusions from the Optical Sorting Test ..... 103
5.1.4 Conclusions from the MW/IR Sorting Test ..... 104
5.1.5 Conclusions from the Impact Evaluation Test ..... 104
5.2 Recommendations ..... 105
5.2.1 Recommendations on Sensor-Based Ore Sorting of This Lead-Zinc Ore ..... 105
5.2.2 Recommendations on Development of Laboratory-Scale Sensor-Based Ore Sorting Evaluation ..... 105
REFERENCES ..... 107
APPENDICES ..... 113
APPENDIX A X-RAY FLUORESCENCE SORTING DATA ..... 113
APPENDIX B X-RAY TRANSMISSION SORTING DAT ..... 132
APPENDIX C OPTICAL SORTING DATA ..... 140
APPENDIX D MICROWAVE-INFRARED SORTING DATA ..... 146
APPENDIX E IMPACT EVALUATION DATA ..... 207

## List of Tables

Table 2-1 Sensing Technologies Currently Available for Automatic Ore Sorters.....7
Table 2-2 Heating Rates of Common Sulphide Minerals and Gangue Minerals.....26
Table 2-3 Comparison of Different Sorting Technologies .....30
Table 3-1 Head Sample Size Analysis and Assays .....31
Table 3-2 Grade-Recovery Relationship Test Results .....37
Table 3-3 Overall Sorting Results of 325 Rocks (Top Size: Bottom Size = 3:1) Sized Above 26.5 mm .....40
Table 3-4 Summary of XRF Sorting Results of Four Size Fractions .....40
Table 3-5 XRT Sorting Results of -37.5+26.5 mm Lead-Zinc Ore Based on Average Brightness Value of the High Energy X-Ray Transmission Image .....48
Table 3-6 XRT Sorting Results of -37.5+26.5 mm Lead-Zinc Ore Based on Average Brightness Value of the Low Energy X-Ray Transmission Image .....49
Table 3-7 XRT Sorting Results of -37.5+26.5 mm Lead-Zinc Ore Based on Ore Indices .....51
Table 3-8 XRT Sorting Results Summary of Different Sorting Criteria .....51
Table 3-9 Results of Quantitative Phase Analysis of Head Sample by XRD (Wt.%) .....53
Table 3-10 XRF Powder Analysis of Waste Rocks and Mineralized Ore .....56
Table 3-11 Average Red, Green and Blue Value for the 10 Matched Patterns for Rock #26 .....59
Table 3-12 Summary of Red, Green and Blue Value for Matched Patterns .....60
Table 3-13 Color Sorting Results Summary .....66
Table 3-14 MW/IR Segregation (Individual 10s 50 Rocks) Results of -26.5+19 mm size fraction Based on Different Separation Average Surface Temperatures.....86
Table 3-15 Summary of MW/IR Sorting Results of -26.5+19 mm Sample.....87
Table 3-16 MW/IR Sorting Results Summary .....89
Table 3-17 Ore Sorting Results Summary .....92
Table 4-1 Bond Ball Charge .....94
Table 4-2 Results of Quantitative Phase Analysis (Wt. %).....97
Table 4-3 $P_{80}$, $F_{80}$ and Work Indices for XRF Feed, XRF Concentrates and XRF Waste98
Table 4-4 Flotation Results Based on Calibrated XRF Powder Readings.....100

## List of Figures

Figure 2-1 Two Sensor Set-Up Methods ..... 5
Figure 2-2 Two Types of Sorting Modes ..... 6
Figure 2-3 Typical XRF Energy Spectrum of a Soil Sample ..... 9
Figure 2-4 Typical XRF Analyzer Basic Components ..... 9
Figure 2-5 Typical Layout of an XRF Ore Sorter ..... 12
Figure 2-6 The Full-Scale RADOS XRF Ore Sorter Installed at Mintek ..... 13
Figure 2-7 Transmission Curves of Mixtures with Different PbS Grades at 83kV/50kV ..... 15
Figure 2-8 The Calibration Curve for Sorting ..... 16
Figure 2-9 Transmission Graph for a Rock Sample ..... 17
Figure 2-10 Layout of an X-Ray Transmission Sorter ..... 18
Figure 2-11 Principle of Single Energy and Dual-Energy X-Ray Transmission Sensing 19
Figure 2-12 Schematic Layout of a Color Ore Sorter ..... 23
Figure 2-13 Schematic Diagram of MW/IR Sorting of Sulfide Ores ..... 27
Figure 3-1 XRF Analysis Station at UBC ..... 32
Figure 3-2 Correlations between XRF Analyzer Surface Reading and Bulk Assays ..... 34
Figure 3-3 Correlations between Pb, Zn and Fe ..... 35
Figure 3-4 Flowsheet of Grade-Recovery Relationship Test Procedures ..... 36
Figure 3-5 Grade-Recovery Relationship Curves for Pb and Zn ..... 38
Figure 3-6 Relationship between Metal Recovery and Percentage Mass Rejected as Waste Based on Different Separation Threshold Values ..... 39
Figure 3-7 Pilot-Scale Dual-Energy XRT Scanner at CommoDas ..... 41
Figure 3-8 Example of a DE-XRT Image Generated by the X-Ray Scanner ..... 42
Figure 3-9 Process of Value Image Generation ..... 43
Figure 3-10 Screenshot of Brightness Value Extraction from the Image ..... 44
Figure 3-11 Image Processing Flowsheet of PACT Software ..... 45
Figure 3-12 Separation Curve for Lead-Zinc Ore Sample Sized -37.5+26.5 mm Based on Average Brightness Values of High/Low Energy Images ..... 46
Figure 3-13 XRT Segregation Sortability Curve of -37.5+26.5 mm Lead-Zinc Ore Based on Average Brightness Values of High/Low Energy Images ..... 47
Figure 3-14 XRT Segregation Sortability Curve of -37.5+26.5 mm Lead-Zinc Ore Based on Ore Indices ..... 50

Figure 3-15 Grade-Recovery Curves of XRT Sorting Based on Different Sorting Criteria ..... 52
Figure 3-16 Optical Bench-Top Image Acquisition System at CommoDas ..... 54
Figure 3-17 Images of Identified Waste Rock and Mineralized Ore ..... 55
Figure 3-18 Schematic Set-Up of the Camera ..... 57
Figure 3-19 Red Spectrum of Selected ROI Pattern for Rock #26-Waste ..... 58
Figure 3-20 Patterns Matching of Rock #26 ..... 59
Figure 3-21 Value Image Selection Methods ..... 61
Figure 3-22 Sample of Threshold Images for Several Rocks ..... 62
Figure 3-23 Histograms of Red Value for the Value Image Before Threshold ..... 63
Figure 3-24 Histograms of Red Value for the Value Image after Threshold ..... 64
Figure 3-25 Correlation between Pb+Zn Grade and Avg. $R_{133-255}$ ..... 65
Figure 3-26 Color Sorting Grade-Recovery Curve for -37.5+26.5 mm Sample ..... 67
Figure 3-27 Flowsheet for Color Ore Sorting Amenability Study in Laboratory-Scale ..... 68
Figure 3-28 BP-110 Lab Use Microwave Oven and FLIR T400 IR Camera ..... 69
Figure 3-29 Rock Position for Individual Testing ..... 70
Figure 3-30 IR (Thermographic) Images of Two Sides of Rocks from -19+13.2 mm Size Fraction After 10s Microwave Heating ..... 71
Figure 3-31 Rock Positions for Group Testing ..... 72
Figure 3-32 IR (Thermographic) Images of Two Sides of Rocks Tested in Groups of 4, 9 and 25 after 10s Microwave Heating ..... 72
Figure 3-33 Average Surface Temperatures of Rocks after 5s, 10s, and 15s Microwave Heating from -19+13.2 mm, -26.5+19 mm and -37.5+26.5 mm Size Fractions ..... 74
Figure 3-34 Average Surface Temperatures after Being Heated for 10s by Individual and Group Heating for Four Size Fractions ..... 77
Figure 3-35 Relationship between Microwave Heating Behaviour of Lead-Zinc Ore and Sample Weight ..... 78
Figure 3-36 Relationship between Microwave Heating Behaviour of Lead-Zinc Ore and Rock Weight: 5s, 10s and 15s ..... 79
Figure 3-37 Relationship between Microwave Heating Behaviour of Lead-Zinc Ore and Rock Weight Heated Individually and Heated Together In a Group of Nine ..... 80
Figure 3-38 Average Surface Temperatures of Rocks from Four Size Fractions after Being Heated for 10s Individually and Together in a Group of Nine ..... 81
Figure 3-39 Average Surface Temperature vs. S /Pb+Zn Grades ..... 83

Figure 3-40 Relationship between Average Surface Temperature and S/Pb+Zn Grades after 5s, 10s and 15s Microwave Heating ..... 84
Figure 3-41 Flowsheet for Laboratory-scale Sensor-based Ore Sorting Study ..... 91
Figure 4-1 Standard Laboratory Bond Test Ball Mill ..... 95

## List of Abbreviations

| | |
|---|---|
| Avg. | Average |
| BWI | Bond Work Index |
| Conc. | Concentrate |
| Cum. | Cumulative |
| Distr. | Distribution |
| MLA | Mineral Liberation Analysis |
| MW/IR | Microwave-Infrared |
| POM | Pend Oreille Mine |
| Tph | Tonnes per hour |
| Wt. | Weight |
| XRD | X-Ray Diffraction |
| XRF | X-Ray Fluorescence |
| XRFC | X-Ray Fluorescence Concentrate |
| XRT | X-Ray Transmission |

## Acknowledgements

I would like to thank my supervisor Dr. Bern Klein for his support and guidance during this research. I also would like to thank Dr. Andrew Bamber, Dr.Maria Holuszko and Dr. Marek Pawlik for their help and instructions during the course of this study. Also I thank Dr. Henry Salomon-De-Friedberg and TECK CESL for their support and sponsorship as well as Pend Oreille Mine for providing the sample for this research.

I thank Dr. Gus van Weert for the kind guidance he has given to me on Microwave-Infrared Sorting and Olivia Wang for her help with the laboratory testing work. I want to thank PROrtech Ltd. as well for their support on the test work.

I also would like to express my thanks to Matthew Kowalczyk for his help and useful suggestions during this research and CommoDas Ultrasort for providing me the laboratory-scale equipment and systems for this ore sorting study. I would like to thank Cindy Collins and Jeff Mabbutt for their support and help with XRF analyzing and related information.

To my partners Amit Kumar, Avinash Tripathi, Chengtie Wang, Jeff Drozdiak, Stefan Nadolski and Zorig Davaanyam thanks a lot for all the help and assistance along the way through this research and the research tips we shared.

Lastly, I would like to thank my husband Jia Wu and all my friends for their encouragement and support through my entire master's program.

# CHAPTER 1 INTRODUCTION

## 1.1 Automatic Sensor-Based Ore Sorting

Automatic sensor-based sorting, together with hand sorting, comminution and size classification, dense media separation and coarse flotation, is the technology commonly used for preconcentration of ores. The automatic sensor-based sorting technique is a dry process needing no or very little water and energy and therefore shows its potential for energy saving and environmental improvement (Kleine, Wotruba, Robben, von Ketelhodt, & Kowalczyk, 2011).

The automatic sensor-based sorting technique has developed rapidly in the recycling, food and industrial mineral industries during the last six decades. However, not until recent decades has it drawn the attention of the mining industry with the development of new sensors, improvement of data processing speed, and increase of the throughput of sorting machines so that it can meet the requirements of mining operations (Fitzpatrick, 2008). Sensors successfully applied to ore sorting include photometric, color (CCD), conductive/magnetic, thermal conductive (Microwave Infrared), radiometric, X-ray fluorescence and X-ray transmission. Ores preconcentrated by automatic sensor-based sorters are mainly uranium, nickel, copper, iron and gold (Kowalczyk & Bartram, 2008).

One or a combination of sensors can be used to discriminate high-grade ore from low-grade waste based on the difference of measured physical properties. A multi-sensor sorter, which is capable of measuring more than one property of the materials, is more suitable for novel mining applications. In a pilot-scale study by Fitzpatrick (2008), a general methodology for determination of an ore's suitability for automatic sorting was developed using a multi-sensor automatic sorter (with both inductive and optical sensors) from CommoDas. This methodology was validated in that study by sorting of a nickel/copper sulfide ore and an iron ore (Fitzpatrick, 2008).

The efficiency of an automatic sensor-based sorter was studied from aspects of the sorter's identification and separation functions using a TiTech Combisense© (BSM 063) automatic sorter. Udoudo (2010) found that the separation efficiency decreased when particle size decreased and throughput increased. Poor separation efficiency was also due to the co-deflection losses (particles meant to go into the "accept" fraction were co-

deflected (deflected together) with the ones meant to go to the “reject” fraction). A separation efficiency model was also established using belt loading (a function of particle size, shape and throughput) and percentage deflected as variables. Using this model, the separation efficiency of the automatic sorter of a specific ore can be calculated (Udoudo, 2010).

Prior to the evaluation of the amenability of an ore to automatic sensor-based sorting and the optimization of the efficiency of the selected sorter in pilot-scale, a preliminary study on the technical amenability of an ore sample to sensor-based sorting should be performed in the laboratory-scale to assess the potential for such application. This research set out to develop a methodology for laboratory-scale quick evaluation of the amenability of an ore sample to automatic sensor-based sorting using bench-top sensor systems. Also, the application of automatic sorting to a lead-zinc ore was investigated to add to the database of successful applications of automatic sorters in the mining industry.

### 1.2 Objectives

The objectives of this research include:

- to evaluate the amenabilities of this lead-zinc ore to sensor-based ore sorting using X-ray Fluorescence, X-ray Transmission, Optical and Microwave-Infrared sensing systems in the laboratory- scale; and
- to assess the effect of sorting on grinding energy saving and flotation performance improvement.

### 1.3 Mine and Mineralogy

The ore sample used for this research was from Pend Oreille Mine, one of the mines owned by Teck Resources Ltd. The Pend Oreille Mine is located in northeast Washington State, approximately two miles north of Metaline Falls, Washington and 95 miles north of Spokane, Washington. Pend Oreille Mine is a Mississippi Valley type metaline replacement high iron content zinc-lead formation (Huntting, 1966). It is an underground zinc-lead mine with a daily production rate of 2200 tons. The processing plant has a capacity of 80,000 tonnes annually with zinc concentrate grading at 60% (Canadian Mining Journal Website, 2004). In 2009, the mine was shut down due to the decreasing metal prices. Primary ore minerals in the Pend Oreille deposit are galena (PbS) and sphalerite (ZnS). Accessory minerals include pyrite, marcasite, pyrrhotite, calcite, palygorskite, fluorite and chalcopyrite. The host rock is mainly coarse dolomite.

### 1.4 Methodology

This thesis is divided into five chapters and five appendices. Chapter 1 introduces the background and objectives of the research, mines where the materials are provided from, mineralogy of the ore and the methodology used. Chapter 2 reviews the literature on automatic sensor-based sorting. Four sensor-based sorting technologies, namely X-ray Fluorescence Sorting, X-ray Transmission Sorting, Optical Sorting and Microwave-Infrared Sorting, are reviewed in detail in this chapter. Chapter 3 describes the sorting test of the Pend Oreille lead-zinc ore sample. The sorting test program used four sensor-based sorting technologies. The chapter summarizes the sorting results of each technology. Chapter 4 describes the impact of sorting on energy saving and flotation metallurgical performance by conducting a bond ball mill work index test and a flotation test. Chapter 5 presents the conclusions derived from this research and the recommendations for further study.

# CHAPTER 2 LITERATURE REVIEW

This chapter reviews the literature on automatic sensor-based sorting technologies and their applications in the metal industry. A general introduction to the development and status of sensor-based sorting is provided, followed by detailed reviews of X-ray Fluorescence Sorting, X-Ray Transmission Sorting, Optical Sorting and Microwave-Infrared Sorting technologies and their applications in the base metal industry. At the end of the chapter, a summary of the characteristics of these four sorting technologies is presented.

## 2.1 Automatic Sensor-Based Sorting

Automatic sensor-based sorting is a method utilizing different sensing technologies to examine the physical properties of each particle and separate these particles into product and waste fractions based on the pre-defined sorting criteria. The reliability and efficiency of automatic sensor-based sorting is highly dependent on the discrimination of physical properties of each particle, such as conductivity, thermal conductivity, magnetic susceptibility, atomic density, reflectance, texture, etc. The particles are separated using an external force generated by air valves or mechanical arms. Automatic sensor-based sorting is capable of sorting materials sized from 2mm to 250mm depending on which physical property is detected (De Jong, 2012).

Ore sorting using automatic sensor-based sorters can be used to preconcentrate the feed ore prior to the beneficiation plant, therefore providing a high grade feed and reducing the costs of grinding and reagents due to the reduction of feed mass. It also helps reduce the fine tailings generated and improves the metallurgical performance of mineral processing. The drawbacks of automatic ore sorting are mainly the preparation needed, such as feeding, sieving and surface cleaning, the large amount of capital, operating and maintenance costs, and the loss of valuable elements to the waste after sorting (Manouchehri, 2003).

There are two ways of sensor set-up: on-belt and free-fall employed by the ore sorter (Figure 2-1). The chute-type sorter utilizes the free-fall sensor set-up method while the belt-type sorter employs the on-belt sensor set-up method. The sorter consists of five components: feed preparation system, feed presentation system, sensing system, data

processing and control system, and separation system. Wotruba and Harbeck (2010) provide a detailed description of these systems, which will be discussed in later sections on ore sorters using different sensing technologies.

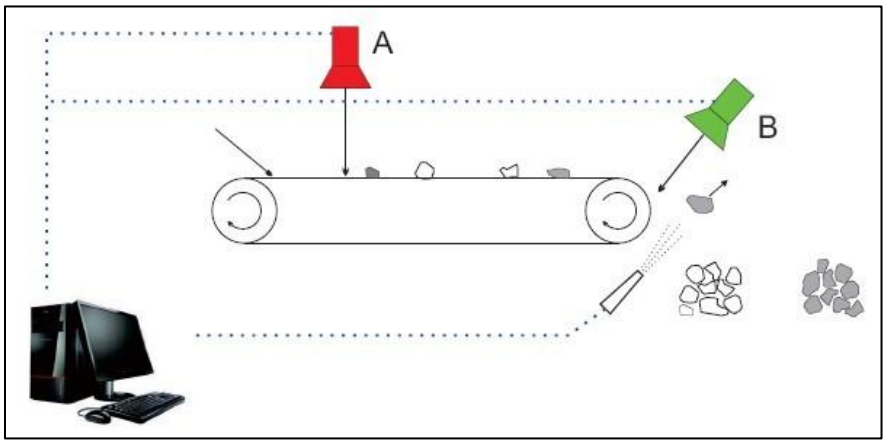


**Figure 2-1 Two Sensor Set-Up Methods**
(De Jong, Van Houwelingen, & Kuilman, 2004)

The ore sorter can be operated in particle-by-particle mode or recovery mode (Figure 2-2). In particle-by-particle mode, materials are present to sensors in a single layer and do not touch each other, for individual detection. When it comes to recovery mode, a layer of materials is transported to the sensing area due to the higher rate of feeding. In this mode, valuable materials together with diluted surrounding materials are ejected together to the product fraction to maximize the recovery. As a result, the particle-by-particle mode can provide a high grade and high recovery product in one run while the recovery mode can produce a diluted high recovery product (Kuilman, 2006). The particle-by-particle mode is used for this research since the sensing systems used in the laboratory-scale ore sorting amenability study are only suitable for individual detection.

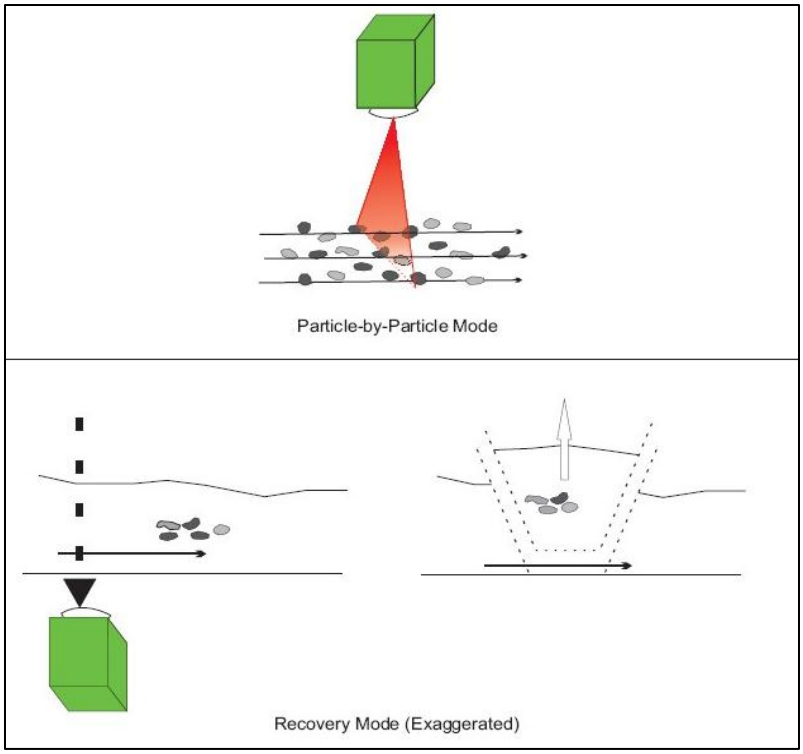


**Figure 2-2 Two Types of Sorting Modes**
(Kuilman, 2006)

Various sensing technologies are currently available for sensor-based ore sorters, some of which are still under development. They are shown in Table 2-1. The present study is concentrated on the most common sorting technique, Optical Sorting, the well-developed X-ray Sorting method, both fluorescence and transmission, and the Microwave-Infrared Sorting technology which is still under development.

**Table 2-1 Sensing Technologies Currently Available for Automatic Ore Sorters** (Kleine, Wotruba, Robben, von Ketelhodt, & Kowalczyk, 2011; Van Weert, Kondos, & Gluck, 2009)

| Sensing Technologies | Physical Properties Detected | Applications |
|---|---|---|
| Radiometric | Natural Gamma Radiation | Uranium, Precious Metals |
| X-Ray Transmission (XRT) | Atomic Density | Base/Precious Metals, Coal, Diamonds, etc. |
| X-Ray Fluorescence (XRF) | Visible Fluorescence under X-Rays | Diamonds |
| X-Ray Fluorescence Spectroscopy (XRF-S)* | Elemental Composition | Base/Precious Metals |
| Near Infra-Red (NIR) | Reflection, Absorption | Industry Minerals, Base Metals |
| Color (CCD) | Colour, Reflection, Brightness, Transparency | Base/Precious Metals, Industrial Minerals, Gem Stones |
| Photometric (PM) | Monochromatic Reflection, Absorption and Transmission | Industry Minerals, Diamond |
| Electromagnetic (EM) | Conductivity/Magnetic Susceptibility | Base Metals |
| **UNDER DEVELOPMENT** | | |
| Microwave-Infrared (MW/IR) | Microwave Absorption, Heat Conductivity | Base Metals, Carbonaceous Materials |
| Laser-Induced Fluorescence (LIF) | | |
| Laser-Induced Breakdown Spectrometry (LIBS) | | |

* The XRF technology discussed in this research is XRF-S, expressed as XRF in short.

Factors influencing the efficiency of the ore sorter include the size, density and liberation of the particle. The smaller the particle size, the better the liberation of the valuable minerals and therefore the better the sorting results are. On the other hand, sorting cost per ton of ore is a function of particle size and density. The larger and heavier the ore, the larger the throughput and therefore the cheaper the cost per ton of ore is (De Jong, 2012).

## 2.2 X-Ray Fluorescence Sorting Technology

### 2.2.1 X-Ray Fluorescence (XRF) Technology and XRF Analyzer

It has been known for a long time that the X-ray Fluorescence (XRF) analysis technique can be applied in the mining industry to facilitate exploration quality control and mineral processing control. It is a simple and efficient method of qualitative and quantitative element analysis, with lower cost and higher speed compared to conventional chemical assays (Wood, 1959). XRF analyzers are available from Olympus (Innov.X), Thermo Scientific (Niton) and other manufacturers. Each of these analyzers has unique advantages but they all work in a similar way. They can quickly and non-destructively determine the element composition of materials with high accuracy and long-term precision.

#### *2.2.1.1 XRF basic theory*

Elements in the sample can be analyzed simultaneously by measuring the emission of characteristic X-rays. An X-ray with sufficient energy bombards the atoms of the sample. X-rays collide with the electrons in the K and L shell resulting in the ejection of electrons from their atomic orbits. Electrons from the higher energy shell then fill the vacancies left and emit characteristic X-rays. The energy of characteristic X-rays is equal to the energy difference between the two shells of the elements. Thus, the emitted X-rays are identical when electrons are dislodged from atoms of the same element. In summary, the energy level of each emitted characteristic X-ray (fluorescence) represents the element being excited; the intensity of the fluorescent X-ray emitted represents the element concentration presence in the sample (Murphy, Maharaj, Lachapelle, & Yuen, 2010). Any element with an atomic number from 22 to 92 when present in sufficient concentration can be analyzed using the XRF analysis method without any special device. However, elements with atomic numbers 12 to 22 can also be analyzed by the XRF method with the help of special analyzing crystals and helium protection against air absorption (Wood, 1959).

A typical XRF Energy Spectrum (Intensity versus Energy) is illustrated in Figure 2-3.The energy level of the peak represents the element presence while the height of the peak represents the concentration of the element detected in the sample.

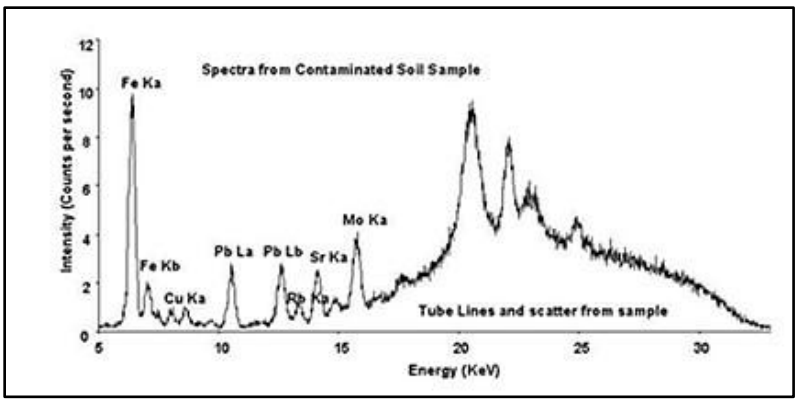


**Figure 2-3 Typical XRF Energy Spectrum of a Soil Sample**
(Murphy, Maharaj, Lachapelle, & Yuen, 2010)

### *2.2.1.2 XRF analyzer*

The basic components of a XRF analyzer are the X-ray tube, detector, multi-channel analyzer and computer (Figure 2-4).

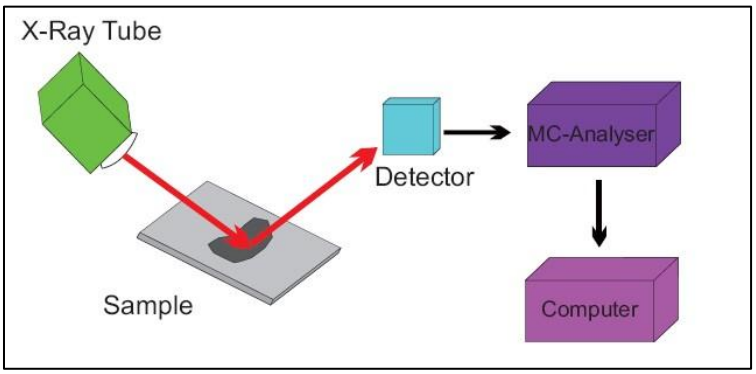


**Figure 2-4 Typical XRF Analyzer Basic Components**
(Murphy, Maharaj, Lachapelle, & Yuen, 2010)

The X-ray tube is the source of the primary X-ray for element excitation. The detector detects fluorescent X-rays emitted from the sample and converts them to voltage pulses. The multi-channel analyzer then generates an energy spectrum of the characteristic X-rays by matching the voltage pulses with energy values and counting how many times each energy value occurs. The energy spectrum is expressed as intensity (counts per second) versus photon energy (keV). After that, the computer modifies the data obtained from the energy spectrum using a few factors and calculates the chemical composition of the sample based on the modified energy spectrum (Murphy, Maharaj, Lachapelle, & Yuen, 2010).

### 2.2.2 The XRF Sorter and Its Application

Not only can XRF technique be used as a tool for chemical composition analysis, but also it provides a sensing method for automatic ore sorting and preconcentration. Full-scale XRF ore sorters are available from RADOS and CommoDas Ultrasort.

Few studies can be found related to the application of XRF ore sorting. Fickling (2011) reviewed the design and operation of an XRF ore sorter from RADOS and demonstrated some preliminary study results on using it in the upgrading of a manganese ore. He indicated that the amenability of a specific ore to XRF sorting depended on the existence of particles with varied grades due to well liberation. He also developed a testwork approach on how to evaluate the amenability of a specific ore to XRF sorting, which provided some guidelines for developing our research methodologies. The three stages involved in his testwork approach are:

- to determine the reliability of the XRF sorter in identifying particles with different grades by comparing the bulk assay and surface XRF analysis of each particle;
- to determine a Grade-Recovery relationship graph characteristic to the specific ore; and
- to determine the efficiency of the sorter. (Fickling, 2011)

The XRF ore sorter utilizes the same technology as the XRF analyzer. It analyzes and sorts rocks based on their chemical compositions by simultaneously measuring the concentration of elements of interest presented on the surface of the rock. A pre-set threshold is used to determine whether a rock reports to product or waste fractions (Fickling, 2011). The XRF ore sorter from RADOS has a capacity of 10-30t/h per module depending on the particle size and ore density. Each module can process particles with a size range of 20-250 mm, up to 8 particles per channel per second. The energy requirement for this ore sorter is from 0.2 to 0.4 kilowatt hour per ton (<6kW). Its detection limits vary from 0.05% to 0.1% for most metals and increase for lighter elements (Fickling, 2011). XRF sorters are also available from CommoDas Ultrasort with capacity up to 70 t/h. Figure 2-5 illustrates the typical layout of a XRF ore sorter. Figure 2-6 shows the full-scale RADOS XRF ore sorter installed at Mintek in Randburg.

Materials are fed to a vibrating feeder from the feed hopper after removal of fines and misplaced particles by a static grizzly. Then the particles are transported to several parallel channels or chutes where the particles are prepared for X-ray detection when

they are falling off. During the free-fall of the particles, X-rays strike the surface of the particle resulting in the emission of characteristic fluorescent X-rays from the rock. The detector then analyzes the characteristic X-rays emitted and their concentration and then calculates the element composition present on the surface of the rock. After comparing the metal concentration of a specific particle with the pre-set sorting threshold value, the control unit will give orders to the mechanical ejector and eject the particle to either the product chute or the waste chute (Fickling, 2011).

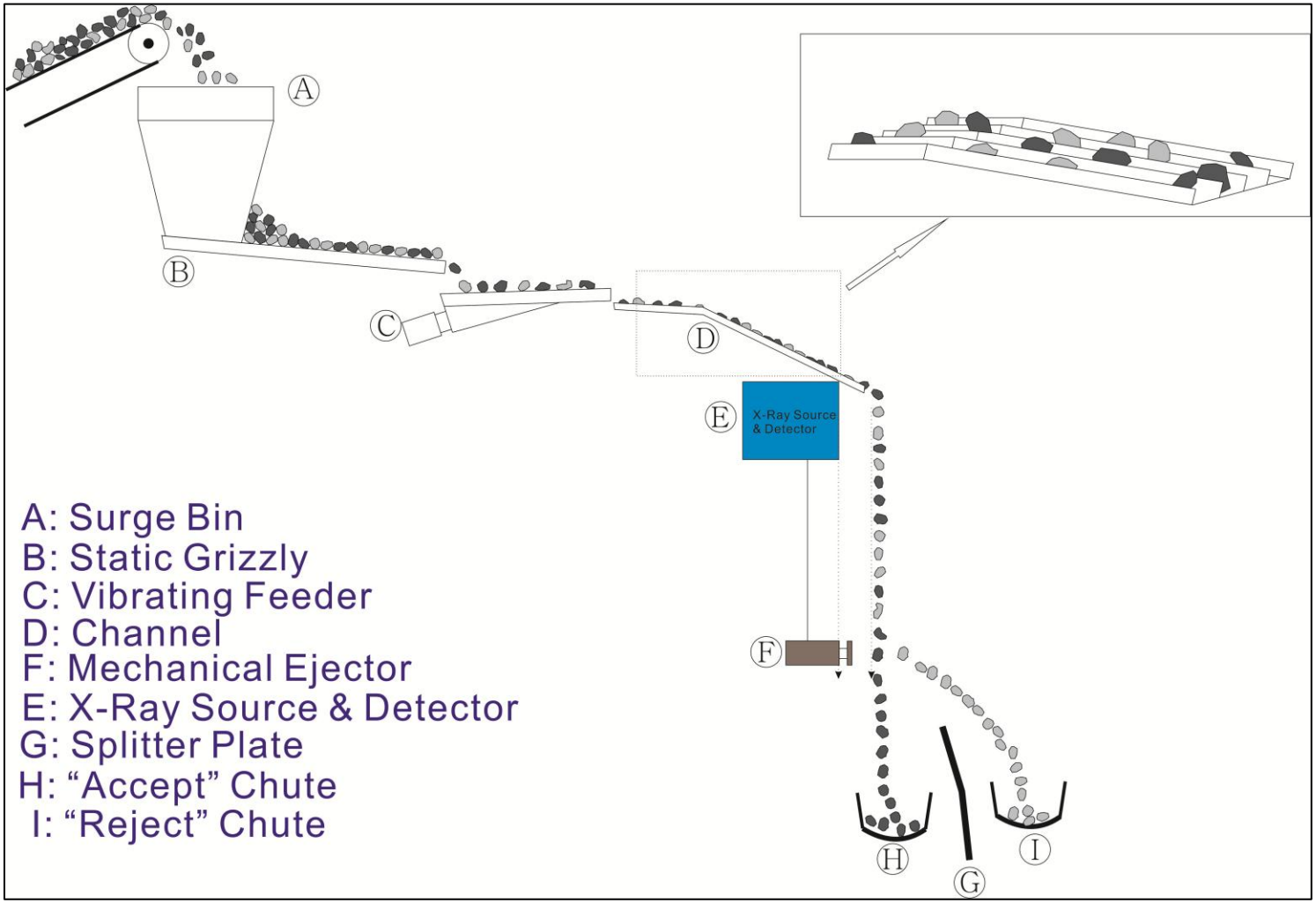


**Figure 2-5 Typical Layout of an XRF Ore Sorter**
(After Fickling, 2011)

**Figure 2-6 The Full-Scale RADOS XRF Ore Sorter Installed at Mintek**
(Fickling, 2011)

In summary, XRF sorting technology provides a green and dry sorting method for preconcentration of ores. A low level of energy is required (Fickling, 2011). However, although it is said that the XRF sorter has successful applications in sorting base metal ores, precious metal ores, ferrous metal ores and industrial minerals, barely any literature demonstrates any actual sorting results of specific ores, especially lead and zinc. More preliminary laboratory-scale and pilot-scale ore sorting tests are needed to prove the reliability of this sorting technique by providing some actual sorting results for specific ores. As a result, it is the goal of this research to evaluate the technical amenability of a lead-zinc ore to XRF sorting in the laboratory-scale using an Innov.X XRF analyzer.

### 2.3 X-Ray Transmission Sorting Technology

Sorting technologies have developed rapidly in the past decade with the development of computing technology and improvement of the sensor resolution. One of these exciting technologies is Dual-Energy X-Ray Transmission Sorting (DE-XRT) which first found successful applications in coal separation and upgrading. The concept of image based DE-XRT Sorting was initially inspired by the X-ray detection unit used for airport security inspection. The dual-energy X-ray system is capable of identifying and evaluating materials based on the atomic number. It is a completely dry process and independent of dust, moisture, surface contamination, shape and size.

#### 2.3.1 X-Ray Transmission Theory

Materials will absorb part of the radiation when exposed to X-rays. The reduction of the initial X-ray intensity is defined as transmission damping. The amount of X-ray transmitted through materials depends on their densities: the heavier the material, the greater the absorption of the X-rays and the smaller the amount of transmission. Transmission damping is a function of density and thickness of material according to Lamber's Law. The Lamber's Law shows that the detected intensity of the X-ray transmitted is proportional to the exponential function of the material density and thickness. Materials with different thicknesses but the same density will transmit X-rays at different degrees. As a result, using single energy X-ray (monochromatic imaging) technique to recognize rocks with different thicknesses will be inaccurate (Strydom, 2010). De Jong and Harbeck applied Lambert's Law to dual energy absorption and therefore eliminated the effect of thickness by using two energy levels of X-ray beam of different wavelengths (dual-energy X-ray transmission imaging)(De Jong & Harbeck, 2005). Detailed physics of X-ray transmission are referred to Strydom's thesis, *The application of dual energy X-ray transmission sorting to the separation of coal form torbanite*.

#### 2.3.2 DE-XRT Sorting Principles

The concept of sorting by dual-energy X-ray transmission imaging was first established by Delft University of Technology in 2000. The dual-energy X-ray transmission imaging system could generate dual-energy images illustrating the shape of the object and the distribution of atomic number and thickness within the object image. A transmission curve characteristic to the specific material type could be generated by plotting the degree of transmission of X-rays of two energy levels (De Jong & Harbeck, 2005). For

mining applications, a transmission curve of each ore type with different grades could be obtained separately. The transmission curves for a PbS/$SiO_2$ mixture of different PbS contents are shown in Figure 2-7 as an example.

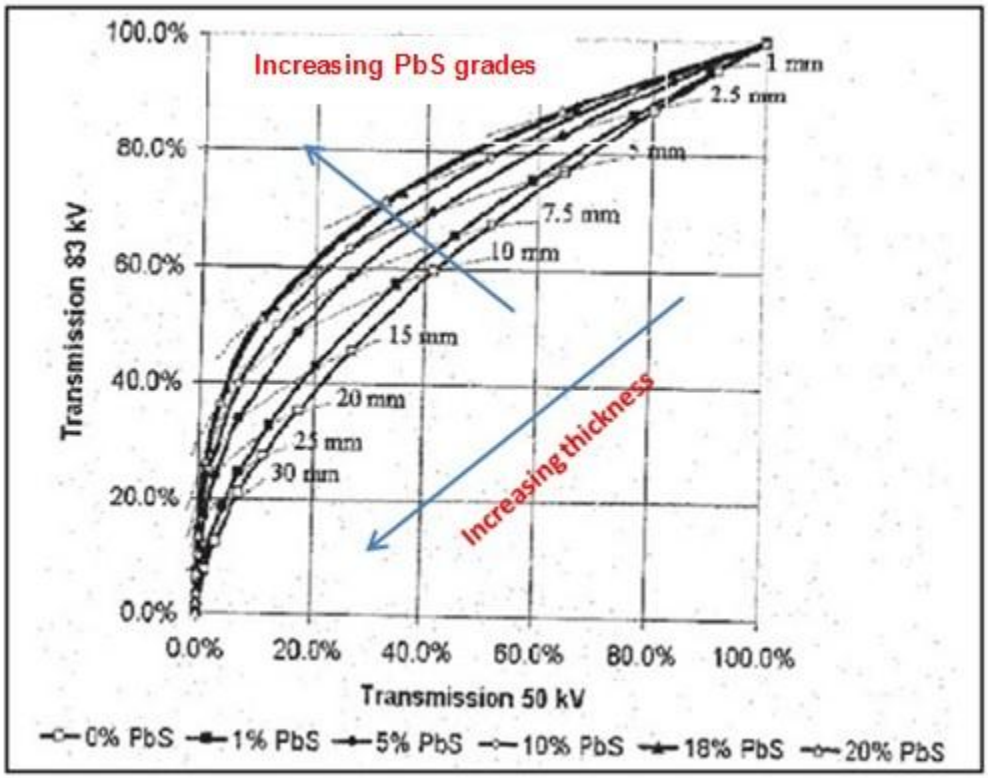


**Figure 2-7 Transmission Curves of Mixtures with Different PbS Grades at 83kV/50kV**
(De Jong & Harbeck, 2005)

The above figure indicates that rocks with different grades can be separated according to their transmission curves if their curves do not coincide. Different software packages employ different methods of analysis of the transmission curve. The Mikrosort® simulation package used by Mikrosort DE-XRT sorter generates a calibration curve as sorting criterion. This curve is plotted using the linear regression of the plotted points from the transmission graph of the typical samples of the material. The curve indicates the average density distribution of the material within the size range for sorting (Figure 2-8). Individual pixels of the high and low energy X-ray images of each particle of the material will be evaluated and plotted on the calibration curve. The pixels are then assigned color according to their position on the curve. If a pixel is plotted in the high density zone it will be assigned as blue and otherwise it will be assigned red. A pre-set

percentage of pixels in the high density zone (blue) is then used as a sorting criterion. This criterion will be used for deciding whether the rock is to be rejected as waste or accepted as product (Strydom, 2010).

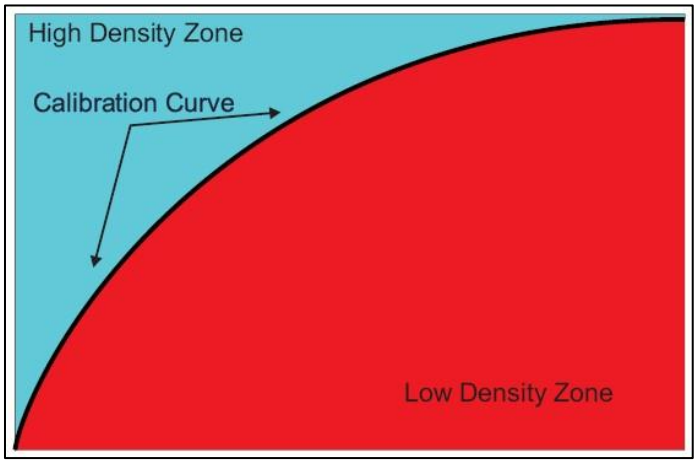


**Figure 2-8 The Calibration Curve for Sorting**
(Strydom, 2010)

The PACT Sorting Control System used by the CommoDas Ultrasort DE-XRT sorter generates an Ore Index for each particle and uses this Ore Index as the sorting criterion. For each particle, a 2D transmission histogram will be created from the low and high energy images showing the distribution of high/low energy brightness combinations of each pixel within the image. The 2D transmission histograms for each rock are then mapped against a weighted reference histogram, called an Ore Index Reference Map. This Ore Index Reference Map is created from the set of histograms and assay results for the sample. The ore index of each particle can be calculated by mapping the 2D histogram of the particle against the reference histogram. The larger the ore index, the more likely the particle reports to the product. Figure 2-9 shows an example of the 2D transmission histogram of a rock and its Ore Index Reference Mapping (Kowalczyk, 2012).

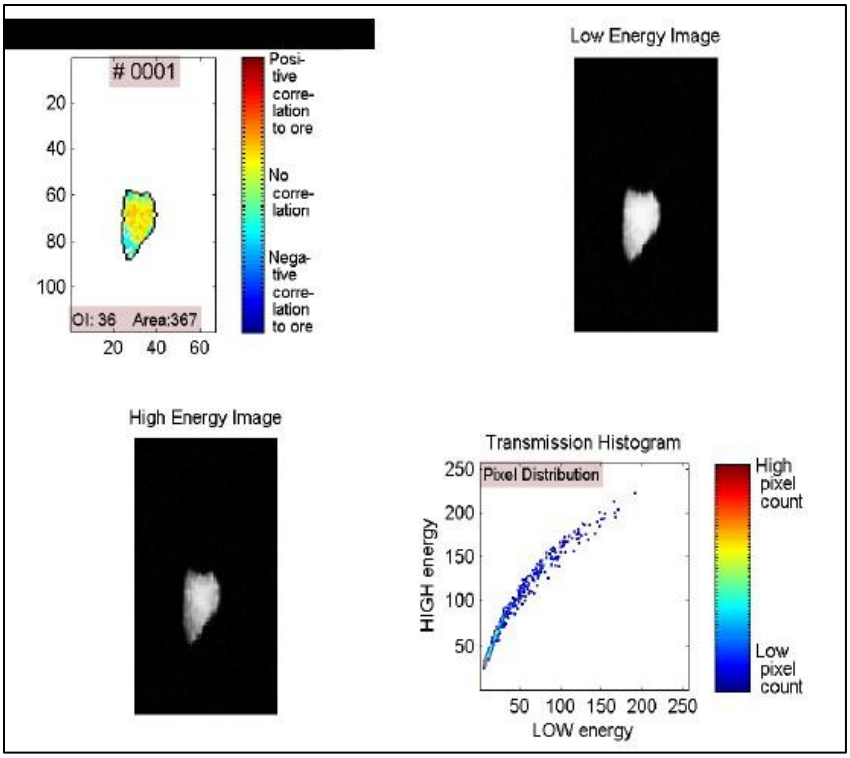


**Figure 2-9 Transmission Graph for a Rock Sample**
(Kowalczyk, 2012)

### 2.3.3 DE-XRT Sorter

The industrial DE-XRT sorter is composed of five major components just like other sorters. These five components are the feed system, feed presentation system, sensing system, data analysis system and separation system. The systematic layout of a DE-XRT sorter is shown in Figure 2-10.

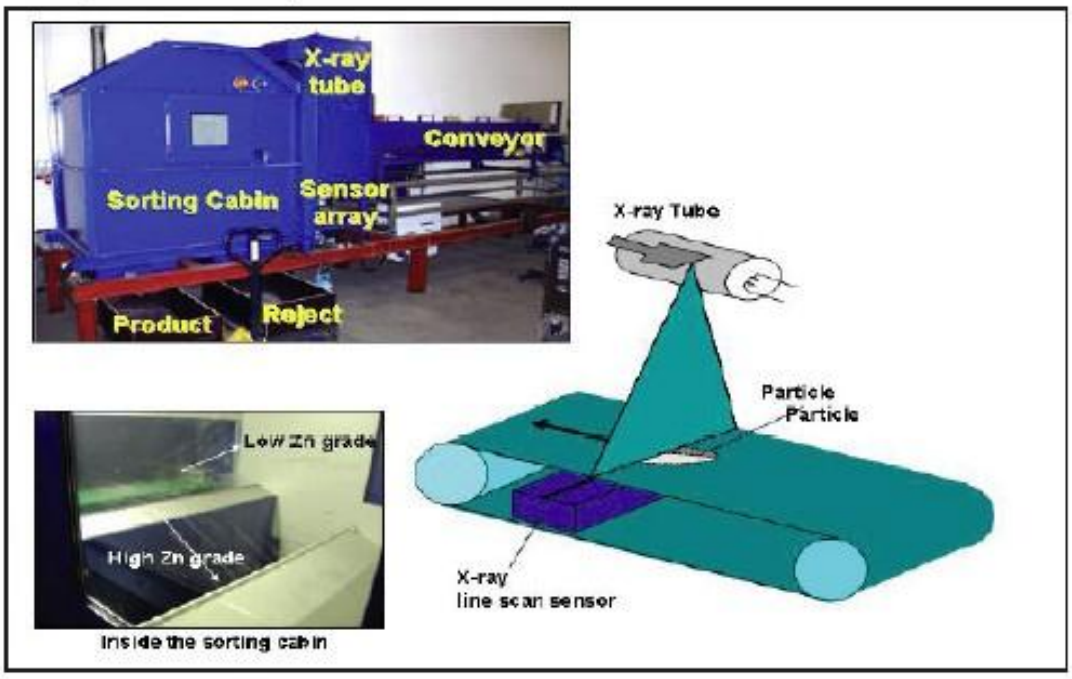


**Figure 2-10 Layout of an X-Ray Transmission Sorter**
(CommoDas, 2004)

1. The materials are fed through the feed bin to the conveyor where they are transported to the sensing system.
2. The materials travel to the sensing area at a speed of 2-4 m/s. The belt width is normally 1-2 m.
3. The sensing system includes an X-ray tube and an X-ray line scanning sensor. X-rays generated from the X-ray tube strike the materials when they are travelling through the sensing area. The transmitted X-rays are then captured by the dual-energy X-ray line scanning sensor which is composed of an array of scintillation crystals. These crystals are used to capture the number of counts of each element in the array. Figure 2-11 shows the principle of the dual-energy X-ray transmission sensing system. An image of the particle is then generated line by line using a similar principle of color line scan camera (Strydom, 2010).
4. The scanning speed is normally 250-500 lines per second. The X-ray components inspection speed is between 0.5-2 m/s at about 1m inspection width. The sensor resolution is between 1.5×1.5 and 5×5 $mm^2$ (De Jong, Dalmijn, & Kattubtudt, 2003).

5. High energy and low energy X-ray transmission images of each particle are generated and analyzed by the data processing system.
6. Depending on the analysis results, the data processing system will signal the separation system whether or not to eject the particle by the air valves.

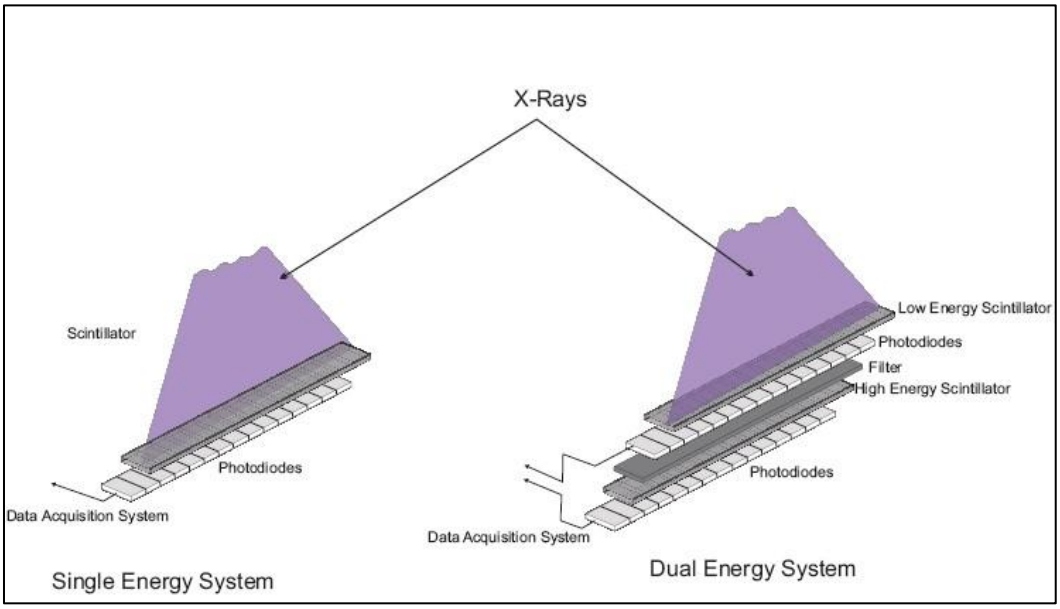


**Figure 2-11 Principle of Single Energy and Dual-Energy X-Ray Transmission Sensing**
(Von Ketelhodt & Bergmann, 2010)

### 2.3.4 Dual-Energy X-Ray Transmission Sorting Applications

Von Ketelhode and Bergmann (2010) found that Dual Energy X-ray Transmission sorting was applicable to dry coarse coal separation in the size range of -120+12 mm with a capacity of 150-80 t/h. Their testwork of different coals was conducted at the XRT sorter pilot plant at Mintek in Randburg, Africa. Test results indicated that this technology was capable of segregating pyrite-bearing coal and shale to produce clean coal product and discriminating coal from torbanite, thereby producing two clean products (Von Ketelhodt & Bergmann, 2010).

Kuilman (2006) also demonstrated the efficiency of the DE-XRT sorter in lowering the ash content of washed coal, preconcentration of Run-of-Mine coal and sorting of coal from waste dump. He indicated that the process should be optimized for sorting of ROM coal finer than 15mm. The sortability of washed coal was strongly dependent on the liberation of coal. DE-XRT Sorting was capable of sorting coal mine waste coarser than 5mm. However, the economy of coal sorting using this technology is strongly dependent

on the characteristics and origin of the material. The sortability of the coal could be only concluded on a case-by-case basis (Kuilman, 2006).

The applications of XRT Sorting for base metal sulfides were first introduced by Harbeck (2004). Testwork using both single energy transmission and dual-energy transmission was conducted and dual-energy transmission indicated greater amenability (Harbeck, 2004). Other successful applications of DE-XRT Sorting include sorting of pentlandite nickel ore (Allen & Gordon, 2009), copper ores such as chalcopyrite and bornite, and pyrite bearing gold ores (Von Ketelhodt, 2009).

It is important to know that the amenability of DE-XRT Sorting of any ore is strongly dependent on the degree of liberation of the ore. Conclusions could be specific to the case studied.

### 2.3.5 Summary

DE-XRT sorting is a fast and reliable dry separation method with many successful applications in the base metal industry. It has several advantages, as follows:

- suitability for high-speed identification, at several thousand particles per second (De Jong, Dalmijn, & Kattubtudt, 2003).
- bulk volume inspection instead of surface (De Jong, Dalmijn, & Kattubtudt, 2003).
- insensitivity to surface conditions, e.g., dust, moisture, and contaminants (De Jong, Dalmijn, & Kattubtudt, 2003).
- on-line analysis of shape, texture, size distribution and composition (Kuilman, 2006).

The present preliminary laboratory DX-XRT testwork was conducted to evaluate the application potential of this technology to the preconcentration of a lead-zinc ore from dolomitic waste rocks. This work will extend the application of DE-XRT sorting technology to a new type of ore and also demonstrate the amenability of preconcentration of this lead-zinc ore using DE-XRT sorting technology.

## 2.4 Optical Sorting Technology

### 2.4.1 Optical Sorting

Optical sorting is the oldest and most mature sorting technology in industry. It has been applied in the recycling, food and industrial mineral industries for a long time and many successful applications can be found. With the help of advanced computing technologies and enhancement of optical resolutions, the capacity of modern optical sorters has been much improved, up to 300t/h, and so has the reliability of this technology. It has only recently been introduced to the metal mining industry, however, and little evaluation of optical sorting of ores has been undertaken in the academic field.

Optical sorting is a separation technique where materials are sorted based on discrimination in reflectance, transparency or color between particles by photo detector or digital cameras. Texture and shape recognition techniques are also available now and could be used in the process of optical sorting by facilitating the recognition of a specific material (Bamber, 2008). The present study is concentrated on the optical sorting under visible light.

Two types of light source are commonly used for this application: continuous spectrum sources (e.g., tungsten bulbs) and discontinuous spectrum sources (e.g., fluorescent tubes and lasers). The detectors used for optical sorting under visible light are mainly photodiodes, photomultipliers (used with lasers) and Charged Couple Devices (CCDs). Optical sorting using photodiodes and photomultiplier detectors is called photometric sorting while that using a CCD detector (digital camera) is commonly called color sorting. Photodiodes and photomultipliers can only detect the intensity of light reflected from the material surface regardless of color while CCDs can analyze different colors. Two major color analyzing methods employing a Bayer filter mask and separate CCDs are used for CCD detector. The Bayer filter mask assigns red, green and blue to each pixel. This filter pattern includes two diagonally opposite green pixels, one red pixel and one blue pixel. The second analyzing method uses a RGB splitter prism to split light into red, green and blue components. Three CCDs are used to respond to each of the three colors (Fitzpatrick, 2008).

There are two major methods to extract color information from the image: first-order statistical method using histogram parameters of RGB image and second-order statistical method, co-occurrence statistics from a gray-level image. The present study

does not aim to review different image processing technologies. For detailed information on image processing methods, readers are referred to Singh and Rao's paper in 2005 (Singh & Rao, 2005) and Tessier, Duchesne and Bartolacci's paper in 2007 (Tessier, Duchesne, & Bartolacci, 2007). The first-order statistical method using histogram parameters is used in this study to obtain color features.

The RGB color model is commonly used for image analysis. An RGB image is composed of three channels of data—red, green and blue—recorded by three CCDs in the camera. Each individual pixel of the image has an intensity value for red, green and blue. This intensity value for each color channel is discrete and ranges from 0 to 255 for the 8-bit camera (Tessier, Duchesne, & Bartolacci, 2007). Sorters can analyze the data directly or convert these data to other color models such as YUV and HS, etc. These color models, unlike the RGB color model, evaluate an image using luminance and chrominance separately. As a result, after converting data from RGB color model to YUV model, sorters can separate materials based on pure color difference only. MikroSort and CommoDas color sorters both use the YUV color model for ore sorting (Fitzpatrick, 2008).

### 2.4.2 The Color Ore Sorter and Its Applications in the Metal Mining Industry

#### *2.4.2.1 Color ore sorter*

Modern color sorters utilize line scan digital cameras together with complicated image processing and analyzing software to discriminate between colors of the materials. Color evaluation can be done within milliseconds (Fattori, 2009). High resolution images can be produced and used to identify small differences in brightness and color. This type of color sorter has many applications in the mining industry.

The color ore sorter includes five components: feed preparation system, feed presentation system, sensing system, data processing system and separation system (Kidd, 1983). The schematic layout of a color ore sorter is shown in Figure 2-12.

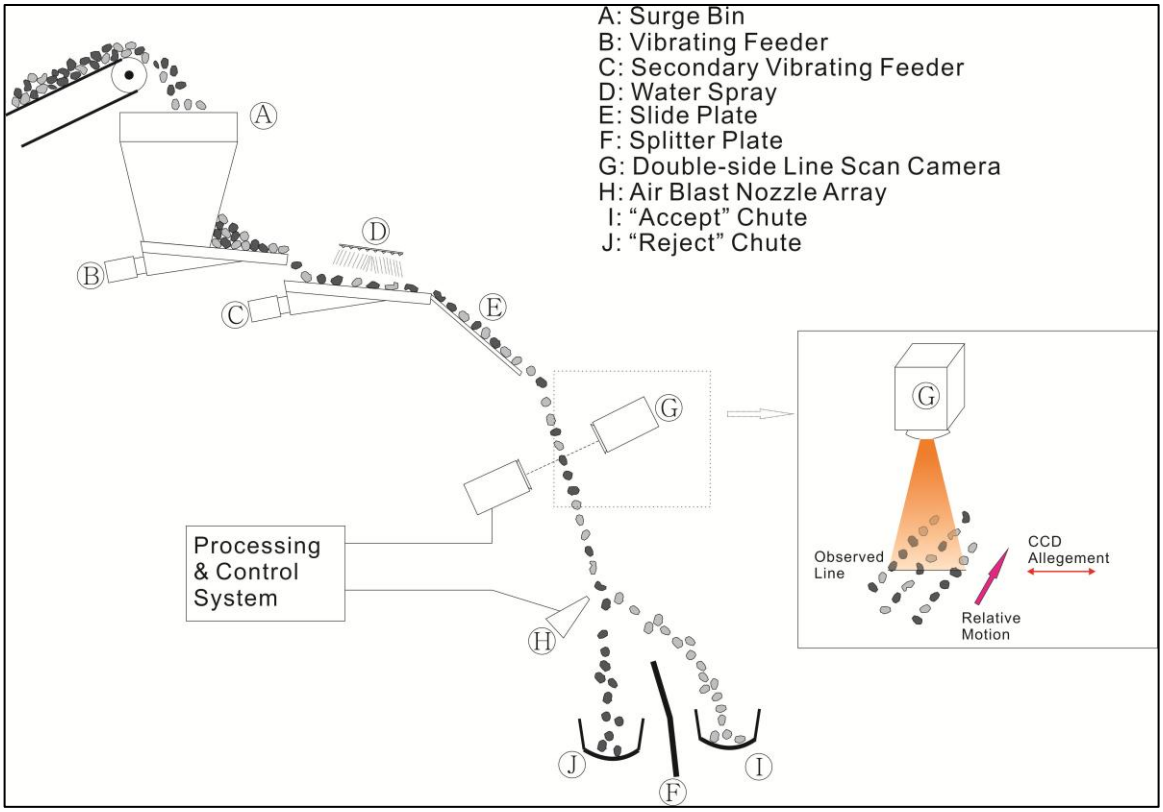


**Figure 2-12 Schematic Layout of a Color Ore Sorter**
(After Fitzpatrick, 2008; Keys, Met, Gordon, & Peverett, 1974)

Preparation of feed is of great importance to achieving efficient sorting results, in two ways. First, rocks need to be present in a specific size range for machine sorting. Second, optical sorting is surface-dependent technology where a clean surface is needed for optical data generation. Therefore, rocks need to be washed to clean off fines prior to sensing. Moisture can also enhance the reflectance of the rock and therefore facilitates sorting based on color properties. Rocks need to travel through the sensing area in a monolayer and be separated from each other. In addition, individual particles should travel at the exact same speed prior to sensing in order to obtain images under constant conditions. Hence, a stable feed presentation system, normally consisting of a vibrating feeder and a conveying belt or a chute, is required for a color ore sorter. Color features of the rocks passing through the optical scanning area are recorded in the image captured by the line scan digital camera. This image is analyzed by the data processing system using sophisticated image processing software and then the decision is made whether the rock is ejected by air jets to the waste chute or continues its trajectory into the product chute. The separation system includes a series

of high-speed valves. When the processer sends a signal to the ejecting system that the rock should be ejected, the corresponding valve or valves will open for a certain time to generate a high-energy blast of air to blow the rock away from its trajectory across the splitter into one chute (Bulled, 1997).

#### *2.4.2.2 Applications of color ore sorting in the metal mining industry*

Modern color ore sorters are available from CommoDas, MikroSort and Comex. They are capable of processing rocks sized from 2 to 300 mm with a capacity up to 300 t/h. Commercial applications of color sorting are mainly found for industrial minerals such as limestone, feldspar and talcum. Not many applications for base metal ore sorting are reviewed in the literature. Only two applications for gold and platinum ores are discussed.

A containerized color sorter from CommoDas was installed at Kloof gold mine in South Africa in October 2003. This color ore sorter was used to sort gold reef from waste rock with a feed rate of about 80 tph. It could process rocks sized -80+16 mm. Five percent mass was rejected as waste after color sorting when concentrate grade was 5 g/t compared to 0.3 g/t in the feed (Von Ketelhodt, 2009).

Another application of color ore sorting was found at Waterval platinum mine in South Africa. A solid CDX-120 chute color ore sorter was installed to upgrade chromite Run-of-Mine ore based on color and brightness differences. The sensor used for this color ore sorter is 30-bit color line scan camera double-side detection. This color ore sorter has a throughput between 100 and 300 tph depending on the size, -300+50 mm. Approximately 20% to 65% mass could be rejected as waste after sorting (Von Ketelhodt, 2009).

A preliminary study of color ore sorting was conducted using an industrial scale CommoDas Sorter installed at University of Exeter. This ore sorter employed multi-sensors, an optical sensor and an inductive sensor. The optical sensor used for this sorter is a Pricolor TVI 2048R. It is a 2048-bit line scan camera using CCDs. Sorting tests were done on an iron ore from the Marandoo deposit in Australia. The experimental results showed that the CommoDas sorter was able to upgrade this iron ore sample based on differences in optical properties. To be specific, a 2.8% increase of grade and a 3.88% decrease of acid oxides level were achieved by rejecting white siliceous waste. A color sorting test of a nickel/copper ore from Raglan mine in northern Canada was conducted for the same study. The experimental results indicated that this CommoDas

sorter could upgrade the nickel/copper ore sample based on color discriminations. Forty percent mass containing basalt and peridotite could be rejected as waste with 93% and 95% recoveries of copper and nickel respectively (Fitzpatrick, 2008).

### 2.4.3 Summary

From the literature review, it can be concluded that optical sorting, and modern color sorting in particular, has demonstrated its potential in the applications of the metal mining industry through industrial applications for gold and platinum ores. Preliminary studies on iron and nickel/copper ores also indicated the potential application of color sorting technology. Color sorting is a proven technology with high throughput and reliability. However, optical sorting is a technique based on the detection of particle surface. It has no penetration power and is not capable of analyzing the bulk particle. In addition, adequate sample preparation and stable sample presentation are required for good sorting results.

## 2.5 Microwave-Infrared Sorting Technology

### 2.5.1 Microwaves and Heating Rates of Minerals

Microwaves are one type of electromagnetic energy with an electric and magnetic field. Dielectrics that have dipoles can absorb the microwave radiation. Those dipoles will align and flip around under microwave radiation when the applied field is changing. As a result, such materials will be heated up when internal energy is stored because of friction (Kingman & Rowson, 1998). Assigned frequencies for microwave heating are 915 and 2450 MHz. Domestic microwave ovens are operating at 2450 MHz (Bradshaw, Van Wyk, & Swardt, 1998).

Hua and Liu (1996) investigated heating rates of over 40 minerals and compounds. Their results showed that most sulphides minerals are good heaters which respond well to microwave radiation, while common gangue minerals such as quartz, calcite and feldspars are transparent to microwaves. This indicated that segregation of sulfide minerals from gangue based on temperature differences will be possible after microwave heating. Some heating rates of the minerals are summarized in the following Table 2-2.

**Table 2-2 Heating Rates of Common Sulphide Minerals and Gangue Minerals** (Hua & Liu, 1996)

| Minerals | Chemical Composition | Heating Rate, $\Delta T$: $\Delta t$ /K·s$^{-1}$ |
|---|---|---|
| **Chalcopyrite** | $CuFeS_2$ | 11.37 |
| **Ferrous sulphide** | FeS | 5.02 |
| **Pyrrhotite** | $Fe_{1-x}S$ | 16.43 |
| **Molybdenite** | $MoS_2$ | 5.08 |
| **Galena** | PbS | 5.93 |
| **Sphalerite** | ZnS | 0.89 |
| **Lead-zinc sulfide concentrate** | PbS-ZnS | 2.81 |
| **Quartz** | $SiO_2$ | 0.32 |
| **Calcium carbonate** | $CaCO_3$ | 1.33 |

### 2.5.2 Microwave Heating and Its Potential for Sorting

The potential applications of selective microwave heating of minerals in mineral processing have been investigated in recent decades. It can assist the comminution process by weakening the ore through inducing differential expansion and increase mineral liberation by enhancing the intergranular fracture of the ore due to the different thermal behaviours of different mineral phases. Microwave heating also found applications in the refractory gold ore treatment process and leaching process to improve mineral separation. Readers are referred to Kobusheshe's 2010 doctoral dissertation *Microwave enhanced processing of ores* for further information on this topic.

The goal of this research is to explore infrared (IR) sensing of sulfide by means of non-contact IR imaging after exposure to microwave radiation. Microwave heating in this case functions as a pre-treatment process for machine sorting using IR sensors. Figure 2-13 illustrates such microwave infrared (MW/IR) sorting of sulfide ore.

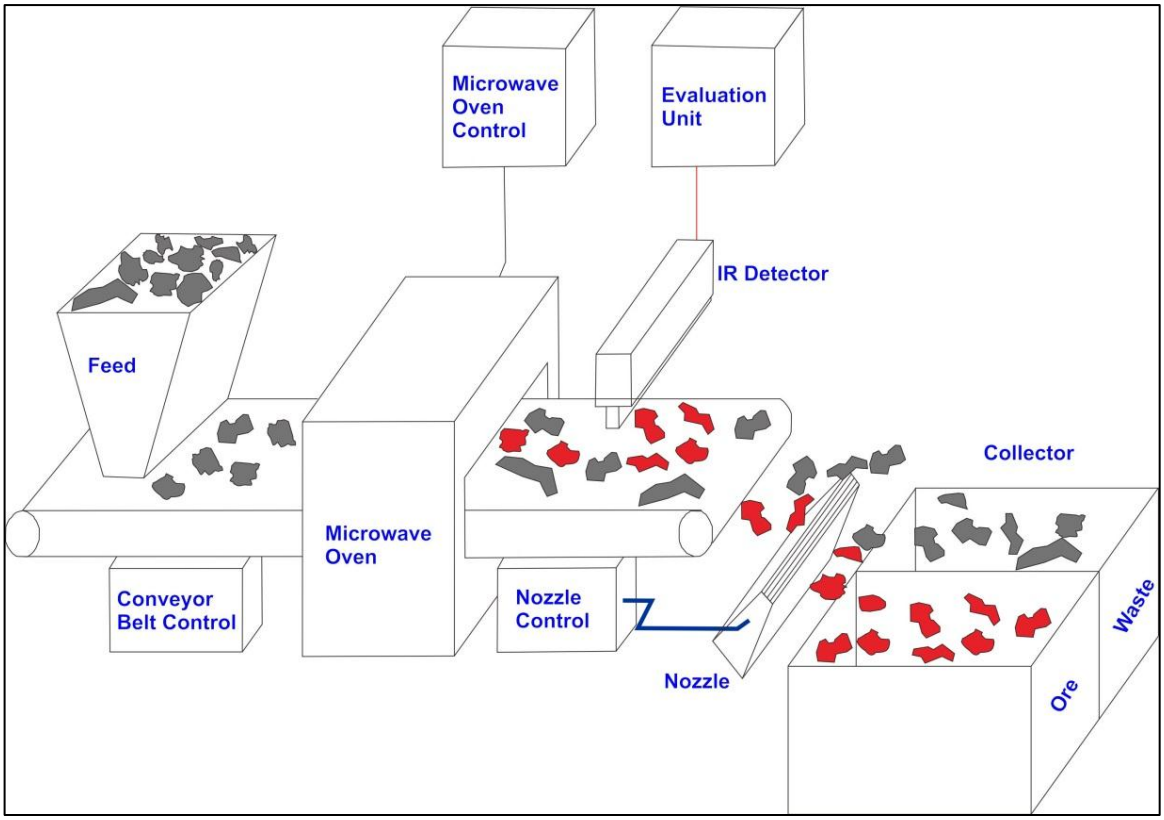


**Figure 2-13 Schematic Diagram of MW/IR Sorting of Sulfide Ores**
(After Labbert, Baloun, Schoenherr, & Kuyumcu, 2012)

MW/IR ore sorting, the segregation of sulphides from barren rock, is still in the development stage compared to other sorting technologies such as X-ray sorting. It is also one of the few sorting techniques enabling entire rock analysis instead of surface. MW/IR was first studied to separate rocks containing graphite or carbonaceous matter, which causes “pre-robbing” problems in the gold milling process. Van Weert and Kondos’s paper, which was given during the 39th Annual Canadian Mineral Processors Conference in 2007 in Ottawa, showed that sulphides and carbonaceous materials bearing rocks responded readily to microwave radiation, which allows for sorting by an infrared sensor (Van Weert & Kondos, 2007). Limited samples were studied using a domestic microwave oven with a turntable. Effects of exposure time, orientation and size of rocks on microwave heating were evaluated. The results showed that the state of rock, i.e., whether it was cleaned, dusty or wet, did not have an impact on separation. Rocks cannot be heated up evenly due to the non-uniform distribution of those components responding to microwave radiation. However, due to the insufficient sample size tested, the conclusions need to be justified by large-scale laboratory tests.

Further work on upgrading sulphide ores by infrared sensing after microwave radiation has demonstrated that successful upgrade of molybdenite or (chalco) pyrite by MW/IR sorting depends on the uneven distribution of sulphides in the host rock, making MW/IR sorting suitable for vein, stockwork or stringer-type sulphide deposits (Van Weert, Kondos, & Gluck, 2009). Maximum temperature as read by an IR sensor was used as sorting criterion in this study. However, average surface temperature could be a better parameter for sorting, which suggests further investigation. The temperature/weight relationship needed to be studied on adequate ore samples of different size range in a laboratory-scale test.

Van Weert and Kondos (Van Weert & Kondos, 2008; Van Weert, Kondos, & Wang, 2011) have demonstrated that particle size has a great effect on microwave heating of pyrite crystals. The results from their research show that crushed clusters of pyrite crystals respond better to microwave radiation and heat up faster than evenly distributed ones. Solid specimens of different sulfide minerals including arsenopyrite, chalcocite, chalcopyrite, cobaltite, covellite, enargite, galena, molybdenite, pyrite, pyrrhotite and sphalerite were crushed to different sizes for MW/IR testing to investigate the effect of particle size and spatial distribution on microwave heating of sulfides (Van Weert, Kondos, & Wang, 2011). The results of their study showed that large sulphide

specimens greater than $1cm^3$ or small sulphide particles smaller than 100 microns responded poorly to 2450 MHz MWs. Sulfides can be heated up faster when touching than when separated, which indicates that corona discharging is of importance to microwave heating of sulfide.

The research on the topic of recognition of sulfides by MW/IR technology has been conducted only on mineral samples and artificial rocks (made of pure minerals and cement) with limited sample size of specific particle sizes. Due to the inadequate sample size and the lack of actual ore samples used for the previous studies on MW/IR sorting, the effect on microwave heating of radiation time, size, surface area or weight of the rock, and quantity of rocks heated at a time needs further investigation. It is the goal of the present research to address the relationship between the average surface temperature and these other factors in a laboratory-scale test on a lead-zinc sulfide ore sample provided by industry. Average surface temperature instead of maximum surface temperature was used sorting criterion, since average surface temperature may represent the overall sulphide content in the rock better, especially when the latter is evenly distributed. A rock with a little sulfide content will be heated up to very high temperature at a spot where the sulfide occurs as aggregates, while a rock with a large sulphide content dispersed within the whole rock will be heated up evenly to a relatively high temperature. If those two rocks are compared using the maximum surface temperature, the one with dispersed sulfides will be considered as waste because of its low maximum surface temperature. This could lead to inefficiency of the separation. Actual sorting results based on different average surface temperatures will also be presented.

## 2.6 Summary

Based on the review of the literatures regarding the four sorting technologies presented in the previous sections, a comparison of these four sorting methods is presented in Table 2-3.

**Table 2-3 Comparison of Different Sorting Technologies**

| Sorting Methods | Physical Properties Detected | Applications | Sensor Set-up Mode | Bulk /Surface | Size Range | Capacity |
|---|---|---|---|---|---|---|
| XRF Sorting | Elemental Composition | Base/Precious Metals | Free-Fall | Surface | 10-300mm | up to 70 tph |
| XRT Sorting | Atomic Density | Base/Precious Metals, Coal, Diamonds, etc. | On-Belt | Bulk | 5-300 mm | up to 150 tph |
| Optical (Color) Sorting | Colour, Reflection, Brightness, Transparency | Base/Precious Metals, Industrial Minerals, Gem Stones | Free-Fall | Surface | 5-250mm | up to 300 tph |
| MW/IR Sorting | Microwave Absorption, Heat Conductivity | Base Metals, Carbonaceous Materials | On-Belt | Bulk | N/A | |

Overall, these sensor-based sorting technologies provide potential applications for preconcentration ores and the technical amenabilities of these sorting methods for the lead-zinc ore can be examined in a laboratory-scale preliminary study prior to large scale test. The flowsheet for laboratory-scale ore sorting study, especially using these four sorting methods, is not yet established. Therefore, it is the aim of this present study to generate a methodology for laboratory-scale ore sorting amenability study using the lead-zinc ore as a case study.

# CHAPTER 3 SORTING TEST PROGRAM

This chapter describes the sorting testwork done to evaluate the amenabilities of this lead-zinc ore to X-ray Fluorescence Sorting, X-ray Transmission Sorting, Optical Sorting and Microwave-Infrared Sorting in the laboratory-scale. The equipment and methodology used for these four sorting tests were described and sorting results obtained were calculated.

## 3.1 Sample Preparation

Two drums of 720 kg ore sample from Pend Oreille Mine were shipped to UBC for this study. This ore sample was already hand-sorted with visible sulfide and meeting the size requirement for sorting study which may create a bias due to the preconcentration of Run of Mine ore. Ore samples were first screened using a US standard 75 mm sieve and the oversize products were fed to a laboratory Jaw Crusher. All the rocks were screened using standard US sieves; the sized fractions were weighted and assayed. The sieve sizes were 75 mm, 53 mm, 37.5 mm, 26.5 mm, 19 mm and 13.2 mm, producing seven size fractions. Subsamples for different ore sorting technologies were taken from each size fraction. Size analysis and assays are shown in Table 3-1.

**Table 3-1 Head Sample Size Analysis and Assays**

| Size Fraction | | Wt. Distribution, % | Cum. Wt. % | | Calibrated Grade, % | | Distribution, % | |
|---|---|---|---|---|---|---|---|---|
| mm | inch | | Oversize | Undersize | Pb | Zn | Pb | Zn |
| +75 | +3 | 24.5 | 24.5 | 75.5 | 2.84 | 5.58 | 16.9 | 14.2 |
| -75+53 | -3+2.12 | 44.9 | 69.3 | 30.7 | 4.66 | 11.80 | 50.9 | 55.1 |
| -53+37.5 | -2.12+1.5 | 14.2 | 83.6 | 16.4 | 5.85 | 9.97 | 20.2 | 14.7 |
| -37.5+26.5 | -1.5+1.06 | 6.3 | 89.9 | 10.1 | 3.65 | 9.52 | 5.6 | 6.3 |
| -26.5+19 | -1.06+0.75 | 2.1 | 92.0 | 8.0 | 1.49 | 12.80 | 0.8 | 2.8 |
| -19+13.2 | -0.75+0.5 | 2.0 | 94.0 | 6.0 | 2.23 | 7.78 | 1.1 | 1.6 |
| -13.2 | -0.5 | 6.0 | 100.0 | 0.0 | 3.10 | 8.61 | 4.5 | 5.3 |
| **Total** | | 100.0 | | | 4.11 | 9.63 | 100.0 | 100.0 |

### 3.2 X-Ray Fluorescence Sorting Test

#### 3.2.1 Materials

Fifty, seventy-five, one hundred and one hundred rocks from +75 mm, -75+53 mm, -53+37.5 mm and -37.5+26.5 mm size fractions respectively of Pend Oreille ore samples were collected. The quantity of rocks being used from each size fraction for XRF sorting test was randomly selected and it is only used to demonstrate the ore's amenability to XRF sorting in laboratory-scale preliminary study. All 325 rocks were cleaned, dried, numbered and weighed before being exposed to XRF sorting tests. Primary ore minerals in this sample are galena and sphalerite. Therefore, elements including Pb, Zn and Fe need to be detected and analyzed by the XRF analyzer.

#### 3.2.2 Equipment

In this preliminary scope test, the amenability of the material to XRF Sorting was evaluated using the XRF analysis station at UBC. The XRF analysis station is mainly composed of a XRF analyzer from Olympus Innov.X, which is illustrated in Figure 3-1. The primary X-ray is produced by an X-ray gun. The rock is placed on the detection area with a diameter of 1cm. An X-ray will shoot on the sample resulting in production of characteristic fluorescence from the rock. This fluorescence will be analyzed and quantified by the detector. Elements and their concentration presented on the surface of the rock will be shown directly on the screen of the HP iPAQ analyzer. Data obtained from this system is used for separation of this lead-zinc ore sample. The analysis process simulates what a real XRF sorter does when sorting the materials.

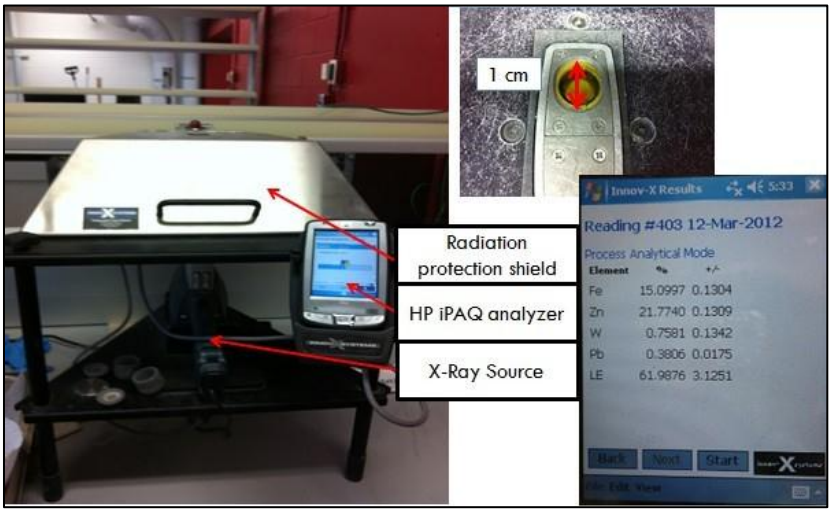


**Figure 3-1 XRF Analysis Station at UBC**

### 3.2.3 Experimental Procedures

In the XRF sorting test, the Innov.X XRF analyzer recorded readings of four, six or eight faces of individual rock, depending on particle size, in order to achieve maximum sorting potential. The average Pb, Zn and Fe grades for each rock were calculated by averaging the face readings; then anticipated XRF sorting results were calculated based on XRF surface readings. According to the anticipated sorting results, rocks in each size fraction were grouped by cut-off grades. They were then crushed in the Jaw Crusher and Gyratory Crusher to reduce size. A small portion of each grade range sample was pulverized and subdivided into two subsamples for XRF powder reading and assay. Pulverized samples from different grade ranges were sent for assay. Calibrations of XRF surface readings and XRF powder readings with real assays were conducted afterwards. Sorting results of four size fractions were finally calculated based on assays.

### 3.2.4 Results and Discussions

#### *3.2.4.1 Sortability of this ore using the Innov.X XRF analyzer*

In order to determine whether the Innov.X XRF analyzer can be employed to identify rocks with different grades of different sizes, all 325 rocks were individually analyzed by the XRF analyzer and then grouped in different grade ranges. After that, the rocks in different grade ranges were crushed and pulverized. Representative samples from each grade range were prepared and sent for chemical assays, which were done at Teck CESL Lab. The typical results, which are illustrated in Figure 3-2, indicate that the Innov.X XRF analyzer can be used to separate ore from waste rock given that there is a good correlation between the analysis of the surface of the rock by the XRF analyzer and the analysis of the bulk rock by chemical assays.

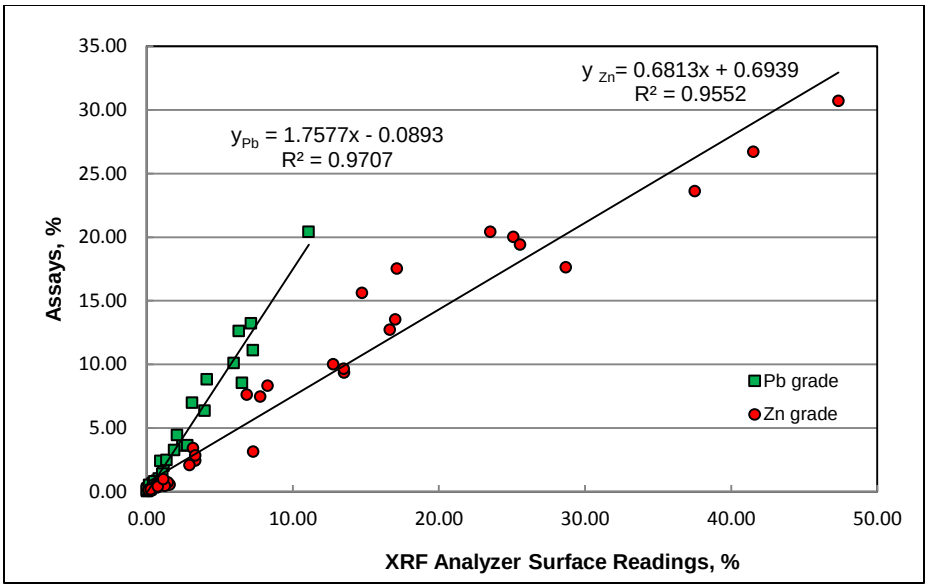


**Figure 3-2 Correlations between XRF Analyzer Surface Reading and Bulk Assays**
Note: these results are not for individual rock analysis. Each point represents the average Pb and Zn grades of several rocks in a grade range.

From the results shown in Figure 3-2, it can be concluded that the valuable minerals in this lead-zinc ore samples are evenly distributed. Consequently, chemical composition analysis of the particle surface has enough confidence in indicating the grade of the bulk particle after calibration. Therefore, this lead-zinc ore is amenable to XRF sorting. Correlation between assays and XRF powder readings were also plotted. The perfect correlation indicated that calibrated XRF powder reading can be used to substitute chemical assays for other sorting tests. Detailed results are shown in Appendix A.

Based on the XRD mineral analysis results, three sulfide minerals are found in this ore sample: galena, sphalerite and pyrite. Pb, Zn and Fe elements are the major metal elements for detection. Correlations between Pb, Zn and Fe grades presented on the rock surface are analyzed. The results are shown in Figure 3-3. It is evident from the figure that some of the rocks have low Pb content but high Zn content. If the Pb grade is used as threshold value, some high-grade zinc rocks will be rejected mistakenly as waste. In the lower part of Figure 3-3, the average Pb grades of the rocks with certain Zn grade range was plotted. It is clear that the larger the Zn grade in the rock, the larger the average Pb grade found. Therefore, the Pb grade has a good correlation with the Zn grade. Fe is also not a good indicator of Pb and Zn grades due to the fact that no evident

correlation is found between Pb/Fe and Zn/Fe. Consequently, the Zn grade is the most suitable threshold value for sorting this lead-zinc ore using XRF sensing system.

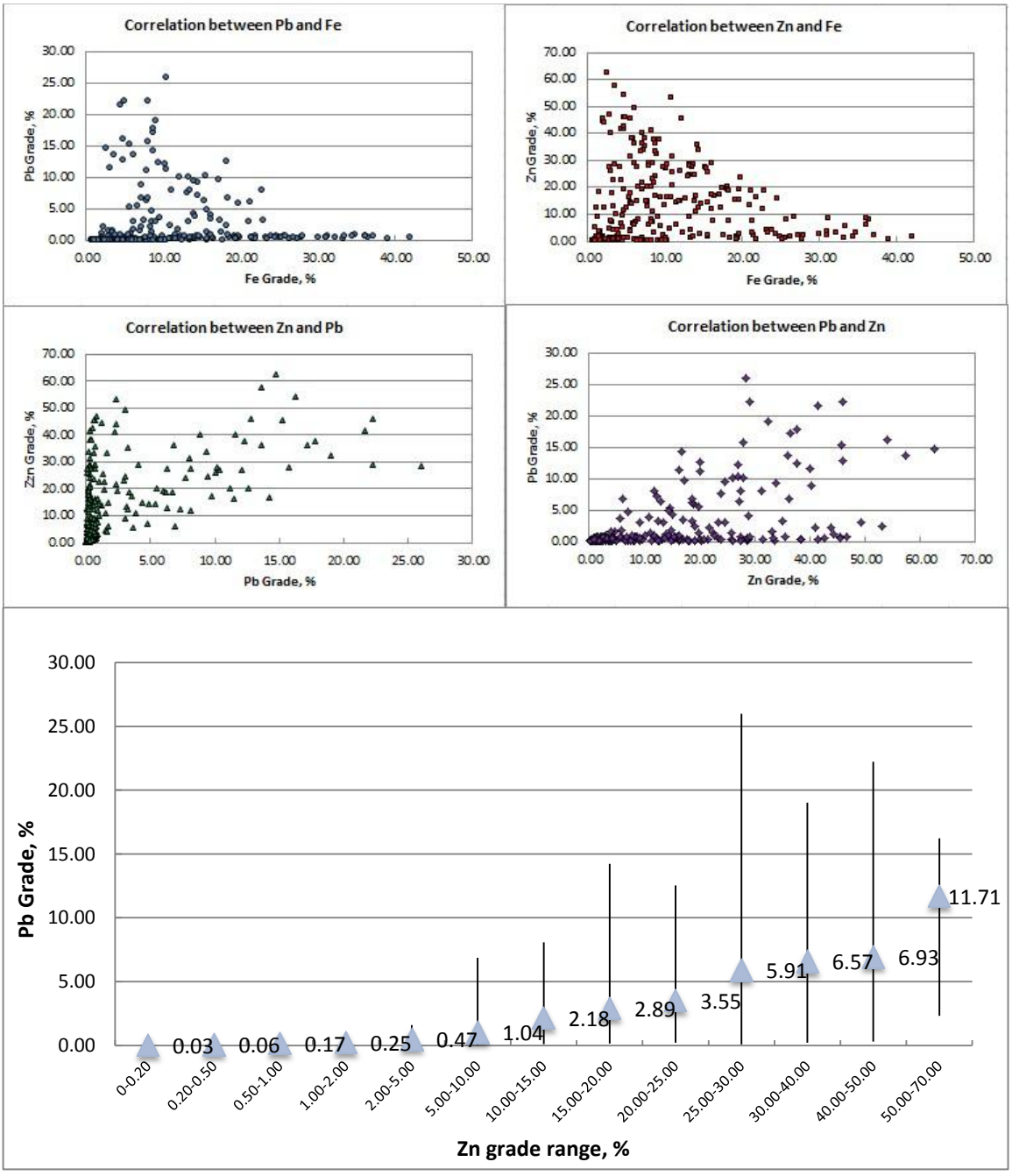


**Figure 3-3 Correlations between Pb, Zn and Fe**

### *3.2.4.2 Grade-Recovery relationship*

The second stage of this preliminary scope study of XRF sorting amenability is to discover the Grade-Recovery relationship for the lead-zinc ore by XRF Sorting using the Innov.X XRF Analyzer. All 325 rocks were analyzed by the XRF analyzer individually and then sorted in multi-stages using different threshold Zn grades. Threshold values used from Test 1 to Test 5 are 20.00% Zn, 10.00% Zn, 5.00% Zn, 2.00% Zn and 1.00% Zn respectively. The test procedures are illustrated in the flowsheet shown in Figure 3-4.

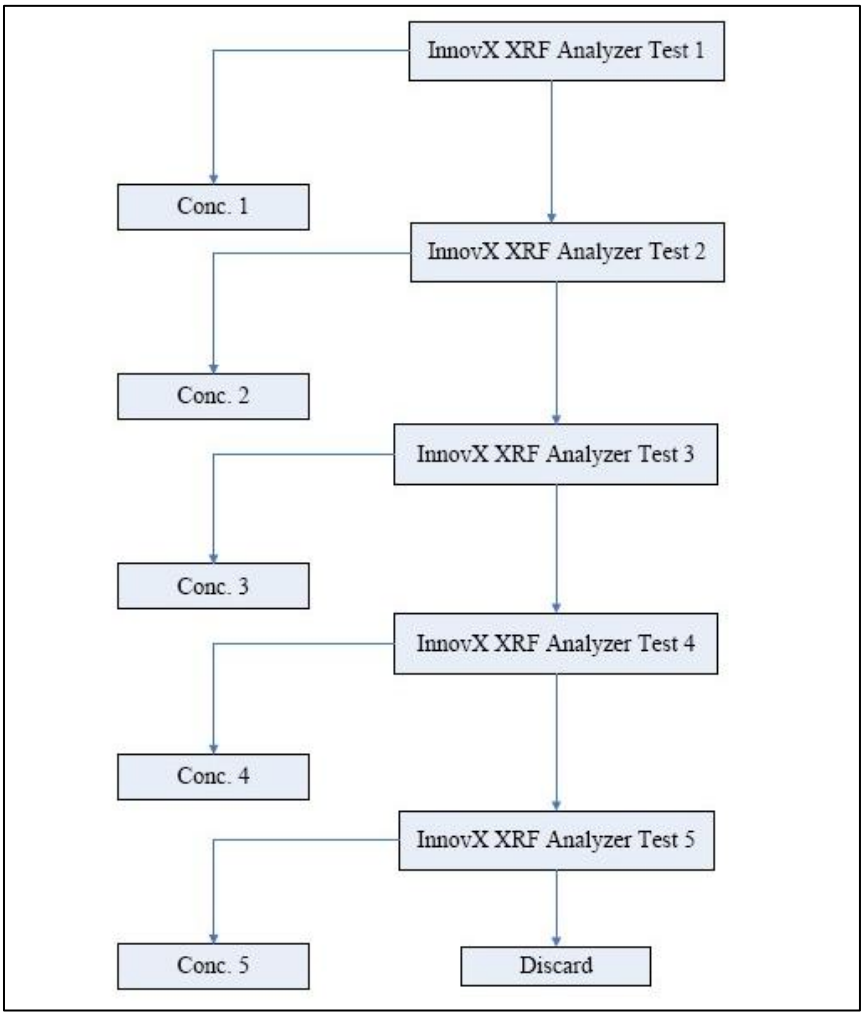


**Figure 3-4 Flowsheet of Grade-Recovery Relationship Test Procedures**

The results of the Grade-Recovery relationship test are shown in Table 3-2. Based on the results, typical Grade-Recovery relationship curves for Pb and Zn can be plotted using the cumulative metal recoveries and concentrate grades in Figure 3-5.

**Table 3-2 Grade-Recovery Relationship Test Results**

| Product | Mass, % | Grade, % | | Distribution, % | |
|---|---|---|---|---|---|
| | | Pb | Zn | Pb | Zn |
| Test 1 Feed | 100.0 | 3.91 | 8.50 | 100.0 | 100.0 |
| Conc.1 | 20.4 | 11.85 | 21.67 | 61.7 | 52.0 |
| Test 2 Feed | 79.6 | 1.88 | 5.12 | 38.3 | 48.0 |
| Conc.2 | 19.9 | 5.62 | 13.53 | 28.6 | 31.7 |
| Test 3 Feed | 59.7 | 0.63 | 2.32 | 9.7 | 16.3 |
| Conc.3 | 12.4 | 1.71 | 7.56 | 5.4 | 11.0 |
| Test 4 Feed | 47.3 | 0.35 | 0.95 | 4.3 | 5.3 |
| Conc.4 | 14.3 | 0.69 | 2.45 | 2.5 | 4.1 |
| Test 5 Feed | 33.0 | 0.21 | 0.29 | 1.7 | 1.2 |
| Conc. 5 | 6.8 | 0.31 | 0.71 | 0.5 | 0.6 |
| Discard | 26.3 | 0.18 | 0.19 | 1.2 | 0.6 |

| Threshold Value (Zn Grades), % | Cumulative, % | | | | Mass Pulled out as Waste, % |
|---|---|---|---|---|---|
| | Pb Recovery | Conc. Grade of Pb | Zn Recovery | Conc. Grade of Zn | |
| 20.00 | 61.7 | 11.85 | 52.0 | 21.67 | 79.6 |
| 10.00 | 90.3 | 8.77 | 83.7 | 17.65 | 59.7 |
| 5.00 | 95.7 | 7.11 | 94.7 | 15.28 | 47.3 |
| 2.00 | 98.3 | 5.74 | 98.9 | 12.54 | 33.0 |
| 1.00 | 98.8 | 5.25 | 99.4 | 11.46 | 26.3 |

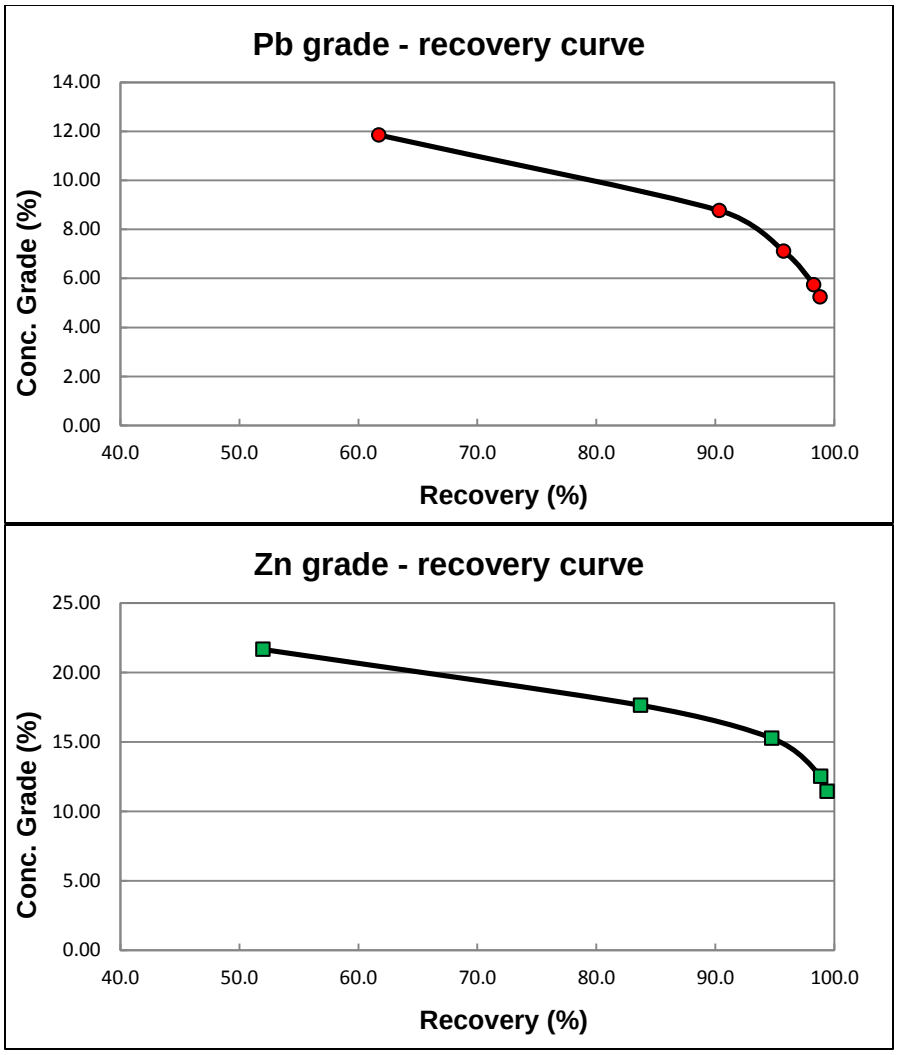


**Figure 3-5 Grade-Recovery Relationship Curves for Pb and Zn**

Data from the above Grade-Recovery relationship curves can be used as reference for selection of threshold value for sorting this lead-zinc ore sample using the Innov.X XRF Analyzer. Figure 3-6 shows the relationship between metal recovery and % mass rejected as waste based on different threshold Zn grades.

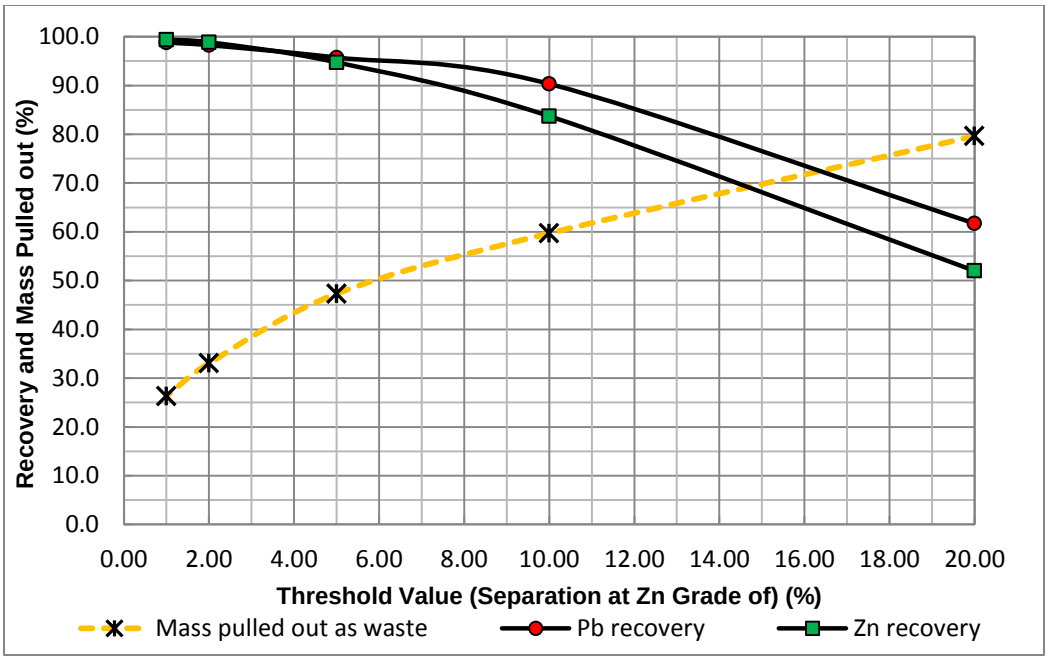


**Figure 3-6 Relationship between Metal Recovery and Percentage Mass Rejected as Waste Based on Different Separation Threshold Values**

From Figure 3-6, it can be concluded that above 45% barren waste can be rejected by mass, while above 95% of metals can be recovered in the concentrate. This indicates that XRF sorting of this lead-zinc ore using the Innov.X XRF Analyzer exhibits great potential.

#### *3.2.4.3 Summary of XRF sorting results*

The overall sorting results of these 325 rocks regardless of size (top size: bottom size = 3:1) are shown in Table 3-3. Sorting tests of +75 mm, -75+53 mm, -53+37.5 mm and -37.5+26.5 mm size fractions were also conducted separately to determine the optimum size for XRF sorting. Optimum results for each size fraction (to reject as much waste as possible with above 95% metal recovery) are shown in summary in Table 3-4. The detailed sorting results for each size fraction can be found in Appendix A.

In summary, in this preliminary scope test sorting of this lead-zinc ore using the Innov.X XRF Analyzer exhibits great potential. Table 3-4 shows that the optimum size for XRF sorting is -37.5+26.5 mm with regard to percentage of mass rejected as waste. At this size, 52.8% waste could be rejected at 97.1% Zn and 96.5% Pb recoveries, with calculated concentrate grades of 21.04% in Zn and 7.61% in Pb. All the other size fractions also showed good sorting results, from 35% to 50% of waste rejected by mass with above 95% metal recoveries.

**Table 3-3 Overall Sorting Results of 325 Rocks (Top Size: Bottom Size = 3:1) Sized Above 26.5 mm**

| Separation at Zn Grade of,% | Conc.,% | Mass Rejected as Waste, % | Metal Recovery, % | | Conc. Grade, % | | Waste Grade, % | |
|---|---|---|---|---|---|---|---|---|
| | | | Pb | Zn | Pb | Zn | Pb | Zn |
| 1.00 | 73.7 | 26.3 | 98.8 | 99.4 | 5.25 | 11.46 | 0.18 | 0.19 |
| 2.00 | 67.0 | 33.0 | 98.3 | 98.9 | 5.74 | 12.54 | 0.21 | 0.29 |
| 5.00 | 52.7 | 47.3 | 95.7 | 94.7 | 7.11 | 15.28 | 0.35 | 0.95 |
| 10.00 | 40.3 | 59.7 | 90.3 | 83.7 | 8.77 | 17.65 | 0.63 | 2.32 |
| 20.00 | 20.4 | 79.6 | 61.7 | 52.0 | 11.85 | 21.67 | 1.88 | 5.12 |
| **Calculated Head Grade:** 3.91% Pb and 8.50% Zn | | | | | | | | |

**Table 3-4 Summary of XRF Sorting Results of Four Size Fractions**

| Size Fraction | Separation at Zn grade of, % | Conc., % | Mass Rejected as Waste, % | Metal Recovery, % | | Conc. Grade, % | | Waste Grade, % | | Calculated Head Grade, % | |
|---|---|---|---|---|---|---|---|---|---|---|---|
| | | | | Zn | Pb | Zn | Pb | Zn | Pb | Zn | Pb |
| +75 mm | 2.00 | 64.1 | 35.9 | 98.2 | 96.1 | 9.68 | 3.27 | 0.31 | 0.24 | 6.32 | 2.18 |
| -75+53 mm | 5.00 | 62.8 | 37.2 | 96.1 | 97.6 | 15.87 | 8.72 | 1.09 | 0.36 | 10.37 | 5.61 |
| -53+37.5 mm | 5.00 | 52.2 | 47.8 | 95.1 | 98.5 | 18.82 | 10.49 | 1.06 | 0.17 | 10.33 | 5.56 |
| -37.5+26.5 mm | 5.00 | 47.2 | 52.8 | 97.1 | 96.5 | 21.04 | 7.61 | 0.56 | 0.25 | 10.21 | 3.72 |

### 3.3 X-Ray Transmission Sorting Test

#### 3.3.1. Equipment

The equipment used for this X-ray Transmission Sorting testwork was from CommoDas's facility in Surrey, British Columbia. It is a dual energy (140kV/77kV) Heimann 6040i X-ray scanner. The scanner was originally designed for airport package security checking and modified for mineral detection purpose (Figure 3-7). A box with four rocks can be scanned at one time with the X-ray scanner and dual energy gray-scale images of these four rocks can be obtained.

**Figure 3-7 Pilot-Scale Dual-Energy XRT Scanner at CommoDas**

The image processing software used for this study is GIMP. GIMP (GNU Image Manipulation Program) is a free image editing and analyzing software. This software features functions like fuzzy selection and free selection for shape contouring, threshold and histogram distribution of color intensity, etc. It can be used as a simplified image analysis tool for DE-XRT image processing, which was developed through this study. Sophisticated image analysis software used in the industrial DE-XRT sorter was inaccessible. However, CommoDas Ultrasort provided analysis results using their sorting control system for comparison purposes.

### 3.3.2. Experimental Procedures

#### *3.3.2.1 Sample preparation*

One hundred rocks from -37.5+26.5 mm size fraction of Pend Oreille lead-zinc ore samples after primary crushing and screening were prepared for this sorting testwork. Individual rocks were marked and weighed prior to testing.

#### *3.3.2.2 Image capture*

A group of four rocks was scanned simultaneously in a wood box using the X-ray scanner described in the previous section. A high energy and low energy gray-scale image was obtained for each rock, four rocks in one image. A sample of a dual-energy image was shown in the Figure 3-8.

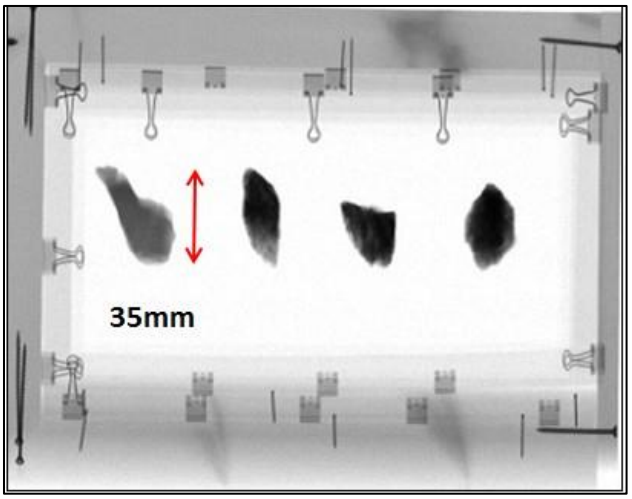


**Figure 3-8 Example of a DE-XRT Image Generated by the X-Ray Scanner**

#### *3.3.2.3 Sample assay*

After imaging, the rocks were individually crushed through a Gyrotary Crusher and Cone Crusher, pulverized and assayed by XRF analyzing of powders. Lead and zinc grades of each rock were obtained for further analysis.

#### *3.3.2.4 Image processing and data extraction*

The author analyzed the DE-XRT images of each rock using GIMP, which is a simple image processing software, and CommoDas Ultrasort analyzed the image using PACT sorting control system. Results based on these two image analysis methods were then compared.

***Simplified image processing by GIMP***

**1. Value image generation**

The image obtained from the X-ray scanner is a tif. format 1024×768 16-bit image with two layers (high and low energy). This image needed to be separated into two layers so that a high energy and a low energy image could be obtained for further analysis. Using GIMP software, the image of each rock was cropped out from the initial image and two layers of the image were saved as separate high energy and low energy images. Since GIMP can only process 8-bit images, images were depressed to 8-bit for this analysis. Data will be lost due to this depression. However, the depression of image will not significantly influence the analysis results since all images are processed and analyzed using the same method. The high energy and low energy images of each rock had a resolution of 320×240. This value image for each rock was used for further analysis. Figure 3-9 shows the process of value image generation.

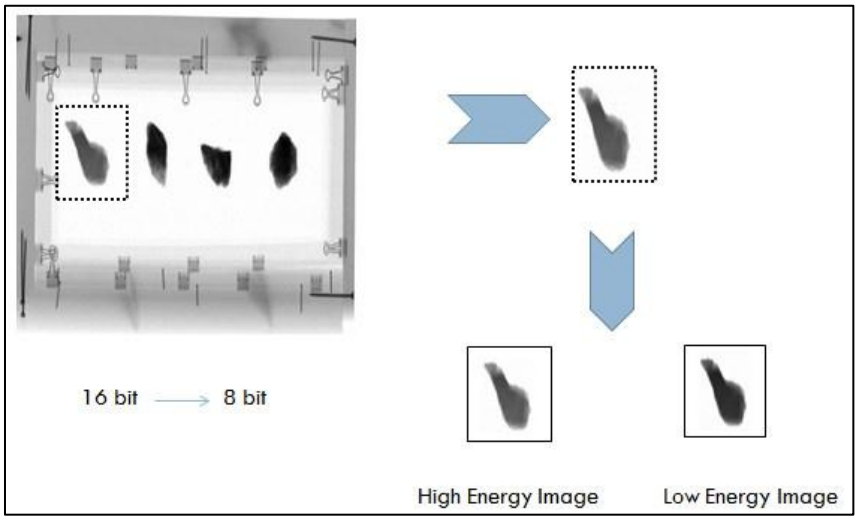


**Figure 3-9 Process of Value Image Generation**

**2. Brightness value extraction**

Individual gray-scale high energy and low energy images of each rock were processed by GIMP software. The shape of the rock was selected using GIMP's fuzzy selection function. The distribution of brightness value within the selected rock image was shown in the histogram. The brightness value ranged from 0 to 255 for an 8-bit image where 0 is blank, 255 is white and numbers between 0 and 255 represent different degrees of gray color. The larger the brightness value, the brighter the image, and the more X-rays

are transmitted. The average brightness value of the rock image (shape contour) was shown in the histogram. Figure 3-10 is a screenshot showing the processing of images using GIMP. In this simplified data extraction process, the average brightness value of the image was used as criterion instead of the brightness distribution for all pixels.

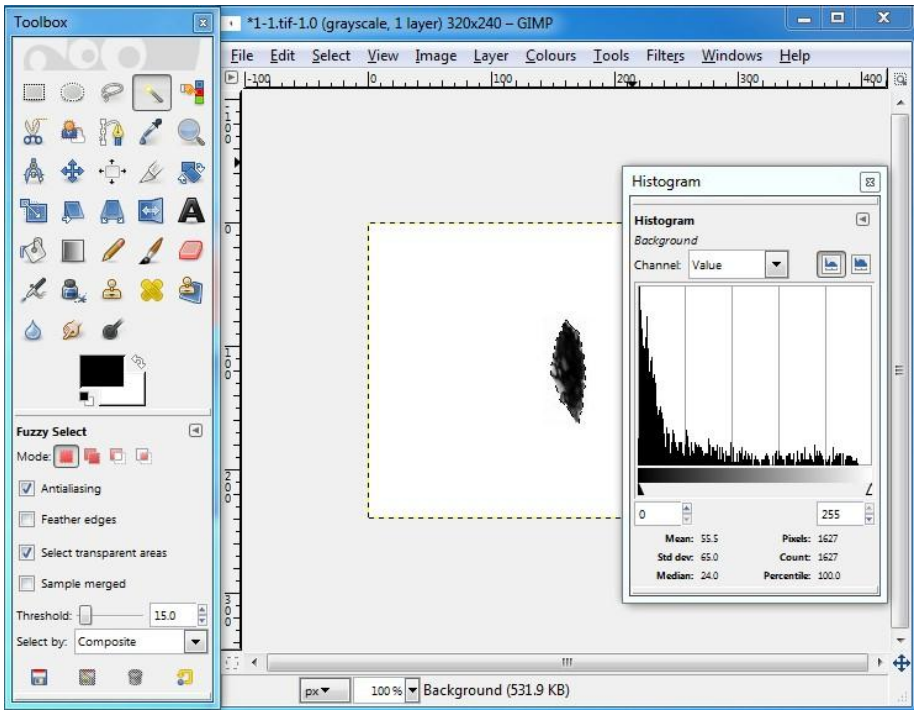


**Figure 3-10 Screenshot of Brightness Value Extraction from the Image**

***Image processing by PACT***

The initial images obtained by the X-ray scanner were also processed and analyzed by CommoDas Ultrasort using the PACT Sorting Control system. A high energy image and a low energy image of each rock were automatically obtained by the software and a 2D transmission histogram for each rock was also obtained showing the distribution of brightness value of the pixels within the image. The 2D transmission histogram and assay of each rock were then analyzed and correlations between them were studied for the generation of the Ore Index Mapping Reference. After that, the Ore Index of each rock was then calculated by mapping the 2D histogram of each rock against the Ore Index Mapping Reference histogram. The image processing flowsheet of PACT software is illustrated in Figure 3-11. The algorithm behind this Ore Index calculation is inaccessible to the author. Therefore, the DE-XRT sorting results based on the Ore Index are used only for comparison. The Ore Index could also demonstrate the actual

technical amenability of DE-XRT sorting of this lead-zinc ore using an industrial-scale DE-XRT sorter.

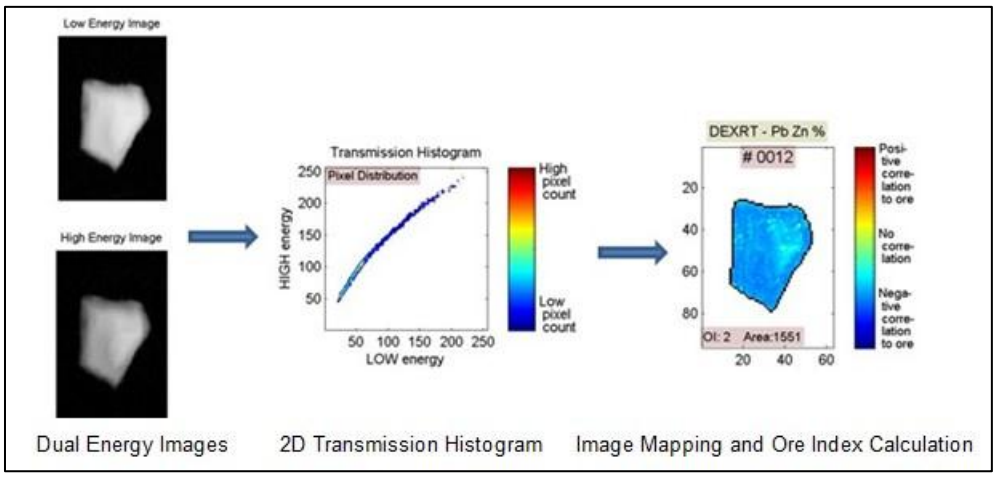


**Figure 3-11 Image Processing Flowsheet of PACT Software**

### *3.3.2.5 DE-XRT Sorting criterion determination*

The data information extracted from the DE-XRT images and assays were studied and analyzed for sorting criterion determination by plotting the correlation curve between the characteristic image data and the chemical composition of the rocks. Two sorting criteria were generated based on two data processing methods.

### 3.3.3 Results and Discussion

#### *3.3.3.1 Simplified image analysis by GIMP*

#### *Sorting potential based on average brightness value*

The average brightness value of the high energy and low energy images of the 100 rocks were read from the histogram through GIMP software. They are shown in Appendix B. The correlation between the total atomic number for valuable elements and the average brightness values of the high/low energy X-ray transmission images of the rock were analyzed by plotting the average brightness values of the high energy image and the low energy image at the X and Y axis respectively (Figure 3-12). The total atomic number for valuable elements is defined as: total atomic number for valuable elements ($Z_{total}$) = atomic number of Pb * Pb grade + atomic number of Zn* Zn grade. For example, if the Pb and Zn grades of the rock are 3.72% and 10.45%, the $Z_{total}$ is equal to 80* 0.0372+ 32* 0.1045 = 6. Each spot shown in Figure 3-12 represents a rock. Rocks were plotted using different colors based on their total valuable atomic numbers. The larger the $Z_{total}$ value, the heavier the rock is.

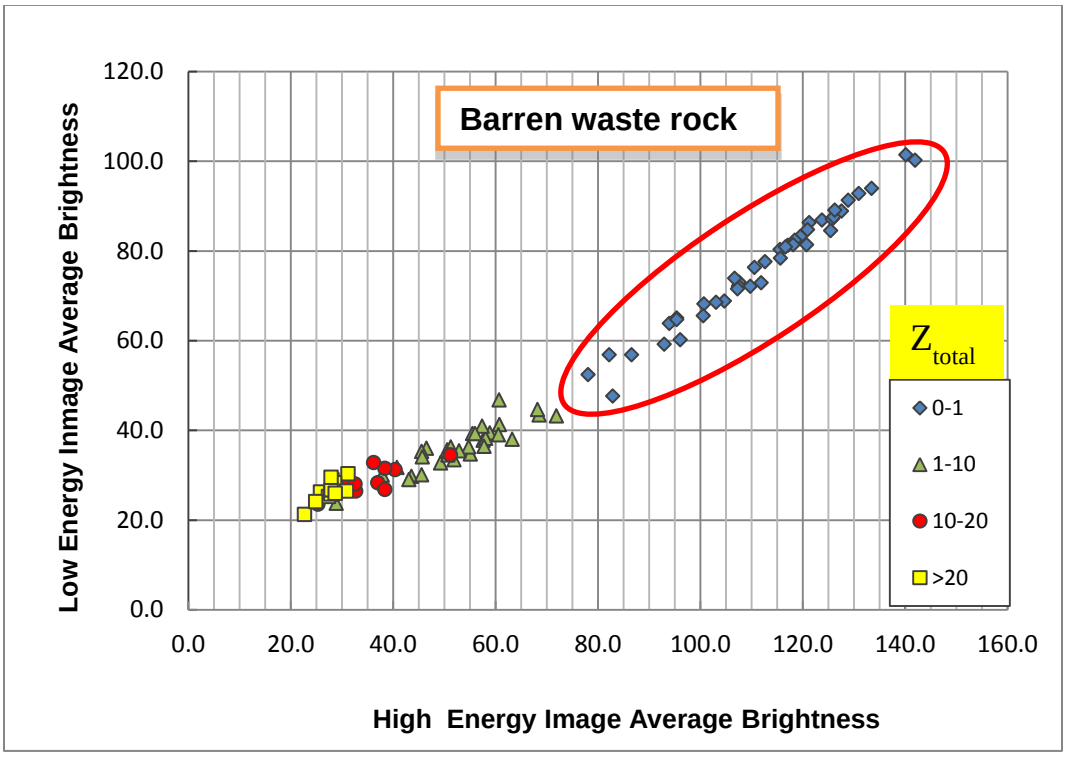


**Figure 3-12 Separation Curve for Lead-Zinc Ore Sample Sized -37.5+26.5 mm Based on Average Brightness Values of High/Low Energy Images**

Figure 3-12 shows rocks with smaller total valuable atomic number (low grade) positioned in the upper right while those with bigger total valuable atomic number are at bottom left, demonstrating good separation potential based on average brightness values of both the high energy image and the low energy image. This indicates that single energy X-ray transmission will also work for this lead-zinc ore sample, sized -37.5+26.5 mm, due to the small variance of rock thickness.

The relationship between the total lead and zinc grades (Pb+Zn) and the average brightness values of the high/low energy images is shown in Figure 3-13. Figure 3-13 also indicates that sorting of this lead-zinc ore based on the average brightness value of the X-ray transmission images would achieve satisfactory results.

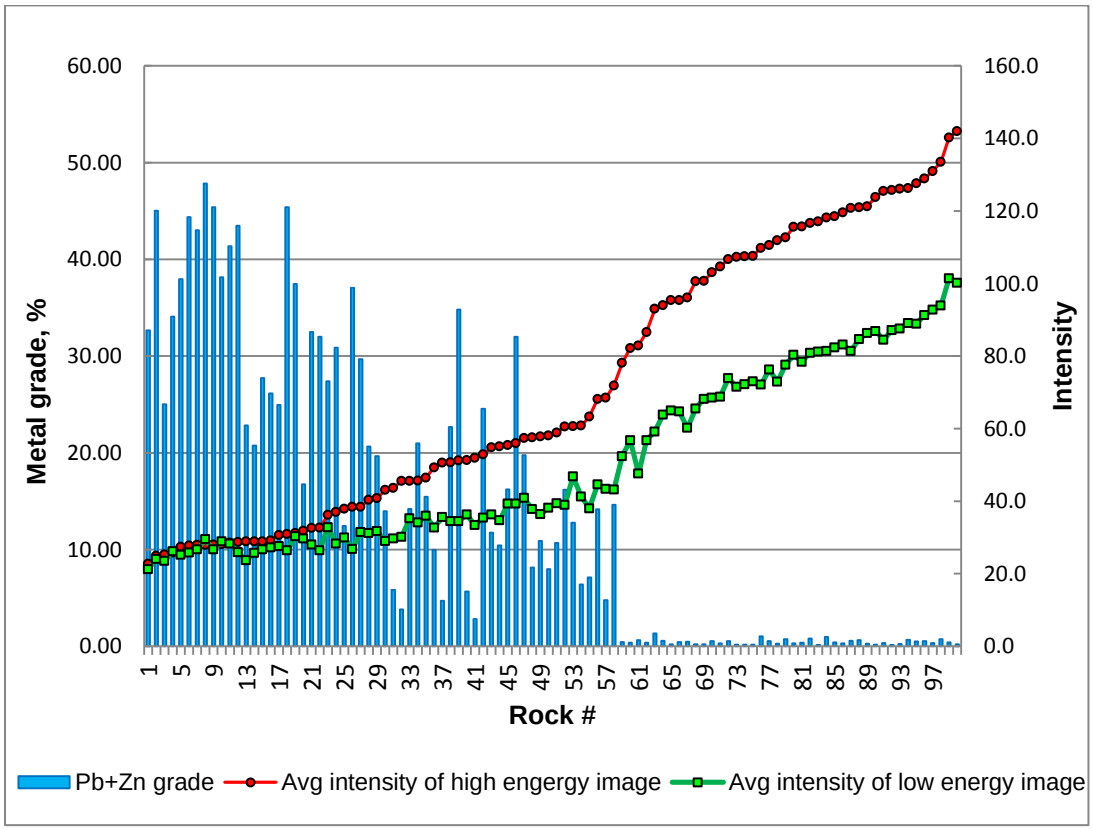


**Figure 3-13 XRT Segregation Sortability Curve of -37.5+26.5 mm Lead-Zinc Ore Based on Average Brightness Values of High/Low Energy Images**

***Sorting results***

Individual rocks with an average brightness value of high/low energy images higher than the separation value will be considered as waste. The sorting results of the 100 rocks based on different separation average brightness values of the high energy and low energy images are shown in Table 3-5 and Table 3-6.

**Table 3-5 XRT Sorting Results of -37.5+26.5 mm Lead-Zinc Ore Based on Average Brightness Value of the High Energy X-Ray Transmission Image**

| Separation at the Avg. Brightness of High Energy Image | Conc. (%) | Mass Rejected (%) | Metal Recovery (%) | | Conc. Grade (%) | | Waste Grade (%) | |
|---|---|---|---|---|---|---|---|---|
| | | | Pb | Zn | Pb | Zn | Pb | Zn |
| **130** | 97.2 | 2.8 | 100.0 | 99.9 | 6.38 | 8.97 | 0.08 | 0.37 |
| **110** | 81.0 | 19.0 | 99.6 | 99.3 | 7.63 | 10.70 | 0.13 | 0.33 |
| **90** | 67.9 | 32.1 | 99.3 | 98.8 | 9.07 | 12.71 | 0.13 | 0.32 |
| **80** | 65.0 | 35.0 | 99.2 | 98.8 | 9.46 | 13.25 | 0.14 | 0.31 |
| **70** | 63.3 | 36.7 | 99.1 | 97.6 | 9.71 | 13.46 | 0.15 | 0.56 |
| **65** | **61.9** | **38.1** | **99.0** | **96.1** | **9.92** | **13.56** | **0.17** | **0.88** |
| **60** | 58.3 | 41.7 | 96.7 | 93.5 | 10.29 | 14.01 | 0.49 | 1.36 |
| **50** | 44.9 | 55.1 | 93.4 | 72.9 | 12.91 | 14.18 | 0.74 | 4.29 |
| **40** | 33.0 | 67.0 | 87.9 | 60.7 | 16.50 | 16.04 | 1.12 | 5.12 |
| **30** | 20.4 | 79.6 | 61.4 | 36.9 | 18.67 | 15.80 | 3.00 | 6.92 |
| **Calculated Head Grade:** 6.20% Pb and 8.73% Zn | | | | | | | | |

As shown in Table 3-5, above 96% of Pb and Zn could be recovered in 62% mass of the feed after XRT sorting based on the average brightness value of the high energy image. The sorting product had calculated Pb and Zn grades of 9.92% and 13.56% (6.20% and 8.73% respectively in the feed) when sorting at an average brightness value of 65 for the high energy X-ray transmission image.

**Table 3-6 XRT Sorting Results of -37.5+26.5 mm Lead-Zinc Ore Based on Average Brightness Value of the Low Energy X-Ray Transmission Image**

| Separation at the Avg. Brightness of Low Energy Image | Conc. (%) | Mass Rejected (%) | Metal Recovery (%) | | Conc. Grade (%) | | Waste Grade (%) | |
|---|---|---|---|---|---|---|---|---|
| | | | Pb | Zn | Pb | Zn | Pb | Zn |
| **90** | 96.4 | 3.6 | 99.9 | 99.8 | 6.43 | 9.04 | 0.10 | 0.37 |
| **80** | 85.1 | 14.9 | 99.7 | 99.4 | 7.26 | 10.20 | 0.12 | 0.32 |
| **70** | 76.5 | 23.5 | 99.5 | 99.1 | 8.07 | 11.32 | 0.12 | 0.33 |
| **65** | 72.3 | 27.7 | 99.5 | 99.0 | 8.53 | 11.94 | 0.12 | 0.32 |
| **60** | 68.6 | 31.4 | 99.4 | 98.9 | 8.98 | 12.57 | 0.12 | 0.31 |
| **50** | 64.5 | 35.5 | 99.2 | 98.7 | 9.54 | 13.35 | 0.13 | 0.29 |
| **45** | **63.1** | **36.9** | **98.1** | **98.2** | **9.64** | **13.57** | **0.31** | **0.43** |
| **40** | 59.4 | 40.6 | 97.8 | 93.6 | 10.20 | 13.74 | 0.34 | 1.38 |
| **35** | 46.3 | 53.7 | 92.9 | 77.1 | 12.44 | 14.53 | 0.81 | 4.32 |
| **30** | 33.0 | 67.0 | 79.2 | 59.0 | 14.86 | 15.60 | 1.93 | 6.37 |
| **Calculated Head Grade:** 6.20% Pb and 8.73% Zn | | | | | | | | |

As shown in Table 3-6, above 98% of Pb and Zn could be recovered in 63% mass of the feed after XRT sorting based on the average brightness value of the low energy image. The sorting product had calculated Pb and Zn grades of 9.64% and 13.57% (6.20% and 8.73% respectively in the feed) when sorting at an average brightness value of 45 for the low energy X-ray transmission image.

Based on these findings, it can be concluded that sorting based on the average brightness value of the high/low energy image of this lead-zinc ore sample with a narrow size range demonstrated great amenability. Above 35% mass could be rejected as waste while upgrading the feed based on the discrimination of average brightness of the XRT image. The results also indicated that single energy X-ray transmission image analysis was also adequate for segregation of this lead-zinc ore sample in this size range.

#### *3.3.3.2 Image analysis by PACT software*

#### *Sorting potential based on Ore Index*

The original dual-energy XRT images were also analyzed using CommoDas Ultrasort PACT software in order to demonstrate the technical amenability of DE-XRT Sorting of this lead-zinc ore by simulating the real separation process of pilot-scale sorter. Ore

Indices for each rock were calculated using the PACT software by investigating correlations between the weighted Pb+Zn grades and the shape of the transmission curve for the 100 rocks. The algorithm of the Ore Index is inaccessible to the author. The calculated ore indices are shown in Appendix B.

The sortability curve base on Ore Indices is illustrated in Figure 3-14. Figure 3-14 indicates that sorting based on Ore Indices will successfully upgrade this lead-zinc ore by rejecting the low grade barren waste rocks.

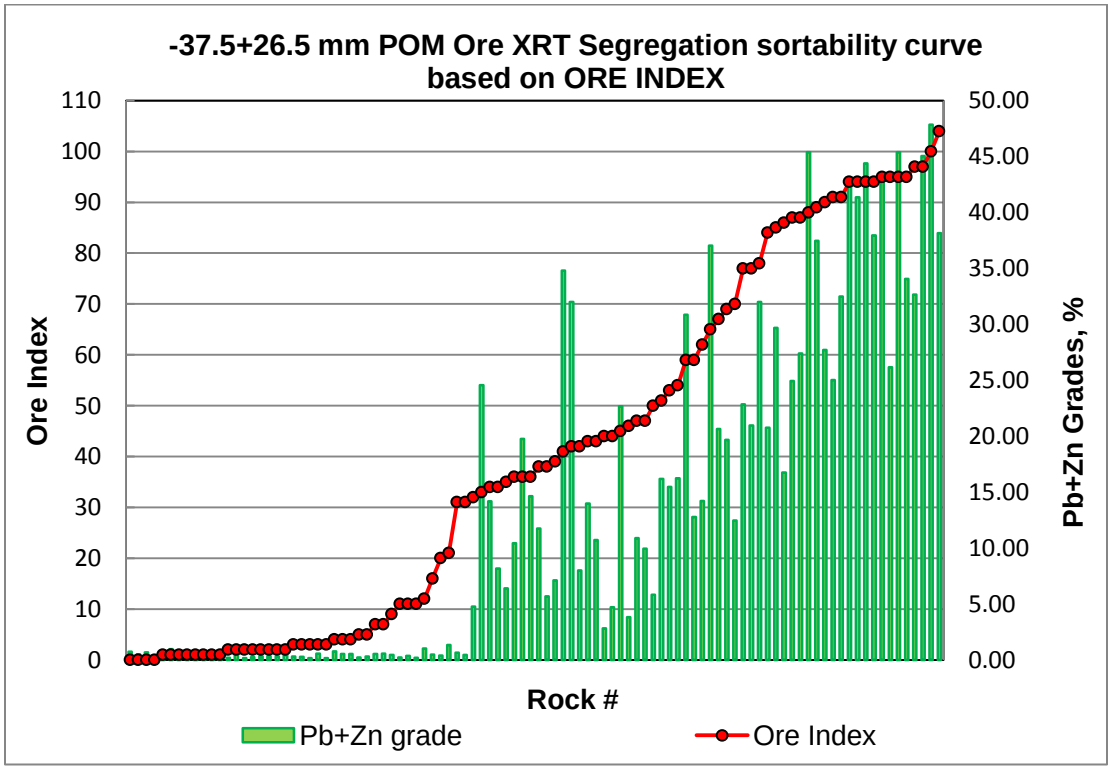


**Figure 3-14 XRT Segregation Sortability Curve of -37.5+26.5 mm Lead-Zinc Ore Based on Ore Indices**

***Sorting results***

Individual rocks with an Ore Index smaller than the separation Ore Index will be considered as waste and rejected. Sorting results based on different separation Ore Indices were calculated and are shown in Table 3-7. Results shown in Table 3-7 confirm the technical amenability of XRT sorting of this lead-zinc ore sample. Above 95% Pb and Zn could be recovered in 62% mass of the feed. The product grades of Pb and Zn were calculated to be 9.86% and 13.39% respectively.

**Table 3-7 XRT Sorting Results of -37.5+26.5 mm Lead-Zinc Ore Based on Ore Indices**

| Separation Ore Index at | Conc. (%) | Mass Rejected (%) | Conc. Grade (%) | | Metal Recovery (%) | | Waste Grade (%) | |
|---|---|---|---|---|---|---|---|---|
| | | | Pb | Zn | Pb | Zn | Pb | Zn |
| 5 | 74.9 | 25.1 | 8.24 | 11.56 | 99.5 | 99.2 | 0.12 | 0.30 |
| 10 | 72.2 | 27.8 | 8.54 | 11.98 | 99.5 | 99.0 | 0.12 | 0.30 |
| 15 | 68.4 | 31.6 | 9.01 | 12.62 | 99.4 | 98.9 | 0.12 | 0.31 |
| 20 | 66.3 | 33.7 | 9.29 | 13.00 | 99.3 | 98.8 | 0.12 | 0.30 |
| 30 | 65.6 | 34.4 | 9.39 | 13.15 | 99.3 | 98.8 | 0.13 | 0.31 |
| **33** | **62.3** | **37.7** | **9.86** | **13.39** | **99.1** | **95.6** | **0.14** | **1.02** |
| 35 | 59.7 | 40.3 | 9.35 | 12.38 | 98.9 | 93.0 | 0.18 | 1.51 |
| 40 | 54.5 | 45.5 | 11.17 | 13.92 | 98.1 | 86.9 | 0.25 | 2.51 |
| 50 | 40.9 | 59.1 | 14.44 | 15.16 | 95.2 | 70.9 | 0.51 | 4.29 |
| 60 | 36.0 | 64.0 | 15.69 | 15.45 | 91.1 | 63.7 | 0.86 | 4.95 |
| **Calculated Head Grade**: 6.20% Pb and 8.73% Zn | | | | | | | | |

***3.3.3.3 Comparison of sorting results by two image analyzing methods***

The optimum sorting results based on different sorting criteria are summarized in Table 3-8. The optimum sorting results were achieved for each sorting criterion when as much waste as mass could be rejected while achieving 95% metal recovery. The Grade-Recovery curves for each sorting criterion are shown in Figure 3-15.

**Table 3-8 XRT Sorting Results Summary of Different Sorting Criteria**

| Separation Criteria | Conc. (%) | Mass Rejected (%) | Conc. Grade (%) | | Metal Recovery (%) | | Waste Grade (%) | |
|---|---|---|---|---|---|---|---|---|
| | | | Pb | Zn | Pb | Zn | Pb | Zn |
| Ore Index at 33 | 62.3 | 37.7 | 9.86 | 13.39 | 99.1 | 95.6 | 0.14 | 1.02 |
| Avg. Brightness of High Energy Image at 65 | 61.9 | 38.1 | 9.92 | 13.56 | 99.0 | 96.1 | 0.17 | 0.88 |
| Avg. Brightness of Low Energy Image at 45 | 63.1 | 36.9 | 9.64 | 13.57 | 98.2 | 98.2 | 0.31 | 0.43 |
| **Calculated Head Grade**: 6.20% Pb and 8.73% Zn | | | | | | | | |

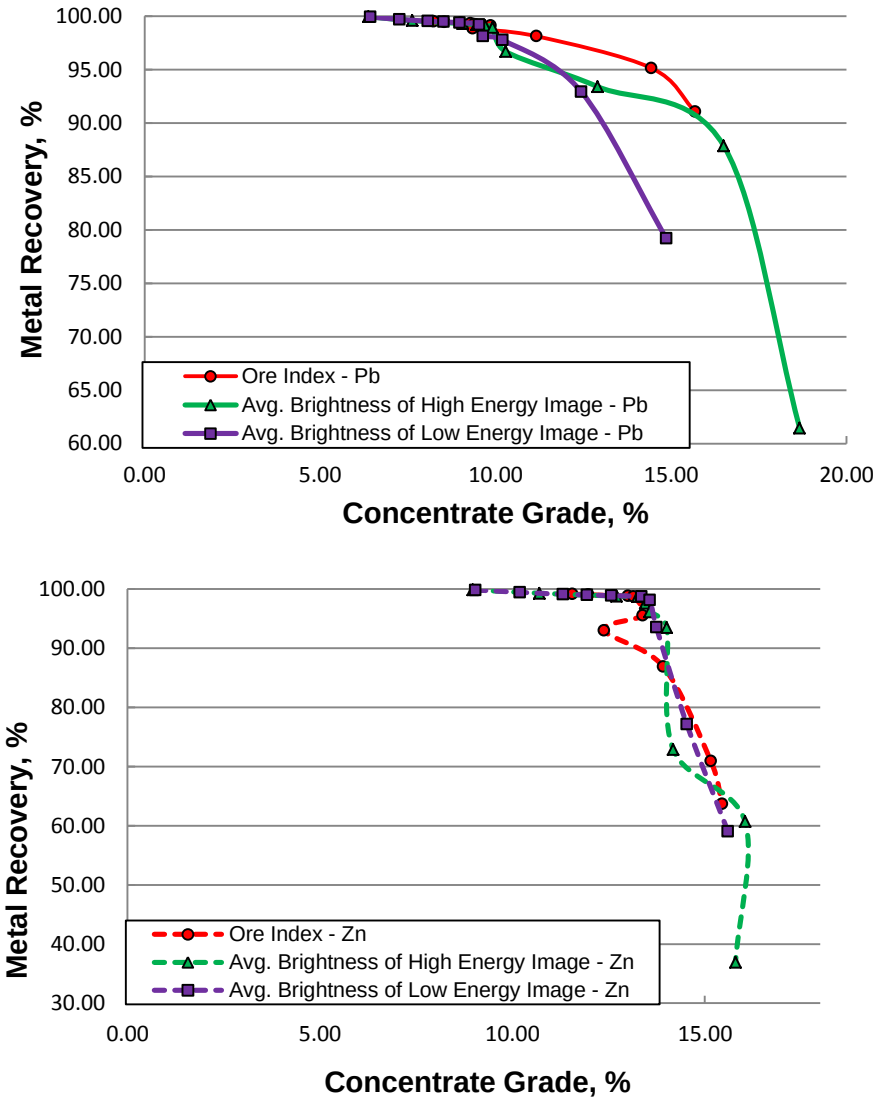


**Figure 3-15 Grade-Recovery Curves of XRT Sorting Based on Different Sorting Criteria**

From the results listed in Table 3-8, it can be concluded that both single and dual energy X-ray transmission imaging technique could be used for sorting of this lead-zinc sample sized -37.5+26.5 mm, due to the negligible effect of thickness. In addition, the satisfactory DE-XRT Sorting results based on different Ore Indices also demonstrate the technical amenability of DE-XRT Sorting of this lead-zinc ore sample using a pilot-scale X-ray sorter.

### 3.4 Optical Sorting Test

#### 3.4.1 Ore Characterization

Ore samples for this optical sorting test are from Pend Oreille Lead Zinc mine. The primary minerals in this ore are sphalerite and galena. Host rock is mainly light-gray bedded dolomite. Other minerals found in this ore include pyrite, cerussite, calcite and quartz. Mineral composition of this ore sample was analyzed by quantitative X-ray Diffraction (XRD). The results of XRD analysis are shown in Table 3-9.

**Table 3-9 Results of Quantitative Phase Analysis of Head Sample by XRD (Wt.%)**

| Mineral | Ideal Formula | Distribution |
|---|---|---|
| Pyrite | $FeS_2$ | 38.5 |
| Sphalerite | (Zn,Fe)S | 10.2 |
| Galena | PbS | 4.6 |
| Cerussite | $PbCO_3$ | 0.1 |
| Dolomite-Ankerite | $CaMg(CO_3)_2$-<br>$Ca(Fe^{2+},Mg,Mn)(CO_3)_2$ | 42.6 |
| Calcite | $CaCO_3$ | 2.2 |
| Plagioclase ? | $NaAlSi_3O_8 – CaAlSi_2O_8$ | 0.8 |
| Quartz | $SiO_2$ | 0.9 |
| Muscovite ? | $KAl_2(AlSi_3O_{10})(OH)_2$ | |
| Total | | 100.0 |

It can be seen from the analysis results that only three sulfide minerals are present in this sample: pyrite, sphalerite and galena. Gangue mineral is mainly dolomite. The aim of this study is then to separate lead-zinc bearing sulfides from dolomitic waste based on the differences in color properties.

#### 3.4.2 Sample Preparation

A subsample of 100 rocks from -37.5+26.5 mm were marked, weighed, cleaned and dried for the color ore sorting test.

### 3.4.3 Equipment

#### *3.4.3.1 Hardware*

In this laboratory-scale color sorting amenability study, an optical bench-top image acquisition system at CommoDas's Surrey facility was used for imaging. This system is equipped with a RGB camera (Opteon USB 1024×768 resolution) mounted with 25mm lens. The camera is installed 50cm above the background surface. The area being imaged is 8.6×6.8 cm. The lighting system is composed of a rectangular arrangement of four standard fluorescent lamps (Philips F39T12/CW 29 Watt Alto). A white blanket is used to protect the imaging from ambient light. The system layout can be seen in Figure 3-16. This system can generate 1024x768 RGB images under different exposure times, e.g., 240 ms, 300 ms, 360 ms.

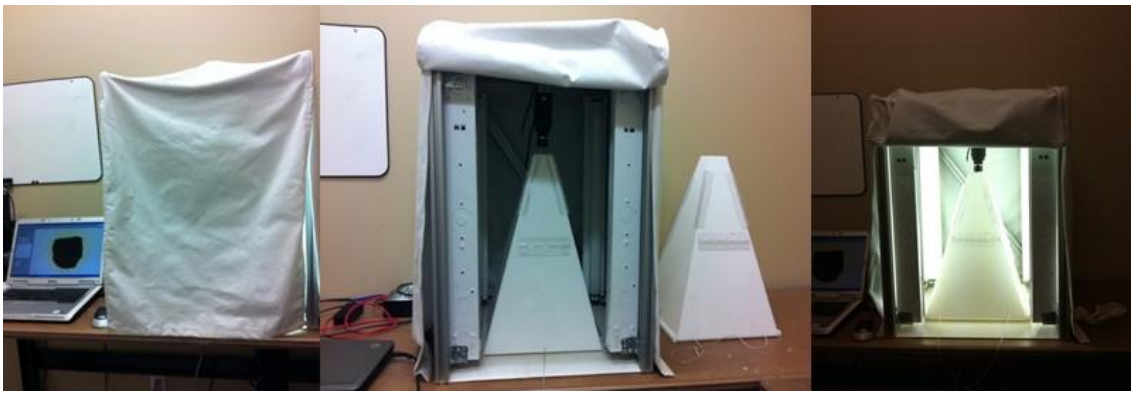

**Figure 3-16 Optical Bench-Top Image Acquisition System at CommoDas**

#### *3.4.3.2 Software*

***National Instrument (NI) Vision Mine Objective Detection and Analysis Software***

The NI Vision Mine Objective Detection and Analysis Software developed at UBC was used for image analysis so as to study the characteristic color data of barren rocks and mineralized ores and to determine the rejection criteria. This software features a function of pattern recognition using fuzzy logic match instead of exact match, which includes pattern learning and pattern matching (Bamber, 2008). This function is used in this study to generate optical features in terms of the RGB values of the object, either mineralized ore or waste rock, therefore providing the sorting threshold for this ore.

***GIMP***

GIMP is used in this study for image editing and data extraction using the first-order statistical histogram method. This software features a free selection function, which can be used for region of interest (ROI) selection, contouring rock shape in our case. It also provides functions such as generating a histogram of each color channel, threshold image, etc. It is a simple, handy and useful software we can get access to for our simplified image analysis.

### 3.4.4 Color Sorting Potential Study

From the subsample of 100 rocks, five light rocks with white and light gray or black green color, and two brass color heavy rocks were picked for a color sorting potential study. The rocks were wetted using water prior to imaging. Images of these rocks were obtained individually by the optical bench-top image acquisition system mentioned earlier. The exposure time was set to 300 ms, which was found most suitable for this sample to prevent overexposure. The rocks are shown in Figure 3-17.

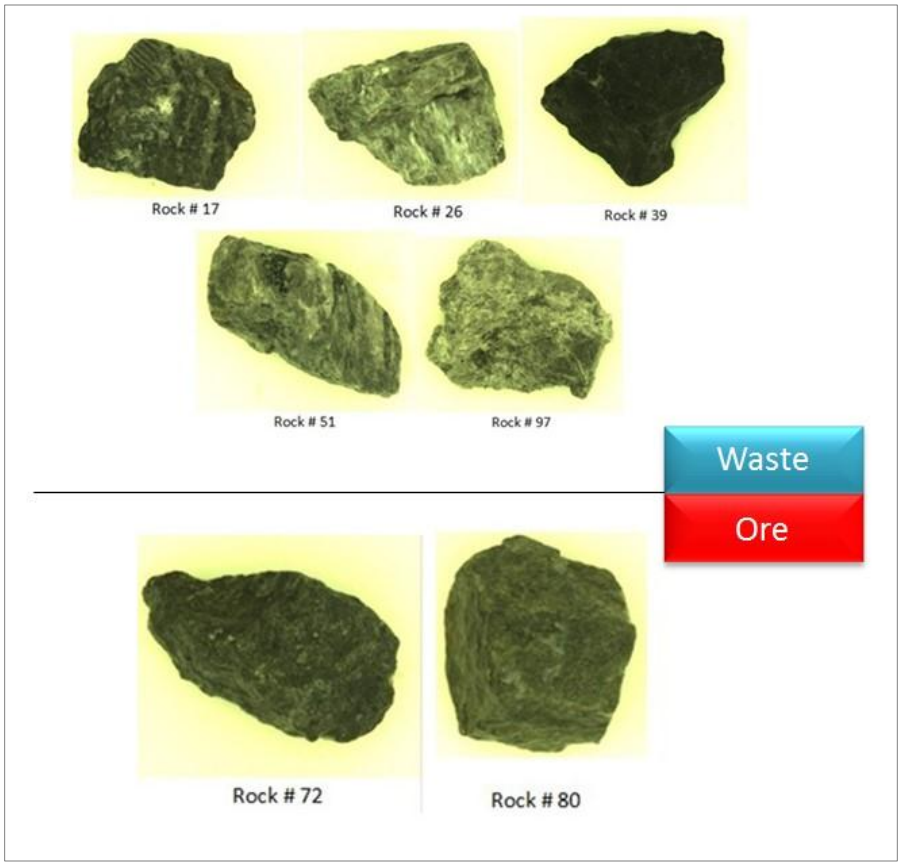


**Figure 3-17 Images of Identified Waste Rock and Mineralized Ore**

Most of the waste rock appears in white or light gray color (Rock #26, 51 and 97) while some waste rock with banded texture appears in bedded white and black (Rock #17). Another type of waste appears in very dark green (Rock #39). Mineralized ores can be divided into two groups based on color property. One type of ore appears in brass yellow with light gray veins (Rock #80). The other type appears in brass yellow with spotted shiny lead gray color (Rock #72).

The rocks were then crushed and pulverized for XRF readings. Previous study of XRF sorting showed that calibrated XRF powder reading, which is calculated using the Assay vs. XRF powder reading correlation function, had enough confidence to predict the chemical composition of the rock. XRF powder analysis of the seven rocks is shown in Table 3-10.

**Table 3-10 XRF Powder Analysis of Waste Rocks and Mineralized Ore**

| Category | Rock ID | Pb grade, % | Zn grade, % |
|---|---|---|---|
| Waste | 17 | 0.37 | 0.39 |
| | 26 | 0.13 | 0.17 |
| | 39 | 0.05 | 0.24 |
| | 51 | 0.19 | 0.33 |
| | 97 | 0.09 | 0.32 |
| Ore | 72 | 19.63 | 18.32 |
| | 80 | 0.10 | 24.47 |

It is evident from Table 3-10 that rocks with light gray and white or dark green color shown as waste rock in Figure 3-17 contain little lead and zinc. The rock with brass yellow color with spotted shiny lead grey contains a high grade of lead and zinc. The rock with brass yellow and light gray color contains a high grade of zinc but a low grade of lead. This indicates the potential of color sorting to remove the barren dolomitic waste rocks from mineralized ores and therefore produce an upgraded lead-zinc preconcentrate.

### 3.4.5 Image Capture

The images of the other 93 rocks were taken with the optical bench-top image acquisition system under wet conditions. The exposure time was 300ms. The rock was placed at the same position each time and was photographed individually. The schematic set-up of the camera is illustrated in Figure 3-18. A 1024×768 revolution RGB image was generated for each of the 100 rocks.

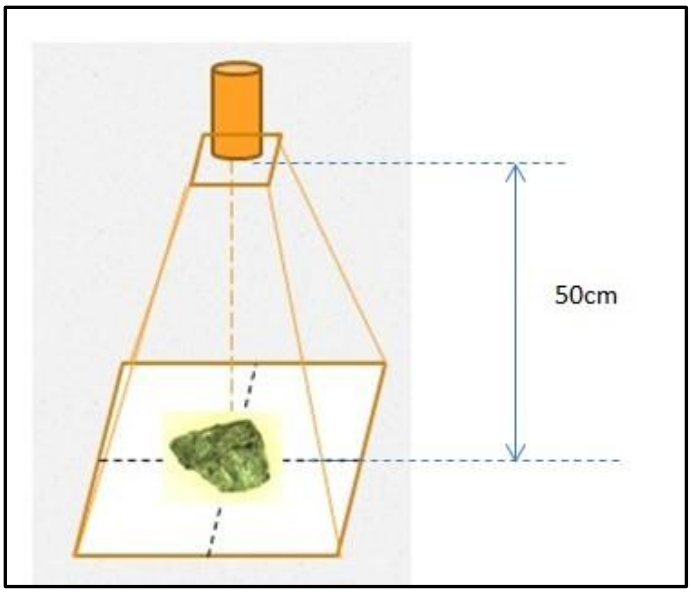


**Figure 3-18 Schematic Set-Up of the Camera**

### 3.4.6 Data Analysis

#### *3.4.6.1 Generation of characteristic color data for waste rock and mineralized ore*

The NI Vision Mine Object Detection and Analysis Software was used to generate characteristic color data in terms of red, green and blue for the waste rock and mineralized ore selected for the color sorting potential study shown in Figure 3-17. Open the image in this software and the red, green and blue value for each pixel can be read directly. The software also features a function of pattern matching with which we can generate the color properties of rock by finding matched patterns (with similar color properties) in the image. This software can only deal with 8-bit coded images with 640×480 pixels resolution therefore the images were resized from the original image size of 1024×768 pixel resolutions to 640×480 pixels resolution prior to analysis.

For the waste rock (Rock #26) image, a region of interest (ROI) was chosen as one pattern. Once the pattern is chosen, a 3D color spectrum of the ROI will be displayed and the color data for red, green and blue for each individual pixel within the interest area will be recorded. Figure 3-19 shows the red spectrum of the selected pattern. The red value of each pixel is recorded in the table on the right side of the figure.

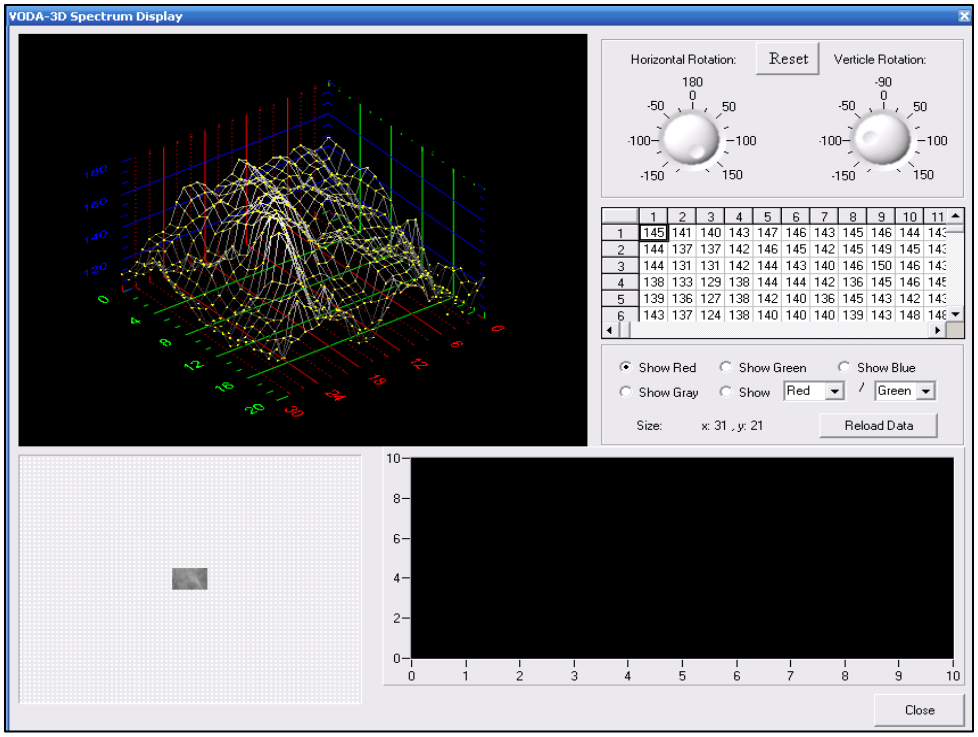


**Figure 3-19 Red Spectrum of Selected ROI Pattern for Rock #26-Waste**

For an 8-bit coded image, the value of red, green and blue varies from 0 to 255. In the above figure, the red value of the selected ROI varies from about 130 to 150. Once this pattern is selected, we can use the pattern-match function of the software to find similar color patterns within the same rock image. A maximum number of 20 matches could be done at one time. However, only 10 color patterns could be recorded. Figure 3-20 shows the matched pattern within the image of Rock #26. The average red, green and blue values of the ten patterns are listed in Table 3-11. The average red, green and blue values for these ten patterns can be used as characteristic color features for this rock.

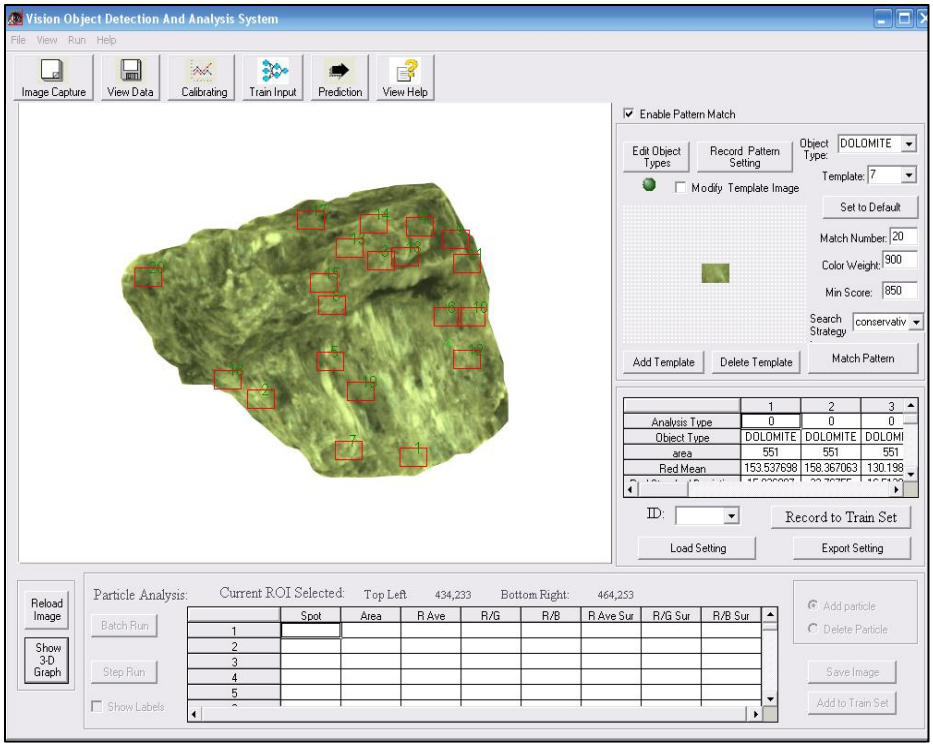


**Figure 3-20 Patterns Matching of Rock #26**

**Table 3-11 Average Red, Green and Blue Value for the 10 Matched Patterns for Rock #26**

| Rock #26 | | 1 | 2 | 3 | 4 | 5 | 6 | 7 | 8 | 9 | 10 | Average |
|---|---|---|---|---|---|---|---|---|---|---|---|---|
| Area | | 551 | 551 | 551 | 551 | 551 | 551 | 551 | 551 | 551 | 551 | |
| **Red** | Mean | 154 | 158 | 130 | 111 | 128 | 118 | 158 | 137 | 98 | 112 | **130** |
| | Standard Deviation | 16 | 23 | 17 | 15 | 23 | 14 | 20 | 14 | 24 | 16 | |
| **Green** | Mean | 170 | 175 | 144 | 123 | 141 | 132 | 175 | 152 | 108 | 125 | **144** |
| | Standard Deviation | 18 | 25 | 18 | 16 | 26 | 16 | 22 | 15 | 24 | 18 | |
| **Blue** | Mean | 95 | 97 | 79 | 67 | 78 | 73 | 98 | 84 | 59 | 67 | **80** |
| | Standard Deviation | 12 | 16 | 12 | 10 | 17 | 10 | 14 | 9 | 24 | 10 | |

Using the same method, two patterns each for rock #51 and rock #97 were selected and matched. All the rocks appearing in light gray and white color are assumed to be waste. One pattern was selected for the dark green rock #39 in order to obtain the color features for this type of waste. However no pattern matching was done for this rock since only five rocks could be found of this type out of one hundred. The selected pattern

could adequately demonstrate the color features of this type of waste. The average characteristic color features in terms of red, green and blue values for these five pattern sets are used for describing and identifying waste rock. Two patterns were selected and matched for rock #72 and one for rock #80, which are assumed to be mineralized ore. The average characteristic color features in terms of red, green and blue values for these three pattern sets are used to describe and identify mineralized ore. The average characteristic red, green and blue value for each pattern set for the rocks are shown in full in Appendix C. Table 3-12 summarizes these values for each of eight pattern sets for the rocks.

**Table 3-12 Summary of Red, Green and Blue Value for Matched Patterns**

| | | | | | | | | | | |
|---|---|---|---|---|---|---|---|---|---|---|
| Waste | Index | 1 | 2 | 3 | 4 | 5 | Ave | Max | Min | Rock 39 |
| | Red | 133 | 149 | 124 | 131 | 130 | 133 | 149 | 124 | 40 |
| | Green | 145 | 163 | 137 | 143 | 144 | 146 | 163 | 137 | 42 |
| | Blue | 79 | 90 | 77 | 79 | 80 | 81 | 90 | 77 | 25 |
| Ore | Index | 1 | 2 | 3 | | | Ave | Max | Min | |
| | Red | 88 | 70 | 69 | | | 76 | 88 | 69 | |
| | Green | 97 | 78 | 77 | | | 84 | 97 | 77 | |
| | Blue | 49 | 41 | 41 | | | 44 | 49 | 41 | |

It is clearly shown in the above table that the patterns of most waste rocks have an average red value of 133 while those of mineralized ore average 76. Differences exist as well for green and blue color. One type of gangue mineral that appears in dark green has a red value of 40. It could also be discriminated from the ores with an average red of 76. As a result, the featured color values could be used to sort this ore. In this laboratory-scale research, the potential of color sorting of this lead-zinc ore was investigated based on the differences of red color only.

### *3.4.6.2 Rejecting criteria determination*

All the 100 images were processed in four stages using GIMP software:

- contouring the value image;
- filtering the image by threshold function;
- extracting the average red value from histogram after threshold; and
- determining the rejection criterion.

***Contouring the value image***

There are three methods to select the value image for analysis: bounding box, centroid and contouring (Kowalczyk & Bartram, 2008). They are shown in Figure 3-21.

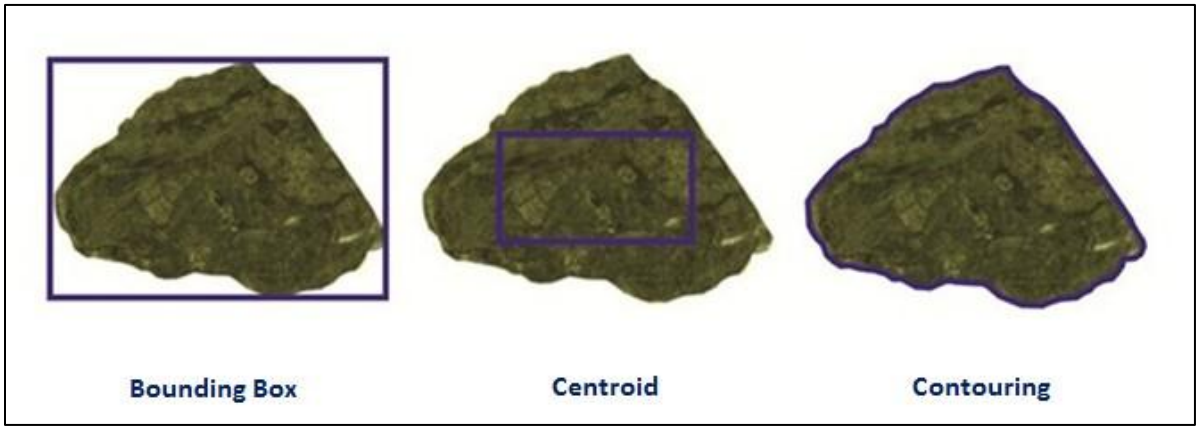


**Figure 3-21 Value Image Selection Methods**

In this study, the contouring method was employed. The value image for each rock was contoured manually using free select tool in the GIMP software.

***Filtering the image by threshold function***

According to the characteristic color data study for the waste rock and mineralized ore discussed in the previous section, it is clear that the waste rock image has an average red value of 133 while the mineralized ore image has an average red value of 76. All the rocks were visually similar as a whole, but it is easy to identify light gray or white gangue minerals in the rock. The percentage of “waste pattern” present in the rock image can be used as criterion for sorting the waste rock from mineralized ore. It is also observed that most of the dolomitic gangue minerals in the image have a red value larger than 133. Therefore it is assumed that any pixel that has a red value between 133 and 255

belongs to the waste pattern. The more the pixels with red value between 133 and 255, the more “waste patterns” present in the rock image, and that rock is more related to waste.

Using the threshold function in GIMP, each value image was color coded with a threshold red value of 133 to 255. Individual pixels with a red value from 133 to 255 will appear in red in the image after threshold and will be given a red value of 1. Any pixel which has a red value between 0 and 132 will appear in green in the image after threshold and will be given a red value of 0. Figure 3-22 shows a sample of threshold images. It is shown clearly in the figure that rocks have great differences in red color after threshold.

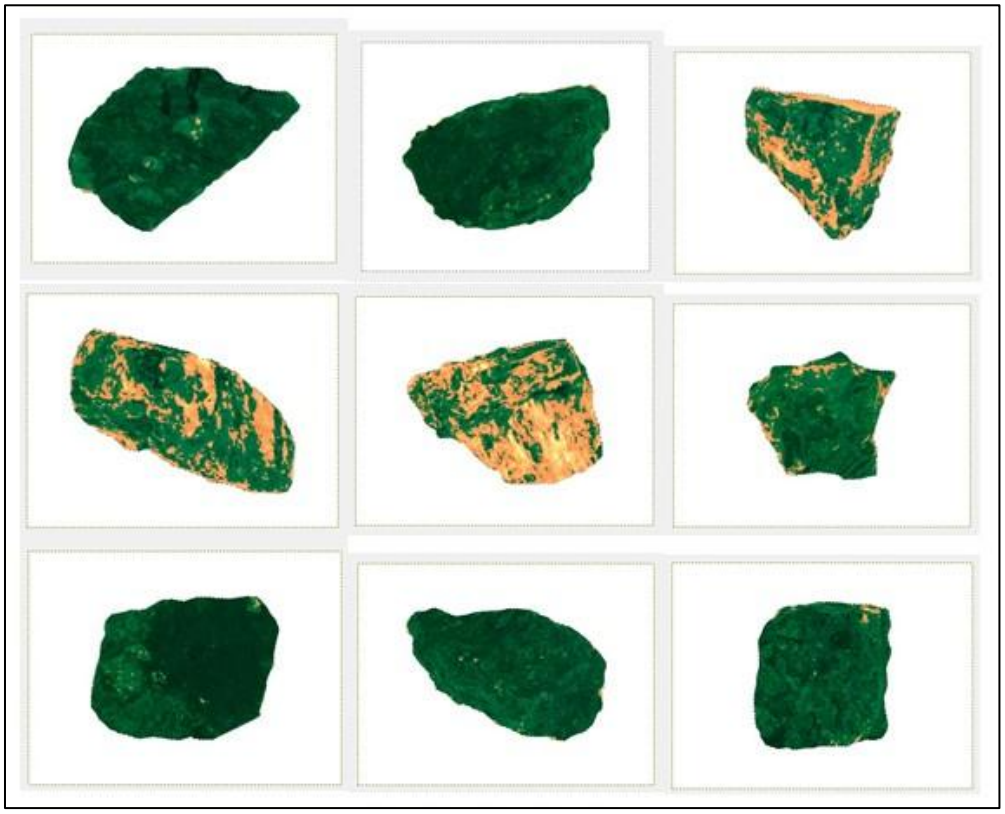

**Figure 3-22 Sample of Threshold Images for Several Rocks**

***Extraction of average red value from histogram after threshold***

The percentage of red area shown in the threshold image represents the correlation of this rock to waste; the more red, the greater the correlation. The percentage of the red area can be expressed as the average red value of the value image after threshold, since pixels were given a red value of 1(shown in red) or 0 (shown in green) in the image

after threshold. More specifically, the larger the average red value of the threshold image, the more percentage of red area in the threshold image, and the more the rock is related to waste. The average red value of the value image after threshold was obtained using the first-order of statistical method using histogram parameters. GIMP features a function of histogram showing the spectrum of red value, the mean, standard deviation, medium of red value, and pixels counted. Figure 3-23 and Figure 3-24 show the histograms of red value for the value images before and after threshold respectively.

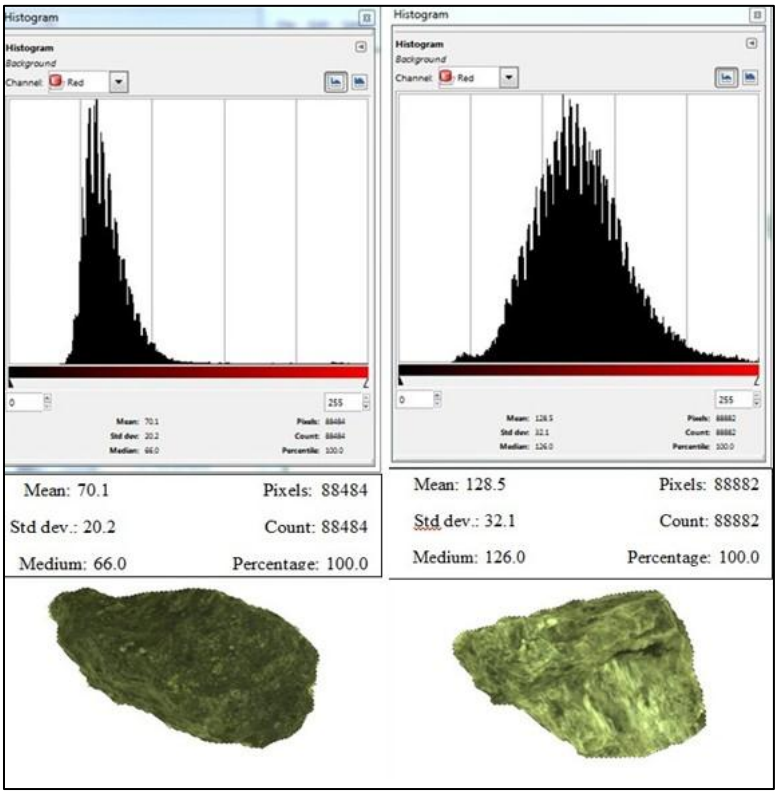


**Figure 3-23 Histograms of Red Value for the Value Image Before Threshold**
Note: left: rock #72, right: rock #26

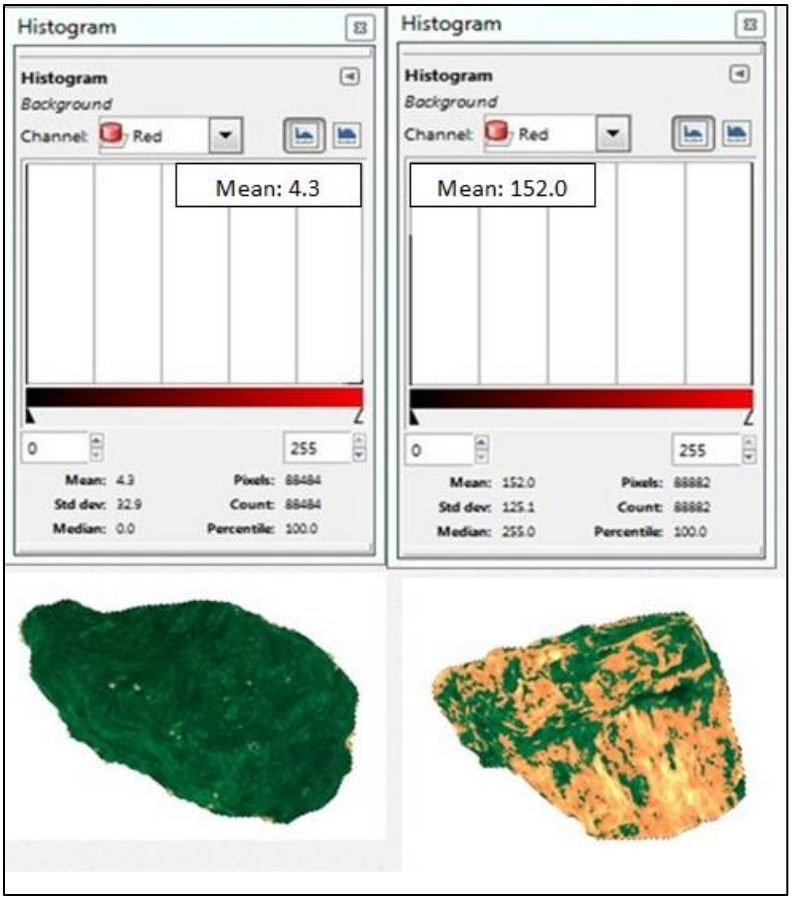


**Figure 3-24 Histograms of Red Value for the Value Image after Threshold**
Note: left: rock #72, right: rock #26

It is evident from Figure 3-23 that the average red values read from the histogram of the value image after threshold differ greatly between rocks. As result, the average red value of the value image after threshold is used as separation criterion.

***Determination of rejecting criteria***

Correlations between Pb+Zn grade and the average red value of the value image after threshold (133-255), Avg. $R_{133\text{-}255,}$ are shown in Figure 3-25. It is clearly shown in the figure that rocks with Avg. $R_{133\text{-}255}$ larger than 50 are totally waste rock. When the Avg. $R_{133\text{-}255}$ is smaller than 50, two types of error occurred only use the Avg. $R_{133\text{-}255}$ as criterion to separate barren rock from mineralized ore.

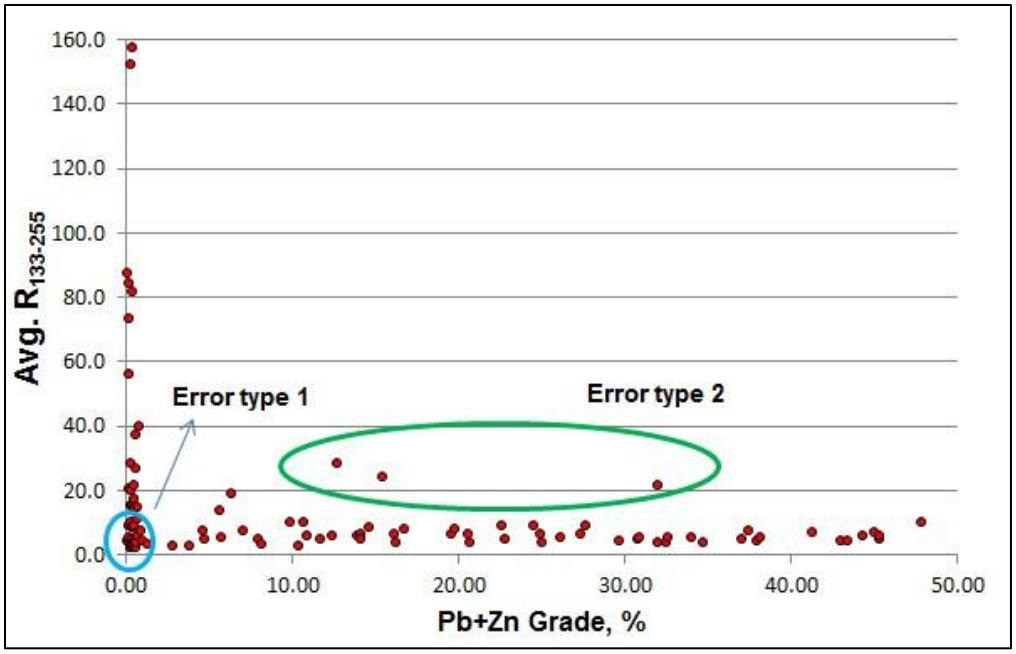


**Figure 3-25 Correlation between Pb+Zn Grade and Avg. $R_{133-255}$**

- error 1: some barren rocks have a smaller Avg. $R_{133-255}$ similar to that of mineralized ore.
- error 2: some mineralized ore rocks have a larger Avg. $R_{133-255}$ similar to that of barren rock.

The first type of error exists partly because there is another type of waste pattern present in the sample appearing in dark green color, which has a red value of approximately 40. Another reason for the first type of error is the existence of barren waste rocks with bedded texture appearing in bedded light grey and dark colors. The second type of error exists because some high zinc grade ore appears in brass yellow color with light grey veins (waste pattern). These light grey veins will contribute much to the Avg. $R_{133-255}$. The first type of error could be partly corrected by an additional step of separation using the average red value of the value image after threshold (0-40), Avg. $_{0-40}$. The second type of error could not be effectively corrected after several trials. Consequently, the rejection criteria were set as follows:

If Avg. $R_{133-255} > X$, then waste

If Avg. $R_{133-255} < X$, then second judgement

If Avg. $_{0-40} > Y$, then waste

If Avg. $_{0\text{-}40}$ < Y, then ore

where X and Y can be optimized based on the sorting results.

### 3.4.7 Sorting Results

Color sorting results based on different Avg. $R_{133\text{-}255}$ values of the rock image, using the rejection criteria described in the previous section, are shown in

Table 3-13. The X value varies while the Y value is set as 7.

**Table 3-13 Color Sorting Results Summary**

| Sorting Criteria | | Conc. % | Waste Rejection % | Metal Recovery, % | | Conc. Grade, % | | Waste Grade, % | |
|---|---|---|---|---|---|---|---|---|---|
| | | | | Pb | Zn | Pb | Zn | Pb | Zn |
| R133-30 | R40-7 | 84.4 | 15.6 | 99.6 | 99.5 | 7.44 | 10.29 | 0.14 | 0.29 |
| **R133-22** | **R40-7** | **81.2** | **18.8** | **98.5** | **97.0** | **7.64** | **10.43** | **0.50** | **0.50** |
| R133-21 | R40-7 | 79.6 | 20.4 | 98.4 | 93.9 | 7.79 | 10.30 | 0.48 | 2.60 |
| R133-15 | R40-7 | 75.8 | 24.2 | 98.3 | 93.2 | 8.17 | 10.74 | 0.43 | 2.45 |
| R133-11 | R40-7 | 70.7 | 29.3 | 98.1 | 92.6 | 8.73 | 11.43 | 0.41 | 2.20 |
| R133-8 | R40-7 | 58.6 | 41.4 | 89.1 | 77.1 | 9.57 | 11.47 | 1.66 | 4.84 |
| **Calculated Head Grade**: 6.20% Pb and 8.73% Zn | | | | | | | | | |

Based on the sorting results shown in Table 3-13, the optimum rejection criterion is as follows:

If Avg. $R_{133\text{-}255}$ > 22, then waste

If Avg. $R_{133\text{-}255}$ < 22, then second judgement

If Avg. $_{0\text{-}40}$ > 7, then waste

If Avg. $_{0\text{-}40}$ < 7, then ore

Using this rejection criterion, color sorting of this lead-zinc ore sample could successfully recover 98.5% lead and 97.0% zinc in 81% of the feed mass. Lead and zinc grades were upgraded to 7.64% and 10.43% respectively from 6.30% and 8.73% calculated in the feed. Figure 3-26 shows the Grade-Recovery curve for color sorting of -37.5+26.5 mm sample.

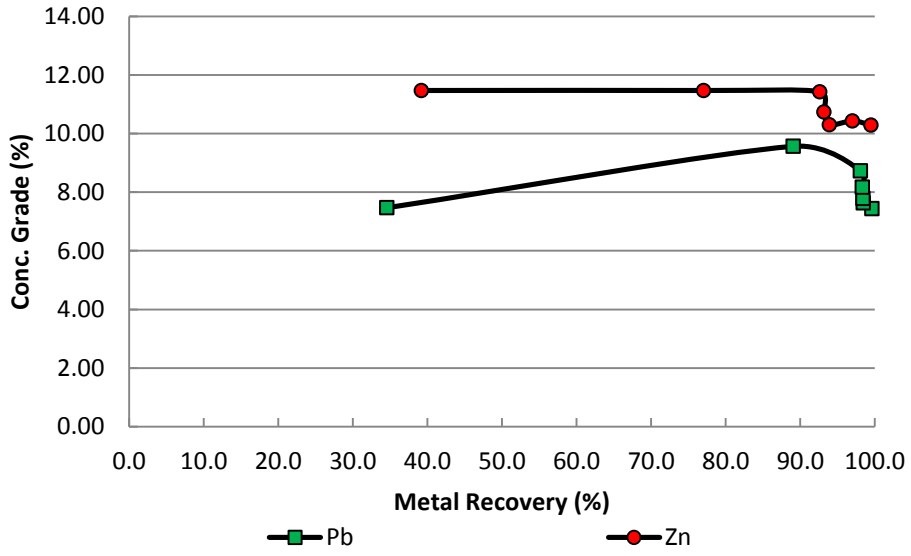


**Figure 3-26 Color Sorting Grade-Recovery Curve for -37.5+26.5 mm Sample**

### 3.4.8 Laboratory-Scale Color Ore Sorting Amenability Study Flowsheet Design

The major steps in this color ore sorting amenability study of an ore sample in the laboratory-scale were sample preparation, sorting potential determination, image capture, data analysis, and sorting result calculation according to the testwork done in this study. The flowsheet for this evaluation process can be seen in Figure 3-27. This flowsheet can be used as a guideline for color ore sorting studies of other ore types in laboratory-scale.

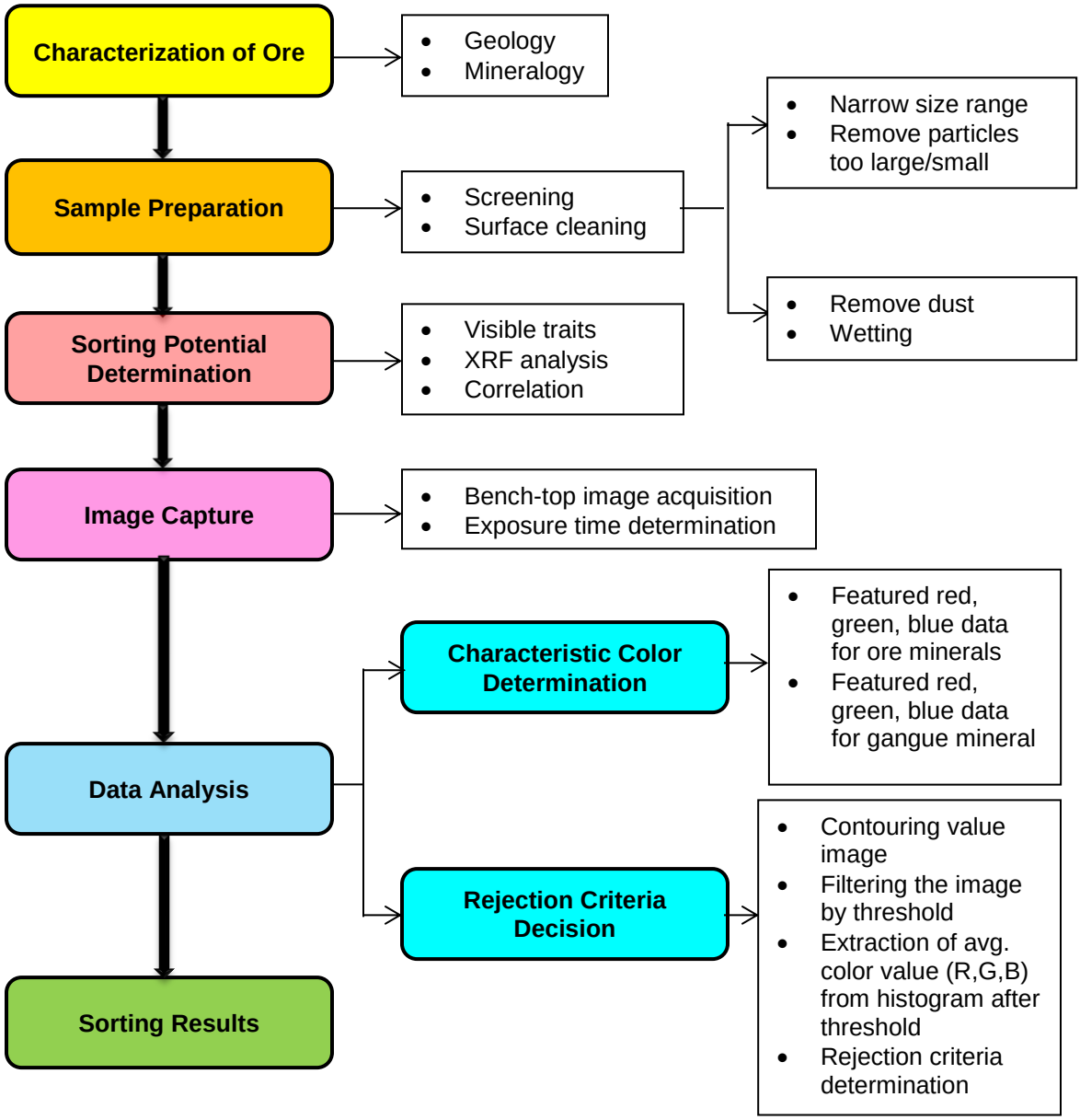


**Figure 3-27 Flowsheet for Color Ore Sorting Amenability Study in Laboratory-Scale**

### 3.5 Microwave-Infrared Sorting Test

#### 3.5.1 Experimental Procedures

##### *3.5.1.1 Equipment*

The microwave oven used in this test was a model BP-110 (2.45 GHz, 12.2 cm wavelength, 1000 w output microwave power) from Microwave Research & Applications, Inc., designed for laboratory use. All tests were conducted using its high energy level setting (maximum output 1000 w).

The infrared camera used in this test was a FLIR T400 Infrared Camera with a 320×240 IR resolution. It can generate an IR picture and a regular digital picture at the same time. The equipment used for this test is shown in Figure 3-28.

**Figure 3-28 BP-110 Lab Use Microwave Oven and FLIR T400 IR Camera**

##### *3.5.1.2 Testing procedures*

Fifty rocks, each sized from -53+37.5 mm, -37.5+26.5 mm, -26.5+19 mm and -19+13.2 mm, were prepared for the microwave/infrared (MW/IR) sorting test. Individual rock samples were marked from 1 to 50 for each size fraction.

***Individual testing***

A batch of fifty rocks from each of the four size fractions were weighed and exposed individually to microwave radiation for different periods of time to evaluate the effect of weight and exposure time on microwave heating. For the -53+37.5 mm size fraction, 10s, 20s and 30s of microwave heating were conducted. For the other three size fractions, rocks were exposed to microwave radiation for 5s, 10s and 15s respectively. One rock at a time was put on the same spot, as shown in Figure 3-29. This is necessary because the MW energy distribution in a MW oven is inhomogeneous. However, each spot shown

in the picture has the same heating effect of individual specimens according to previous studies (Van Weert, Kondos, & Gluck, 2009).

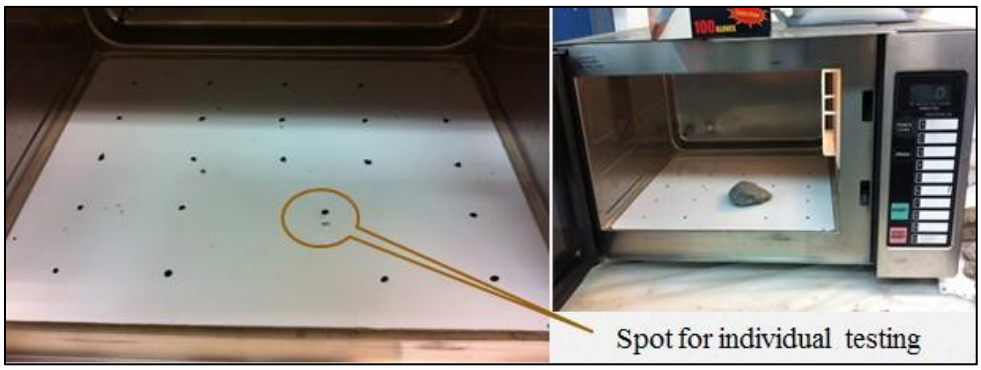


**Figure 3-29 Rock Position for Individual Testing**

An IR image was taken using the FLIR T400 IR camera for two sides of each rock right after microwave heating by the oven. One could argue that it takes time with the larger rocks for internal heat to diffuse to the surface and that the surface temperature may actually increase with time. Work at Process Research ORTECH has shown this not to occur with 50 mm rocks (Wang, 2012) and this variant was not pursued in this work. The average surface temperature of each rock was obtained by contouring the shape of the rock and averaging the temperatures of both sides using FLIR Quick Reporter 9.0. Figure 3-30 shows the IR (Thermographic) images of both sides of rock samples (one mineralized ore and one waste). XRF surface reading of each rock was done for Pb, Zn, Fe and S analysis. Calibrated XRF surface readings were used as assays for data analysis since assays and XRF surface reading have a strong correlation according to XRF sorting studies.

**Figure 3-30 IR (Thermographic) Images of Two Sides of Rocks from -19+13.2 mm Size Fraction After 10s Microwave Heating**
Note: the left appears to be mineralized ore and the right appears to be waste) Average surface temperature of both sides were calculated.

***Group testing***

Rock samples from each size fraction were grouped and exposed to microwave radiation for 10s in order to discover the microwave heating performance of different quantities of rock being heated at the same time.

Assume that individual rock has a cubic shape with the side being the particle size (13.2 mm, 19 mm, 26.5 mm and 37.5 mm) and each rock has the same density, which is the average density of the sample. As a result, the weight of each rock is proportional to the third power of the particle size. Therefore, the weight of a rock with a side of 37.5 mm approximately equals the weights of four, nine and thirty rocks with a side of 26.5 mm, 19 mm and 13.2 mm, respectively.

However, only a maximum of 25 rocks can be treated at the same time in the lab microwave oven due to its size. Consequently, after being exposed to microwave for 10s, the surface temperatures of separate groups of four, nine and twenty-five rocks from -37.5+26.5 mm, -26.5+19 mm and -19+13.2 mm size fraction were measured.

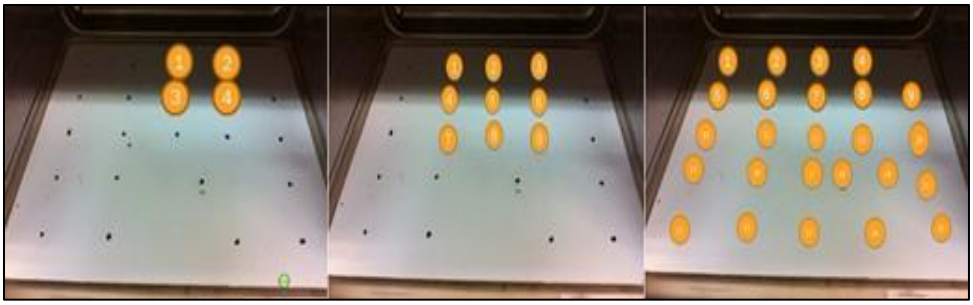

**Figure 3-31 Rock Positions for Group Testing**

Also, the surface temperatures of a group of nine rocks from each of the four size fractions were measured after 10 seconds microwave heating so that a comparison of heating performance of a group of nine rocks from different size fractions could be made.

Rock positioning in the oven for grouped sample tests is shown in Figure 3-31. A glass plate, which is used in the domestic microwave oven, was put inside the Lab BP-110 microwave oven for conveniently moving the rocks for IR imaging. The rocks were then placed on the glass plate according to the positions illustrated in the above figure. After being heated for 10s, the plate was quickly and carefully taken out and photographed using the IR camera. The rocks were then turned around and an IR image was taken on the second side of the rocks. Figure 3-32 shows an example of the digital and IR images for the group test.

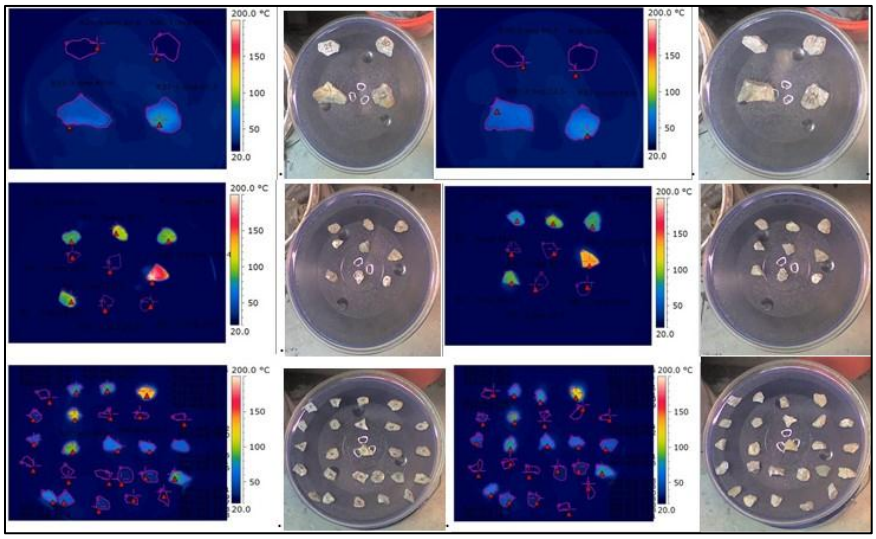

**Figure 3-32 IR (Thermographic) Images of Two Sides of Rocks Tested in Groups of 4, 9 and 25 after 10s Microwave Heating**
Note: -19+13.2 mm rocks were grouped in 9 and 25 while -26.5+19 mm rocks are tested 4 rocks at a time as shown in this figure.

### 3.5.2 Results and Discussion

#### *3.5.2.1 Factors influencing microwave heating of lead-zinc sulfide ore*

***Effect of heating time***

In order to illustrate the effect of heating time on microwave heating of lead-zinc sulfide ore, 50 rock samples from each of the four size fractions were exposed to microwave radiation for different periods of time. It takes approximately five seconds for this type of microwave oven to come to full power. Hence, a minimum of five seconds heating was used in this study. Figure 3-32 shows the average surface temperatures of the fifty rocks each from -19+13.2 mm, -26.5+19 mm and -37.5+26.5 mm size fractions after being heated by microwave for 5s, 10s and 15s. The rocks were numbered in ascending order of temperature after exposure. It is interesting to note that the 10 seconds microwave exposure did yield a more irregular curve. Future work should explore the repeatability of the readings as a function of rock position on the plate, to gain information for scale-up.

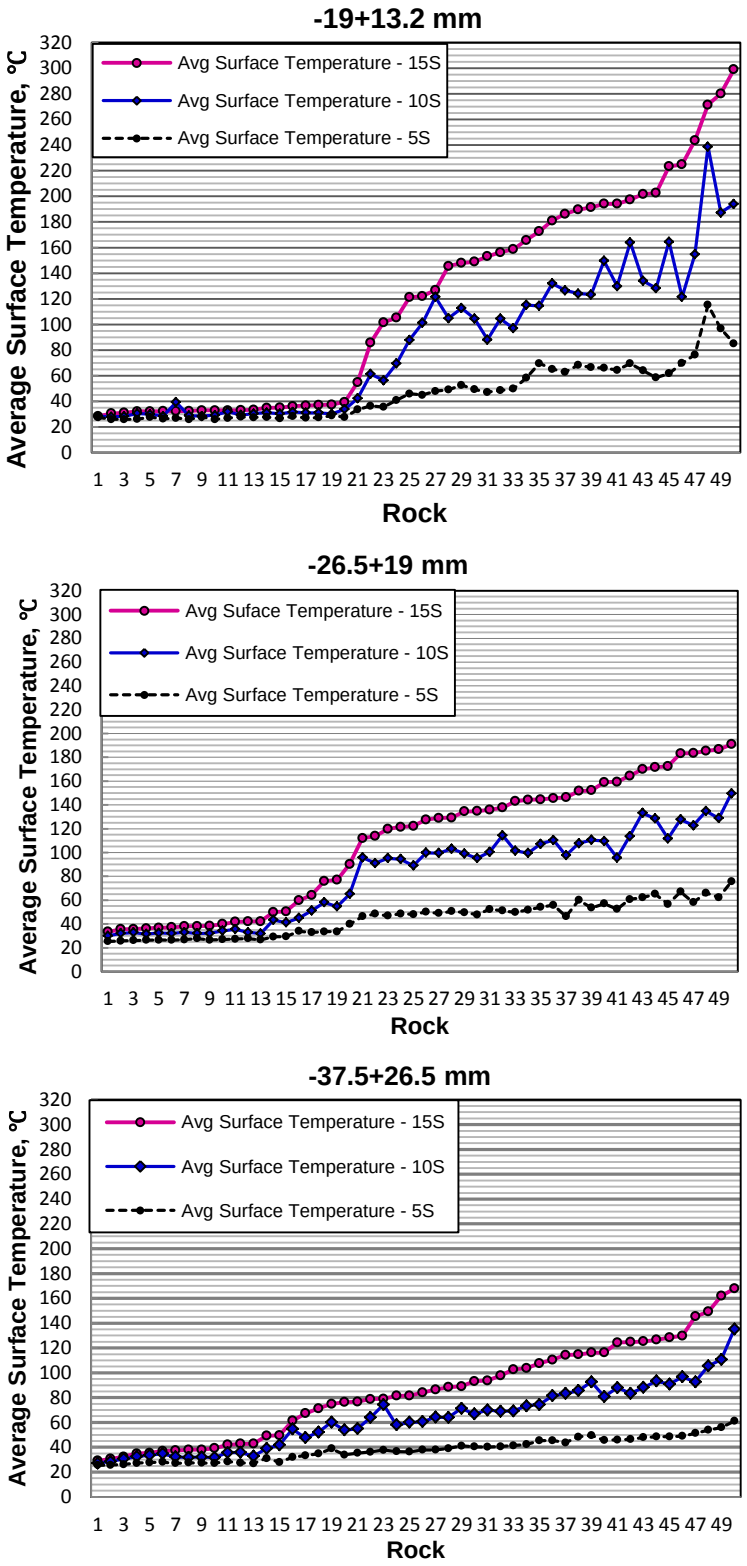


**Figure 3-33 Average Surface Temperatures of Rocks after 5s, 10s, and 15s Microwave Heating from -19+13.2 mm, -26.5+19 mm and -37.5+26.5 mm Size Fractions**

It is shown clearly in Figure 3-33 that microwave heating of this lead-zinc ore is a function of heating time; the longer the heating time, the higher the increase in temperature. Also evident is that the smaller the particle size, the greater the influence of heating time on microwave heating of this material, based on the fact that microwave power was in excess of that needed (details are shown in Appendix D).

***Effect of quantity of rocks heated at the same time***

The effect of quantity of rocks heated at the same time on microwave heating was investigated by exposing one, four, nine and twenty-five rocks at a time to microwave radiation in the lab microwave oven. Figure 3-34 shows the average surface temperatures of rocks after being heated for 10s individual and group heating. The rocks were numbered in ascending order of temperature after individually exposure to 10 seconds microwaving.

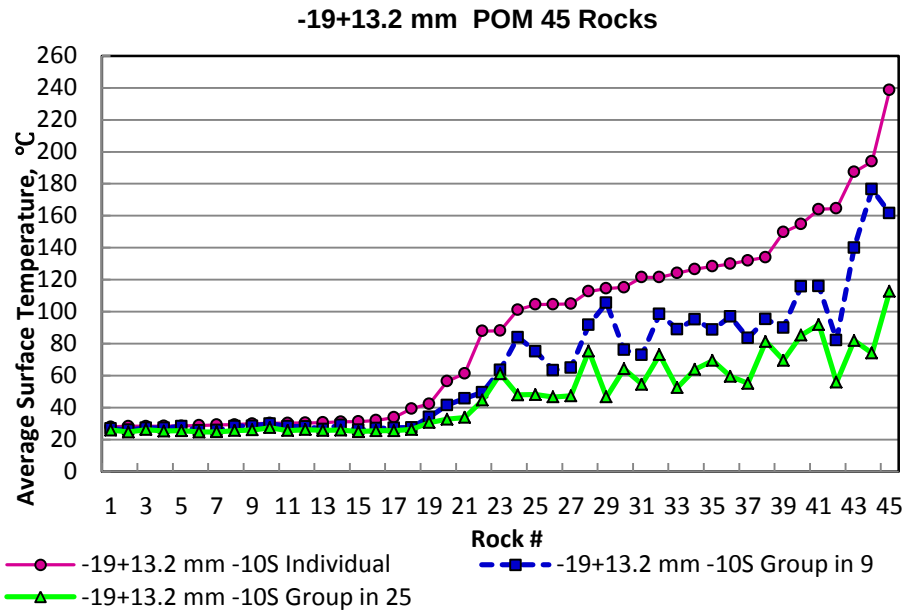
-19+13.2 mm POM 45 Rocks
Average Surface Temperature, °C
260
240
220
200
180
160
140
120
100
80
60
40
20
0
1 3 5 7 9 11 13 15 17 19 21 23 25 27 29 31 33 35 37 39 41 43 45
Rock #
-19+13.2 mm -10S Individual
-19+13.2 mm -10S Group in 9
-19+13.2 mm -10S Group in 25

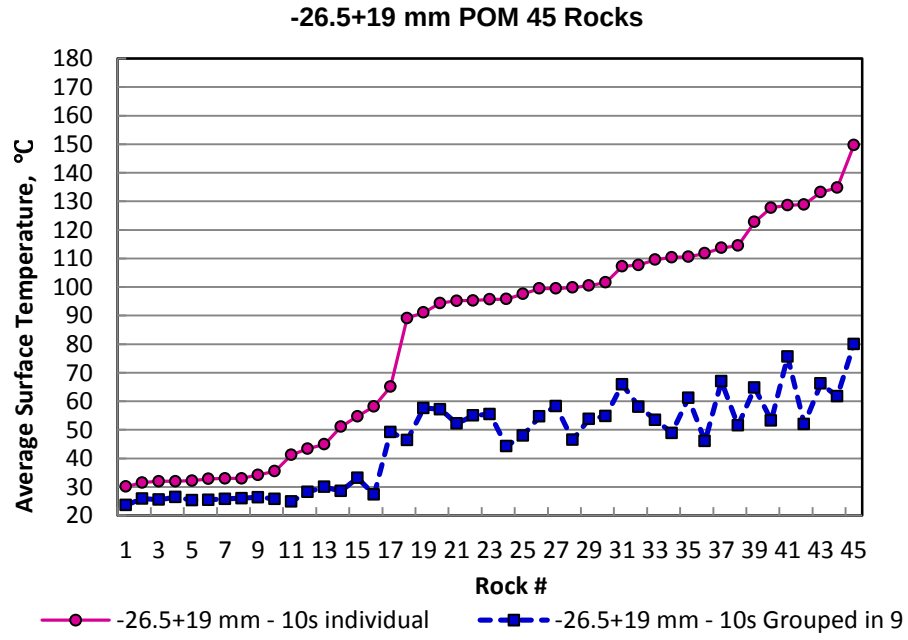
-26.5+19 mm POM 45 Rocks
Average Surface Temperature, °C
180
170
160
150
140
130
120
110
100
90
80
70
60
50
40
30
20
1 3 5 7 9 11 13 15 17 19 21 23 25 27 29 31 33 35 37 39 41 43 45
Rock #
-26.5+19 mm - 10s individual
-26.5+19 mm - 10s Grouped in 9

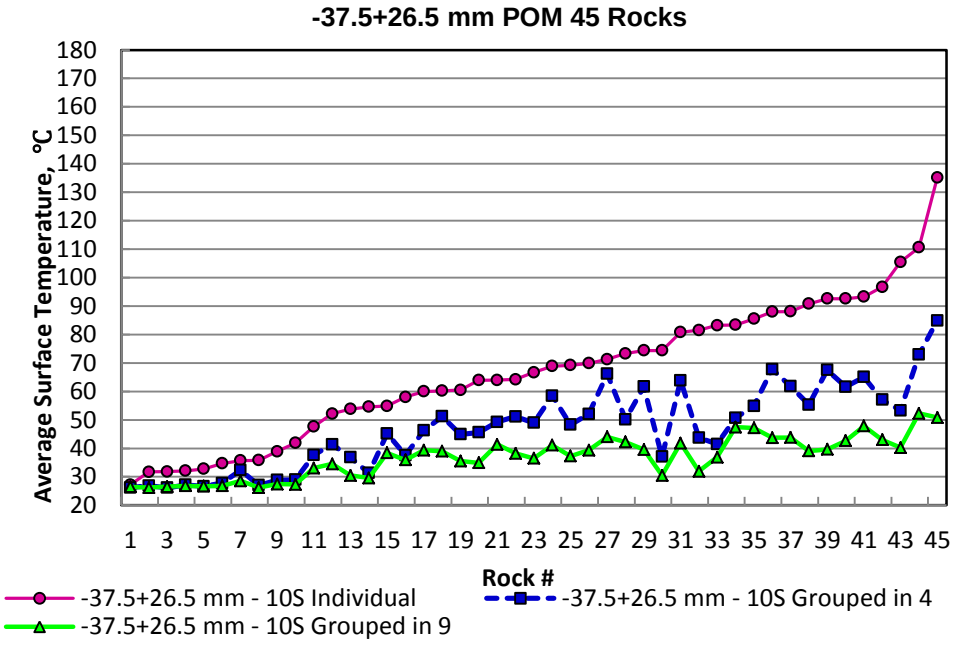


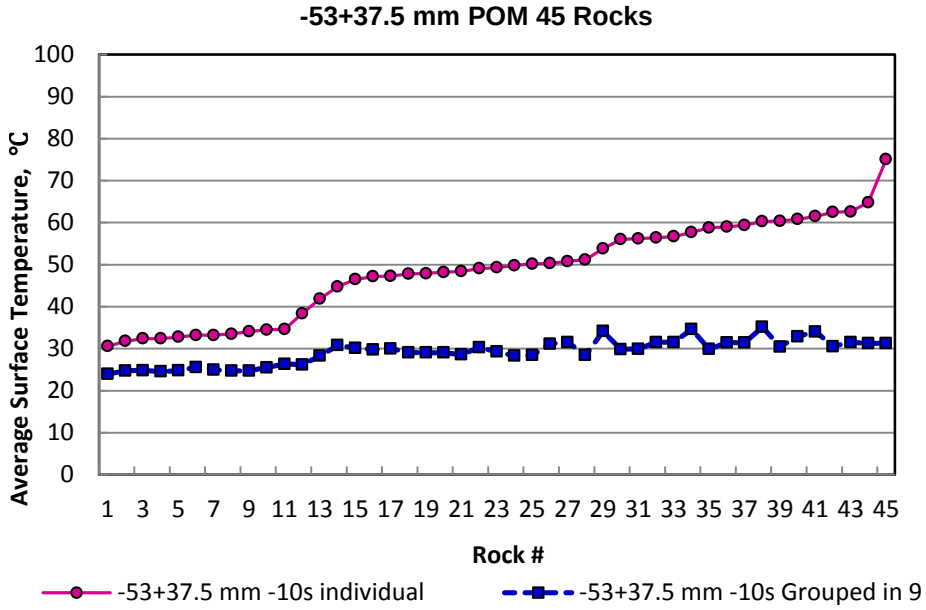


**Figure 3-34 Average Surface Temperatures after Being Heated for 10s by Individual and Group Heating for Four Size Fractions**

As seen in Figure 3-34, the highest temperatures are measured for samples being heated individually for 10s for all of the four size fractions. The rocks being heated together, the lower the temperature to which the rocks were heated.

***Effect of particle size/weight***

It has been found that microwave heating of sulfide minerals is a function of their size. In order to investigate the effect of particle size on microwave heating of this lead-zinc sulfide ore, two hundred rocks between 53 and 13.2 mm were exposed to microwave heating for 10s. In this study, the relationship between average surface temperature and weight of the rocks was assessed to address the effect of particle size on microwave heating, based on the assumptions that weight is proportional to the third power of particle size and all tests had sufficient MW power. The results are shown in Figure 3-35.

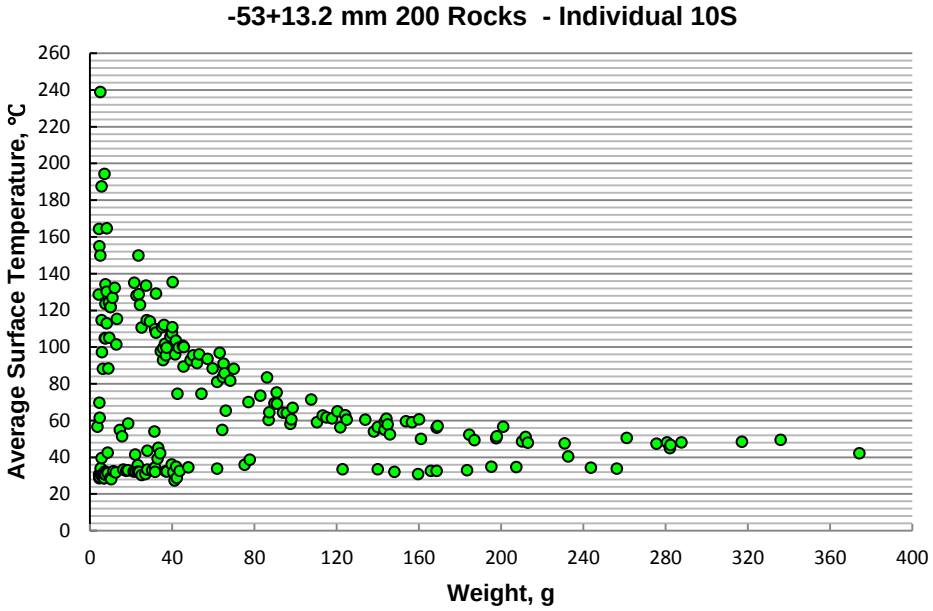


**Figure 3-35 Relationship between Microwave Heating Behaviour of Lead-Zinc Ore and Sample Weight**

As shown in Figure 3-35, microwave heating of rocks containing sulfides is a function of weight. The heavier the sample, the lower temperature it can be heated up to in 10s. The temperatures of rocks barely containing sulfides remain almost the same regardless of weight. This is most significant, because it allows efficient rejection of waste. It is also evident that the smaller the rock is, the greater the difference of average surface temperatures between valuable ore and waste rock. Figure 3-36 shows clearly that the longer the heating time, the greater effect of weight on microwave heating of rocks containing sulfides.

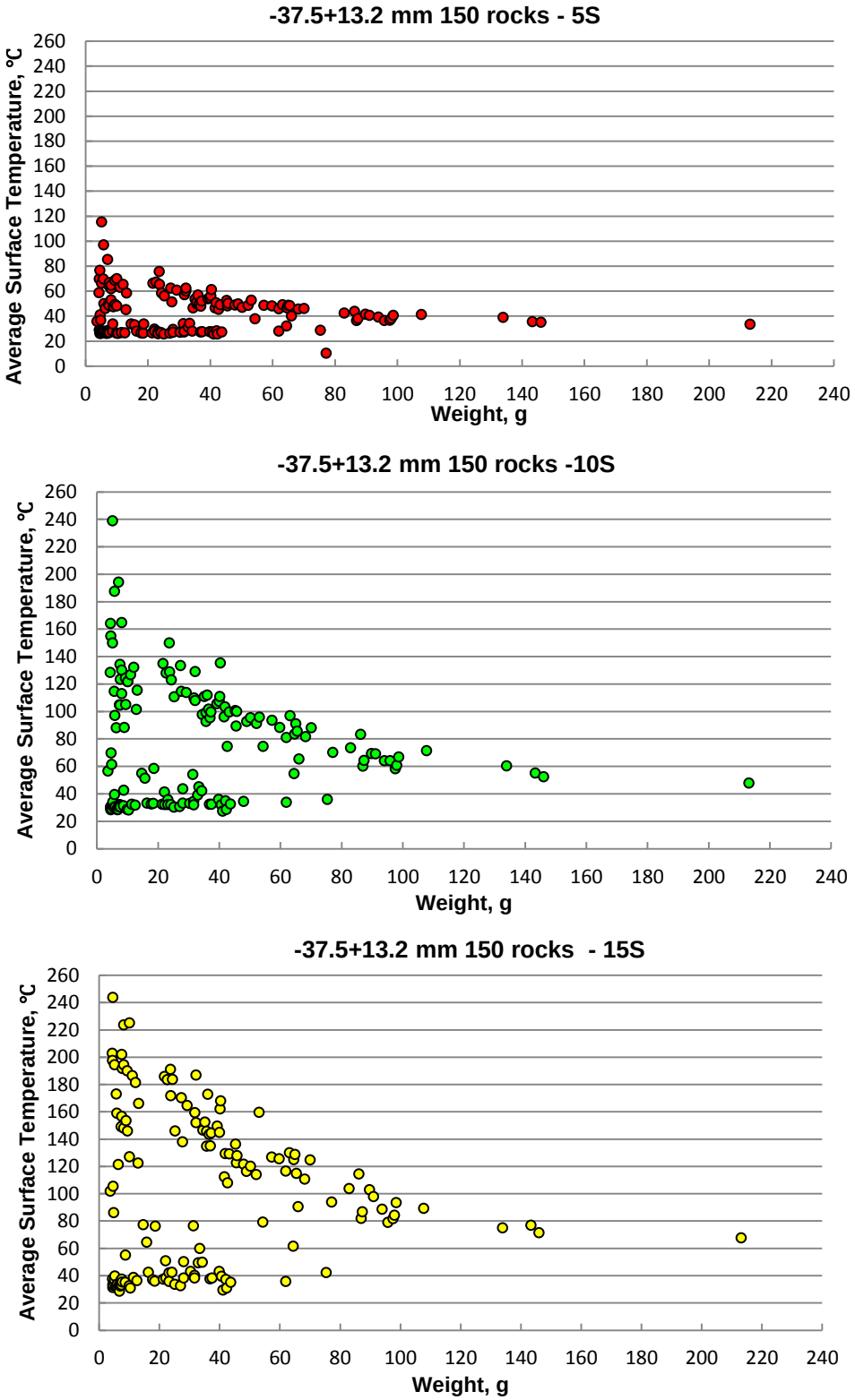


**Figure 3-36 Relationship between Microwave Heating Behaviour of Lead-Zinc Ore and Rock Weight: 5s, 10s and 15s**

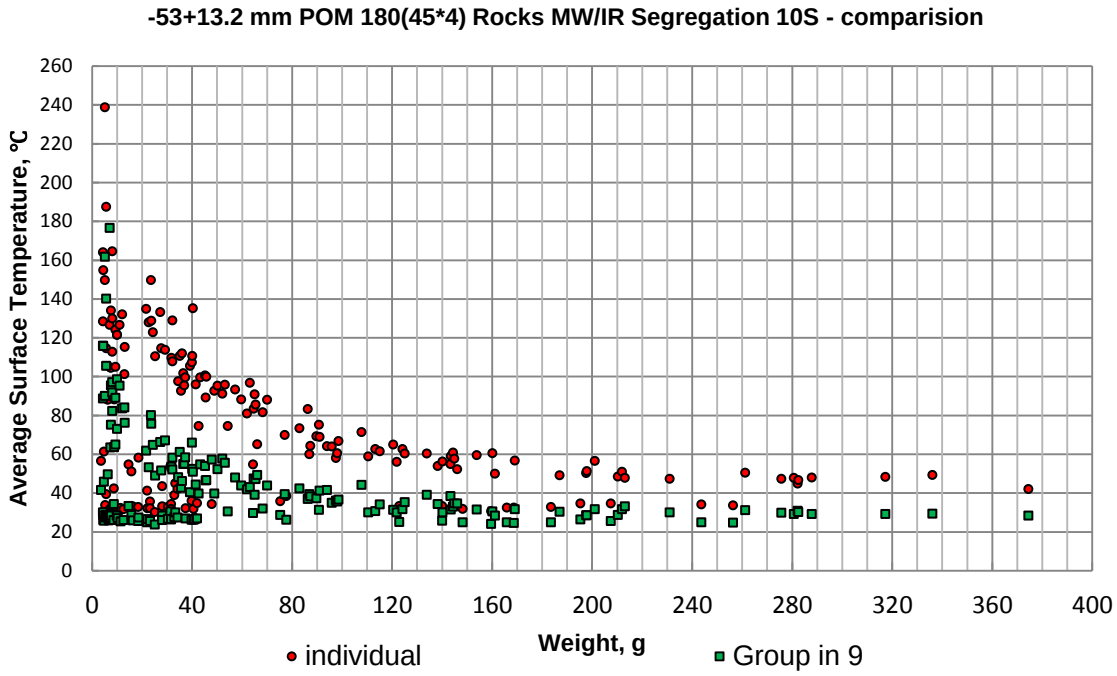


**Figure 3-37 Relationship between Microwave Heating Behaviour of Lead-Zinc Ore and Rock Weight Heated Individually and Heated Together In a Group of Nine**

Figure 3-37 illustrates that rocks can be heated to higher temperature when being exposed to microwave individually rather than being heated together.

It is evident that the finer the particle, the higher the average surface temperature after 10s microwave heating regardless of the quantity of rocks being heated at the same time (see Figure 3-38).

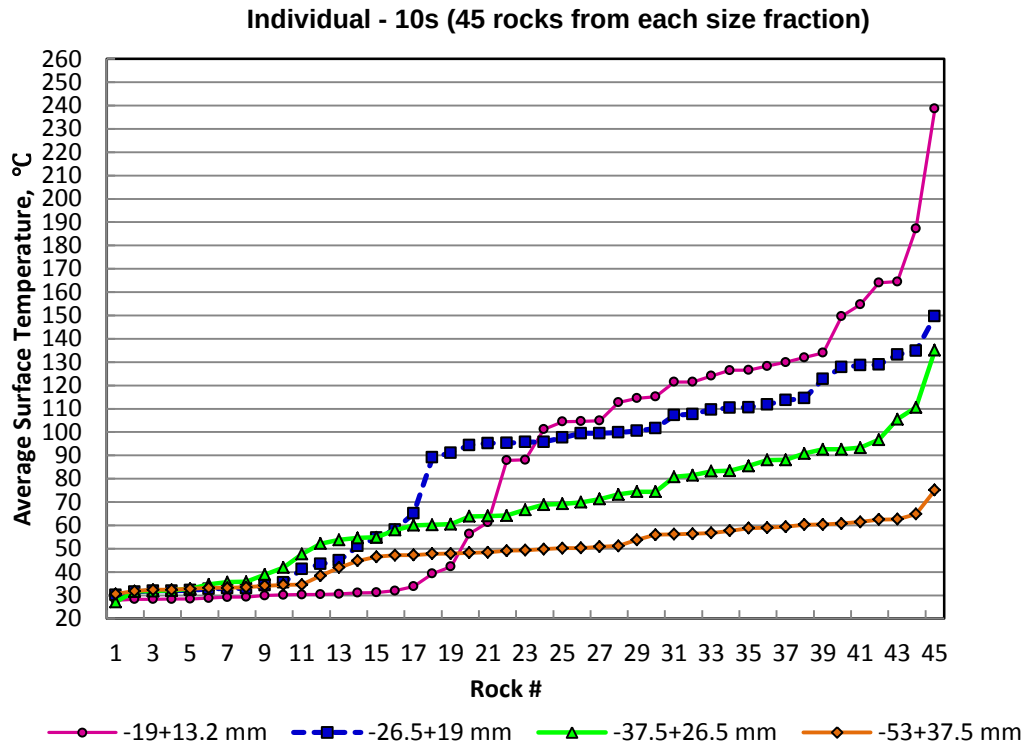


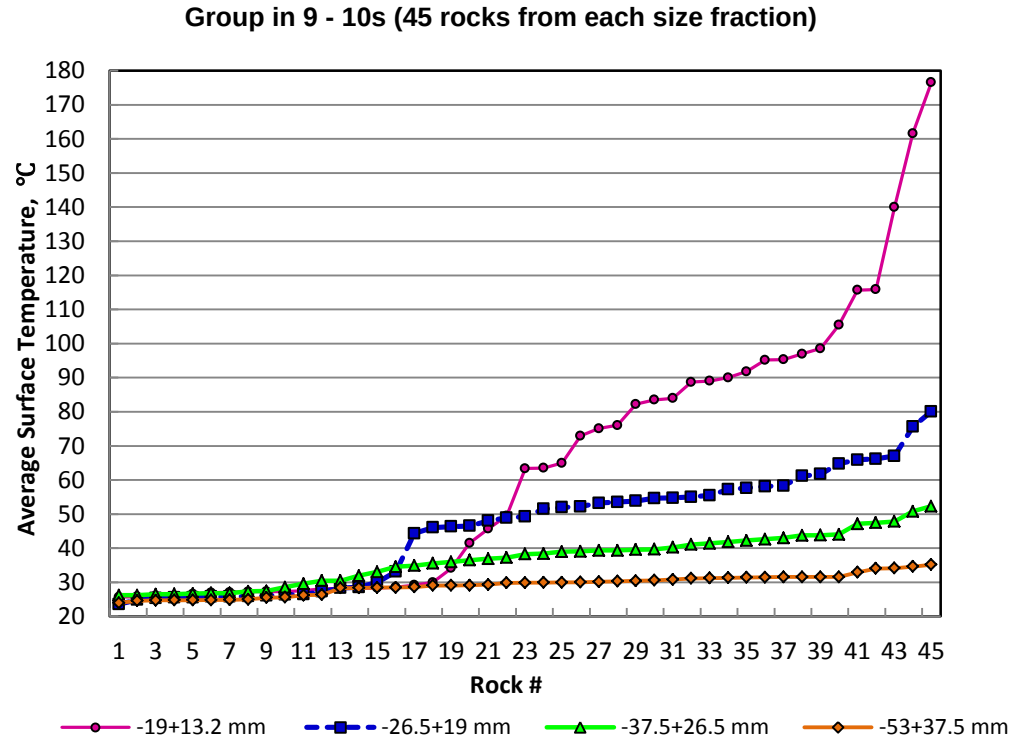


**Figure 3-38 Average Surface Temperatures of Rocks from Four Size Fractions after Being Heated for 10s Individually and Together in a Group of Nine**

Figure 3-33 to Figure 3-38 prove that microwave heating of lead-zinc sulfide ores is a function of particle size, weight, heating time and quantity of rocks being heated at one time. All these factors affect the segregation of barren waste from lead-zinc ore.

#### *3.5.2.2 Distinguishability of waste rock from lead-zinc sulfide ore*

Since sulfides respond well to microwave heating while waste rocks such as dolomite and quartz do not, it is possible to distinguish valuable mineralized sulfide ores from waste rock by measuring the average surface temperature of rocks after being selectively heated by microwave. MW/IR sorting tests were done on four size fractions. In this section only the sorting results of the -26.5+19 mm size fraction are discussed to demonstrate the distinguishability of waste rock from lead-zinc sulfide ore by means of MW/IR sensing. Results for all the four size fractions are shown in Appendices D.

Figure 3-39 shows that the higher the S content, the higher the average surface temperature after 10s microwave heating. The XRD results indicate that only three kinds of sulfide are found in this ore sample, namely galena, sphalerite and pyrite. Sulfur content in our case represents the overall sulfide content present in this sample. However, Pb from galena and Zn from sphalerite are the only elements of interest that need to be recovered during the MW/IR segregation. It is also evident that some rocks containing a low Pb+Zn grade were heated to above 100°C after 10s microwave heating. It is believed that this is related to the high content in the rock of pyrite, which also responds well to microwave radiation. Figure 3-40 also illustrates the fact that microwave can selectively heat up the rocks with higher sulfide content but not those with higher Pb+Zn content. Figure 3-34 and Figure 3-38 also show a perfect rejection of waste because temperatures of ore vary as a function of MW time/power, but the temperatures of the waste rock do not. Therefore, sorting of waste from this lead-zinc ore by means of MW/IR sensing is much easier than sorting of lead-zinc sulfides from waste.

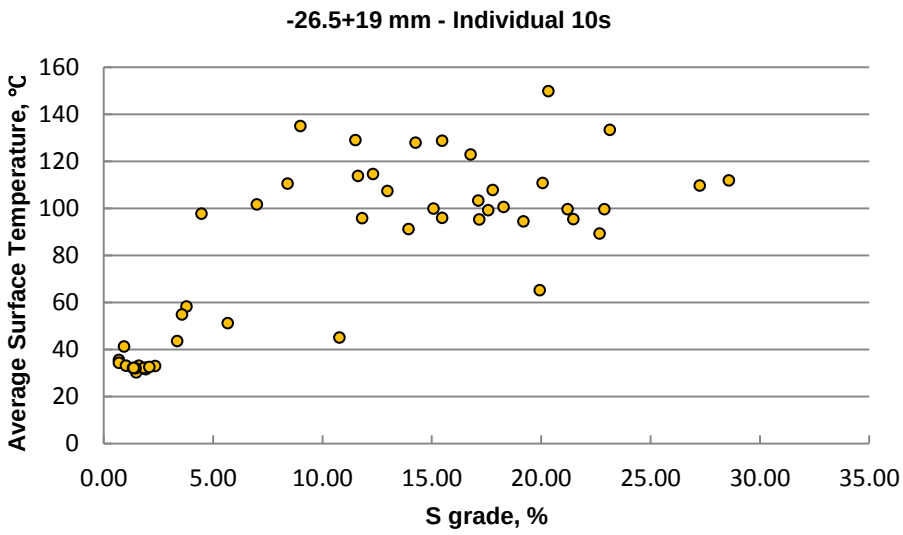


(1)

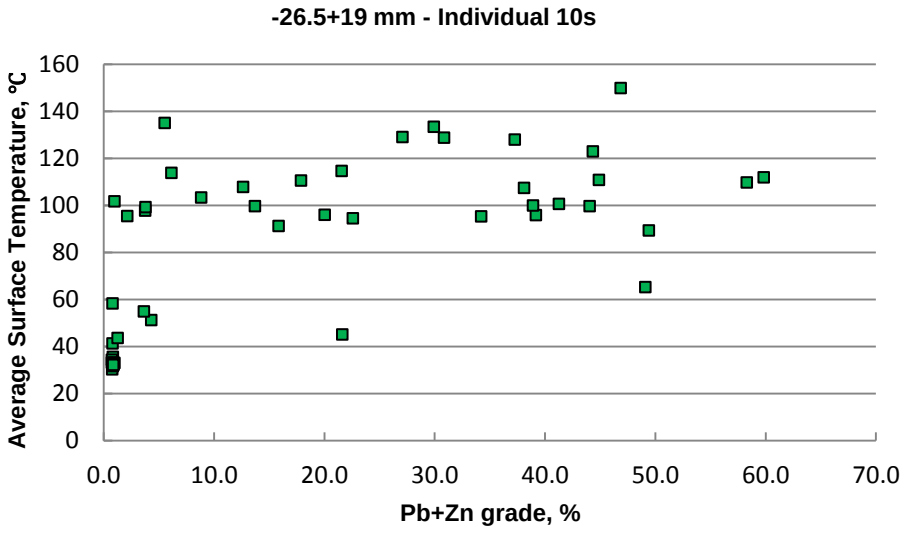


(2)

**Figure 3-39 Average Surface Temperature vs. S /Pb+Zn Grades**

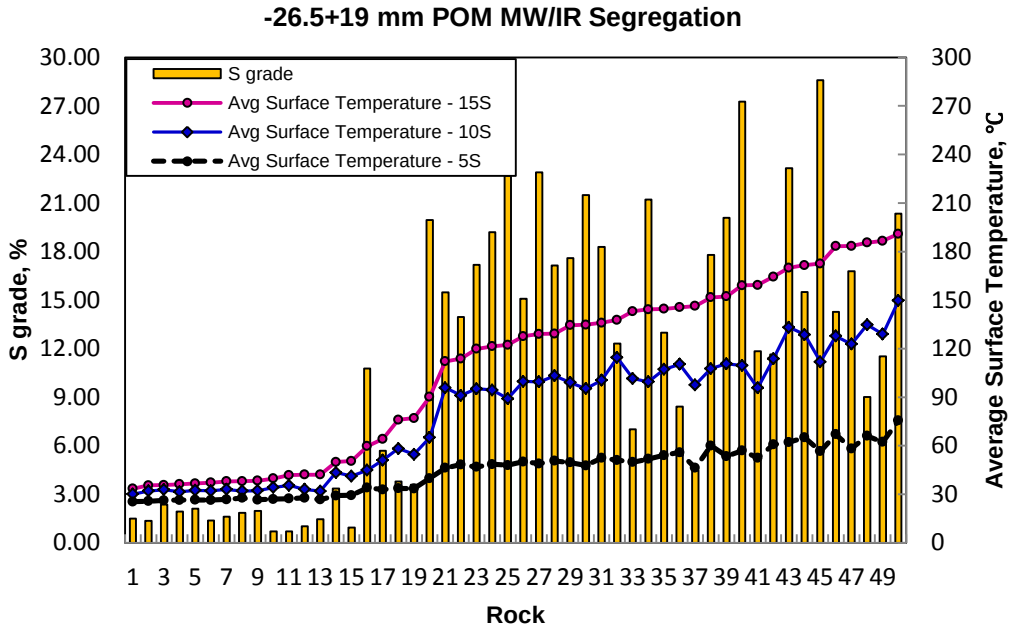


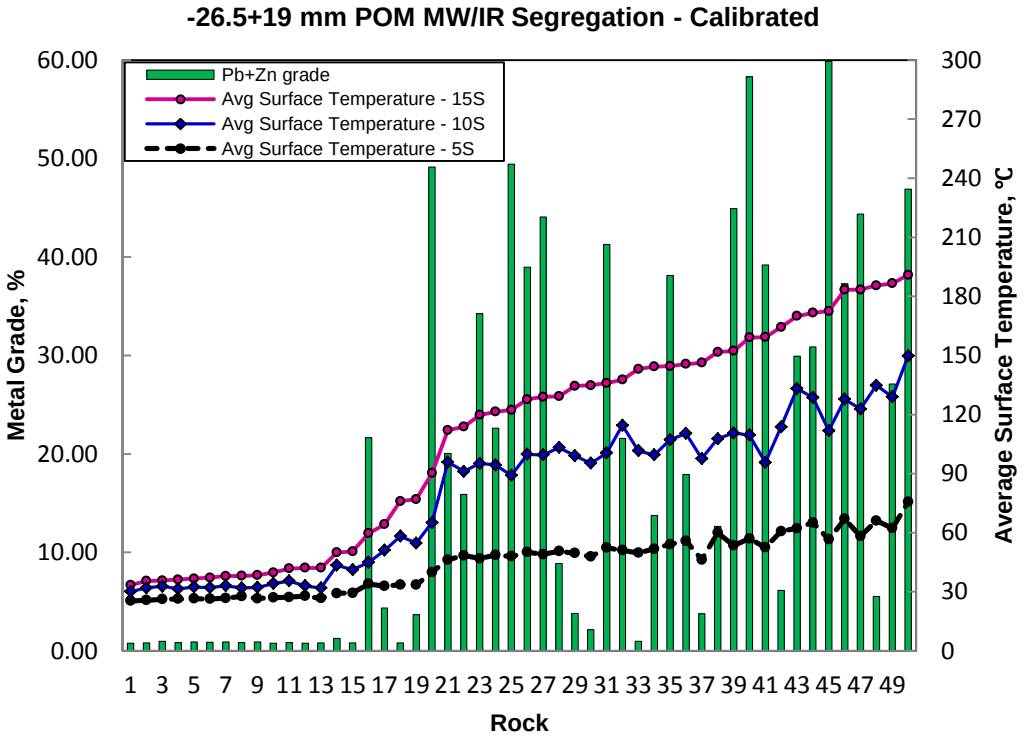


**Figure 3-40 Relationship between Average Surface Temperature and S/Pb+Zn Grades after 5s, 10s and 15s Microwave Heating**

Sorting results of MW/IR sensing of -26.5+19 mm after 10s microwave heating are taken as an example to demonstrate the capability of selective microwave heating (Table 3-14). A series of separation temperatures were chosen to separate waste rock from mineralized ore. Table 3-14 shows that 99.9% of the Pb and 95% of the Zn in the head sample were sorted into 77% of the weight after 10s microwave heating. Table 3-14 lists the MW/IR sorting results of rocks from -26.5+19 mm size fraction under different testing conditions.

.

**Table 3-14 MW/IR Segregation (Individual 10s 50 Rocks) Results of -26.5+19 mm size fraction Based on Different Separation Average Surface Temperatures**

| Separation Temperature, °C | Hot Fraction | Cold Fraction | Wt.% in Hot Fraction | | | Wt.% in Cold Fraction | | | % in Hot Fraction | | | % in Cold Fraction | | |
|---|---|---|---|---|---|---|---|---|---|---|---|---|---|---|
| | | | Concentrate Grades, % | | | Waste Grades, % | | | Metal Recovery, % | | | Metal Recovery, % | | |
| | Conc. Wt. % | Waste Wt. % | Pb | Zn | S | Pb | Zn | S | Pb | Zn | S | Pb | Zn | S |
| **32** | 89.8 | 10.2 | 10.31 | 14.18 | 14.44 | 0.03 | 0.82 | 1.64 | 100.0 | 99.3 | 99.3 | 0.0 | 0.7 | 0.7 |
| **33** | 85.8 | 14.2 | 10.79 | 14.81 | 15.05 | 0.03 | 0.83 | 1.62 | 100.0 | 99.1 | 99.0 | 0.0 | 0.9 | 1.0 |
| **45** | **76.9** | **23.1** | **12.03** | **15.84** | **16.36** | **0.04** | **2.77** | **2.43** | **99.9** | **95.0** | **97.0** | **0.1** | **5.0** | **3.0** |
| **60** | 73.7 | 26.3 | 12.53 | 16.42 | 16.88 | 0.08 | 2.73 | 2.66 | 99.8 | 94.4 | 96.3 | 0.2 | 5.6 | 3.7 |
| **80** | 69.5 | 30.5 | 11.09 | 16.62 | 16.69 | 5.09 | 4.17 | 5.06 | 83.2 | 90.1 | 90.0 | 16.8 | 9.9 | 10.0 |
| **95** | 54.5 | 45.5 | 12.05 | 16.25 | 16.16 | 5.92 | 8.72 | 9.53 | 70.9 | 69.1 | 70.2 | 29.1 | 30.9 | 29.8 |
| **100** | 35.8 | 64.2 | 14.39 | 15.44 | 16.48 | 6.40 | 11.36 | 11.28 | 55.6 | 43.1 | 45.3 | 44.4 | 56.9 | 54.7 |
| **105** | 27.8 | 72.2 | 16.42 | 16.67 | 17.02 | 6.50 | 11.34 | 11.65 | 49.4 | 36.2 | 37.7 | 50.6 | 63.8 | 62.3 |
| **110** | 19.5 | 80.5 | 16.52 | 16.71 | 17.12 | 7.50 | 11.88 | 12.18 | 34.8 | 25.5 | 27.8 | 65.2 | 74.5 | 72.2 |
| **120** | 11.3 | 88.7 | 13.75 | 18.02 | 15.83 | 8.69 | 12.16 | 12.80 | 16.8 | 15.9 | 15.1 | 83.2 | 84.1 | 84.9 |
| **130** | 4.7 | 95.3 | 11.73 | 16.45 | 18.02 | 9.14 | 12.64 | 12.90 | 5.9 | 6.0 | 7.1 | 94.1 | 94.0 | 92.9 |
| **Calculated Head Grade**: 9.26% Pb and 12.82% Zn, 13.10% S | | | | | | | | | | | | | | |

**Table 3-15 Summary of MW/IR Sorting Results of -26.5+19 mm Sample**

| Test Condition | Separation at °C | Mass % of Cold | Pb in Hot Fraction, % | | Zn in Hot Fraction, % | |
|---|---|---|---|---|---|---|
| | | | Grade | Recovery | Grade | Recovery |
| 5s | 30 | 21.0 | 11.71 | 99.9 | 16.00 | 98.6 |
| 10s | 45 | 23.1 | 12.03 | 99.9 | 15.84 | 95.0 |
| 15s | 60 | 23.1 | 12.03 | 99.9 | 15.84 | 95.0 |
| **Calculated Head Grade**: 9.26% Pb and 12.82% of Zn 50 rocks being tested | | | | | | |
| **Test Condition** | **Separation at, °C** | **Mass % of Cold** | **Pb in Hot Fraction, %** | | **Zn in Hot Fraction, %** | |
| | | | **Grade** | **Recovery** | **Grade** | **Recovery** |
| Individual | 45 | 20.9 | 12.75 | 99.9 | 16.60 | 95.2 |
| Group in 9 | 26 | 16.6 | 12.09 | 100.0 | 16.38 | 99.0 |
| **Calculated Head Grade**: 10.09% Pb and 13.79% Zn 45 rocks being tested | | | | | | |

It is clearly shown in the above table that MW/IR sensing has the same segregation effect on this lead-zinc ore after 5s and 15s microwave heating. However, at 15s rocks are heated to higher temperatures, meaning that a higher separation temperature is needed for distinguishing waste rock from valuable mineralized ore. Based on these results, it appears that a heating time of 10s will be quite enough for effective elimination of waste rock from this ore sample. However, it also appears that batch heating of rocks, especially the larger ones, for short periods (<10 seconds) introduces errors, which can be avoided by heating the rocks in continuous microwave device. This should be the subject of further testwork.

#### *3.5.2.3 Sorting results summary*

All of the samples from the four size fractions exhibited good MW/IR sorting results. Microwave heating time of 10s and 15s achieved a similar segregation effect while heating for 5s did not provide as great a difference in average surface temperature as did 10s, probably due to the fact that the oven needs about 5 seconds to warm up and reach full power. As a result, the optimum heating time for MW/IR segregation of this lead-zinc ore on a batch laboratory-scale is 10 seconds. Table 3-16 summarizes the optimum sorting results for each test condition.

For individual testing, samples from the -19+13.2 mm size fraction yield the best MW/IR sorting results, with lead and zinc recoveries exceeding 95% and mass rejection exceeding 30%. The other three larger size fractions exhibited similarly good sorting

results. About 20-25% mass could be rejected with above 95% metal recovery of lead and zinc. Whether the larger ore particles contained more lead and zinc still needs to be established but appears likely, in which case less mass can be rejected, setting a 95% metal recovery.

For group testing, microwave heating of the samples in a group of nine yielded similar sorting results as the individual test. Although lower average surface temperatures were obtained for all the rocks when heated together in a group of nine rather than individually, no significant improvement or inefficiency of the optimum MW/IR sorting of this material was identified. Only a lower separation temperature needed to be chosen for similar sorting results. About 20-30% mass could be rejected in the cold fraction depending on the size of rock in order to recover above 95% of the element of interest, Pb and Zn in our case. However, for the large rocks sized -53+37.5 mm, sorting results varied a lot when separation was at 26°C and 29°C (metal recoveries dropped from 99.8% to 59.8% for Pb and 97.5% to.66.7% for Zn). Previous study by Olive showed that duplicate MW heating test on the same rock could give 2-3°C difference. For the rocks with higher average temperature, the error could be more when duplicate tests were done (Wang, O., personal communication, July 18, 2012). Thus, sorting results of 26°C and 29°C should be of less difference in order to justify the reliability of the MW/IR segregation. Therefore, it can be concluded that heating individually achieved better segregation result than group heating for -53+37.5 mm rocks after 10s microwave heating since consistent sorting results were achieved based on different separation temperatures by individual heating. It is also evident that the finer the particle size, the more consistent the sorting results of group heating were based on separation temperatures with a difference of 2-3°C.

Similar optimum sorting results in terms of mass rejection were achieved when exposing the same weight of rocks, in groups of one, four, nine and twenty-five rocks based on different rock size, to microwave heating. This indicates that high capacity of microwave treatment will be possible, which enables the application of this sorting technology to base metal sulfide ore sorting. Shape recognition technologies now available will also allow scanners to determine the size of the individual rocks and adjust the separation temperature for each rock, eliminating the need for elaborate sizing of the sorting machine feed.

**Table 3-16 MW/IR Sorting Results Summary**

| Size, mm | Separation Limit, °C | Mass % of Cold | Pb, % | | | Zn, % | | |
|---|---|---|---|---|---|---|---|---|
| | | | Grade in Head | Grade in Hot | Recovery in Hot | Grade in Head | Grade in Hot | Recovery in Hot |
| -53+37.5 | 26 | 24.4 | 11.10 | 14.66 | 99.8 | 8.30 | 10.70 | 97.5 |
| -37.5+26.5 | 31 | 17.3 | 5.13 | 6.20 | 99.8 | 10.51 | 12.13 | 95.4 |
| -26.5+19 | 30 | 23.4 | 10.09 | 13.15 | 99.8 | 13.79 | 17.06 | 94.8 |
| -19+13.2 | 28 | 31.1 | 4.46 | 6.45 | 99.7 | 7.12 | 9.82 | 95.0 |
| 45 rocks grouped in 9 -10s | | | | | | | | |
| **Particle #** | **Separation Limit, °C** | **Mass % of Cold** | **Pb, %** | | | **Zn, %** | | |
| | | | **Grade in Head** | **Grade in Hot** | **Recovery in Hot** | **Grade in Head** | **Grade in Hot** | **Recovery in Hot** |
| Individual (-53+37.5 mm) | 35 | 23.5 | 11.10 | 14.49 | 99.8 | 8.30 | 10.59 | 97.7 |
| Group in 4 (-37.5+26.5 mm) | 37 | 17.3 | 5.13 | 6.20 | 99.8 | 10.51 | 12.13 | 95.4 |
| Group in 9 (-26.5+19 mm) | 30 | 23.4 | 10.09 | 13.15 | 99.8 | 13.79 | 17.06 | 94.8 |
| Group in 25 (-19+13.2 mm) | 26 | 35.1 | 4.46 | 6.84 | 99.7 | 7.12 | 10.37 | 94.6 |
| 45 rocks -10S same weight being heated at the same time | | | | | | | | |
| **Size, mm** | **Separation Limit, °C** | **Mass % of Cold** | **Pb, %** | | | **Zn, %** | | |
| | | | **Grade in Head** | **Grade in Hot** | **Recovery in Hot** | **Grade in Head** | **Grade in Hot** | **Recovery in Hot** |
| -53+37.5 | 35 | 21.3 | 11.06 | 14.03 | 99.8 | 8.54 | 10.63 | 98.0 |
| -37.5+26.5 | 50 | 24.3 | 4.82 | 6.23 | 98.0 | 10.06 | 12.76 | 96.1 |
| -26.5+19 | 45 | 23.1 | 9.26 | 12.03 | 99.9 | 12.82 | 15.84 | 95.0 |
| -19+13.2 | 31 | 29.7 | 4.16 | 5.90 | 99.7 | 7.30 | 9.92 | 95.6 |
| 50 rocks individual - 10s | | | | | | | | |

### 3.6 Ore Sorting Test Summary

The amenabilities of the four sorting technologies X-ray fluorescence sorting, X-ray transmission sorting, optical sorting and microwave-infrared sorting to this ore have been investigated in laboratory-scale in this chapter. Sorting results are summarized in Table 3-17, except for the microwave-infrared sorting which is still under development. Table 3-17 indicates that pilot-scale sorting tests of the other three sorting techniques could be performed to further confirm the technical feasibilities of sorting this lead-zinc ore using automatic sensor-based ore sorters, since promising results were obtained in the laboratory-scale evaluation.

Technically speaking, XRF sorting provided the most satisfactory sorting results in terms of waste rejection. Above 50% mass could be rejected as waste and above 96% Pb and Zn could be recovered from 47% of the test feed. XRT sorting also presents almost 40% waste mass rejections. Color sorting could only achieve about 20% waste mass rejection, which is not as promising as the X-ray technologies.

A flowsheet for a technical amenability study of sensor-based ore sorting in laboratory-scale was generated and provides a reference for similar studies. The flowsheet can be seen in Figure 3-41.

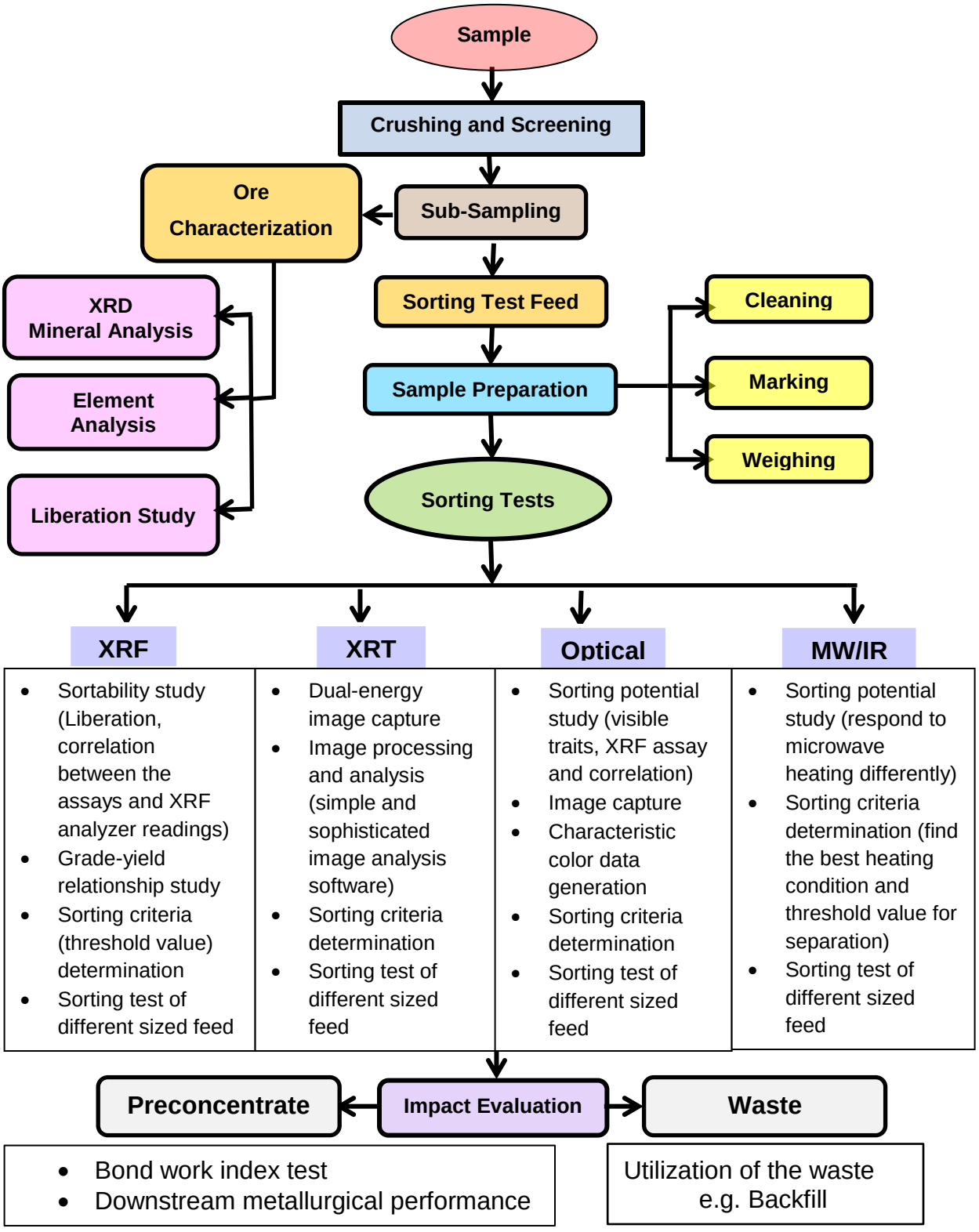


**Figure 3-41 Flowsheet for Laboratory-scale Sensor-based Ore Sorting Study**

**Table 3-17 Ore Sorting Results Summary**

| Sample Size, mm | Sorting Technique | Sorting Criteria | Conc., % | Mass Rejected as Waste, % | Metal Recovery, % | | Calculated Head Grade | | Conc. Grade, % | | Waste Grade, % | | Note |
|---|---|---|---|---|---|---|---|---|---|---|---|---|---|
| | | | | | Pb | Zn | Pb | Zn | Pb | Zn | Pb | Zn | |
| -37.5+26.5 | XRF | 5.00% Zn Grade | 47.2 | 52.8 | 96.5 | 97.1 | 3.72 | 10.21 | 7.61 | 21.04 | 0.25 | 0.56 | Assays |
| -37.5+26.5 | XRT | Avg. Brightness Value of High Energy Image of 65 | 61.9 | 38.1 | 99.0 | 96.1 | 6.20 | 8.73 | 9.92 | 13.56 | 0.17 | 0.88 | Calibrated XRF Powder |
| | | Ore Index of 33 | 62.3 | 37.7 | 99.1 | 95.6 | 6.20 | 8.73 | 9.86 | 13.39 | 0.14 | 1.02 | Calibrated XRF Powder |
| -37.5+26.5 | Optical (Color) | R133-22, R40-7 | 81.2 | 18.8 | 98.5 | 97.0 | 6.20 | 8.73 | 7.64 | 10.43 | 0.50 | 0.50 | Calibrated XRF Powder |
| -19+13.2 | MW/IR | 31°C (Individual Heating) | 70.3 | 29.7 | 99.7 | 95.6 | 4.16 | 7.30 | 5.90 | 9.92 | 0.04 | 1.09 | Calibrated XRF Surface |

# CHAPTER 4 SORTING IMPACT EVALUATION

It has been demonstrated that automatic sensor-based ore sorting is beneficial to the ore beneficiation process in terms of energy saving and metallurgical performance improvement. Bamber (2008) demonstrated that preconcentration of ores by sorting had three benefits regarding power savings at the mill: reduction in tonnage of feed to the mill; rejection of hard siliceous waste rock which has high grinding work index; and providing finer feed to mill plant. Therefore, energy consumption could be considered as one of the indices used for sorting impact evaluation. It can be calculated by measuring the Bond Ball Mill Work Index for the material. Better metallurgical performance may also be achieved with higher grade and finer feed due to the upgrading effect of ore sorting and the removal of hard gangue minerals.

In order to evaluate the sorting impact of this lead-zinc ore, the Bond Ball Mill Work Indices for the head ore, X-ray fluorescence (XRF) sorting concentrate and XRF waste were calculated for the evaluation of grinding energy savings. Flotation tests were also conducted with the feed of head sample and XRF concentrate using similar reagent conditions to those employed by the mine site.

## 4.1 Experimental Procedures

### 4.1.1 X-Ray Diffraction Analysis

Sub-samples of head ore, XRF concentrate and XRF waste were prepared for the Quantitative X-Ray Diffraction analysis for mineral composition characterization.

### 4.1.2 Grinding Energy Consumption Test

The impact of ore sorting on grinding energy consumption can be calculated from the Bond equation as follows (Bamber, 2008):

$$\Delta \mathrm{P} = \Delta \mathrm{t} 10 \Delta W_i \left( \frac{1}{\sqrt{P_{80}}} - \frac{1}{\sqrt{F_{80}}} \right) \quad (1)$$

Where: Δt = Waste Rejection (tph)

$\Delta W_i$ = Change in Bond Work Index

$P_{80}$ = 80% passing size of the product (μm)

$F_{80}$ = 80% passing size of the feed (μm)

Waste rejection data can be achieved from different sorting tests. Bond Ball Mill Work Indices for the materials can be determined by Standard Laboratory Bond Ball Mill Index Test. Representative samples from -37.5+26.5 mm size fraction Pend Oreille ore head sample, XRF sorting concentrate and XRF sorting waste were crushed by gyratory crusher and cone crusher. Then the crushed products were screened at 2800 μm and prepared for the Laboratory Bond Ball Mill Index test. The Bond Ball Mill (Figure 4-1) is 305 mm in length and 305 mm in diameter. Ball charge used is shown in Table 4-1.

**Table 4-1 Bond Ball Charge**

| Ball, Inches | Diameter, Inches | Number | Unit Weight, lbs | Total Weight, lbs |
|---|---|---|---|---|
| 1 1/2 | 1.5 | 43 | 0.500555 | 21.5 |
| 1 1/4 | 1.25 | 67 | 0.289673 | 19.4 |
| 1 | 1 | 10 | 0.148313 | 1.5 |
| 3/4 | 0.75 | 71 | 0.062569 | 4.4 |
| 5/8 | 0.625 | 94 | 0.036209 | 3.4 |
| Sum | | | | 50.3 |
| Steel SG=7.85<br>Calculated surface area: 842 sq. in. | | | | |

**Figure 4-1 Standard Laboratory Bond Test Ball Mill**

The Bond Work Index of the POM feed was determined through a full Standard Bond Ball Mill Work Index test with a closing screen of 180 µm and considered as the reference. Tests were done according to the standard Bond Ball Mill Work Index Test procedures developed by Bond (1961). The work indices of the XRF sorting concentrate and waste were then determined by a comparative Bond Ball Mill Work Index test (Berry & Bruce, 1966). The Bond Ball Mill Work Indices can be calculated employing equations (2) and (3).

$$W_i = 44.5/(P_i)^{0.23} \times (Gbp)^{0.82} \left(\frac{1}{\sqrt{P_{80}}} - \frac{1}{\sqrt{F_{80}}}\right) \quad (2)$$

$$W_{i2} = W_{i1} \times \left(\frac{10}{\sqrt{P_1}} - \frac{10}{\sqrt{F_1}}\right) \Big/ \left(\frac{10}{\sqrt{P_2}} - \frac{10}{\sqrt{F_2}}\right) \quad (3)$$

### 4.1.3 Flotation Test

Flotation tests of different feed samples (Head and XRF concentrate) were conducted to evaluate the impact of ore sorting on the downstream flotation performance.

One 1 kg subsample of the head ore and two 1 kg subsamples of XRF concentrate were prepared as the feed for the flotation tests. According to the grindability test results shown in Appendix E, a 500 g sample could be ground dry for 5 min in a laboratory rod mill to have a product of P80 being about 100 microns. As a result, each flotation feed was divided into two portions and dry ground to have a grinding product size of 80%

passing 100 microns. Then the ground materials were transferred into a batch scale Denver laboratory flotation cell (4L). The flotation test was conducted at 20% solid content with tap water. The temperature under which this test was conducted is room temperature. The reagents used in sequence were pH modifier, activator or depressant and collector. The pH of the slurry was adjusted by adding lime until it was 10.5 in the lead flotation circuit. After the pH of the slurry was stabilized, the depressant sodium cyanide with a concentration of 100 g/t was added in the lead flotation circuit to depress pyrite and sphalerite. After three min conditioning, the Potassium Amyl Xanthate (PAX) with a concentration of 50g/t was added as collector. Conditioning time for the pH modifier, activator or depressant and collector was one min each. The methylisobutylcarbinol (MIBC) was used as frother. In the zinc flotation circuit, the pH was set as 11. The activator used for Zn flotation was copper sulphate with a concentration of 700 g/t. 100 g/t PAX was used in the Zn flotation circuit.

Froth was collected from the cell by scraping by hand at an interval of three seconds in the first minute and five seconds thereafter. At the very beginning, froth was allowed to build up for five seconds before scraping. Fresh tap water was added to slurry during the test in order to maintain pulp volume and clean sides of the cell. Each product was then dried in the oven and prepared for XRF powder reading for assays.

## 4.2 Results and Discussion

### 4.2.1 X-Ray Diffraction Analysis

The quantitative X-Ray Diffraction analysis of the head ore, XRF concentrate and XRF waste are shown in Table 4-2. Results indicate that XRF sorting rejected many hard dolomitic gangue minerals that are hard to grind. Lead and zinc were upgraded in the XRF concentrate (XRFC) which meant that feed with higher grades was reported to flotation circuit. Almost no valuable metal contents of lead and zinc were lost in the XRF waste.

**Table 4-2 Results of Quantitative Phase Analysis (Wt. %)**

| Mineral | Ideal Formula | Feed | XRFC | Waste |
|---|---|---|---|---|
| Pyrite | $FeS_2$ | 38.5 | 48.4 | 3.2 |
| Sphalerite | (Zn,Fe)S | 10.2 | 19.5 | |
| Galena | PbS | 4.6 | 4.9 | |
| Cerussite | $PbCO_3$ | 0.1 | | |
| Dolomite-Ankerite | $CaMg(CO_3)_2$-<br>$Ca(Fe^{2+},Mg,Mn)(CO_3)_2$ | 42.6 | 23.7 | 88.4 |
| Calcite | $CaCO_3$ | 2.2 | 1.9 | 6.8 |
| Plagioclase ? | $NaAlSi_3O_8$ – $CaAlSi_2O_8$ | 0.8 | 1.0 | 0.2 |
| Quartz | $SiO_2$ | 0.9 | 0.6 | 0.7 |
| Muscovite ? | $KAl_2(AlSi_3O_{10})(OH)_2$ | | | 0.7 |
| Total | | 100.0 | 100.0 | 100.0 |

### 4.2.2 Grinding Energy Savings

Results of the Work Index tests are shown in Table 4-3.

**Table 4-3 $P_{80}$, $F_{80}$ and Work Indices for XRF Feed, XRF Concentrates and XRF Waste**

| Sample | $F_{80}$, microns | $P_{80}$, microns | BWI, kwh/tonne | % Saving of Wi |
|---|---|---|---|---|
| Head Ore | 2338 | 99 | 8.33 | |
| XRF Conc. | 2230 | 77 | 7.20 | 13.6 |
| XRFConc.-2 | 2362 | 82 | 7.40 | 11.2 |
| XRF Waste | 2365 | 101 | 8.43 | |

Results shown in Table 4-3 indicated that the Bond Work Index of the XRF concentrate was smaller than the head ore which meant that ore sorting could provide softer feed to the mill. Even though the Bond Work Indices were similar for the head ore and XRF concentrate, considerable amount of energy could still be saved due to the large mass rejection rate by XRF sorting. The grinding energy savings can be calculated based on the following conditions as an example.

The F80 and P80 of the ball mill at the mine site were 4.17 mm and 0.47 mm respectively (Lin, D., personal communication, October 27, 2011). The waste rejection achieved by XRF sorting of -37.5+26.5 mm size fraction was 52.8%. The average calculated Bond Work Index for the XRF concentrate was 7.30 kwh/tonne. The Bond Work Index for head ore was 8.33 kwh/tonne. The capacity of the XRF sorter was assumed to be 60 tph. The grinding energy savings after ore sorting can be calculated then using the Equation (1).

$$\Delta \mathrm{P} = \Delta \mathrm{t}10\Delta W_i \left(\frac{1}{\sqrt{P_{80}}} - \frac{1}{\sqrt{F_{80}}}\right) = (52.80\% * 60) \times 10 \times (8.33 - 7.30) \times \left(\frac{1}{\sqrt{0.47}} - \frac{1}{\sqrt{4.17}}\right) = 316.2 \text{ kW}$$

### 4.2.3 Flotation Test Results

Flotation results are shown in Table 4-4 based on XRF powder readings.

The metal recoveries for Pb and Zn after XRF sorting were 96.5% and 97.1% respectively. As a result, the overall metal recoveries of Pb and Zn for XRF concentrate after flotation process were 73.9% Pb in the lead concentrate and 73.0% Zn in the zinc

concentrate. The overall metal recoveries of Pb and Zn for XRFconcentrate-2 were 75.6% Pb in the lead concentrate and 85.4% Zn in the zinc concentrate. It is clearly shown that the overall metal recoveries of Pb and Zn both increased after preconcentration by XRF sorting. The grades of the lead concentrate and zinc concentrate were also higher after preconcentration. However, the results obtained in this test could only be seen as tentative. Repeated flotation tests should be conducted in the future work to justify the reliability of the results obtained in this study

**Table 4-4 Flotation Results Based on Calibrated XRF Powder Readings**

| POM | Weight, g | Weight Distr. % | Pb Grade, % | Zn Grade, % | Fe Grade, % | Pb Recovery, % | Zn Recovery, % |
|---|---|---|---|---|---|---|---|
| Pb Conc. | 101.85 | 10.6 | 23.2 | 11.4 | 7.3 | 62.3 | 13.6 |
| Zn Conc. | 200.66 | 20.9 | 4.9 | 30.4 | 5.6 | 25.8 | 71.8 |
| Tailings | 656.1 | 68.4 | 0.7 | 1.9 | 17.7 | 11.8 | 14.6 |
| Total | 958.61 | 100.0 | 4.0 | 8.9 | 14.0 | 100.0 | 100.0 |
| **XRF** | Weight, g | Weight Distr. % | Pb Grade, % | Zn Grade, % | Fe Grade, % | Pb Recovery, % | Zn Recovery, % |
| Pb Conc. | 109.28 | 11.4 | 30.6 | 18.1 | 6.0 | 76.6 | 15.8 |
| Zn Conc. | 212.9 | 22.2 | 2.4 | 44.2 | 5.5 | 11.8 | 75.2 |
| Tailings | 635.1 | 66.3 | 0.8 | 1.8 | 27.5 | 11.6 | 9.0 |
| | 957.28 | 100.0 | 4.6 | 13.1 | 20.1 | 100.0 | 100.0 |
| **XRF2** | Weight, g | Weight Distr. % | Pb Grade, % | Zn Grade, % | Fe Grade, % | Pb Recovery, % | Zn Recovery, % |
| Pb Conc. | 98.36 | 10.2 | 50.7 | 4.5 | 6.1 | 78.3 | 7.0 |
| Zn Conc. | 258.6 | 26.8 | 3.2 | 46.1 | 5.0 | 13.0 | 88.0 |
| Tailings | 609.74 | 63.1 | 0.9 | 1.9 | 24.9 | 8.7 | 5.0 |
| Total | 966.7 | 100.0 | 6.6 | 14.0 | 17.7 | 100.0 | 100.0 |

# CHAPTER 5 CONCLUSIONS AND RECOMMENDATIONS

## 5.1 Conclusions

This thesis summarized the research testwork done on the technical evaluation of sensor-based ore sorting (XRF, XRT, Color and MW/IR) of a Mississippi Valley type lead-zinc ore sample from Pend Oreille Mine. A literature review found that automatic sensor-based ore sorting has been successfully applied to many base metal cases such as copper, nickel and gold. This laboratory-scale ore sorting amenability study of a lead-zinc ore, using different sensing technologies, will add valuable knowledge to the study of sensor-based ore sorting and will provide guidelines for ore sorting evaluation of other ore types.

Several conclusions can be drawn according to the testwork described in this thesis. The most valuable contribution of this work is the generation of a detailed evaluation process and methodology for ore sorting amenability study at laboratory-scale using certain sensor-based sorting techniques.

The X-ray sorting methods of fluorescence and transmission showed greatest potential for preconcentration of this lead-zinc ore based on the sorting results obtained in this study and therefore are recommended for large-scale testing and justification of the reliability. Optical sorting seemed to be not very effective for sorting this lead-zinc ore and hence not studied further. MW/IR sorting of lead-zinc bearing sulfide ore is promising but the sorting technique itself needs more development until industrial application.

### 5.1.1 Conclusions from the XRF Sorting Test

1. The procedures for laboratory-scale XRF sorting amenability study using a XRF analyzer were established. The grades of elements of interest are read using the XRF analyzer by averaging different faces' readings; sorting potential using this XRF analyzer is demonstrated by plotting the chemical assay results and XRF analyzer surface readings of the rocks on a sortability curve; a Grade-Recovery curve is obtained by separation at different threshold metal grades for sorting criterion determination; sorting results using this XRF analyzer are calculated.

2. X-Ray Fluorescence Sorting has been applied successfully in the separation of dolomitic waste rock from lead-zinc mineralized ore in this preliminary scope study using the Innov.X XRF Analyzer. The results have demonstrated that discrimination of element compositions on the surface of rock could be used and detected by a XRF analyzer to sort ores from barren gangues when:
    - a degree of “liberation” at certain particle size provides particles with different grades to be sorted (liberation here means the enrichment of valuable minerals/gangue minerals in the rock); and
    - a good correlation exists between the analysis of particle surface by XRF analyzer/XRF sorter and the analysis of bulk particle by chemical assay (a strong correlation between XRF surface reading and assays existed for our material).
3. It is observed that XRF sorting provided satisfactory results in rejecting barren waste rocks and therefore upgrading the mill feed. The overall sorting results of the 325 rocks sized above 26.5 mm (top size: bottom size = 3:1) demonstrated that above 95% of the Pb and Zn reporting to the feed could be recovered when rejecting 47.3% of mass as waste. Pb and Zn grades in the concentrate were calculated to be 7.11% and 15.28% compared to those in the head being 3.91% and 8.50% respectively (upgrade the head by a factor of approximate 1.8 for both Pb and Zn).
4. The finer the particle size, the better the sorting results are in terms of percentage mass rejected as waste. The -37.5+26.5 mm size fraction showed the best sorting results. When a Zn grade of 5.00% was selected as sorting threshold (cut-off grade), 96.5% Pb and 97.1% Zn could be recovered in the concentrate product with calculated grades of 7.61% of Pb and 21.04 % of Zn at a waste rejection of 52.8% by mass.

### 5.1.2 Conclusions from the XRT Sorting Test

1. A simple X-ray transmission image processing and analyzing method was developed in this study using GIMP software to determine the sorting criterion for XRT sorting of an ore sample. This method can be used as laboratory quick evaluation of an ore’s amenability to XRT sorting.
2. Sorting criteria used in this study included threshold average brightness value of single energy X-ray transmission image (high/low energy) and Ore Index

generated from dual-energy X-ray images (by CommoDas). The smaller the average brightness value of the X-ray image and the larger the Ore Index of the rock, the more likely the rock reported to the product fraction.

3. Clear distinction between lead-zinc bearing sulfide and dolomitic waste rock were observed using the XRT sorting technique. It is observed from the sorting results that above 36% mass of the feed can be rejected as waste when above 95% of Pb and Zn were recovered in the product by X-Ray transmission sorting. The calculated product grades of Pb and Zn were about 10% Pb and 14% Zn compared to 6% Pb and 9% Zn in the feed.
4. Similar sorting results were obtained using single energy X-ray transmission imaging (high/low energy) and dual-energy transmission imaging techniques primarily because the sample tested for this sorting technique had a narrow size range and therefore the effect of thickness on X-ray transmission could be neglected. The average brightness value of the X-ray image could be used as sorting criterion instead of the characteristic distribution of the brightness for all pixels within the image (each pixel is analyzed) because the ore sample sized –37.5+26.5 mm was well “liberated” (the rock either enriched in valuable minerals or gangue minerals) The average brightness value of the image could represent the average density composition (atomic number) of the rock due to the well liberation of the rock at this size. The sortability of the lead-zinc ore using X-Ray Transmission sorting could only be concluded for this specific case. The technical amenability of XRT sorting of other types of lead-zinc ore could be evaluated using similar procedures as this study.

### 5.1.3 Conclusions from the Optical Sorting Test

1. A methodology for laboratory-scale color sorting amenability studies was established based on the process of this color sorting study. The major steps are characterization of ore, sample preparation, sorting potential determination, image capture, data analysis and sorting result calculation. This methodology provides useful guidelines for designing and conducting future laboratory-scale color ore sorting amenability studies using optical bench-top image acquisition systems.
2. The results of color sorting of the Pend Oreille lead-zinc ore using simple and handy image analysis software indicated that color sorting was capable of

upgrading a sample of this lead-zinc ore sized -37.5+26.5 mm based on color differences. More specifically, the rejection of light grey dolomitic waste rocks led to about 19% reduction of the mass while recovering 98.5% and 97% of lead and zinc. Lead and zinc grades were upgraded to 7.64% and 10.43% respectively from 6.30% and 8.73% in the feed.

### 5.1.4 Conclusions from the MW/IR Sorting Test

1. The effect on microwave heating behaviour of heating time and weight/size of rock, as well as quantity of rocks being heated at the same time was investigated using a lead-zinc ore from industry.
2. The longer the heating time, the higher the average surface temperature of the rock. The finer the rock size, the smaller the rock weight, the less time the rocks are heated, and the smaller the quantity of rocks being heated at the same time, the more efficiently the microwave heating performs in terms of ore sorting.
3. This MW/IR sorting test work has indicated that carbonate gangue minerals in mineralized sulfide ore does not heat when exposed to microwave heating. This suggests that MW exposure of this type of ore, followed by IR sensing, is a possible method to metallurgically concentrate this lead-zinc ore by rejecting waste rock. While performance of samples from different size fractions varied a little, they all showed high metal recoveries as well as about 20-30% barren mass rejection. The smaller the size, the better the segregation of valuable ore and barren rock, and therefore the better the sorting results were in terms of grade/recovery.

### 5.1.5 Conclusions from the Impact Evaluation Test

1. The results of sorting impact evaluation testwork showed that the preconcentrate of X-ray fluorescence sorting had a Bond Work Index 12% smaller than that of the feed ore, which indicated potential grinding energy saving due to the removal of hard waste rock. The reduction of feed mass by up to 50% will also contribute to energy savings.
2. Flotation test results also presented the improvement of the overall lead and zinc recovery in the lead rougher flotation concentrate and zinc rougher flotation concentrate as well as the concentrate grade after XRF sorting. The reduction of feed mass by removing the dolomitic gangue minerals up to 50% by mass could also contribute to reagent savings in the flotation process.

## 5.2 Recommendations

Several recommendations are proposed for further study in two directions: recommendations on further evaluation of this lead-zinc ore's amenability to sensor-based ore sorting and recommendations on development of laboratory-scale sensor-based ore sorting evaluation.

### 5.2.1 Recommendations on Sensor-Based Ore Sorting of This Lead-Zinc Ore

1. Further tests using representative Run-of-Mine ore sample from different mineralization zones in the deposit should be conducted to evaluate the amenabilities of this lead-zinc ore to sensor-based ore sorting due to the limitation of the sample used in this study.
2. Large-scale testwork should include sorting tests of different particle sizes and degree of liberation and therefore optimizing the top size and top/bottom size ratio for sorting process using different sensing technologies.
3. Pilot-scale or full-scale sorting tests by commercial ore sorters should be conducted to justify the reliability of the sorting results obtained by this laboratory-scale preliminary study.

### 5.2.2 Recommendations on Development of Laboratory-Scale Sensor-Based Ore Sorting Evaluation

1. Ore sample mineral liberation study by optical thin section study or MLA should also be conducted to characterize the ore.
2. Advanced and updated XRF analyzer should be used in future XRF sorting study in order to achieve more accurate results.
3. Integration of advanced image analysis software into the bench-top image acquisition system to extract color information and determine sorting criterion for color sorting study.
4. Advanced DE- XRT image analysis system, which is capable of automated analyzing individual pixel in both of the high and low energy images and generating sorting criterion, should be considered for interpretation of the dual-energy image obtained in future DE-XRT sorting study.
5. Continuous microwave heating device should be used for further MW/IR study to eliminate the microwave oven warm-up characteristic, creating uncertainty in this work whether heating selectivity is lost for larger rocks (5 cm).

6. Limitations such as high cost of microwave generation, lack of reliable design of continuous microwave generator meeting the processing requirements of the automated MW/IR sorter and slow data processing speed of IR image are major problems need to be considered in the development of the MW/IR sorting technology in future study.

# REFERENCES


Allen, A., & Gordon, H. (2009, May). X-ray sorting and other technologies for upgrading nickel ore. *ALTA 2009 Nickel-Cobalt, Copper and Uranium Conference,* Perth, Australia.

Bamber, A. S. (2008). Integrated mining, preconcentration and waste disposal system for the increased sustainability of hard rock metal mining (Doctoral dissertation, University of British Columbia, Vancouver). Retrieved August 20, 2012 from http://circle.ubc.ca/handle/2429/779

Berry, T. F., & Bruce, R. W. (1966). A simple method of determining the grindability of ores. *Canadian Mining Journal, 6*(6), 63–65.

Bond, F. C. (1961). Crushing and grinding calculations part I and II. *British Chemical Engineering, 6*(6,8).

Bradshaw, S. M., Van Wyk, E. J., & Swardt, J. B. (1998). Microwave heating principles and the application to the regeneration of granular activated carbon. *Journal of the South African Institute of Mining and Metallurgy, 98*(4), 201–212.

Bulled, D. (1997). A new full colour sorter for rocks too small to hand sort*. 2 Endüstriyel Hammaddeler Sempozyumu, 16-17 Ekim 1997*, İzmir, Türkiye (pp. 92–96). Retrieved July 23, 2012 from http://www.google.ca/url?sa=t&rct=j&q=&esrc=s&frm=1&source=web&cd=1&ved=0CGwQFjAA&url=http%3A%2F%2Fwww.maden.org.tr%2Fresimler%2Fekler%2F613e70fd9f59310_ek.pdf&ei=qwMOULWaIoHkqAGByoCYCQ&usg=AFQjCNHkqLa7cUiKWht0vEvrMf_OUTg89g&sig2=ykE7eRYSOXaxGlAMWW3Yog

CommoDas GmbH. (2004). Product Brochures and Marketing Material, Wedel, Germany.

De Jong, T. P. R. (2012). Automatic rock sorting. Retrieved July 31, 2012, from http://citg.tudelft.nl/index.php?id=19616&L=1

De Jong, T. P. R., Dalmijn, W. L., & Kattubtudt, H. U. R. (2003). Dual energy X-ray transmission imaging for the concentration and control of solids. *Proceedings of the XXII International Mineral Processing Congress, IMPC-2003,* Cape Town, South Africa.

De Jong, T. P. R., & Harbeck, H. (2005). Automatic sorting of minerals: Current status and future outlook. *Proceedings of the 37th Annual Meeting of the Canadian Mineral Processors,* Ottawa, Canada (pp. 629–648).

Fattori, L. (2009). Optical electromagnetic and X-ray sorters improve efficiencies for the mineral industry. *Ontario Mineral Exploration Review* (Spring), 15–17. Retrieved July 20, 2012 from http://www.google.ca/url?sa=t&rct=j&q=&esrc=s&frm=1&source=web&cd=1&ved=0CFAQFjAA&url=http%3A%2F%2Fwww.CommoDas-ultrasort.com%2Fassets%2Fx%2F50133&ei=zuwJULqDC9L3rAGaotDVCg&usg=AFQjCNHpnQuWTFRDLATk32jyLBvvVG9jrQ&sig2=bnoiYMsa5FK-tzu82ZD_LQ

Fickling, R. S. (2011). An introduction to the RADOS XRF ore sorter. *The Southern African Institute of Mining and Metallurgy 6th Southern African Base Metals Conference 2011,* Phalaborwa, South Africa (pp. 99-110). Retrieved on July 15th, 2012 from http://www.google.ca/url?sa=t&rct=j&q=&esrc=s&frm=1&source=web&cd=1&ved=0CDEQFjAA&url=http%3A%2F%2Fwww.saimm.co.za%2FConferences%2FBM2011%2F099-Fickling.pdf&ei=6Og_UP29KoiVjALX3YDgDw&usg=AFQjCNHQhX_bthXMhJ5lr89ahUKgXF8M5Q&sig2=2dglzwx8RjtB6Wsvz-mQ7g

Fitzpatrick, R. (2008). The development of a methodology for automated sorting in the minerals industry. (Doctoral dissertation, University of Exeter). Retrieved from https://eric.exeter.ac.uk/repository/handle/10036/68635

Harbeck, H. (2004, May). Classification of minerals with the use of X-ray transmission. *Colloquim Sensorgestutzte Sortierung,* Stolberg, Germany.

Hua, Y., & Liu, C. (1996). Heating rate of minerals and compounds in microwave field. *Transactions of Nonferrous Metals Society of China, 6*(1), 35–40.

Huntting, M. T. (1966). Washington mineral deposits. Washington Division of Mines and Geology Reprint No. 10. (Reprinted from *C.I.M.* Special Volume No.8, 209–214). Retrieved July 24, 2012, from http://www.google.ca/url?sa=t&rct=j&q=&esrc=s&frm=1&source=web&cd=4&ved=0CFAQFjAD&url=http%3A%2F%2Fwww.dnr.wa.gov%2FPublications%2Fger_reprint10_wa_min_dep.pdf&ei=4PAOUN3aO9DwiQKPoID4Dg&usg=AFQjCNHYesqsaAQaiiNIZKSf-xLi0ivUMw&sig2=PIGIjN5sundvtM5pERgZ8Q

Keys, N. J., Met, B. E., Gordon, R. J., & Peverett, N. F. (1974). Photometric sorting of ore on a South African gold mine. *Journal of the South African Institute of Mining and Metallurgy, 75*, 13–21.

Kidd, D. G. (1983). Photometric ore sorting. *Society of Mining Engineers of AIME Annual Meeting* (pp. 83–92.

Kingman, S. W., & Rowson, N. A. (1998). Microwave treatment of minerals: a review. *Minerals Engineering, 11*(11), 1081–1087. doi:10.1016/S0892-6875(98)00094-6

Kleine, C., Wotruba, H., Robben, M., von Ketelhodt, L., & Kowalczyk, M. (2011). Potential of sensor-based sorting for the gold mining industry. *Conference of Metallurgists 2011, World Gold Symposium,* Montreal, Quebec.

Kowalczyk, M. (2012). Preliminary ore sorting investigation bench-top amenability test: Radiometric, X-ray transmission, Optical for a project. (Project report). CommoDas Ultrasort, Surrey, Canada.

Kowalczyk, M., & Bartram, K. (2008). Sensor based sorting in the mining world. *Innovation in Global Mining. Terra Vision Ore Sorting Solutions, CommoDas Ulfrasort, Surrey, Canada.*

Kuilman, W. (2006). DE-XRT sorting of coal. *Sensor Based Sorting Conference* GDMB, Aachen, Germany. Retrieved July 31, 2012 from http://www.citg.tudelft.nl/en/about-faculty/departments/structural-

engineering/sections/materials-and-environment/chairs/recycling-technology/research/automatic-sorting/de-xrt-sorting-of-coal/.

Labbert, M., Baloun, T. A., Schoenherr, J. I., & Kuyumcu, H. Z. (2012). Studies on thermo-sensitive sorting of plastics. *Proceedings of Sensor Based Sorting 2012,* Aachen, Germany.

Manouchehri, H. R. (2003). Sorting: Possibilities, limitations and future. *Proceedings of Swedish Mineral Processing Research Association,* Stockholm. Retrieved July 20th, 2012 from http://www.google.ca/url?sa=t&rct=j&q=&esrc=s&frm=1&source=web&cd=1&ved=0CCYQFjAA&url=http%3A%2F%2Fpure.ltu.se%2Fportal%2Ffiles%2F299975%2Farticle&ei=Qvc_UOzyGKSEygHAt4DgDw&usg=AFQjCNHq8-aHnHQX2IdErKiewQdCKlYFbg&sig2=_kWn4bY2rTBrxy4GVzT9oA

Murphy, R. V., Maharaj, H., Lachapelle, J. & Yuen, P. K. (2010). Certification information and examination preparation booklet - operator of portable XRF analyzers (version 3). Retrieved July 12, 2012 from http://www.nrcan.gc.ca/minerals-metals/non-destructive-testing/application/2914

Singh, V., & Rao, S. M. (2005). Application of image processing and radial basis neural network techniques for ore sorting and ore classification. *Minerals Engineering, 18*, 1412–1420.

Strydom, H. (2010). The application of dual energy x-ray transmission sorting to the separation of coal from torbanite. (Master's thesis, University of the Witwatersrand, South Africa). Retrieved August 15, 2012 from http://wiredspace.wits.ac.za/handle/10539/9804

Tessier, J., Duchesne, C., & Bartolacci, G. (2007). A machine vision approach to on-line estimation of run-of-mine ore composition on conveyor belts. *Minerals Engineering, 20*, 1129–1144.

Udoudo, O. B. (2010). Modelling the efficiency of an automated sensor-based sorter. (Doctoral dissertation, University of Exeter, United Kingdom. Retrieved August 19, 2012 from https://eric.exeter.ac.uk/repository/handle/10036/118786

Van Weert, G., & Kondos, P. (2007). Infrared recognition of high sulphide and carbonaceous rocks after microwave heating. *Proceedings of 39 The Annual Meeting of the Canadian Mineral Processors Conference,* Ottawa, ON. 345–363. Retrieved July 14th, 2012 from http://www.google.ca/url?sa=t&rct=j&q=&esrc=s&frm=1&source=web&cd=1&ved=0CCcQFjAA&url=http%3A%2F%2Fwww.infomine.com%2Fpublications%2Fdocs%2FVanWeert2007.pdf&ei=afM_UN7OJcjdigLYrID4AQ&usg=AFQjCNF8p5oHugQpoCHJUz6EfOTS6YPGsw&sig2=pLj4Zmqy6WE4UyrUmZLk8A

Van Weert, G., & Kondos, P. (2008, March). Effects of susceptor size and concentration on the efficiency of microwave/infrared (MW/IR) sorting. *RWTH Aachen University's Sensorgestuetzte Sortierung (Sensor Based Sorting) Conference,* Aachen, Germany.

Van Weert, G., Kondos, P., & Gluck, E. (2009). Upgrading molybdenite ores between mine and mill using microwave/infrared (MW/IR) sorting technology. *Proceedings of the Forty-First Canadian Mineral Processors Conference,* Ottawa, Canada (pp. 509–521). Copy supplied by G. Van Weert.

Van Weert, G., Kondos, P., & Wang, O. (2011). Microwave heating of sulphide minerals as a function of their size and spatial distribution. *Journal of Canadian Institute of Mining, Metallurgy and Petroleum, 2*(3), 117–124.

Von Ketelhodt, L. (2009). Sensor based sorting: New developments. *Mintek 75th Anniversary Conference, June 4th 2009. CommoDas Ultrasort*, Randburg, South Africa.

Von Ketelhodt, L., & Bergmann, C. (2010). Dual energy X-ray transmission sorting of coal. *Journal of the South African Institute of Mining and Metallurgy, 110*, 371–378.

Wood, R. E. (1959). X-ray mineral analysis techniques. *Mining Engineering, 11*, 602-604.

Wotruba, H., & Harbeck, H. (2010). Sensor-based sorting. In *Ullmann's Encyclopedia of Industrial. Chemistry*, Wiley-VCH Verlag.

Zinc mining news: Pend Oreille Mine to reopen. (2004, March 3). *Canadian Mining Journal*. Retrieved August 10th, 2011 from http://www.canadianminingjournal.com/news/zinc-mining-news--pend-oreille-mine-to-reopen/1000013128/

# APPENDICES

## APPENDIX A X-RAY FLUORESCENCE SORTING DATA

**Surface Analysis of Rocks from Four Size Fractions by the Innov.X XRF Analyzer**
**-37.5+26.5 mm Size Fraction**

| Sample ID | Weight, g | Metal Grade, % | | |
|---|---|---|---|---|
| | | Pb | Zn | Fe |
| PO106-1 | 83.7 | 1.54 | 4.70 | 2.83 |
| PO106-2 | 125.5 | 4.01 | 28.89 | 16.11 |
| PO106-3 | 140.2 | 3.03 | 49.22 | 6.10 |
| PO106-4 | 62.6 | 0.05 | 0.38 | 2.68 |
| PO106-5 | 72.7 | 0.04 | 0.29 | 0.87 |
| PO106-6 | 86.7 | 9.75 | 17.20 | 17.14 |
| PO106-7 | 68.2 | 0.06 | 0.38 | 1.24 |
| PO106-8 | 107.5 | 21.66 | 41.42 | 4.39 |
| PO106-9 | 70.1 | 0.06 | 0.28 | 1.49 |
| PO106-10 | 59.8 | 0.07 | 0.29 | 1.37 |
| PO106-11 | 68.9 | 0.09 | 12.58 | 1.10 |
| PO106-12 | 47.9 | 0.21 | 33.67 | 7.23 |
| PO106-13 | 55.6 | 0.03 | 0.13 | 1.08 |
| PO106-14 | 149.9 | 0.05 | 1.74 | 2.02 |
| PO106-15 | 54.7 | 0.03 | 0.14 | 1.05 |
| PO106-16 | 57.9 | 11.54 | 40.07 | 2.98 |
| PO106-17 | 118.4 | 0.52 | 0.85 | 27.81 |
| PO106-18 | 55.2 | 0.02 | 0.15 | 2.40 |
| PO106-19 | 87.9 | 0.87 | 3.13 | 34.78 |
| PO106-20 | 74.3 | 0.07 | 0.52 | 0.92 |
| PO106-21 | 115.5 | 2.31 | 53.06 | 10.78 |
| PO106-22 | 78.7 | 0.36 | 38.36 | 5.96 |
| PO106-23 | 186.6 | 12.55 | 20.09 | 18.07 |
| PO106-24 | 190.7 | 14.72 | 62.55 | 2.52 |
| PO106-25 | 103.7 | 13.59 | 57.45 | 3.46 |
| PO106-26 | 53.7 | 0.06 | 0.45 | 2.36 |
| PO106-27 | 59.2 | 3.67 | 5.68 | 9.37 |
| PO106-28 | 92.5 | 0.60 | 1.71 | 41.92 |
| PO106-29 | 63.7 | 9.33 | 33.96 | 14.40 |
| PO106-30 | 115.0 | 1.33 | 25.70 | 15.51 |
| PO106-31 | 120.9 | 0.04 | 0.21 | 3.77 |

| Sample ID | Weight, g | Metal Grade, % | | |
|---|---|---|---|---|
| | | Pb | Zn | Fe |
| PO106-32 | 101.6 | 0.57 | 23.44 | 19.75 |
| PO106-33 | 45.9 | 0.03 | 0.15 | 3.12 |
| PO106-34 | 36.6 | 0.30 | 28.96 | 6.01 |
| PO106-35 | 64.5 | 3.10 | 13.56 | 20.91 |
| PO106-36 | 56.7 | 1.43 | 19.86 | 17.37 |
| PO106-37 | 52.7 | 0.68 | 45.51 | 12.16 |
| PO106-38 | 101.3 | 0.05 | 0.29 | 3.66 |
| PO106-39 | 103.9 | 0.04 | 0.18 | 1.67 |
| PO106-40 | 78.9 | 0.18 | 1.93 | 3.92 |
| PO106-41 | 41.9 | 0.03 | 1.83 | 1.53 |
| PO106-42 | 101.8 | 0.10 | 1.37 | 3.31 |
| PO106-43 | 71.7 | 0.03 | 0.15 | 0.71 |
| PO106-44 | 79.6 | 0.31 | 25.69 | 10.92 |
| PO106-45 | 47.3 | 0.05 | 0.59 | 1.39 |
| PO106-46 | 71.1 | 0.08 | 0.72 | 1.13 |
| PO106-47 | 80.6 | 0.04 | 0.24 | 2.47 |
| PO106-48 | 70.6 | 0.21 | 16.28 | 9.51 |
| PO106-49 | 83.5 | 1.60 | 3.97 | 3.34 |
| PO106-50 | 137.1 | 0.79 | 46.72 | 2.91 |
| PO106-51 | 93.0 | 0.29 | 16.64 | 13.95 |
| PO106-52 | 142.0 | 0.04 | 0.29 | 1.93 |
| PO106-53 | 53.7 | 0.20 | 2.11 | 9.82 |
| PO106-54 | 109.9 | 0.31 | 9.03 | 13.15 |
| PO106-55 | 150.7 | 1.21 | 44.39 | 1.97 |
| PO106-56 | 55.5 | 0.05 | 3.55 | 1.66 |
| PO106-57 | 164.7 | 0.19 | 28.54 | 3.49 |
| PO106-58 | 47.0 | 0.03 | 0.22 | 1.44 |
| PO106-59 | 79.0 | 0.04 | 0.24 | 1.17 |
| PO106-60 | 50.0 | 0.03 | 0.17 | 9.50 |
| PO106-61 | 125.9 | 0.30 | 15.01 | 11.99 |
| PO106-62 | 118.5 | 0.29 | 14.78 | 7.70 |
| PO106-63 | 40.8 | 0.09 | 2.37 | 17.57 |
| PO106-64 | 45.6 | 0.07 | 4.90 | 0.89 |
| PO106-65 | 62.8 | 0.03 | 0.20 | 4.48 |
| PO106-66 | 156.5 | 0.31 | 1.73 | 26.31 |
| PO106-67 | 89.2 | 0.20 | 20.40 | 8.13 |
| PO106-68 | 49.2 | 0.15 | 3.12 | 12.31 |

| Sample ID | Weight, g | Metal Grade, % | | |
|---|---|---|---|---|
| | | Pb | Zn | Fe |
| PO106-69 | 109.0 | 0.30 | 23.91 | 8.72 |
| PO106-70 | 85.0 | 0.04 | 0.38 | 8.32 |
| PO106-71 | 62.9 | 25.99 | 28.30 | 10.35 |
| PO106-72 | 50.1 | 0.05 | 0.32 | 1.14 |
| PO106-73 | 40.5 | 0.07 | 0.39 | 1.39 |
| PO106-74 | 79.1 | 0.81 | 5.87 | 36.08 |
| PO106-75 | 44.6 | 0.07 | 1.43 | 3.79 |
| PO106-76 | 53.7 | 0.02 | 0.14 | 0.73 |
| PO106-77 | 37.2 | 0.02 | 0.11 | 0.84 |
| PO106-78 | 52.9 | 0.42 | 0.94 | 38.94 |
| PO106-79 | 166.7 | 0.30 | 41.55 | 4.72 |
| PO106-80 | 85.4 | 0.06 | 0.28 | 1.66 |
| PO106-81 | 80.5 | 0.55 | 3.14 | 32.20 |
| PO106-82 | 79.6 | 0.73 | 2.07 | 37.06 |
| PO106-83 | 60.1 | 0.19 | 1.30 | 13.31 |
| PO106-84 | 39.3 | 0.53 | 7.82 | 36.34 |
| PO106-85 | 41.8 | 0.15 | 11.38 | 4.64 |
| PO106-86 | 132.3 | 0.72 | 1.35 | 25.62 |
| PO106-87 | 67.0 | 0.24 | 28.71 | 13.22 |
| PO106-88 | 73.3 | 0.06 | 0.41 | 2.69 |
| PO106-89 | 55.1 | 0.05 | 0.32 | 1.18 |
| PO106-90 | 77.2 | 0.10 | 0.33 | 6.75 |
| PO106-91 | 50.9 | 0.25 | 21.44 | 8.55 |
| PO106-92 | 62.0 | 0.02 | 0.15 | 1.41 |
| PO106-93 | 63.2 | 0.04 | 1.31 | 2.78 |
| PO106-94 | 85.1 | 0.59 | 1.67 | 24.82 |
| PO106-95 | 44.8 | 0.02 | 0.12 | 7.58 |
| PO106-96 | 55.7 | 0.11 | 26.02 | 3.00 |
| PO106-97 | 76.8 | 2.95 | 23.35 | 8.50 |
| PO106-98 | 59.6 | 0.10 | 1.53 | 15.53 |
| PO106-99 | 77.9 | 0.02 | 0.18 | 0.89 |
| PO106-100 | 80.0 | 6.27 | 27.32 | 15.16 |

**-53+37.5 mm Size Fraction**

| Sample ID | Weight, g | Metal Grade, % | | |
|---|---|---|---|---|
| | | Pb | Zn | Fe |
| PO150-1 | 91.2 | 0.07 | 0.29 | 1.06 |
| PO150-2 | 165.8 | 0.05 | 0.38 | 10.33 |
| PO150-3 | 197.4 | 0.05 | 1.26 | 1.13 |
| PO150-4 | 254.4 | 0.44 | 7.52 | 21.40 |
| PO150-5 | 229.1 | 0.02 | 0.20 | 1.03 |
| PO150-6 | 231.6 | 0.04 | 0.27 | 1.00 |
| PO150-7 | 150.1 | 0.09 | 1.29 | 1.86 |
| PO150-8 | 337.5 | 0.22 | 20.03 | 8.26 |
| PO150-9 | 254.1 | 0.54 | 3.51 | 31.02 |
| PO150-10 | 261.8 | 0.33 | 1.95 | 13.64 |
| PO150-11 | 93.5 | 2.29 | 43.80 | 2.09 |
| PO150-12 | 184.3 | 0.04 | 0.33 | 1.37 |
| PO150-13 | 281.5 | 0.06 | 0.39 | 2.24 |
| PO150-14 | 129.2 | 0.31 | 31.41 | 5.49 |
| PO150-15 | 619.1 | 12.82 | 46.03 | 4.67 |
| PO150-16 | 234.9 | 15.27 | 45.66 | 5.50 |
| PO150-17 | 136.9 | 0.51 | 0.78 | 25.17 |
| PO150-18 | 166.7 | 0.10 | 1.73 | 1.15 |
| PO150-19 | 358.0 | 9.42 | 24.73 | 13.91 |
| PO150-20 | 105.3 | 0.10 | 1.29 | 3.44 |
| PO150-21 | 285.4 | 0.08 | 0.54 | 1.32 |
| PO150-22 | 324.9 | 0.35 | 16.94 | 16.36 |
| PO150-23 | 154.9 | 0.08 | 0.38 | 9.18 |
| PO150-24 | 179.9 | 12.10 | 27.04 | 10.10 |
| PO150-25 | 134.9 | 0.08 | 0.39 | 1.61 |
| PO150-26 | 397.1 | 16.23 | 54.14 | 4.78 |
| PO150-27 | 292.4 | 10.04 | 26.15 | 12.03 |
| PO150-28 | 204.6 | 0.56 | 28.56 | 13.69 |
| PO150-29 | 225.0 | 10.33 | 27.11 | 15.38 |
| PO150-30 | 92.9 | 0.09 | 3.75 | 1.53 |
| PO150-31 | 150.4 | 0.03 | 0.22 | 0.86 |
| PO150-32 | 444.5 | 0.13 | 3.96 | 3.89 |
| PO150-33 | 223.1 | 0.08 | 0.58 | 1.78 |
| PO150-34 | 93.4 | 0.04 | 0.15 | 1.12 |
| PO150-35 | 221.4 | 0.33 | 38.33 | 7.48 |
| PO150-36 | 298.3 | 0.03 | 0.12 | 0.61 |
| PO150-37 | 207.0 | 0.04 | 0.17 | 0.90 |

| Sample ID | Weight, g | Metal Grade, % | | |
|---|---|---|---|---|
| | | Pb | Zn | Fe |
| PO150-38 | 127.7 | 0.08 | 0.37 | 0.91 |
| PO150-39 | 142.9 | 0.05 | 0.23 | 0.89 |
| PO150-40 | 200.2 | 0.28 | 16.32 | 10.88 |
| PO150-41 | 239.0 | 0.07 | 0.30 | 2.84 |
| PO150-42 | 106.6 | 0.05 | 0.35 | 9.40 |
| PO150-43 | 379.4 | 5.37 | 14.59 | 5.55 |
| PO150-44 | 218.0 | 0.69 | 4.13 | 23.87 |
| PO150-45 | 122.6 | 0.12 | 0.45 | 1.66 |
| PO150-46 | 85.4 | 0.09 | 6.47 | 4.41 |
| PO150-47 | 150.3 | 0.11 | 4.24 | 5.47 |
| PO150-48 | 324.3 | 0.25 | 2.22 | 15.58 |
| PO150-49 | 268.5 | 0.13 | 1.31 | 5.12 |
| PO150-50 | 288.1 | 22.22 | 29.02 | 7.99 |
| PO150-51 | 153.0 | 0.33 | 15.30 | 19.54 |
| PO150-52 | 119.3 | 0.06 | 0.26 | 1.03 |
| PO150-53 | 88.4 | 0.07 | 0.95 | 2.74 |
| PO150-54 | 143.8 | 0.06 | 0.23 | 1.01 |
| PO150-55 | 273.2 | 0.09 | 0.23 | 7.80 |
| PO150-56 | 253.4 | 7.99 | 31.32 | 10.98 |
| PO150-57 | 306.8 | 0.40 | 1.20 | 33.13 |
| PO150-58 | 149.8 | 0.14 | 19.19 | 7.16 |
| PO150-59 | 209.5 | 3.01 | 24.71 | 13.10 |
| PO150-60 | 93.9 | 0.17 | 8.21 | 6.58 |
| PO150-61 | 182.7 | 0.54 | 45.57 | 2.07 |
| PO150-62 | 146.3 | 0.10 | 12.70 | 3.41 |
| PO150-63 | 345.6 | 0.46 | 1.53 | 19.20 |
| PO150-64 | 235.2 | 0.60 | 12.29 | 5.09 |
| PO150-65 | 199.7 | 0.72 | 29.19 | 8.51 |
| PO150-66 | 153.1 | 0.04 | 0.28 | 7.15 |
| PO150-67 | 252.9 | 0.82 | 8.74 | 36.06 |
| PO150-68 | 250.1 | 0.42 | 2.11 | 27.23 |
| PO150-69 | 156.1 | 0.17 | 8.01 | 8.32 |
| PO150-70 | 93.1 | 0.06 | 0.25 | 0.84 |
| PO150-71 | 165.2 | 8.07 | 11.81 | 22.68 |
| PO150-72 | 568.4 | 17.21 | 36.46 | 8.69 |
| PO150-73 | 131.1 | 0.28 | 17.75 | 3.15 |
| PO150-74 | 89.4 | 0.07 | 0.25 | 2.25 |
| PO150-75 | 95.3 | 0.07 | 0.27 | 1.40 |
| PO150-76 | 138.2 | 0.05 | 0.21 | 1.06 |

| Sample ID | Weight, g | Metal Grade, % | | |
|---|---|---|---|---|
| | | Pb | Zn | Fe |
| PO150-77 | 20.2 | 0.07 | 0.29 | 1.08 |
| PO150-78 | 147.1 | 0.08 | 9.20 | 1.38 |
| PO150-79 | 111.2 | 0.07 | 0.28 | 1.33 |
| PO150-80 | 225.0 | 0.44 | 42.58 | 4.67 |
| PO150-81 | 109.6 | 0.07 | 0.60 | 2.59 |
| PO150-82 | 246.5 | 1.35 | 22.44 | 3.30 |
| PO150-83 | 100.6 | 0.05 | 0.30 | 1.78 |
| PO150-84 | 211.6 | 0.09 | 2.49 | 4.03 |
| PO150-85 | 322.2 | 3.02 | 9.25 | 9.03 |
| PO150-86 | 218.3 | 3.22 | 12.41 | 17.29 |
| PO150-87 | 133.1 | 0.09 | 0.49 | 1.96 |
| PO150-88 | 137.7 | 0.14 | 18.09 | 1.44 |
| PO150-89 | 190.8 | 0.11 | 0.46 | 1.63 |
| PO150-90 | 146.7 | 0.07 | 0.36 | 2.84 |
| PO150-91 | 271.5 | 19.03 | 32.38 | 8.87 |
| PO150-92 | 236.1 | 4.37 | 15.08 | 13.88 |
| PO150-93 | 185.2 | 2.38 | 19.23 | 18.07 |
| PO150-94 | 305.2 | 0.78 | 2.75 | 19.60 |
| PO150-95 | 286.4 | 0.24 | 13.16 | 10.03 |
| PO150-96 | 137.3 | 0.13 | 7.16 | 6.30 |
| PO150-97 | 302.9 | 3.81 | 10.78 | 14.10 |
| PO150-98 | 84.9 | 0.07 | 0.39 | 1.13 |
| PO150-99 | 285.7 | 0.44 | 14.82 | 7.59 |
| PO150-100 | 73.8 | 0.13 | 1.40 | 6.99 |

**-75+53 mm Size Fraction**

| Sample | Weight, g | Metal Grade, % | | |
|---|---|---|---|---|
| | | Pb | Zn | Fe |
| PO212-1 | 363 | 3.32 | 18.64 | 22.87 |
| PO212-2 | 750.1 | 0.21 | 0.67 | 6.41 |
| PO212-3 | 766.9 | 0.22 | 27.59 | 4.11 |
| PO212-4 | 673.1 | 0.08 | 0.71 | 2.82 |
| PO212-5 | 667.5 | 8.86 | 40.34 | 7.06 |
| PO212-6 | 208.3 | 0.11 | 1.23 | 1.65 |
| PO212-7 | 598.5 | 0.77 | 8.17 | 25.66 |
| PO212-8 | 340.1 | 0.08 | 0.66 | 6.14 |
| PO212-9 | 543.3 | 0.43 | 7.69 | 16.16 |
| PO212-10 | 857.6 | 0.42 | 2.15 | 21.57 |
| PO212-11 | 617.9 | 2.24 | 41.06 | 8.28 |
| PO212-12 | 1104.7 | 6.29 | 12.93 | 7.72 |
| PO212-13 | 535.5 | 11.45 | 16.43 | 10.32 |
| PO212-14 | 421.4 | 0.39 | 27.69 | 6.45 |
| PO212-15 | 782.7 | 0.03 | 0.15 | 0.92 |
| PO212-16 | 454.3 | 0.04 | 0.20 | 1.04 |
| PO212-17 | 475.6 | 0.03 | 0.15 | 0.97 |
| PO212-18 | 855.3 | 0.03 | 0.27 | 1.24 |
| PO212-19 | 454.8 | 0.03 | 0.48 | 0.70 |
| PO212-20 | 820.5 | 0.30 | 20.90 | 10.94 |
| PO212-21 | 492.8 | 0.34 | 3.91 | 5.54 |
| PO212-22 | 436.6 | 22.23 | 46.02 | 4.92 |
| PO212-23 | 917.6 | 0.03 | 0.24 | 0.99 |
| PO212-24 | 919.4 | 0.67 | 15.60 | 24.56 |
| PO212-25 | 409.0 | 1.59 | 33.16 | 6.94 |
| PO212-26 | 438.5 | 1.02 | 10.17 | 3.62 |
| PO212-27 | 273.0 | 0.03 | 0.31 | 0.86 |
| PO212-28 | 528.5 | 0.34 | 38.30 | 5.65 |
| PO212-29 | 411.8 | 0.14 | 17.88 | 5.54 |
| PO212-30 | 930.7 | 0.51 | 4.39 | 23.18 |
| PO212-31 | 916.9 | 0.72 | 16.09 | 21.88 |
| PO212-32 | 438.1 | 5.99 | 19.00 | 19.70 |
| PO212-33 | 769.9 | 15.73 | 27.89 | 7.98 |
| PO212-34 | 355.1 | 0.24 | 0.36 | 1.75 |
| PO212-35 | 439.5 | 0.65 | 27.50 | 9.73 |
| PO212-36 | 340.0 | 0.09 | 0.35 | 2.43 |
| PO212-37 | 262.4 | 1.24 | 13.97 | 5.73 |

| Sample | Weight, g | Metal Grade, % | | |
|---|---|---|---|---|
| | | Pb | Zn | Fe |
| PO212-38 | 393.2 | 0.15 | 12.55 | 2.10 |
| PO212-39 | 388.1 | 0.35 | 9.70 | 4.61 |
| PO212-40 | 457.8 | 0.19 | 0.61 | 10.14 |
| PO212-41 | 323.1 | 3.26 | 35.18 | 7.38 |
| PO212-42 | 684.3 | 0.56 | 33.42 | 8.76 |
| PO212-43 | 348.1 | 0.04 | 5.03 | 4.55 |
| PO212-44 | 462.9 | 0.81 | 1.64 | 34.41 |
| PO212-45 | 668.1 | 0.10 | 1.10 | 4.36 |
| PO212-46 | 517.0 | 0.06 | 1.23 | 4.72 |
| PO212-47 | 382.6 | 0.04 | 0.30 | 2.09 |
| PO212-48 | 532.0 | 7.68 | 23.96 | 12.97 |
| PO212-49 | 740.7 | 1.03 | 14.48 | 11.47 |
| PO212-50 | 663.1 | 4.74 | 7.13 | 8.42 |
| PO212-51 | 422.2 | 0.05 | 0.30 | 1.77 |
| PO212-52 | 827.9 | 13.60 | 36.08 | 6.08 |
| PO212-53 | 733.3 | 6.21 | 18.62 | 21.14 |
| PO212-54 | 214.9 | 0.12 | 0.49 | 1.89 |
| PO212-55 | 425.5 | 0.20 | 1.09 | 10.04 |
| PO212-56 | 1025.6 | 0.66 | 2.24 | 27.88 |
| PO212-57 | 542.6 | 0.10 | 0.66 | 3.56 |
| PO212-58 | 786.4 | 0.68 | 16.00 | 12.74 |
| PO212-59 | 454.9 | 0.61 | 13.66 | 14.76 |
| PO212-60 | 405.8 | 0.07 | 0.40 | 2.41 |
| PO212-61 | 335.2 | 17.82 | 37.58 | 8.65 |
| PO212-62 | 631.0 | 2.28 | 21.67 | 7.13 |
| PO212-63 | 1148.5 | 11.16 | 20.21 | 7.67 |
| PO212-64 | 719.4 | 0.67 | 8.37 | 31.15 |
| PO212-65 | 786.0 | 12.32 | 37.69 | 9.23 |
| PO212-66 | 474.0 | 0.10 | 0.71 | 3.29 |
| PO212-67 | 566.4 | 14.23 | 16.86 | 8.69 |
| PO212-68 | 506.8 | 0.19 | 15.00 | 6.40 |
| PO212-69 | 482.0 | 3.54 | 17.09 | 16.13 |
| PO212-70 | 664.4 | 0.93 | 11.83 | 16.06 |
| PO212-71 | 682.3 | 5.44 | 19.98 | 6.61 |
| PO212-72 | 770.3 | 7.29 | 12.33 | 14.41 |
| PO212-73 | 860.7 | 0.14 | 2.99 | 8.59 |
| PO212-74 | 1024.9 | 0.40 | 4.43 | 10.67 |
| PO212-75 | 937.6 | 0.70 | 35.55 | 14.27 |

**+75 mm Size Fraction**

| Sample | Weight, g | Metal Grade,% | | |
|---|---|---|---|---|
| | | Pb | Zn | Fe |
| PO300-1 | 1081.9 | 0.24 | 6.34 | 11.47 |
| PO300-2 | 1570.5 | 0.59 | 1.02 | 18.43 |
| PO300-3 | 897.1 | 0.07 | 0.47 | 6.36 |
| PO300-4 | 2509.9 | 0.86 | 16.21 | 5.44 |
| PO300-5 | 1237.3 | 0.14 | 19.26 | 4.75 |
| PO300-6 | 1281.3 | 0.29 | 3.14 | 23.30 |
| PO300-7 | 898.4 | 0.93 | 7.65 | 18.30 |
| PO300-8 | 1097.1 | 0.08 | 27.52 | 2.87 |
| PO300-9 | 1551.3 | 0.03 | 0.22 | 6.87 |
| PO300-10 | 801.7 | 0.03 | 0.14 | 2.26 |
| PO300-11 | 1106.9 | 1.46 | 11.09 | 8.38 |
| PO300-12 | 820.1 | 0.01 | 0.10 | 0.91 |
| PO300-13 | 1326.9 | 0.56 | 9.11 | 26.68 |
| PO300-14 | 1907.9 | 0.68 | 5.73 | 33.30 |
| PO300-15 | 925.9 | 6.87 | 6.10 | 7.85 |
| PO300-16 | 1461.6 | 0.09 | 7.05 | 3.15 |
| PO300-17 | 1143.2 | 0.49 | 2.69 | 24.41 |
| PO300-18 | 977.0 | 0.02 | 0.22 | 1.71 |
| PO300-19 | 874.9 | 0.26 | 0.67 | 21.77 |
| PO300-20 | 979.8 | 0.13 | 6.68 | 5.85 |
| PO300-21 | 1049.1 | 0.03 | 0.28 | 9.40 |
| PO300-22 | 1000.3 | 0.09 | 0.62 | 4.09 |
| PO300-23 | 933.5 | 0.69 | 6.87 | 8.27 |
| PO300-24 | 1380.6 | 8.12 | 27.54 | 13.44 |
| PO300-25 | 1048.7 | 0.03 | 0.16 | 1.16 |
| PO300-26 | 1381.5 | 6.81 | 36.19 | 7.12 |
| PO300-27 | 1477.0 | 0.47 | 2.83 | 29.96 |
| PO300-28 | 885.6 | 1.75 | 5.90 | 6.03 |
| PO300-29 | 1063.4 | 1.01 | 22.82 | 4.29 |
| PO300-30 | 1753.8 | 0.48 | 2.09 | 31.05 |
| PO300-31 | 769.5 | 0.03 | 7.45 | 3.02 |
| PO300-32 | 794.4 | 0.04 | 0.18 | 1.95 |
| PO300-33 | 1659.8 | 0.69 | 2.55 | 14.55 |
| PO300-34 | 881.6 | 0.05 | 0.28 | 2.67 |
| PO300-35 | 1291.6 | 4.87 | 14.38 | 15.48 |
| PO300-36 | 1100.0 | 0.12 | 0.75 | 2.41 |
| PO300-37 | 1010.6 | 0.01 | 0.10 | 10.11 |

| Sample | Weight, g | Metal Grade,% | | |
|---|---|---|---|---|
| | | Pb | Zn | Fe |
| PO300-38 | 1824.2 | 0.64 | 3.20 | 21.34 |
| PO300-39 | 1813.8 | 10.17 | 28.00 | 13.23 |
| PO300-40 | 1266.6 | 0.04 | 0.14 | 9.69 |
| PO300-41 | 1307.2 | 0.66 | 15.39 | 19.17 |
| PO300-42 | 854.6 | 0.03 | 0.17 | 1.61 |
| PO300-43 | 1381.6 | 0.56 | 4.30 | 13.35 |
| PO300-44 | 1349.9 | 0.52 | 1.01 | 19.37 |
| PO300-45 | 1322.7 | 6.70 | 18.65 | 18.26 |
| PO300-46 | 1135.6 | 1.74 | 14.82 | 11.81 |
| PO300-47 | 588.4 | 0.02 | 0.17 | 0.88 |
| PO300-48 | 656.9 | 0.03 | 1.73 | 1.41 |
| PO300-49 | 1060.9 | 0.15 | 0.10 | 0.96 |
| PO300-50 | 1305.4 | 0.24 | 0.95 | 19.23 |

**XRF Surface Readings, XRF Powder Readings and Assays for Grouped Rocks for Four Size Fractions**
**-37.5+26.5 mm Size Fraction**

| Separation at Zn Grade of, % | -37.5+26.5 mm | Weight, g | XRF Surface Readings | | | XRF Powder Readings | | | Assay Results | | |
|---|---|---|---|---|---|---|---|---|---|---|---|
| | | | Pb Grade, % | Zn Grade, % | Fe Grade, % | Pb Grade, % | Zn Grade, % | Fe Grade, % | Pb Grade, % | Zn Grade, % | Fe Grade, % |
| **0.20** | 0-0.20 | 775.4 | 0.03 | 0.16 | 2.73 | 0.04 | 0.07 | 2.76 | 0.03 | 0.03 | 1.38 |
| **0.50** | 0.20-0.50 | 1424.2 | 0.05 | 0.31 | 2.50 | 0.12 | 0.12 | 5.60 | 0.09 | 0.06 | 4.32 |
| **1.00** | 0.50-1.00 | 364.1 | 0.26 | 0.74 | 14.04 | 0.40 | 0.63 | 19.99 | 0.28 | 0.31 | 16.70 |
| **2.00** | 1.00-2.00 | 1066.3 | 0.29 | 1.59 | 13.74 | 0.37 | 1.42 | 27.13 | 0.24 | 0.53 | 24.40 |
| **5.00** | 2.00-5.00 | 660.0 | 0.71 | 3.34 | 15.25 | 1.13 | 4.24 | 18.87 | 0.84 | 2.42 | 17.70 |
| **10.00** | 5.00-10.00 | 287.5 | 1.17 | 7.30 | 23.74 | 2.50 | 5.14 | 21.85 | 2.02 | 3.12 | 20.60 |
| **15.00** | 10.00-15.00 | 293.5 | 0.84 | 13.51 | 8.59 | 1.23 | 13.75 | 19.06 | 1.00 | 9.33 | 20.10 |
| **20.00** | 15.00-20.00 | 432.9 | 2.45 | 16.64 | 13.99 | 4.32 | 17.13 | 20.10 | 3.59 | 12.70 | 21.30 |
| **30.00** | 20.00-30.00 | 1401.0 | 3.98 | 25.10 | 11.03 | 7.46 | 26.92 | 15.58 | 6.34 | 20.00 | 18.00 |
| | +30.00 | 1413.1 | 6.31 | 47.35 | 6.12 | 13.65 | 37.69 | 9.76 | 12.60 | 30.70 | 11.30 |
| **Total/Head Grade, %** | | 8118.0 | 2.11 | 14.79 | 9.24 | 4.21 | 13.39 | 14.16 | 3.72 | 10.21 | 13.95 |

**-53+37.5 mm Size Fraction**

| Separation at Zn Grade of, % | -53+37.5 mm | Weight, g | XRF Surface Readings | | | XRF Powder Readings | | | Assay Results | | |
|---|---|---|---|---|---|---|---|---|---|---|---|
| | | | Pb Grade, % | Zn Grade, % | Fe Grade, % | Pb Grade, % | Zn Grade, % | Fe Grade, % | Pb Grade, % | Zn Grade, % | Fe Grade, % |
| **0.25** | 0-0.25 | 1858.8 | 0.05 | 0.20 | 1.97 | 0.06 | 0.42 | 2.87 | 0.03 | 0.19 | 1.56 |
| **0.50** | 0.25-0.50 | 2995.3 | 0.07 | 0.35 | 3.12 | 0.19 | 0.56 | 2.84 | 0.14 | 0.23 | 1.53 |
| **1.00** | 0.50-1.00 | 843.4 | 0.15 | 0.64 | 5.63 | 0.23 | 0.93 | 7.37 | 0.16 | 0.48 | 6.99 |
| **2.00** | 1.00-2.00 | 1876.0 | 0.25 | 1.46 | 12.43 | 0.23 | 1.42 | 16.46 | 0.16 | 0.70 | 16.30 |
| **5.00** | 2.00-5.00 | 2251.0 | 0.36 | 3.18 | 15.32 | 0.49 | 6.29 | 22.54 | 0.35 | 3.41 | 23.40 |
| **10.00** | 5.00-10.00 | 1449.3 | 0.95 | 8.29 | 14.37 | 2.70 | 12.70 | 18.72 | 2.39 | 8.31 | 21.50 |
| **20.00** | 10.00-20.00 | 3537.4 | 2.08 | 14.74 | 11.15 | 5.50 | 21.93 | 15.15 | 4.42 | 15.60 | 19.00 |
| **30.00** | 20.00-30.00 | 2541.2 | 7.28 | 25.57 | 10.59 | 12.39 | 25.93 | 15.01 | 11.10 | 19.40 | 20.60 |
| | +30.00 | 3196.2 | 11.09 | 41.52 | 6.32 | 22.38 | 32.57 | 10.26 | 20.40 | 26.70 | 12.30 |
| **Total/Head Grade, %** | | 20548.6 | 3.13 | 13.32 | 8.90 | 6.27 | 13.92 | 12.33 | 5.56 | 10.33 | 13.95 |

**-75+53 mm Size Fraction**

| Separation at Zn Grade of, % | -75+53 mm | Weight, g | XRF Surface Readings | | | XRF Powder Readings | | | Assay Results | | |
|---|---|---|---|---|---|---|---|---|---|---|---|
| | | | Pb Grade, % | Zn Grade, % | Fe Grade, % | Pb Grade, % | Zn Grade, % | Fe Grade, % | Pb Grade, % | Zn Grade, % | Fe Grade, % |
| **1.00** | 0-1.0 | 8148.4 | 0.07 | 0.37 | 8.12 | 0.32 | 0.41 | 11.37 | 0.24 | 0.18 | 8.94 |
| **2.00** | 1.0-2.0 | 2281.8 | 0.25 | 1.25 | 9.85 | 0.21 | 0.81 | 12.26 | 0.17 | 0.43 | 11.5 |
| **5.00** | 2.0-5.0 | 5192.3 | 0.43 | 3.32 | 8.11 | 0.79 | 4.71 | 24.21 | 0.63 | 2.81 | 24.6 |
| **10.00** | 5.0-10.0 | 3260.5 | 1.37 | 7.77 | 10.43 | 3.05 | 12.00 | 21.41 | 2.47 | 7.46 | 24.3 |
| **15.00** | 10.0-15.0 | 4829.1 | 3.12 | 12.76 | 10.41 | 7.97 | 14.00 | 16.45 | 6.96 | 10.0 | 20.2 |
| **20.00** | 15.0-20.0 | 6978.9 | 4.12 | 17.03 | 10.50 | 10.14 | 19.25 | 21.00 | 8.80 | 13.5 | 24.1 |
| **30.00** | 20.0-30.0 | 4762.8 | 6.54 | 23.52 | 11.79 | 10.52 | 28.78 | 13.88 | 8.52 | 20.4 | 16.7 |
| | +30.00 | 6553.6 | 7.15 | 37.52 | 9.91 | 17.57 | 33.37 | 12.71 | 13.2 | 23.6 | 14.3 |
| **Total/Head Grade, %** | | 42007.4 | 3.09 | 13.97 | 9.75 | 6.94 | 14.91 | 16.46 | 5.61 | 10.37 | 17.74 |

**+75 mm Size Fraction**

| Separation at Zn Grade of, % | +75 mm | Weight, g | XRF Surface Readings | | | XRF Powder Readings | | | Assay Results | | |
|---|---|---|---|---|---|---|---|---|---|---|---|
| | | | Pb Grade, % | Zn Grade, % | Fe Grade, % | Pb Grade, % | Zn Grade, % | Fe Grade, % | Pb Grade, % | Zn Grade, % | Fe Grade, % |
| **0.20** | 0-0.20 | 8246.00 | 0.04 | 0.14 | 11.24 | 0.10 | 0.28 | 3.25 | 0.06 | 0.10 | 1.34 |
| **0.50** | 0.20-0.50 | 5356.10 | 0.04 | 0.28 | 12.33 | 0.15 | 0.27 | 7.74 | 0.13 | 0.15 | 3.72 |
| **1.00** | 0.50-1.00 | 4280.60 | 0.18 | 0.77 | 9.27 | 0.76 | 0.88 | 38.92 | 0.51 | 0.39 | 33.30 |
| **2.00** | 1.00-2.00 | 3577.30 | 0.46 | 1.15 | 12.51 | 0.64 | 1.82 | 31.14 | 0.49 | 0.95 | 28.50 |
| **5.00** | 2.00-5.00 | 10520.90 | 0.53 | 2.94 | 10.46 | 1.01 | 3.57 | 22.82 | 0.79 | 2.07 | 22.20 |
| **10.00** | 5.00-10.00 | 11171.00 | 1.07 | 6.86 | 10.67 | 1.76 | 11.54 | 18.02 | 1.39 | 7.61 | 18.90 |
| **15.00** | 10.00-15.00 | 3534.10 | 2.80 | 13.49 | 13.84 | 4.70 | 14.93 | 22.62 | 3.63 | 9.65 | 23.90 |
| **20.00** | 15.00-20.00 | 6377.10 | 1.89 | 17.14 | 13.14 | 3.74 | 23.83 | 16.09 | 3.26 | 17.50 | 18.90 |
| | +20.00 | 6736.40 | 5.97 | 28.69 | 6.50 | 12.83 | 25.65 | 16.05 | 10.10 | 17.60 | 17.60 |
| **Total/Head Grade, %** | | 59799.5 | 1.38 | 7.82 | 10.85 | 2.75 | 9.33 | 18.03 | 2.18 | 6.32 | 17.45 |

**Sorting Results of Each Size Fraction Based on Different Threshold Values (Zn Grades)**

| Separation at Zn Grade of, % | Conc., % | Waste Rejection, % | Metal Recovery, % | | Conc. Grade, % | |
|---|---|---|---|---|---|---|
| | | | Zn | Pb | Zn | Pb |
| **0.20** | 90.4 | 9.6 | 100.0 | 99.9 | 11.29 | 4.11 |
| **0.50** | 72.9 | 27.1 | 99.9 | 99.5 | 13.99 | 5.07 |
| **1.00** | 68.4 | 31.6 | 99.7 | 99.2 | 14.89 | 5.39 |
| **2.00** | 55.3 | 44.7 | 99.1 | 98.3 | 18.30 | 6.61 |
| **5.00** | **47.2** | **52.8** | **97.1** | **96.5** | **21.04** | **7.61** |
| **10.00** | 43.6 | 56.4 | 96.0 | 94.6 | 22.49 | 8.06 |
| **15.00** | 40.0 | 60.0 | 92.7 | 93.6 | 23.68 | 8.70 |
| **20.00** | 34.7 | 65.3 | 86.1 | 88.4 | 25.37 | 9.48 |
| **30.00** | 17.4 | 82.6 | 52.3 | 59.0 | 30.70 | 12.60 |
| **Calculated Head Grade: 3.72% Pb and 10.21 % Zn (-37.5+26.5 mm size fraction 100 rocks)** | | | | | | |

| Separation at Zn Grade of, % | Conc., % | Waste Rejection, % | Metal Recovery, % | | Conc. Grade, % | |
|---|---|---|---|---|---|---|
| | | | Zn | Pb | Zn | Pb |
| **0.25** | 91.0 | 9.0 | 99.8 | 100.0 | 11.34 | 6.11 |
| **0.50** | 76.4 | 23.6 | 99.5 | 99.6 | 13.46 | 7.25 |
| **1.00** | 72.3 | 27.7 | 99.3 | 99.5 | 14.20 | 7.65 |
| **2.00** | 63.1 | 36.9 | 98.7 | 99.2 | 16.15 | 8.73 |
| **5.00** | **52.2** | **47.8** | **95.1** | **98.5** | **18.82** | **10.49** |
| **10.00** | 45.1 | 54.9 | 89.4 | 95.5 | 20.47 | 11.76 |
| **20.00** | 27.9 | 72.1 | 63.4 | 81.8 | 23.47 | 16.28 |
| **30.00** | 15.6 | 84.4 | 40.2 | 57.1 | 26.70 | 20.40 |
| **Calculated Head Grade: 5.56% Pb and 10.33 % Zn (-53+37.5 mm size fraction 100 rocks)** | | | | | | |

| Separation at Zn Grade of, % | Conc., % | Waste Rejection, % | Metal Recovery, % | | Conc. Grade, % | |
|---|---|---|---|---|---|---|
| | | | Zn | Pb | Zn | Pb |
| **1.00** | 80.6 | 19.4 | 99.7 | 99.2 | 12.82 | 6.91 |
| **2.00** | 75.2 | 24.8 | 99.4 | 99.0 | 13.72 | 7.39 |
| **5.00** | **62.8** | **37.2** | **96.1** | **97.6** | **15.87** | **8.72** |
| **10.00** | 55.0 | 45.0 | 90.5 | 94.2 | 17.05 | 9.61 |
| **15.00** | 43.6 | 56.4 | 79.4 | 79.9 | 18.91 | 10.30 |
| **20.00** | 26.9 | 73.1 | 57.8 | 53.9 | 22.25 | 11.23 |
| **30.00** | 15.6 | 84.4 | 35.5 | 36.7 | 23.60 | 13.20 |
| **Calculated Head Grade: 5.61% Pb and 10.37 % Zn (-75+53 mm size fraction 75 rocks)** | | | | | | |

| Separation at Zn Grade of, % | Conc., % | Waste Rejection, % | Metal Recovery, % | | Conc. Grade, % | |
|---|---|---|---|---|---|---|
| | | | Zn | Pb | Zn | Pb |
| **0.20** | 86.2 | 13.8 | 99.8 | 99.6 | 7.31 | 2.52 |
| **0.50** | 77.3 | 22.7 | 99.6 | 99.1 | 8.14 | 2.80 |
| **1.00** | 70.1 | 29.9 | 99.1 | 97.4 | 8.93 | 3.04 |
| **2.00** | **64.1** | **35.9** | **98.2** | **96.1** | **9.68** | **3.27** |
| **5.00** | 46.5 | 53.5 | 92.5 | 89.7 | 12.56 | 4.21 |
| **10.00** | 27.8 | 72.2 | 70.0 | 77.8 | 15.87 | 6.11 |
| **15.00** | 21.9 | 78.1 | 60.9 | 68.0 | 17.55 | 6.77 |
| **20.00** | 11.3 | 88.7 | 31.4 | 52.1 | 17.60 | 10.10 |
| **Calculated Head Grade: 2.18% Pb and 6.32 % Zn (+75 mm size fraction 50 rocks)** | | | | | | |

All sorting results were calculated based on chemical assays.

**Correlations Between XRF Analyzer Surface Readings and Bulk Assays for Each Size Fraction**

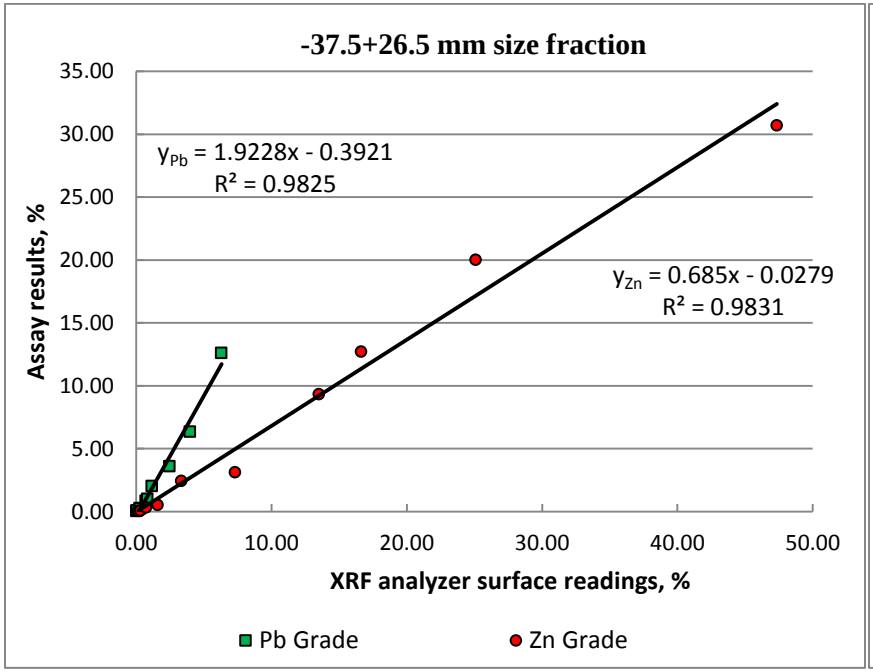


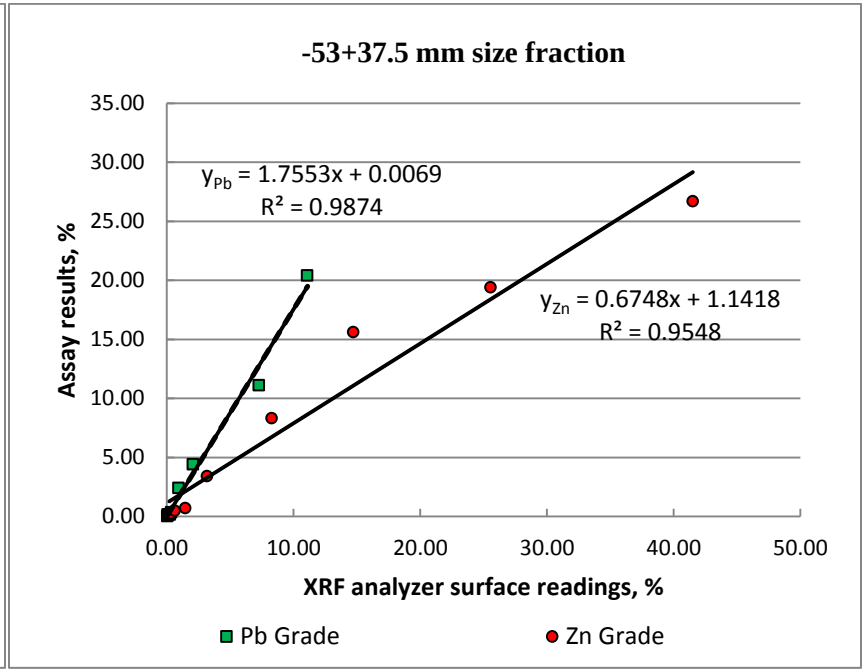

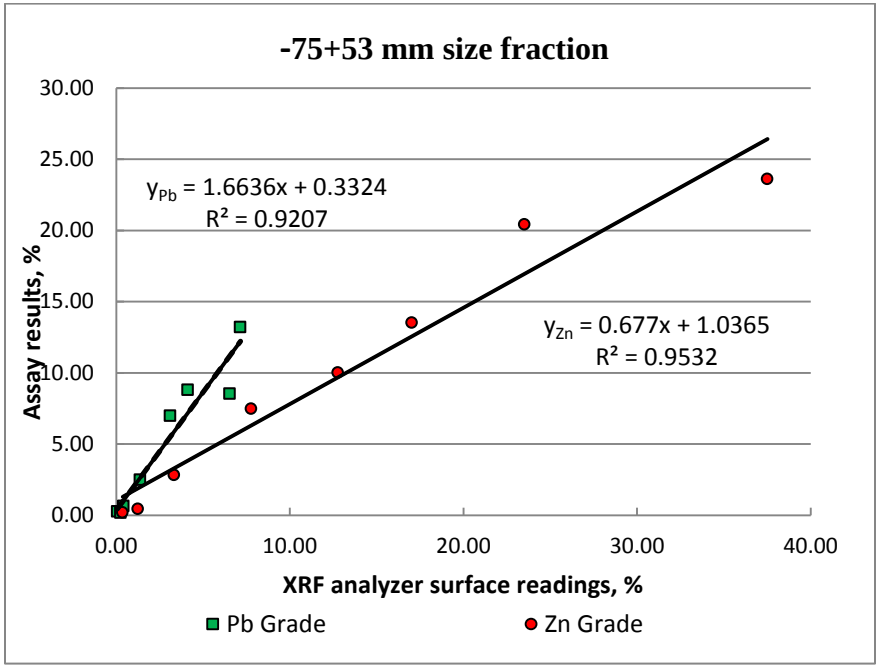


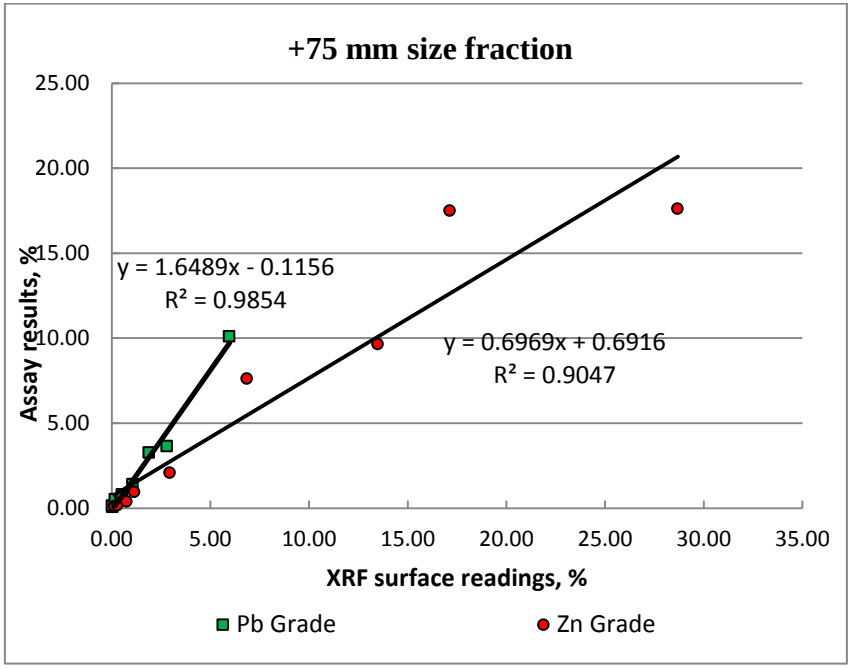


It is evident from the above graphs, the finer the particle size, the better the correlation between XRF analyzer surface readings and assays was. This indicated that a better sorting result will be achieved by the finer size fraction. This is primarily due to the limitation of our XRF analyzer. The detection window for our XRF analyzer is about 1cm$^2$. Although eight faces (8 cm$^2$ detection area) of the rock sized above 75 mm (about 400 cm$^2$ of the total surface area) were analyzed by the XRF analyzer, which account for 1/50 of the rock surface, the average reading of these faces was still not adequate for precisely predicting the grades of the bulk rock. In addition, the coarser the particle size, the less precisely the surface analysis can be used to predict the grades of the bulk rock. Consequently, a poorer correlation exhibited.

**Correlation between XRF Powder Readings and Assays**

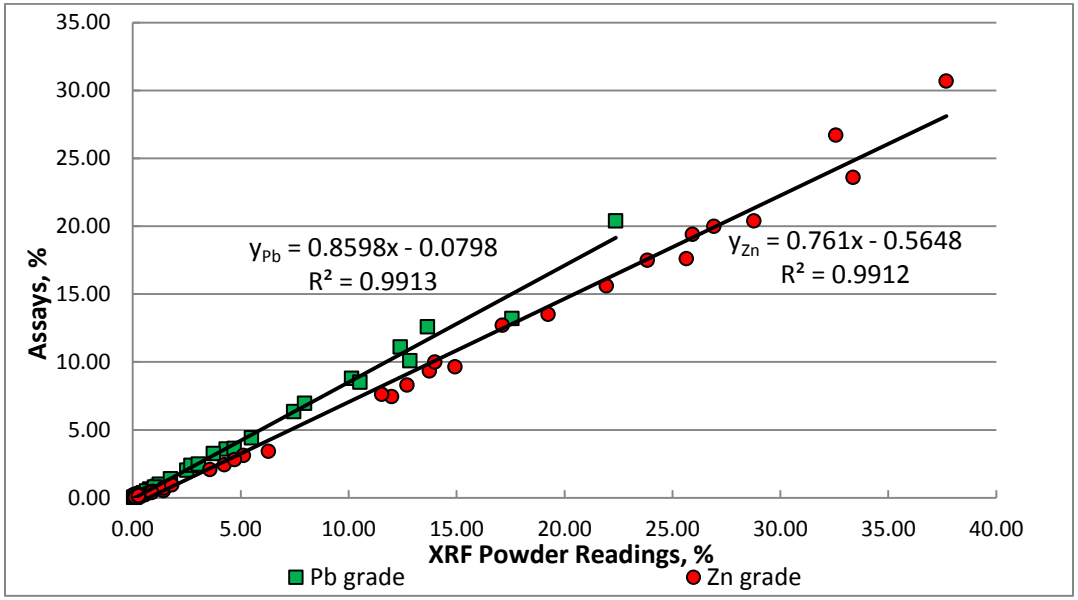


It is clearly shown in the above figure that XRF powder readings and assays have a very strong correlation between each other. All samples were prepared following the same procedures (jaw and cone crushing and pulverizing for 45s) to obtain same particle size for consistent analysis results from XRF analyzer. The calibrated XRF powder readings using the above calibration function have enough confidence in predicting real assays. Therefore, other sorting tests using XRT and optical sorting technologies were calculated and analyzed based on calibrated XRF powder reading. MW/IR sorting tests were calculated and analyzed based on XRF surface reading. Rock samples from -19+13.2 mm are too small to have enough pulverized powder for XRF power analysis. In order to have consistent results for MW/IR sorting tests, calibrated XRF surface readings were used as assays which are also quite confident in predicting real assays.

## APPENDIX B X-RAY TRANSMISSION SORTING DAT

**Initial Data Set of Avg. Brightness Value**

| Rock ID | High Energy Image | | Low Energy Image | | 320*240 | Weight, g | Pb, % | Zn, % | Pb+Zn | $Z_{Pb}$ | $Z_{zn}$ | $Z_{total}$ |
|---|---|---|---|---|---|---|---|---|---|---|---|---|
| | Avg. Intensity (0,255) | Pixels Counted | Avg. Intensity (0,255) | Pixels Counted | Total Pixels | | | | | 82.00 | 30.00 | 112.00 |
| 1 | 55.5 | 1627 | 39.3 | 1667 | 76800 | 105.84 | 5.68 | 10.56 | 16.23 | 465.41 | 316.68 | 782.09 |
| 2 | 22.7 | 1491 | 21.2 | 1514 | 76800 | 141.79 | 21.17 | 11.48 | 32.66 | 1736.27 | 344.45 | 2080.72 |
| 3 | 82.2 | 1323 | 56.8 | 1361 | 76800 | 108.18 | 0.18 | 0.21 | 0.39 | 14.58 | 6.27 | 20.85 |
| 4 | 100.7 | 1154 | 68.2 | 1190 | 76800 | 70.11 | 0.03 | 0.17 | 0.20 | 2.49 | 5.18 | 7.68 |
| 5 | 45.6 | 1519 | 30.1 | 1556 | 76800 | 140.78 | 2.58 | 1.24 | 3.81 | 211.42 | 37.09 | 248.52 |
| 6 | 30.7 | 1362 | 27.6 | 1402 | 76800 | 129.54 | 12.87 | 12.07 | 24.94 | 1055.70 | 362.01 | 1417.71 |
| 7 | 93.0 | 1204 | 59.2 | 1241 | 76800 | 68.04 | 0.60 | 0.74 | 1.34 | 49.00 | 22.25 | 71.24 |
| 8 | 133.5 | 1988 | 93.9 | 2057 | 76800 | 77.99 | 0.17 | 0.55 | 0.72 | 13.97 | 16.59 | 30.56 |
| 9 | 95.4 | 1427 | 65.0 | 1483 | 76800 | 91.09 | 0.04 | 0.17 | 0.21 | 3.58 | 5.05 | 8.63 |
| 10 | 100.6 | 1374 | 65.5 | 1407 | 76800 | 82.25 | 0.09 | 0.11 | 0.20 | 7.22 | 3.24 | 10.46 |
| 11 | 28.7 | 1495 | 25.9 | 1524 | 76800 | 93.26 | 32.82 | 10.65 | 43.47 | 2691.27 | 319.46 | 3010.73 |
| 12 | 116.7 | 1601 | 80.9 | 1656 | 76800 | 81.09 | 0.51 | 0.27 | 0.79 | 42.19 | 8.19 | 50.38 |
| 13 | 125.8 | 1095 | 87.1 | 1130 | 76800 | 48.65 | 0.05 | 0.09 | 0.14 | 4.11 | 2.82 | 6.93 |
| 14 | 32.7 | 1539 | 26.4 | 1578 | 76800 | 138.02 | 7.91 | 24.08 | 31.99 | 648.72 | 722.25 | 1370.98 |
| 15 | 25.3 | 1491 | 23.5 | 1519 | 76800 | 137.01 | 8.50 | 16.51 | 25.01 | 697.05 | 495.29 | 1192.35 |
| 16 | 36.2 | 990 | 32.8 | 1018 | 76800 | 97.66 | 19.01 | 8.37 | 27.38 | 1559.20 | 251.00 | 1810.20 |
| 17 | 112.7 | 1966 | 77.6 | 2025 | 76800 | 110.2 | 0.37 | 0.39 | 0.75 | 29.96 | 11.56 | 41.52 |
| 18 | 126.1 | 1461 | 87.6 | 1496 | 76800 | 65.62 | 0.08 | 0.17 | 0.25 | 6.45 | 5.16 | 11.61 |
| 19 | 111.9 | 2071 | 72.9 | 2130 | 76800 | 101.88 | 0.08 | 0.20 | 0.29 | 6.88 | 6.13 | 13.01 |

| Rock ID | High Energy Image | | Low Energy Image | | 320*240 | Weight, g | Pb, % | Zn, % | Pb+Zn | $Z_{Pb}$ | $Z_{zn}$ | $Z_{total}$ |
|---|---|---|---|---|---|---|---|---|---|---|---|---|
| | Avg. Intensity (0,255) | Pixels Counted | Avg. Intensity (0,255) | Pixels Counted | Total Pixels | | | | | 82.00 | 30.00 | 112.00 |
| 20 | 27.9 | 1190 | 26.7 | 1219 | 76800 | 89.88 | 26.07 | 16.92 | 43.00 | 2138.09 | 507.63 | 2645.72 |
| 21 | 29.2 | 1325 | 27.2 | 1347 | 76800 | 128.33 | 16.94 | 9.21 | 26.15 | 1389.46 | 276.17 | 1665.63 |
| 22 | 31.2 | 1054 | 30.3 | 1095 | 76800 | 95.65 | 21.08 | 16.37 | 37.45 | 1728.41 | 491.20 | 2219.61 |
| 23 | 30.9 | 1492 | 26.4 | 1527 | 76800 | 89.97 | 30.67 | 14.73 | 45.40 | 2514.58 | 442.03 | 2956.61 |
| 24 | 121.0 | 1092 | 84.7 | 1131 | 76800 | 52.92 | 0.29 | 0.34 | 0.64 | 24.07 | 10.32 | 34.39 |
| 25 | 86.6 | 1350 | 56.8 | 1391 | 76800 | 98.03 | 0.18 | 0.18 | 0.36 | 15.04 | 5.37 | 20.41 |
| 26 | 104.7 | 1421 | 68.8 | 1452 | 76800 | 82.63 | 0.13 | 0.17 | 0.31 | 10.72 | 5.25 | 15.96 |
| 27 | 96.1 | 1395 | 60.2 | 1440 | 76800 | 75.72 | 0.22 | 0.26 | 0.48 | 18.33 | 7.81 | 26.14 |
| 28 | 43.1 | 1183 | 29.0 | 1213 | 76800 | 98.39 | 0.98 | 12.98 | 13.96 | 80.30 | 389.54 | 469.84 |
| 29 | 28.6 | 942 | 28.3 | 972 | 76800 | 75.53 | 24.94 | 16.42 | 41.36 | 2045.03 | 492.68 | 2537.71 |
| 30 | 60.6 | 1435 | 39.0 | 1473 | 76800 | 68.51 | 8.10 | 8.07 | 16.17 | 664.38 | 242.17 | 906.54 |
| 31 | 28.9 | 1831 | 23.7 | 1879 | 76800 | 161.29 | 5.62 | 17.21 | 22.83 | 461.00 | 516.30 | 977.30 |
| 32 | 57.8 | 1526 | 36.4 | 1552 | 76800 | 96.08 | 3.31 | 7.59 | 10.90 | 271.32 | 227.60 | 498.92 |
| 33 | 56.0 | 1010 | 39.3 | 1046 | 76800 | 75.2 | 0.35 | 31.66 | 32.01 | 28.70 | 949.77 | 978.47 |
| 34 | 28.9 | 1305 | 25.7 | 1341 | 76800 | 125.26 | 8.03 | 12.73 | 20.76 | 658.53 | 381.80 | 1040.33 |
| 35 | 60.8 | 1084 | 41.3 | 1122 | 76800 | 83.05 | 0.53 | 5.87 | 6.39 | 43.07 | 176.05 | 219.13 |
| 36 | 51.9 | 1638 | 33.4 | 1693 | 76800 | 135.41 | 0.67 | 2.15 | 2.82 | 55.25 | 64.45 | 119.70 |
| 37 | 131.0 | 1316 | 92.8 | 1359 | 76800 | 56.55 | 0.00 | 0.33 | 0.33 | 0.37 | 9.86 | 10.23 |
| 38 | 125.5 | 1581 | 84.5 | 1613 | 76800 | 68.01 | 0.08 | 0.25 | 0.34 | 6.91 | 7.62 | 14.53 |
| 39 | 119.6 | 1474 | 83.2 | 1527 | 76800 | 71.12 | 0.05 | 0.24 | 0.30 | 4.31 | 7.33 | 11.64 |
| 40 | 32.6 | 1043 | 28.0 | 1067 | 76800 | 85.88 | 15.60 | 16.89 | 32.49 | 1279.57 | 506.70 | 1786.26 |
| 41 | 31.8 | 1088 | 29.7 | 1130 | 76800 | 111.87 | 6.21 | 10.55 | 16.76 | 509.60 | 316.37 | 825.97 |
| 42 | 103.1 | 2256 | 68.5 | 2327 | 76800 | 131.62 | 0.14 | 0.40 | 0.54 | 11.84 | 11.88 | 23.72 |

| Rock ID | High Energy Image | | Low Energy Image | | 320*240 | Weight, g | Pb, % | Zn, % | Pb+Zn | $Z_{Pb}$ | $Z_{zn}$ | $Z_{total}$ |
|---|---|---|---|---|---|---|---|---|---|---|---|---|
| | Avg. Intensity (0,255) | Pixels Counted | Avg. Intensity (0,255) | Pixels Counted | Total Pixels | | | | | 82.00 | 30.00 | 112.00 |
| 43 | 28.0 | 1090 | 26.7 | 1116 | 76800 | 105.99 | 21.52 | 23.88 | 45.40 | 1764.66 | 716.30 | 2480.96 |
| 44 | 55.1 | 1430 | 34.7 | 1473 | 76800 | 104.12 | 0.72 | 9.70 | 10.42 | 59.34 | 291.00 | 350.33 |
| 45 | 57.4 | 871 | 40.9 | 906 | 76800 | 56.49 | 0.44 | 19.32 | 19.76 | 36.48 | 579.52 | 616.00 |
| 46 | 110.6 | 1509 | 76.3 | 1553 | 76800 | 85.55 | 0.05 | 0.48 | 0.53 | 4.23 | 14.45 | 18.69 |
| 47 | 121.3 | 1045 | 86.3 | 1087 | 76800 | 51.21 | 0.09 | 0.20 | 0.29 | 7.02 | 5.99 | 13.00 |
| 48 | 49.3 | 1127 | 32.7 | 1155 | 76800 | 101.87 | 0.32 | 9.63 | 9.95 | 26.45 | 288.86 | 315.31 |
| 49 | 127.6 | 1543 | 88.9 | 1588 | 76800 | 68.72 | 0.00 | 0.50 | 0.50 | 0.25 | 14.88 | 15.13 |
| 50 | 25.8 | 1120 | 26.2 | 1149 | 76800 | 121.39 | 19.75 | 14.32 | 34.07 | 1619.68 | 429.58 | 2049.26 |
| 51 | 95.4 | 1578 | 64.7 | 1622 | 76800 | 105.46 | 0.19 | 0.27 | 0.45 | 15.18 | 8.02 | 23.20 |
| 52 | 40.8 | 1190 | 31.7 | 1234 | 76800 | 95.35 | 5.84 | 13.81 | 19.65 | 479.10 | 414.36 | 893.46 |
| 53 | 37.0 | 1206 | 28.3 | 1237 | 76800 | 82.08 | 5.68 | 25.18 | 30.86 | 465.47 | 755.45 | 1220.93 |
| 54 | 106.7 | 1242 | 73.9 | 1283 | 76800 | 74.18 | 0.19 | 0.33 | 0.53 | 15.76 | 10.03 | 25.79 |
| 55 | 107.5 | 1501 | 72.2 | 1536 | 76800 | 85.47 | 0.04 | 0.13 | 0.17 | 3.29 | 3.94 | 7.23 |
| 56 | 38.4 | 1704 | 26.8 | 1752 | 76800 | 123.07 | 7.76 | 29.29 | 37.05 | 635.98 | 878.73 | 1514.71 |
| 57 | 118.2 | 1211 | 81.4 | 1260 | 76800 | 58.57 | 0.16 | 0.80 | 0.95 | 12.72 | 23.96 | 36.68 |
| 58 | 68.5 | 1013 | 43.4 | 1051 | 76800 | 62.74 | 0.47 | 4.30 | 4.77 | 38.60 | 129.02 | 167.62 |
| 59 | 82.9 | 1042 | 47.6 | 1077 | 76800 | 46.52 | 0.50 | 0.15 | 0.65 | 40.77 | 4.50 | 45.27 |
| 60 | 126.3 | 1602 | 89.1 | 1660 | 76800 | 72.8 | 0.39 | 0.28 | 0.67 | 32.27 | 8.41 | 40.68 |
| 61 | 45.7 | 1338 | 34.1 | 1372 | 76800 | 86.23 | 6.27 | 14.69 | 20.97 | 514.30 | 440.84 | 955.15 |
| 62 | 50.7 | 958 | 34.5 | 992 | 76800 | 81.98 | 0.77 | 21.90 | 22.67 | 63.40 | 656.85 | 720.26 |
| 63 | 120.8 | 2212 | 81.4 | 2291 | 76800 | 97.74 | 0.02 | 0.55 | 0.57 | 2.05 | 16.39 | 18.44 |
| 64 | 128.9 | 1664 | 91.3 | 1730 | 76800 | 71.44 | 0.17 | 0.35 | 0.53 | 14.27 | 10.58 | 24.85 |
| 65 | 123.8 | 1382 | 86.9 | 1425 | 76800 | 66.73 | 0.00 | 0.16 | 0.16 | 0.02 | 4.75 | 4.77 |

| Rock ID | High Energy Image | | Low Energy Image | | 320*240 | Weight, g | Pb, % | Zn, % | Pb+Zn | $Z_{Pb}$ | $Z_{zn}$ | $Z_{total}$ |
|---|---|---|---|---|---|---|---|---|---|---|---|---|
| | Avg. Intensity (0,255) | Pixels Counted | Avg. Intensity (0,255) | Pixels Counted | Total Pixels | | | | | 82.00 | 30.00 | 112.00 |
| 66 | 37.9 | 1155 | 30.0 | 1186 | 76800 | 98.78 | 5.57 | 6.88 | 12.46 | 457.00 | 206.50 | 663.50 |
| 67 | 27.8 | 1290 | 25.8 | 1319 | 76800 | 86.85 | 21.85 | 22.53 | 44.38 | 1791.40 | 675.97 | 2467.37 |
| 68 | 28.9 | 1438 | 26.7 | 1474 | 76800 | 146.86 | 13.27 | 14.44 | 27.71 | 1088.47 | 433.12 | 1521.59 |
| 69 | 24.9 | 1322 | 24.1 | 1348 | 76800 | 133.86 | 25.88 | 19.15 | 45.03 | 2122.31 | 574.53 | 2696.84 |
| 70 | 43.6 | 1702 | 29.7 | 1748 | 76800 | 170.94 | 1.30 | 4.51 | 5.81 | 106.64 | 135.39 | 242.03 |
| 71 | 60.7 | 1095 | 46.8 | 1129 | 76800 | 79.19 | 7.29 | 5.49 | 12.78 | 598.13 | 164.60 | 762.73 |
| 72 | 27.4 | 1460 | 25.2 | 1492 | 76800 | 131.7 | 19.63 | 18.32 | 37.95 | 1610.03 | 549.46 | 2159.49 |
| 73 | 40.4 | 1312 | 31.2 | 1351 | 76800 | 95.31 | 7.49 | 13.16 | 20.65 | 614.36 | 394.67 | 1009.03 |
| 74 | 50.6 | 1127 | 35.6 | 1163 | 76800 | 100.17 | 0.56 | 4.14 | 4.70 | 45.76 | 124.21 | 169.97 |
| 75 | 115.6 | 1027 | 80.3 | 1068 | 76800 | 52.06 | 0.09 | 0.21 | 0.30 | 7.43 | 6.17 | 13.59 |
| 76 | 94.0 | 911 | 63.8 | 945 | 76800 | 59.25 | 0.06 | 0.51 | 0.57 | 5.31 | 15.22 | 20.53 |
| 77 | 46.5 | 975 | 36.0 | 1007 | 76800 | 97.89 | 0.58 | 14.88 | 15.46 | 47.32 | 446.52 | 493.84 |
| 78 | 109.8 | 1663 | 72.1 | 1715 | 76800 | 82.66 | 0.05 | 0.98 | 1.03 | 3.95 | 29.43 | 33.38 |
| 79 | 118.5 | 1370 | 82.4 | 1420 | 76800 | 67.64 | 0.05 | 0.36 | 0.41 | 4.31 | 10.83 | 15.14 |
| 80 | 52.9 | 1197 | 35.4 | 1252 | 76800 | 89.23 | 0.10 | 24.47 | 24.57 | 7.91 | 734.07 | 741.98 |
| 81 | 71.9 | 1074 | 43.2 | 1117 | 76800 | 62 | 0.85 | 13.79 | 14.64 | 69.72 | 413.67 | 483.39 |
| 82 | 27.9 | 931 | 29.5 | 960 | 76800 | 71.41 | 30.42 | 17.43 | 47.85 | 2494.25 | 522.94 | 3017.20 |
| 83 | 54.8 | 1118 | 36.3 | 1155 | 76800 | 90.55 | 1.41 | 10.34 | 11.75 | 116.03 | 310.18 | 426.21 |
| 84 | 115.7 | 1432 | 78.4 | 1480 | 76800 | 71.62 | 0.13 | 0.24 | 0.37 | 10.34 | 7.30 | 17.64 |
| 85 | 117.1 | 1642 | 81.2 | 1706 | 76800 | 82.36 | 0.02 | 0.13 | 0.15 | 1.68 | 3.82 | 5.50 |
| 86 | 78.1 | 1181 | 52.4 | 1226 | 76800 | 92.89 | 0.14 | 0.29 | 0.43 | 11.42 | 8.79 | 20.22 |
| 87 | 68.2 | 1118 | 44.6 | 1164 | 76800 | 65.93 | 0.73 | 13.44 | 14.17 | 59.59 | 403.20 | 462.79 |
| 88 | 63.3 | 1344 | 38.0 | 1382 | 76800 | 91.9 | 0.84 | 6.27 | 7.11 | 68.73 | 188.23 | 256.96 |

| Rock ID | High Energy Image | | Low Energy Image | | 320*240 | Weight, g | Pb, % | Zn, % | Pb+Zn | $Z_{Pb}$ | $Z_{zn}$ | $Z_{total}$ |
|---|---|---|---|---|---|---|---|---|---|---|---|---|
| | Avg. Intensity (0,255) | Pixels Counted | Avg. Intensity (0,255) | Pixels Counted | Total Pixels | | | | | 82.00 | 30.00 | 112.00 |
| 89 | 45.6 | 1052 | 35.3 | 1089 | 76800 | 71.53 | 6.03 | 8.16 | 14.19 | 494.65 | 244.85 | 739.50 |
| 90 | 28.1 | 795 | 28.9 | 814 | 76800 | 73.43 | 23.87 | 14.27 | 38.14 | 1957.54 | 428.10 | 2385.64 |
| 91 | 57.6 | 1153 | 37.8 | 1197 | 76800 | 82.05 | 0.65 | 7.51 | 8.16 | 53.21 | 225.21 | 278.41 |
| 92 | 58.9 | 864 | 39.4 | 904 | 76800 | 62.51 | 0.77 | 9.93 | 10.70 | 62.91 | 298.04 | 360.95 |
| 93 | 51.3 | 735 | 36.3 | 762 | 76800 | 61.34 | 0.69 | 4.99 | 5.68 | 56.63 | 149.58 | 206.20 |
| 94 | 51.2 | 1109 | 34.5 | 1148 | 76800 | 78.59 | 0.67 | 34.12 | 34.79 | 54.67 | 1023.73 | 1078.40 |
| 95 | 38.4 | 1081 | 31.5 | 1107 | 76800 | 74.25 | 16.83 | 12.84 | 29.67 | 1379.72 | 385.23 | 1764.95 |
| 96 | 58.1 | 1189 | 38.2 | 1223 | 76800 | 77.87 | 3.67 | 4.32 | 7.99 | 301.12 | 129.66 | 430.78 |
| 97 | 140.2 | 1667 | 101.4 | 1731 | 76800 | 64.19 | 0.09 | 0.32 | 0.41 | 7.28 | 9.65 | 16.93 |
| 98 | 142.0 | 1511 | 100.2 | 1559 | 76800 | 53.95 | 0.01 | 0.21 | 0.22 | 0.75 | 6.24 | 6.99 |
| 99 | 107.3 | 1268 | 71.5 | 1323 | 76800 | 66.87 | 0.05 | 0.13 | 0.18 | 4.03 | 3.89 | 7.92 |
| 100 | 107.6 | 1707 | 73.0 | 1757 | 76800 | 96.44 | 0.04 | 0.13 | 0.17 | 2.89 | 3.91 | 6.80 |

**Initial Data Set of Ore Index**

| Rock ID | Weight, g | Pb, % | Zn, % | SUM Pb + Zn (%) | Weighted by Atomic Number Pb + Zn (%) | Ore Index SPECTRAL Correl = 0.8944 |
|---|---|---|---|---|---|---|
| 1 | 105.8 | 5.68 | 10.56 | 16.23 | 6.98 | 54 |
| 2 | 141.8 | 21.17 | 11.48 | 32.66 | 18.58 | 97 |
| 3 | 108.2 | 0.18 | 0.21 | 0.39 | 0.19 | 20 |
| 4 | 70.1 | 0.03 | 0.17 | 0.20 | 0.07 | 5 |
| 5 | 140.8 | 2.58 | 1.24 | 3.81 | 2.22 | 46 |
| 6 | 129.5 | 12.87 | 12.07 | 24.94 | 12.66 | 87 |
| 7 | 68.0 | 0.60 | 0.74 | 1.34 | 0.64 | 21 |
| 8 | 78.0 | 0.17 | 0.55 | 0.72 | 0.27 | 0 |
| 9 | 91.1 | 0.04 | 0.17 | 0.21 | 0.08 | 11 |
| 10 | 82.3 | 0.09 | 0.11 | 0.20 | 0.09 | 2 |
| 11 | 93.3 | 32.82 | 10.65 | 43.47 | 26.88 | 95 |
| 12 | 81.1 | 0.51 | 0.27 | 0.79 | 0.45 | 2 |
| 13 | 48.7 | 0.05 | 0.09 | 0.14 | 0.06 | 2 |
| 14 | 138.0 | 7.91 | 24.08 | 31.99 | 12.24 | 78 |
| 15 | 137.0 | 8.50 | 16.51 | 25.01 | 10.65 | 91 |
| 16 | 97.7 | 19.01 | 8.37 | 27.38 | 16.16 | 87 |
| 17 | 110.2 | 0.37 | 0.39 | 0.75 | 0.37 | 4 |
| 18 | 65.6 | 0.08 | 0.17 | 0.25 | 0.10 | 2 |
| 19 | 101.9 | 0.08 | 0.20 | 0.29 | 0.12 | 5 |
| 20 | 89.9 | 26.07 | 16.92 | 43.00 | 23.62 | 94 |
| 21 | 128.3 | 16.94 | 9.21 | 26.15 | 14.87 | 95 |
| 22 | 95.7 | 21.08 | 16.37 | 37.45 | 19.82 | 89 |
| 23 | 90.0 | 30.67 | 14.73 | 45.40 | 26.40 | 88 |
| 24 | 52.9 | 0.29 | 0.34 | 0.64 | 0.31 | 1 |
| 25 | 98.0 | 0.18 | 0.18 | 0.36 | 0.18 | 11 |
| 26 | 82.6 | 0.13 | 0.17 | 0.31 | 0.14 | 3 |
| 27 | 75.7 | 0.22 | 0.26 | 0.48 | 0.23 | 16 |
| 28 | 98.4 | 0.98 | 12.98 | 13.96 | 4.19 | 43 |
| 29 | 75.5 | 24.94 | 16.42 | 41.36 | 22.66 | 94 |
| 30 | 68.5 | 8.10 | 8.07 | 16.17 | 8.09 | 51 |
| 31 | 161.3 | 5.62 | 17.21 | 22.83 | 8.73 | 77 |
| 32 | 96.1 | 3.31 | 7.59 | 10.90 | 4.45 | 47 |
| 33 | 75.2 | 0.35 | 31.66 | 32.01 | 8.74 | 42 |
| 34 | 125.3 | 8.03 | 12.73 | 20.76 | 9.29 | 84 |

| Rock ID | Weight, g | Pb, % | Zn, % | SUM Pb + Zn (%) | Weighted by Atomic Number Pb + Zn (%) | Ore Index SPECTRAL Correl = 0.8944 |
|---|---|---|---|---|---|---|
| 35 | 83.1 | 0.53 | 5.87 | 6.39 | 1.96 | 35 |
| 36 | 135.4 | 0.67 | 2.15 | 2.82 | 1.07 | 44 |
| 37 | 56.6 | 0.00 | 0.33 | 0.33 | 0.09 | 2 |
| 38 | 68.0 | 0.08 | 0.25 | 0.34 | 0.13 | 2 |
| 39 | 71.1 | 0.05 | 0.24 | 0.30 | 0.10 | 2 |
| 40 | 85.9 | 15.60 | 16.89 | 32.49 | 15.95 | 91 |
| 41 | 111.9 | 6.21 | 10.55 | 16.76 | 7.37 | 86 |
| 42 | 131.6 | 0.14 | 0.40 | 0.54 | 0.21 | 4 |
| 43 | 106.0 | 21.52 | 23.88 | 45.40 | 22.15 | 95 |
| 44 | 104.1 | 0.72 | 9.70 | 10.42 | 3.13 | 36 |
| 45 | 56.5 | 0.44 | 19.32 | 19.76 | 5.50 | 36 |
| 46 | 85.6 | 0.05 | 0.48 | 0.53 | 0.17 | 4 |
| 47 | 51.2 | 0.09 | 0.20 | 0.29 | 0.12 | 3 |
| 48 | 101.9 | 0.32 | 9.63 | 9.95 | 2.82 | 47 |
| 49 | 68.7 | 0.00 | 0.50 | 0.50 | 0.14 | 0 |
| 50 | 121.4 | 19.75 | 14.32 | 34.07 | 18.30 | 95 |
| 51 | 105.5 | 0.19 | 0.27 | 0.45 | 0.21 | 9 |
| 52 | 95.4 | 5.84 | 13.81 | 19.65 | 7.98 | 69 |
| 53 | 82.1 | 5.68 | 25.18 | 30.86 | 10.90 | 59 |
| 54 | 74.2 | 0.19 | 0.33 | 0.53 | 0.23 | 7 |
| 55 | 85.5 | 0.04 | 0.13 | 0.17 | 0.06 | 3 |
| 56 | 123.1 | 7.76 | 29.29 | 37.05 | 13.52 | 65 |
| 57 | 58.6 | 0.16 | 0.80 | 0.95 | 0.33 | 1 |
| 58 | 62.7 | 0.47 | 4.30 | 4.77 | 1.50 | 32 |
| 59 | 46.5 | 0.50 | 0.15 | 0.65 | 0.40 | 31 |
| 60 | 72.8 | 0.39 | 0.28 | 0.67 | 0.36 | 0 |
| 61 | 86.2 | 6.27 | 14.69 | 20.97 | 8.53 | 77 |
| 62 | 82.0 | 0.77 | 21.90 | 22.67 | 6.43 | 45 |
| 63 | 97.7 | 0.02 | 0.55 | 0.57 | 0.16 | 3 |
| 64 | 71.4 | 0.17 | 0.35 | 0.53 | 0.22 | 1 |
| 65 | 66.7 | 0.00 | 0.16 | 0.16 | 0.04 | 1 |
| 66 | 98.8 | 5.57 | 6.88 | 12.46 | 5.92 | 70 |
| 67 | 86.9 | 21.85 | 22.53 | 44.38 | 22.03 | 94 |
| 68 | 146.9 | 13.27 | 14.44 | 27.71 | 13.59 | 90 |
| 69 | 133.9 | 25.88 | 19.15 | 45.03 | 24.08 | 97 |
| 70 | 170.9 | 1.30 | 4.51 | 5.81 | 2.16 | 50 |
| 71 | 79.2 | 7.29 | 5.49 | 12.78 | 6.81 | 59 |
| 72 | 131.7 | 19.63 | 18.32 | 37.95 | 19.28 | 94 |

| Rock ID | Weight, g | Pb, % | Zn, % | SUM Pb + Zn (%) | Weighted by Atomic Number Pb + Zn (%) | Ore Index SPECTRAL Correl = 0.8944 |
|---|---|---|---|---|---|---|
| 73 | 95.3 | 7.49 | 13.16 | 20.65 | 9.01 | 67 |
| 74 | 100.2 | 0.56 | 4.14 | 4.70 | 1.52 | 44 |
| 75 | 52.1 | 0.09 | 0.21 | 0.30 | 0.12 | 1 |
| 76 | 59.3 | 0.06 | 0.51 | 0.57 | 0.18 | 7 |
| 77 | 97.9 | 0.58 | 14.88 | 15.46 | 4.41 | 53 |
| 78 | 82.7 | 0.05 | 0.98 | 1.03 | 0.30 | 12 |
| 79 | 67.6 | 0.05 | 0.36 | 0.41 | 0.14 | 2 |
| 80 | 89.2 | 0.10 | 24.47 | 24.57 | 6.62 | 33 |
| 81 | 62.0 | 0.85 | 13.79 | 14.64 | 4.32 | 36 |
| 82 | 71.4 | 30.42 | 17.43 | 47.85 | 26.94 | 100 |
| 83 | 90.6 | 1.41 | 10.34 | 11.75 | 3.81 | 38 |
| 84 | 71.6 | 0.13 | 0.24 | 0.37 | 0.16 | 1 |
| 85 | 82.4 | 0.02 | 0.13 | 0.15 | 0.05 | 1 |
| 86 | 92.9 | 0.14 | 0.29 | 0.43 | 0.18 | 31 |
| 87 | 65.9 | 0.73 | 13.44 | 14.17 | 4.13 | 34 |
| 88 | 91.9 | 0.84 | 6.27 | 7.11 | 2.29 | 39 |
| 89 | 71.5 | 6.03 | 8.16 | 14.19 | 6.60 | 62 |
| 90 | 73.4 | 23.87 | 14.27 | 38.14 | 21.30 | 104 |
| 91 | 82.1 | 0.65 | 7.51 | 8.16 | 2.49 | 34 |
| 92 | 62.5 | 0.77 | 9.93 | 10.70 | 3.22 | 43 |
| 93 | 61.3 | 0.69 | 4.99 | 5.68 | 1.84 | 38 |
| 94 | 78.6 | 0.67 | 34.12 | 34.79 | 9.63 | 41 |
| 95 | 74.3 | 16.83 | 12.84 | 29.67 | 15.76 | 85 |
| 96 | 77.9 | 3.67 | 4.32 | 7.99 | 3.85 | 42 |
| 97 | 64.2 | 0.09 | 0.32 | 0.41 | 0.15 | 1 |
| 98 | 54.0 | 0.01 | 0.21 | 0.22 | 0.06 | 0 |
| 99 | 66.9 | 0.05 | 0.13 | 0.18 | 0.07 | 11 |
| 100 | 96.4 | 0.04 | 0.13 | 0.17 | 0.06 | 3 |

## APPENDIX C OPTICAL SORTING DATA

### Initial Data for Color Sorting

| Sample ID | Weight, g | Pb, % | Zn, % | Red Threshold | |
|---|---|---|---|---|---|
| | | | | 133-255 | 0-40 |
| | | | | Avg. $R_{133-255}$ | Avg. $R_{0-40}$ |
| 1 | 105.8 | 5.68 | 10.56 | 4.0 | 5.7 |
| 2 | 141.8 | 21.17 | 11.48 | 5.5 | 0.4 |
| 3 | 108.2 | 0.18 | 0.21 | 15.3 | 26.1 |
| 4 | 70.1 | 0.03 | 0.17 | 84.1 | 0.0 |
| 5 | 140.8 | 2.58 | 1.24 | 2.8 | 1.8 |
| 6 | 129.5 | 12.87 | 12.07 | 6.4 | 1.6 |
| 7 | 68.0 | 0.60 | 0.74 | 3.4 | 11.6 |
| 8 | 78.0 | 0.17 | 0.55 | 5.7 | 10.2 |
| 9 | 91.1 | 0.04 | 0.17 | 9.2 | 0.8 |
| 10 | 82.3 | 0.09 | 0.11 | 5.3 | 41.2 |
| 11 | 93.3 | 32.82 | 10.65 | 4.5 | 1.8 |
| 12 | 81.1 | 0.51 | 0.27 | 39.8 | 0.0 |
| 13 | 48.7 | 0.05 | 0.09 | 87.5 | 0.0 |
| 14 | 138.0 | 7.91 | 24.08 | 3.8 | 0.2 |
| 15 | 137.0 | 8.50 | 16.51 | 3.6 | 0.2 |
| 16 | 97.7 | 19.01 | 8.37 | 6.6 | 0.0 |
| 17 | 110.2 | 0.37 | 0.39 | 14.9 | 0.0 |
| 18 | 65.6 | 0.08 | 0.17 | 8.8 | 0.1 |
| 19 | 101.9 | 0.08 | 0.20 | 2.3 | 135.1 |
| 20 | 89.9 | 26.07 | 16.92 | 4.3 | 0.4 |
| 21 | 128.3 | 16.94 | 9.21 | 5.3 | 3.0 |
| 22 | 95.7 | 21.08 | 16.37 | 7.7 | 0.1 |
| 23 | 90.0 | 30.67 | 14.73 | 5.7 | 0.0 |
| 24 | 52.9 | 0.29 | 0.34 | 26.9 | 0.1 |
| 25 | 98.0 | 0.18 | 0.18 | 3.0 | 6.2 |
| 26 | 82.6 | 0.13 | 0.17 | 152.0 | 0.0 |
| 27 | 75.7 | 0.22 | 0.26 | 4.0 | 0.0 |
| 28 | 98.4 | 0.98 | 12.98 | 5.8 | 0.1 |
| 29 | 75.5 | 24.94 | 16.42 | 6.8 | 0.1 |
| 30 | 68.5 | 8.10 | 8.07 | 6.3 | 0.0 |
| 31 | 161.3 | 5.62 | 17.21 | 5.0 | 0.1 |
| 32 | 96.1 | 3.31 | 7.59 | 5.9 | 0.0 |
| 33 | 75.2 | 0.35 | 31.66 | 21.7 | 0.0 |
| 34 | 125.3 | 8.03 | 12.73 | 3.8 | 0.8 |
| 35 | 83.1 | 0.53 | 5.87 | 19.1 | 0.9 |
| 36 | 135.4 | 0.67 | 2.15 | 2.6 | 0.0 |
| 37 | 56.6 | 0.00 | 0.33 | 28.4 | 0.0 |
| 38 | 68.0 | 0.08 | 0.25 | 10.1 | 0.0 |
| 39 | 71.1 | 0.05 | 0.24 | 2.3 | 61.0 |
| 40 | 85.9 | 15.60 | 16.89 | 4.0 | 0.3 |
| 41 | 111.9 | 6.21 | 10.55 | 8.1 | 0.0 |

| Sample ID | Weight, g | Pb, % | Zn, % | Red Threshold | |
|---|---|---|---|---|---|
| | | | | 133-255 | 0-40 |
| | | | | Avg. $R_{133-255}$ | Avg. $R_{0-40}$ |
| 42 | 131.6 | 0.14 | 0.40 | 14.5 | 2.0 |
| 43 | 106.0 | 21.52 | 23.88 | 4.7 | 0.1 |
| 44 | 104.1 | 0.72 | 9.70 | 2.8 | 2.6 |
| 45 | 56.5 | 0.44 | 19.32 | 8.1 | 0.0 |
| 46 | 85.6 | 0.05 | 0.48 | 17.4 | 2.3 |
| 47 | 51.2 | 0.09 | 0.20 | 20.0 | 0.0 |
| 48 | 101.9 | 0.32 | 9.63 | 10.1 | 0.0 |
| 49 | 68.7 | 0.00 | 0.50 | 21.4 | 0.0 |
| 50 | 121.4 | 19.75 | 14.32 | 5.4 | 0.0 |
| 51 | 105.5 | 0.19 | 0.27 | 81.8 | 0.2 |
| 52 | 95.4 | 5.84 | 13.81 | 6.5 | 0.0 |
| 53 | 82.1 | 5.68 | 25.18 | 4.8 | 0.8 |
| 54 | 74.2 | 0.19 | 0.33 | 14.3 | 0.5 |
| 55 | 85.5 | 0.04 | 0.13 | 55.9 | 0.0 |
| 56 | 123.1 | 7.76 | 29.29 | 4.8 | 0.0 |
| 57 | 58.6 | 0.16 | 0.80 | 7.6 | 0.0 |
| 58 | 62.7 | 0.47 | 4.30 | 4.8 | 0.0 |
| 59 | 46.5 | 0.50 | 0.15 | 3.6 | 0.0 |
| 60 | 72.8 | 0.39 | 0.28 | 11.0 | 0.2 |
| 61 | 86.2 | 16.27 | 14.69 | 5.6 | 0.4 |
| 62 | 82.0 | 0.77 | 21.90 | 9.2 | 0.0 |
| 63 | 97.7 | 0.02 | 0.55 | 2.1 | 66.2 |
| 64 | 71.4 | 0.17 | 0.35 | 9.1 | 11.9 |
| 65 | 66.7 | 0.00 | 0.16 | 20.4 | 0.1 |
| 66 | 98.8 | 5.57 | 6.88 | 5.7 | 0.0 |
| 67 | 86.9 | 21.85 | 22.53 | 5.9 | 0.1 |
| 68 | 146.9 | 13.27 | 14.44 | 9.1 | 0.0 |
| 69 | 133.9 | 25.88 | 19.15 | 6.7 | 2.0 |
| 70 | 170.9 | 1.30 | 4.51 | 5.5 | 0.6 |
| 71 | 79.2 | 7.29 | 5.49 | 28.1 | 0.0 |
| 72 | 131.7 | 19.63 | 18.32 | 4.3 | 0.0 |
| 73 | 95.3 | 7.49 | 13.16 | 6.3 | 0.1 |
| 74 | 100.2 | 0.56 | 4.14 | 7.7 | 0.3 |
| 75 | 52.1 | 0.09 | 0.21 | 15.2 | 0.1 |
| 76 | 59.3 | 0.06 | 0.51 | 37.3 | 0.0 |
| 77 | 97.9 | 0.58 | 14.88 | 24.1 | 0.0 |
| 78 | 82.7 | 0.05 | 0.98 | 4.5 | 0.3 |
| 79 | 67.6 | 0.05 | 0.36 | 4.8 | 1.2 |
| 80 | 89.2 | 0.10 | 24.47 | 8.8 | 0.0 |
| 81 | 62.0 | 0.85 | 13.79 | 8.3 | 0.0 |
| 82 | 71.4 | 30.42 | 17.43 | 9.9 | 0.0 |
| 83 | 90.6 | 1.41 | 10.34 | 4.9 | 0.1 |
| 84 | 71.6 | 0.13 | 0.24 | 8.6 | 0.4 |
| 85 | 82.4 | 0.02 | 0.13 | 4.3 | 0.0 |
| 86 | 92.9 | 0.14 | 0.29 | 3.2 | 5.3 |
| 87 | 65.9 | 0.73 | 13.44 | 6.6 | 0.1 |

| Sample ID | Weight, g | Pb, % | Zn, % | Red Threshold | |
|---|---|---|---|---|---|
| | | | | 133-255 | 0-40 |
| | | | | Avg. $R_{133-255}$ | Avg. $R_{0-40}$ |
| 88 | 91.9 | 0.84 | 6.27 | 7.4 | 0.0 |
| 89 | 71.5 | 6.03 | 8.16 | 4.7 | 1.4 |
| 90 | 73.4 | 23.87 | 14.27 | 5.6 | 0.2 |
| 91 | 82.1 | 0.65 | 7.51 | 3.4 | 2.6 |
| 92 | 62.5 | 0.77 | 9.93 | 10.0 | 0.0 |
| 93 | 61.3 | 0.69 | 4.99 | 13.9 | 0.0 |
| 94 | 78.6 | 0.67 | 34.12 | 3.7 | 0.0 |
| 95 | 74.3 | 16.83 | 12.84 | 4.3 | 0.1 |
| 96 | 77.9 | 3.67 | 4.32 | 5.1 | 0.7 |
| 97 | 64.2 | 0.09 | 0.32 | 157.6 | 0.0 |
| 98 | 54.0 | 0.01 | 0.21 | 73.3 | 0.0 |
| 99 | 66.9 | 0.05 | 0.13 | 4.0 | 68.3 |
| 100 | 96.4 | 0.04 | 0.13 | 5.0 | 0.1 |

**Characteristic Color Data for Each Selected Pattern for Selected Rocks**

| Waste rock-26 | | 1 | 2 | 3 | 4 | 5 | 6 | 7 | 8 | 9 | 10 | Average |
|---|---|---|---|---|---|---|---|---|---|---|---|---|
| | Area | 551 | 551 | 551 | 551 | 551 | 551 | 551 | 551 | 551 | 551 | |
| Red | Mean | 154 | 158 | 130 | 111 | 128 | 118 | 158 | 137 | 98 | 112 | **130** |
| | Standard Deviation | 16 | 23 | 17 | 15 | 23 | 14 | 20 | 14 | 24 | 16 | |
| Green | Mean | 170 | 175 | 144 | 123 | 141 | 132 | 175 | 152 | 108 | 125 | **144** |
| | Standard Deviation | 18 | 25 | 18 | 16 | 26 | 16 | 22 | 15 | 24 | 18 | |
| Blue | Mean | 95 | 97 | 79 | 67 | 78 | 73 | 98 | 84 | 59 | 67 | **80** |
| | Standard Deviation | 12 | 16 | 12 | 10 | 17 | 10 | 14 | 9 | 24 | 10 | |

| Waste rock -51 pattern 1 | | 1 | 2 | 3 | 4 | 5 | 6 | 7 | 8 | 9 | 10 | Average |
|---|---|---|---|---|---|---|---|---|---|---|---|---|
| | Area | 368 | 368 | 368 | 368 | 368 | 368 | 368 | 368 | 368 | 368 | |
| Red | Mean | 119 | 150 | 145 | 139 | 130 | 121 | 109 | 111 | 104 | 115 | **124** |
| | Standard Deviation | 29 | 26 | 17 | 22 | 34 | 18 | 16 | 16 | 9 | 18 | |
| Green | Mean | 132 | 164 | 161 | 152 | 143 | 134 | 121 | 124 | 115 | 129 | **137** |
| | Standard Deviation | 31 | 28 | 18 | 24 | 37 | 19 | 17 | 17 | 10 | 20 | |
| Blue | Mean | 74 | 93 | 91 | 85 | 80 | 75 | 68 | 69 | 65 | 72 | **77** |
| | Standard Deviation | 17 | 17 | 12 | 14 | 22 | 11 | 10 | 10 | 7 | 12 | |
| Waste rock -51-pattern 2 | | 1 | 2 | 3 | 4 | 5 | 6 | 7 | 8 | 9 | 10 | Average |
| | Area | 378 | 378 | 378 | 378 | 378 | 378 | 378 | 378 | 378 | 378 | |
| Red | Mean | 152 | 123 | 129 | 127 | 143 | 147 | 112 | 121 | 118 | 134 | **131** |
| | Standard Deviation | 8 | 24 | 13 | 11 | 24 | 15 | 15 | 20 | 18 | 26 | |
| Green | Mean | 165 | 136 | 141 | 140 | 156 | 160 | 123 | 133 | 130 | 146 | **143** |
| | Standard Deviation | 9 | 26 | 15 | 13 | 27 | 17 | 16 | 23 | 19 | 27 | |
| Blue | Mean | 92 | 76 | 79 | 77 | 86 | 90 | 68 | 74 | 72 | 82 | **79** |
| | Standard Deviation | 6 | 15 | 9 | 8 | 17 | 10 | 10 | 13 | 11 | 15 | |

| Waste rock-97-pattern 1 | | 1 | 2 | 3 | 4 | 5 | 6 | 7 | 8 | 9 | 10 | Average |
|---|---|---|---|---|---|---|---|---|---|---|---|---|
| | Area | 1452 | 1452 | 1452 | 1452 | 1452 | 1452 | 1452 | 1452 | 1452 | 1452 | |
| Red | Mean | 145 | 144 | 139 | 155 | 127 | 140 | 124 | 139 | 97 | 120 | **133** |
| | Standard Deviation | 21 | 21 | 26 | 20 | 22 | 22 | 24 | 22 | 13 | 25 | |
| Green | Mean | 157 | 157 | 150 | 168 | 139 | 152 | 135 | 151 | 106 | 131 | **145** |
| | Standard Deviation | 23 | 22 | 28 | 22 | 22 | 24 | 27 | 24 | 14 | 27 | |
| Blue | Mean | 86 | 86 | 82 | 91 | 77 | 81 | 73 | 83 | 57 | 72 | **79** |
| | Standard Deviation | 14 | 13 | 17 | 13 | 22 | 14 | 16 | 19 | 8 | 16 | |

| Waste rock-97-pattern 2 | | 1 | 2 | 3 | 4 | 5 | 6 | 7 | 8 | 9 | 10 | Average |
|---|---|---|---|---|---|---|---|---|---|---|---|---|
| | Area | 609 | 609 | 609 | 609 | 609 | 609 | 609 | 609 | 609 | 609 | |
| Red | Mean | 171 | 153 | 164 | 162 | 149 | 141 | 127 | 142 | 136 | 143 | **149** |
| | Standard Deviation | 16 | 23 | 21 | 18 | 23 | 14 | 27 | 19 | 28 | 24 | |
| Green | Mean | 187 | 166 | 179 | 179 | 164 | 153 | 140 | 156 | 147 | 156 | **163** |
| | Standard Deviation | 17 | 26 | 22 | 19 | 25 | 15 | 30 | 21 | 30 | 26 | |
| Blue | Mean | 103 | 92 | 99 | 99 | 91 | 84 | 77 | 85 | 81 | 85 | **90** |
| | Standard Deviation | 12 | 15 | 14 | 13 | 15 | 10 | 18 | 13 | 17 | 16 | |

| Mineralized rock-80 | | 1 | 2 | 3 | 4 | 5 | 6 | 7 | 8 | 9 | 10 | Average |
|---|---|---|---|---|---|---|---|---|---|---|---|---|
| | Area | 840 | 840 | 840 | 840 | 840 | 840 | 840 | 840 | 840 | 840 | |
| Red | Mean | 97 | 90 | 94 | 79 | 82 | 80 | 93 | 83 | 95 | 92 | 88 |
| | Standard Deviation | 9 | 8 | 9 | 10 | 12 | 12 | 10 | 10 | 17 | 12 | |
| Green | Mean | 106 | 98 | 102 | 87 | 89 | 87 | 101 | 92 | 105 | 101 | 97 |
| | Standard Deviation | 10 | 9 | 9 | 10 | 13 | 12 | 11 | 11 | 18 | 14 | |
| Blue | Mean | 53 | 50 | 51 | 44 | 45 | 45 | 52 | 47 | 54 | 51 | 49 |
| | Standard Deviation | 6 | 5 | 5 | 5 | 6 | 7 | 6 | 6 | 11 | 8 | |

| Mineralized rock -72-pattern 1 | | 1 | 2 | 3 | 4 | 5 | 6 | 7 | 8 | 9 | 10 | Average |
|---|---|---|---|---|---|---|---|---|---|---|---|---|
| | Area | 456 | 456 | 456 | 456 | 456 | 456 | 456 | 456 | 456 | 456 | |
| Red | Mean | 88 | 77 | 55 | 78 | 63 | 81 | 66 | 64 | 59 | 67 | 70 |
| | Standard Deviation | 10 | 12 | 6 | 11 | 8 | 14 | 8 | 11 | 16 | 11 | |
| Green | Mean | 97 | 85 | 61 | 87 | 71 | 90 | 74 | 72 | 65 | 74 | 78 |
| | Standard Deviation | 12 | 13 | 6 | 12 | 8 | 16 | 9 | 12 | 18 | 11 | |
| Blue | Mean | 53 | 46 | 33 | 46 | 37 | 49 | 40 | 38 | 35 | 38 | 41 |
| | Standard Deviation | 6 | 8 | 4 | 7 | 4 | 9 | 5 | 7 | 10 | 5 | |

| Mineralized rock-72-pattern 2 | | 1 | 2 | 3 | 4 | 5 | 6 | 7 | 8 | 9 | 10 | Average |
|---|---|---|---|---|---|---|---|---|---|---|---|---|
| | Area | 540 | 540 | 540 | 540 | 540 | 540 | 540 | 540 | 540 | 540 | |
| Red | Mean | 82 | 60 | 54 | 69 | 71 | 55 | 82 | 57 | 85 | 79 | 69 |
| | Standard Deviation | 14 | 8 | 7 | 11 | 17 | 6 | 13 | 6 | 10 | 20 | |
| Green | Mean | 91 | 66 | 60 | 77 | 78 | 60 | 92 | 63 | 96 | 87 | 77 |
| | Standard Deviation | 15 | 9 | 7 | 12 | 18 | 7 | 14 | 6 | 11 | 21 | |
| Blue | Mean | 49 | 36 | 32 | 40 | 42 | 32 | 50 | 33 | 52 | 45 | 41 |
| | Standard Deviation | 8 | 6 | 5 | 6 | 17 | 4 | 7 | 4 | 7 | 11 | |

## APPENDIX D MICROWAVE-INFRARED SORTING DATA

### Calculation of the Absorbed Microwave Energy

The weight of rock #50 (RockID #37) in the following figure for -37.5+26.5 mm size fraction is 40.4 g. Grades for Pb, Zn, Fe and Light elements are 13.85%, 61.67%, 3.68% and 20.80%. The specific heat capacities for Pb, Zn, Fe, S and Ca (S and Ca are major light elements in this ore sample) are 0.16, 0.39, 0.45, 0.73 and 0.65(Engineering Toolbox) respectively. The specific heat capacity for light elements is 0.70 used for the calculation. The average specific heat capacity for this rock is then Cp=0.42.

$P*t=Cp*\Delta T*M=0.42*(168-23)*40.4=2460.36J$

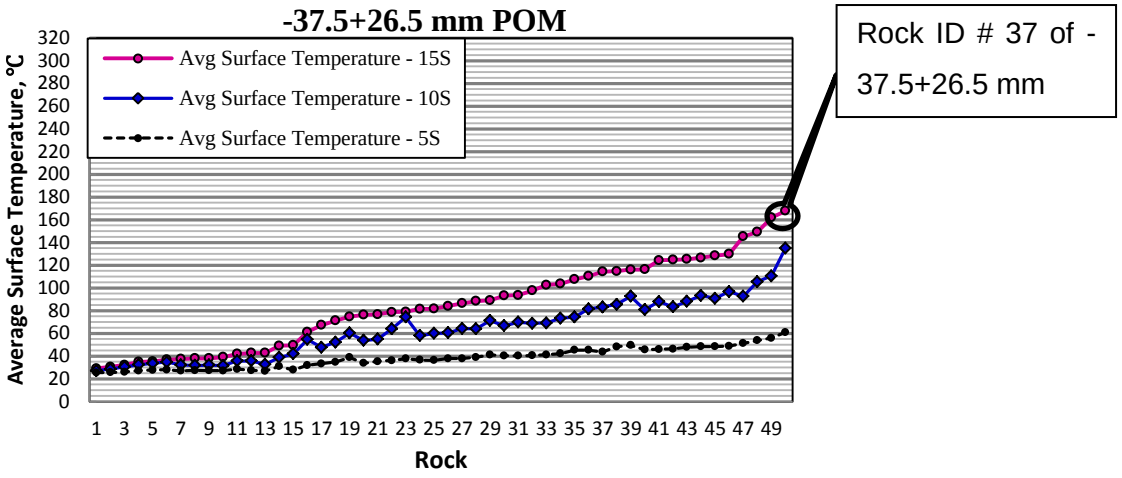


Efficiency of microwave heating of 15s =2460.36/(1000*15)=16%

Based on the results derived from the above calculation, it can be concluded that the large rock (-37.5+26.5 mm) can be only heated up to 168 °C (compared to 300 °C for the rock sized -19+13.2 mm) after 15s microwave heating is not because of shortage of microwave energy.

The calculation above is based on the XRF surface reading of metal grades. Assumptions are made that the average temperature of measured surface equals to the average temperature of the bulk rock. This assumption may be valid for small rocks with mass of 30 g -50 g, but may cause bias on the large rocks with mass of 300 g-400 g due to the limit of penetration depth. Thus, the energy calculation here is only approximate and is only used for the above conclusion.

**-53+37.5 mm Size Fraction MW/IR Sorting**

**Initial Data Set**

| Sample ID | Weight, g | Metal Content, % | | | Average Temperature, °C | | | |
|---|---|---|---|---|---|---|---|---|
| | | Pb | Zn | Pb+Zn | 10s | 20s | 30s | G9-10s |
| 1 | 201.1 | 56.87 | 20.04 | 76.91 | 56 | 98 | 141 | 32 |
| 2 | 287.9 | 16.13 | 9.85 | 25.98 | 48 | 81 | 111 | 29 |
| 3 | 187.1 | 3.26 | 8.36 | 11.62 | 49 | 80 | 113 | 30 |
| 4 | 140.1 | 0.02 | 0.84 | 0.86 | 33 | 49 | 62 | 26 |
| 5 | 124.2 | 23.79 | 10.08 | 33.87 | 63 | 106 | 154 | 32 |
| 6 | 115.2 | 0.52 | 21.84 | 22.37 | 62 | 114 | 148 | 34 |
| 7 | 161.2 | 18.87 | 9.64 | 28.51 | 50 | 92 | 122 | 28 |
| 8 | 159.7 | 0.01 | 0.82 | 0.83 | 31 | 39 | 50 | 24 |
| 9 | 231.1 | 11.41 | 18.43 | 29.84 | 47 | 75 | 106 | 30 |
| 10 | 243.8 | 0.02 | 0.75 | 0.77 | 34 | 47 | 60 | 25 |
| 11 | 120.5 | 44.05 | 23.91 | 67.96 | 65 | 114 | 158 | 31 |
| 12 | 256.4 | 0.05 | 0.81 | 0.86 | 34 | 47 | 61 | 25 |
| 13 | 140.2 | 6.06 | 3.98 | 10.04 | 56 | 101 | 139 | 30 |
| 14 | 197.7 | 4.50 | 9.92 | 14.42 | 50 | 89 | 120 | 28 |
| 15 | 261.3 | 0.85 | 8.19 | 9.05 | 50 | 81 | 115 | 31 |
| 16 | 113.4 | 0.48 | 8.10 | 8.58 | 63 | 107 | 149 | 31 |
| 17 | 198.0 | 0.71 | 1.39 | 2.10 | 51 | 82 | 117 | 28 |
| 18 | 153.9 | 0.53 | 12.26 | 12.79 | 59 | 101 | 138 | 31 |
| 19 | 144.4 | 33.11 | 7.32 | 40.42 | 61 | 102 | 141 | 33 |
| 20 | 77.8 | 0.09 | 1.67 | 1.75 | 38 | 58 | 76 | 26 |
| 21 | 123.0 | 0.05 | 0.77 | 0.82 | 33 | 46 | 56 | 25 |
| 22 | 138.3 | 0.39 | 1.20 | 1.59 | 54 | 94 | 127 | 34 |
| 23 | 169.2 | 3.74 | 10.44 | 14.18 | 57 | 97 | 138 | 32 |
| 24 | 282.3 | 0.80 | 1.14 | 1.94 | 45 | 73 | 99 | 31 |
| 25 | 148.3 | 0.02 | 0.76 | 0.78 | 32 | 44 | 61 | 25 |

| Sample ID | Weight, g | Metal Content, % | | | Average Temperature, °C | | | |
|---|---|---|---|---|---|---|---|---|
| | | Pb | Zn | Pb+Zn | 10s | 20s | 30s | G9-10s |
| 26 | 212.0 | 3.68 | 5.85 | 9.53 | 51 | 85 | 122 | 32 |
| 27 | 90.9 | 52.80 | 19.71 | 72.51 | 75 | 138 | 181 | 31 |
| 28 | 145.0 | 31.81 | 17.90 | 49.72 | 58 | 102 | 146 | 35 |
| 29 | 160.2 | 67.84 | 16.27 | 84.11 | 60 | 112 | 151 | 30 |
| 30 | 125.1 | 0.88 | 10.00 | 10.88 | 60 | 103 | 140 | 35 |
| 31 | 143.6 | 6.28 | 10.97 | 17.24 | 59 | 98 | 128 | 31 |
| 32 | 336.2 | 13.33 | 8.58 | 21.92 | 49 | 77 | 107 | 29 |
| 33 | 166.0 | 0.15 | 0.79 | 0.95 | 32 | 42 | 56 | 25 |
| 34 | 317.3 | 53.58 | 14.81 | 68.38 | 48 | 76 | 106 | 29 |
| 35 | 121.9 | 1.71 | 14.33 | 16.05 | 56 | 98 | 136 | 30 |
| 36 | 110.6 | 2.00 | 2.37 | 4.37 | 59 | 102 | 138 | 30 |
| 37 | 280.8 | 16.92 | 15.29 | 32.21 | 48 | 72 | 101 | 29 |
| 38 | 210.4 | 2.28 | 2.36 | 4.63 | 48 | 79 | 104 | 29 |
| 39 | 374.5 | 6.17 | 7.07 | 13.24 | 42 | 69 | 85 | 28 |
| 40 | 168.8 | 0.10 | 0.83 | 0.94 | 32 | 45 | 55 | 25 |
| 41 | 275.8 | 0.58 | 14.08 | 14.65 | 47 | 76 | 107 | 30 |
| 42 | 183.6 | 0.22 | 0.93 | 1.15 | 33 | 48 | 59 | 25 |
| 43 | 195.4 | 0.09 | 0.81 | 0.90 | 35 | 51 | 68 | 26 |
| 44 | 207.6 | 0.15 | 0.87 | 1.02 | 35 | 52 | 63 | 26 |
| 45 | 282.6 | 13.18 | 16.67 | 29.85 | 47 | 74 | 102 | 30 |
| 46 | 156.8 | 3.73 | 21.17 | 24.90 | 59 | 100 | 146 | |
| 47 | 184.7 | 43.55 | 26.98 | 70.53 | 52 | 90 | 116 | |
| 48 | 232.8 | 0.18 | 0.89 | 1.07 | 40 | 61 | 79 | |
| 49 | 117.8 | 2.17 | 5.41 | 7.58 | 61 | 111 | 142 | |
| 50 | 168.7 | 1.21 | 1.55 | 2.76 | 56 | 92 | 132 | |

## Sortability Graph

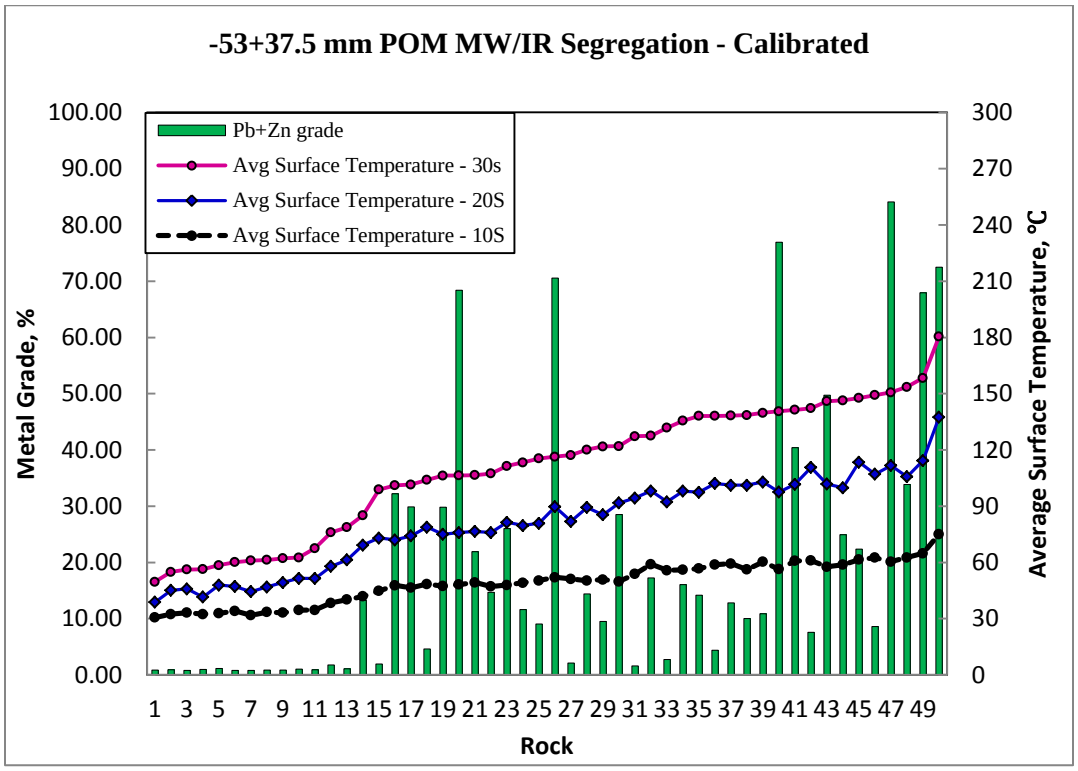


## Individual and Group Tests

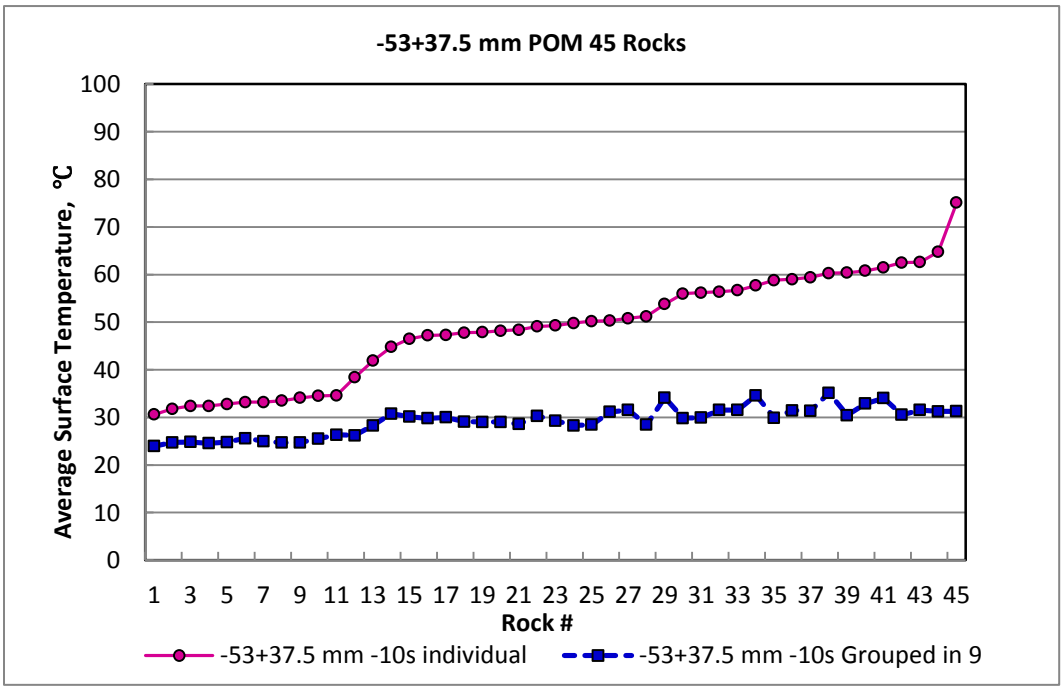

**-53+37.5 mm MW/IR Sorting Results –Individual 10s (Calibrated XRF Surface Readings)**

| Separation Temperature, °C | Hot Fraction | Cold Fraction | Wt. % in Hot Fraction | | Wt. % in Cold Fraction | | % in Hot Fraction | | % in Cold Fraction | |
|---|---|---|---|---|---|---|---|---|---|---|
| | | | Concentrate Grades, % | | Waste Grades, % | | Metal Recovery, % | | Metal Recovery, % | |
| | Conc. % | Waste % | Pb | Zn | Pb | Zn | Pb | Zn | Pb | Zn |
| **32** | 93.1 | 6.9 | 11.87 | 9.11 | 0.07 | 0.80 | 100.0 | 99.4 | 0.0 | 0.6 |
| **33** | 88.3 | 11.7 | 12.51 | 9.56 | 0.09 | 0.83 | 99.9 | 98.9 | 0.1 | 1.1 |
| **35** | **78.7** | **21.3** | **14.03** | **10.63** | **0.08** | **0.82** | **99.8** | **98.0** | **0.2** | **2.0** |
| **45** | 68.3 | 31.7 | 15.75 | 11.72 | 0.93 | 1.67 | 97.3 | 93.8 | 2.7 | 6.2 |
| **47** | 59.9 | 40.1 | 16.81 | 11.08 | 2.47 | 4.74 | 91.0 | 77.7 | 9.0 | 22.3 |
| **48** | 48.1 | 51.9 | 14.93 | 11.04 | 7.46 | 6.21 | 65.0 | 62.3 | 35.0 | 37.7 |
| **49** | 42.5 | 57.5 | 15.62 | 11.38 | 7.68 | 6.44 | 60.1 | 56.7 | 39.9 | 43.3 |
| **50** | 35.9 | 64.1 | 17.27 | 11.79 | 7.58 | 6.72 | 56.1 | 49.6 | 43.9 | 50.4 |
| **55** | 28.1 | 71.9 | 18.66 | 12.55 | 8.09 | 6.97 | 47.3 | 41.2 | 52.7 | 58.8 |
| **56** | 21.3 | 78.7 | 18.20 | 13.22 | 9.13 | 7.27 | 35.1 | 33.0 | 64.9 | 67.0 |
| **60** | 8.8 | 91.2 | 22.04 | 13.37 | 9.99 | 8.07 | 17.6 | 13.8 | 82.4 | 86.2 |
| **Calculated Head Grade: 11.06% Pb and 8.54% Zn** | | | | | | | | | | |

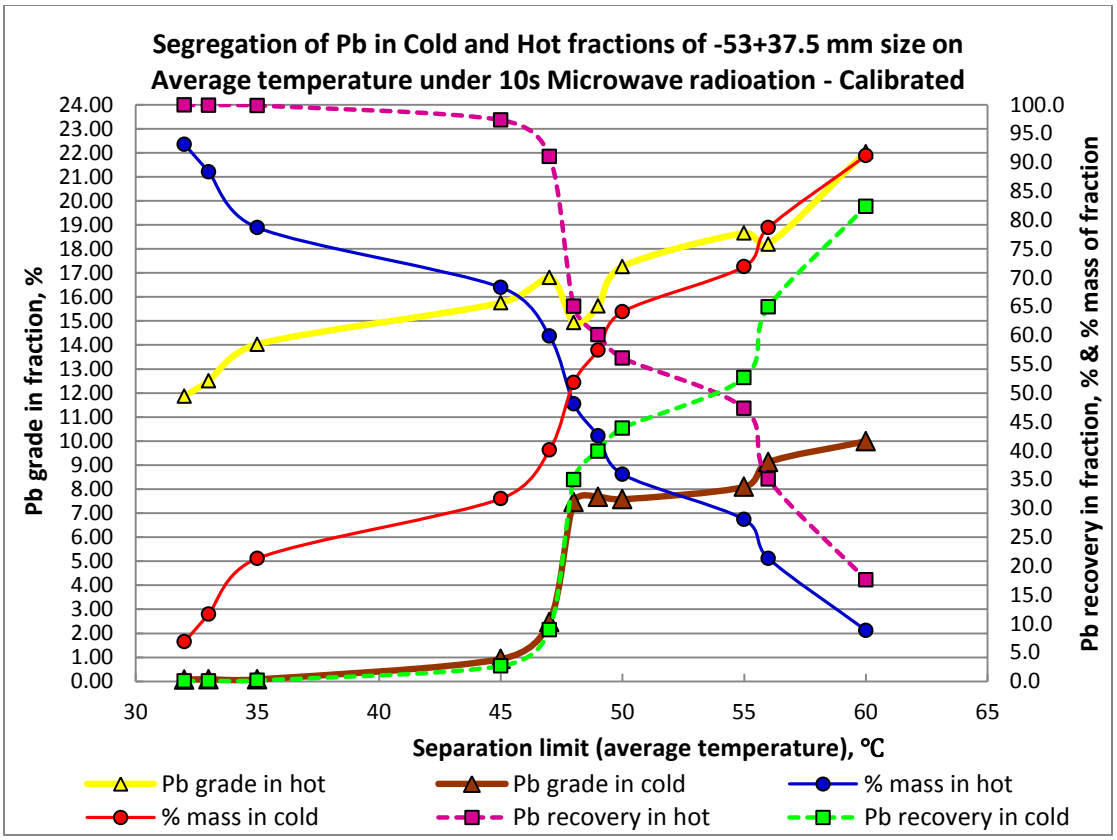
Segregation of Pb in Cold and Hot fractions of -53+37.5 mm size on Average temperature under 10s Microwave radioation - Calibrated
Pb grade in fraction, %
Pb recovery in fraction, % & % mass of fraction
Separation limit (average temperature), ℃
Pb grade in hot
Pb grade in cold
% mass in hot
% mass in cold
Pb recovery in hot
Pb recovery in cold

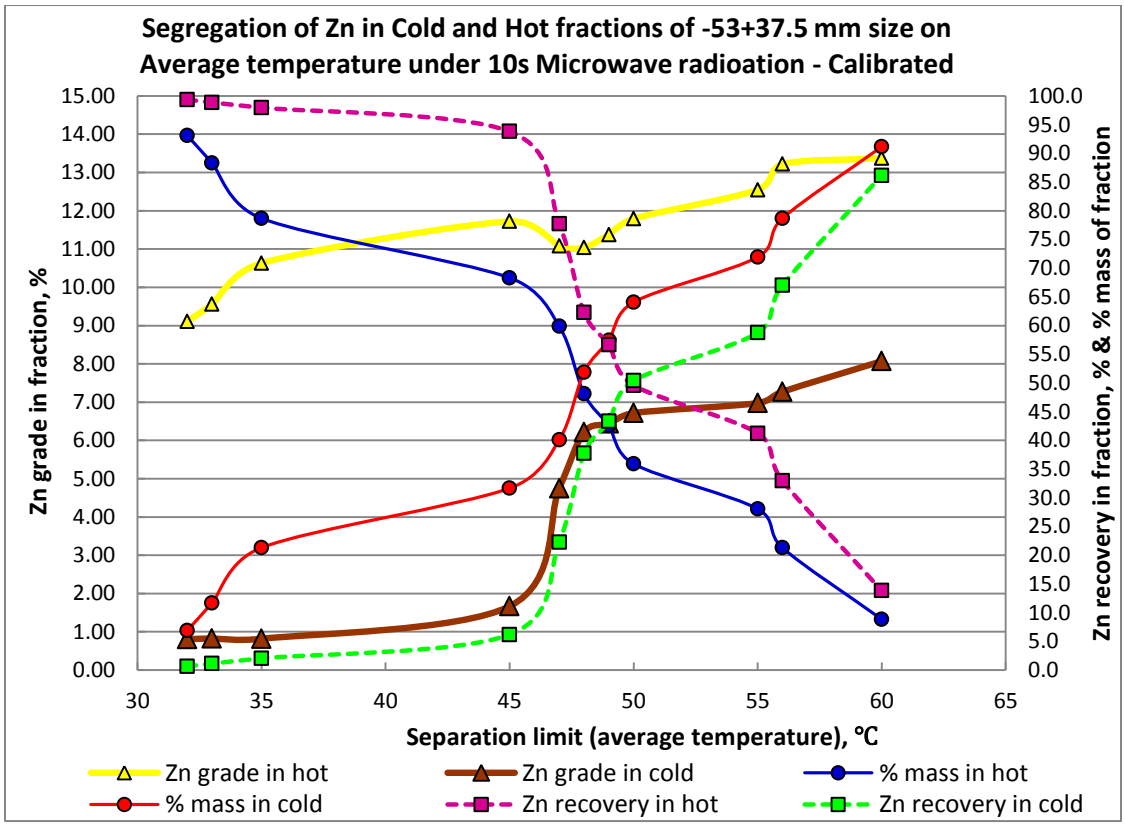
Segregation of Zn in Cold and Hot fractions of -53+37.5 mm size on Average temperature under 10s Microwave radioation - Calibrated
Zn grade in fraction, %
Zn recovery in fraction, % & % mass of fraction
Separation limit (average temperature), ℃
Zn grade in hot
Zn grade in cold
% mass in hot
% mass in cold
Zn recovery in hot
Zn recovery in cold

**-53+37.5 mm MW/IR Sorting Results –Individual 20s (Calibrated XRF Surface Readings)**

| Separation Temperature, °C | Hot Fraction | Cold Fraction | Wt. % in Hot Fraction | | Wt. % in Cold Fraction | | % in Hot Fraction | | % in Cold Fraction | |
|---|---|---|---|---|---|---|---|---|---|---|
| | | | Concentrate Grades, % | | Waste Grades, % | | Metal Recovery, % | | Metal Recovery, % | |
| | Conc. % | Waste % | Pb | Zn | Pb | Zn | Pb | Zn | Pb | Zn |
| **45** | 93.1 | 6.9 | 11.87 | 9.11 | 0.07 | 0.80 | 100.0 | 99.4 | 0.0 | 0.6 |
| **47** | 86.5 | 13.5 | 12.78 | 9.75 | 0.06 | 0.79 | 99.9 | 98.7 | 0.1 | 1.3 |
| **52** | **78.7** | **21.3** | **14.03** | **10.63** | **0.08** | **0.82** | **99.8** | **98.0** | **0.2** | **2.0** |
| **70** | **71.3** | **28.7** | **15.12** | **11.28** | **0.94** | **1.72** | **97.6** | **94.2** | **2.4** | **5.8** |
| **75** | 59.8 | 40.2 | 16.00 | 11.02 | 3.69 | 4.85 | 86.6 | 77.2 | 13.4 | 22.8 |
| **80** | 45.6 | 54.4 | 15.65 | 11.27 | 7.20 | 6.24 | 64.6 | 60.2 | 35.4 | 39.8 |
| **85** | 35.4 | 64.6 | 18.45 | 12.58 | 7.02 | 6.33 | 59.0 | 52.1 | 41.0 | 47.9 |
| **90** | 31.3 | 68.7 | 17.80 | 11.85 | 7.99 | 7.03 | 50.3 | 43.4 | 49.7 | 56.6 |
| **92** | 27.7 | 72.3 | 18.82 | 12.66 | 8.08 | 6.96 | 47.2 | 41.1 | 52.8 | 58.9 |
| **100** | 17.8 | 82.2 | 21.04 | 12.17 | 8.90 | 7.75 | 33.8 | 25.3 | 66.2 | 74.7 |
| **105** | 9.0 | 91.0 | 28.85 | 14.96 | 9.30 | 7.90 | 23.5 | 15.8 | 76.5 | 84.2 |
| **Calculated Head Grade: 11.06% Pb and 8.54% Zn** | | | | | | | | | | |

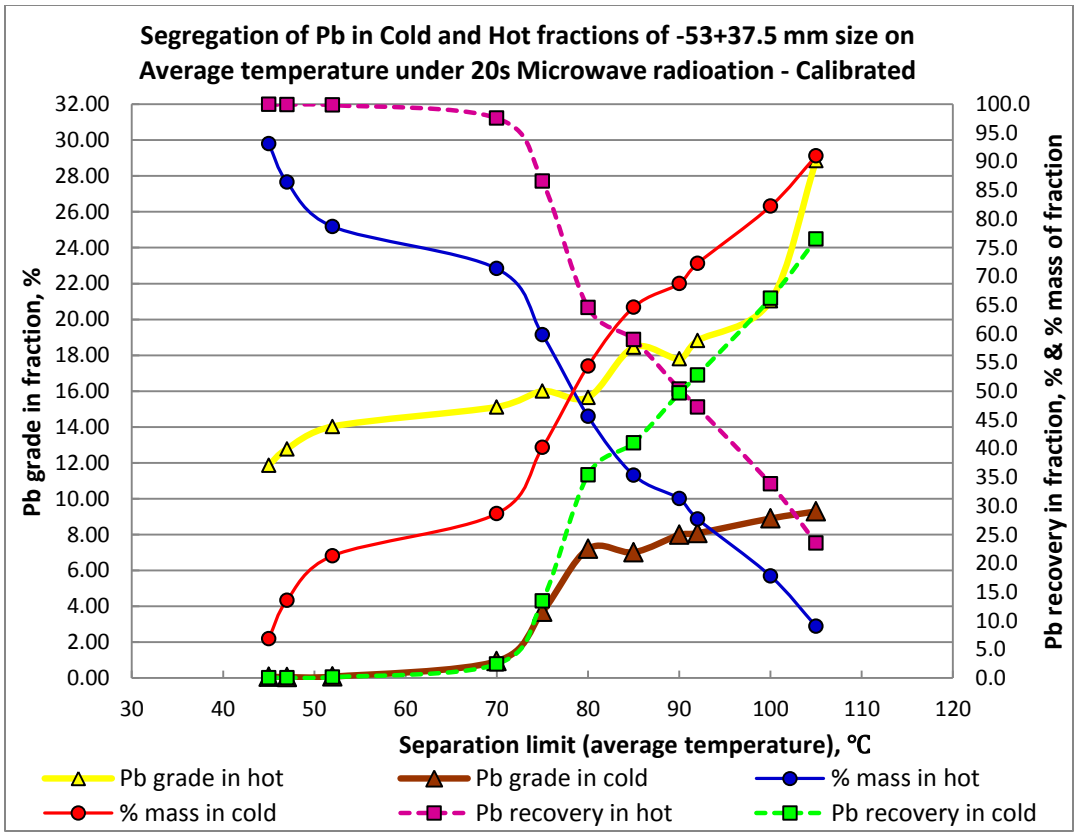
Segregation of Pb in Cold and Hot fractions of -53+37.5 mm size on
Average temperature under 20s Microwave radioation - Calibrated
Pb grade in fraction, %
Pb recovery in fraction, % & % mass of fraction
Separation limit (average temperature), ℃
Pb grade in hot
Pb grade in cold
% mass in hot
% mass in cold
Pb recovery in hot
Pb recovery in cold

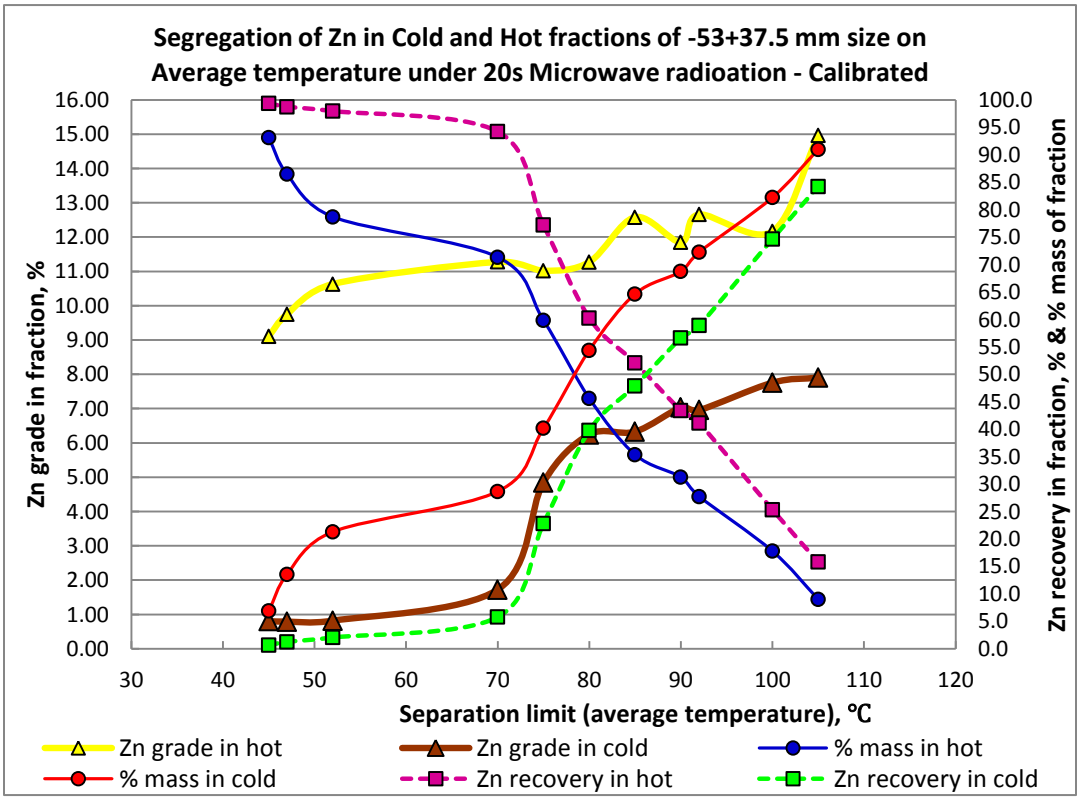
Segregation of Zn in Cold and Hot fractions of -53+37.5 mm size on
Average temperature under 20s Microwave radioation - Calibrated
Zn grade in fraction, %
Zn recovery in fraction, % & % mass of fraction
Separation limit (average temperature), ℃
Zn grade in hot
Zn grade in cold
% mass in hot
% mass in cold
Zn recovery in hot
Zn recovery in cold

**-53+37.5 mm MW/IR Sorting Results –Individual 30s (Calibrated XRF Surface Reading)**

| Separation Temperature, °C | Hot Fraction | Cold Fraction | Wt. % in Hot Fraction | | Wt. % in Cold Fraction | | % in Hot Fraction | | % in Cold Fraction | |
|---|---|---|---|---|---|---|---|---|---|---|
| | | | Concentrate Grades, % | | Waste Grades, % | | Metal Recovery, % | | Metal Recovery, % | |
| | Conc. % | Waste % | Pb | Zn | Pb | Zn | Pb | Zn | Pb | Zn |
| **56** | 93.4 | 6.6 | 11.83 | 9.09 | 0.08 | 0.81 | 100.0 | 99.4 | 0.0 | 0.6 |
| **60** | 88.8 | 11.2 | 12.44 | 9.51 | 0.09 | 0.81 | 99.9 | 98.9 | 0.1 | 1.1 |
| **70** | **78.7** | **21.3** | **14.03** | **10.63** | **0.08** | **0.82** | **99.8** | **98.0** | **0.2** | **2.0** |
| **90** | **71.3** | **28.7** | **15.12** | **11.28** | **0.94** | **1.72** | **97.6** | **94.2** | **2.4** | **5.8** |
| **105** | 60.0 | 40.0 | 16.33 | 11.65 | 3.13 | 3.87 | 88.7 | 81.9 | 11.3 | 18.1 |
| **110** | 47.6 | 52.4 | 15.13 | 11.15 | 7.35 | 6.16 | 65.2 | 62.2 | 34.8 | 37.8 |
| **120** | 33.5 | 66.5 | 16.85 | 11.45 | 8.14 | 7.07 | 51.1 | 45.0 | 48.9 | 55.0 |
| **130** | 26.5 | 73.5 | 16.43 | 10.72 | 8.06 | 7.06 | 46.5 | 39.3 | 53.5 | 60.7 |
| **140** | 15.9 | 84.1 | 30.69 | 15.85 | 7.33 | 7.15 | 44.2 | 29.6 | 55.8 | 70.4 |
| **150** | 5.3 | 94.7 | 48.27 | 17.20 | 8.97 | 8.05 | 23.2 | 10.7 | 76.8 | 89.3 |
| **160** | 1.0 | 99.0 | 52.80 | 19.71 | 10.65 | 8.43 | 4.6 | 2.2 | 95.4 | 97.8 |
| **Calculated Head Grade: 11.06% Pb and 8.54% Zn** | | | | | | | | | | |

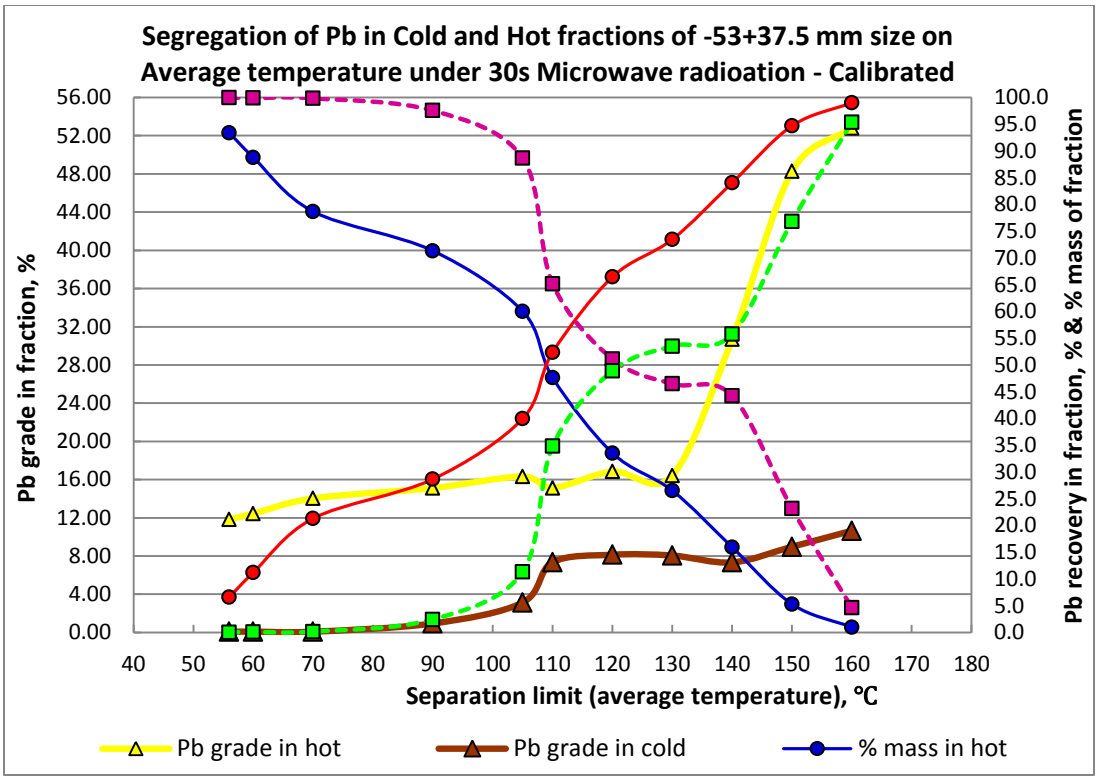
Segregation of Pb in Cold and Hot fractions of -53+37.5 mm size on Average temperature under 30s Microwave radioation - Calibrated
Pb grade in fraction, %
Pb recovery in fraction, % & % mass of fraction
Separation limit (average temperature), ℃
Pb grade in hot
Pb grade in cold
% mass in hot

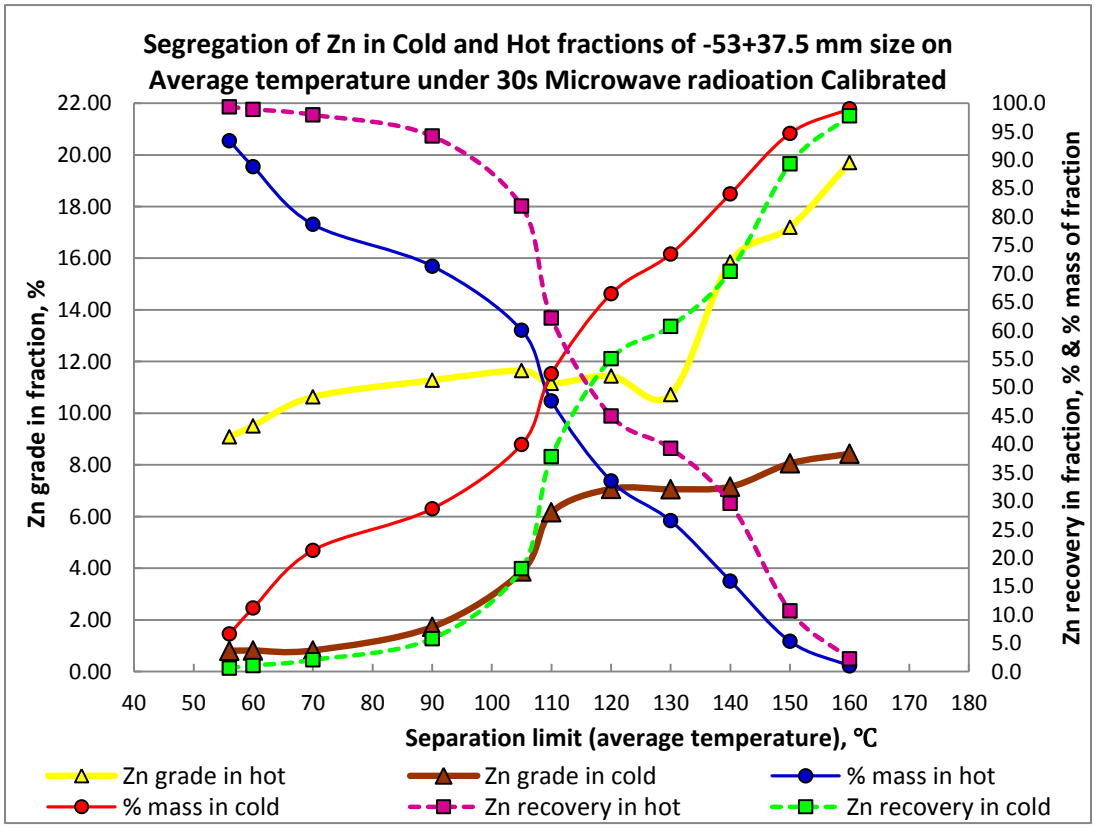
Segregation of Zn in Cold and Hot fractions of -53+37.5 mm size on Average temperature under 30s Microwave radioation Calibrated
Zn grade in fraction, %
Zn recovery in fraction, % & % mass of fraction
Separation limit (average temperature), ℃
Zn grade in hot
Zn grade in cold
% mass in hot
% mass in cold
Zn recovery in hot
Zn recovery in cold

**-53+37.5 mm MW/IR Sorting Results –Individual 10s for 45 Rocks (Calibrated XRF Surface Reading)**

| Separation Temperature, °C | Hot Fraction | Cold Fraction | Wt. % in Hot Fraction | | Wt. % in Cold Fraction | | % in Hot Fraction | | % in Cold Fraction | |
|---|---|---|---|---|---|---|---|---|---|---|
| | | | Concentrate Grades, % | | Waste Grades, % | | Metal Recovery, % | | Metal Recovery, % | |
| | Conc. % | Waste % | Pb | Zn | Pb | Zn | Pb | Zn | Pb | Zn |
| **32** | 92.4 | 7.6 | 12.01 | 8.91 | 0.07 | 0.80 | 99.9 | 99.3 | 0.1 | 0.7 |
| **33** | 87.2 | 12.8 | 12.73 | 9.40 | 0.09 | 0.83 | 99.9 | 98.7 | 0.1 | 1.3 |
| **35** | **76.5** | **23.5** | **14.49** | **10.59** | **0.08** | **0.82** | **99.8** | **97.7** | **0.2** | **2.3** |
| **45** | 67.9 | 32.1 | 15.89 | 11.41 | 0.99 | 1.73 | 97.1 | 93.3 | 2.9 | 6.7 |
| **47** | 58.5 | 41.5 | 17.11 | 10.63 | 2.62 | 5.00 | 90.2 | 75.0 | 9.8 | 25.0 |
| **48** | 45.6 | 54.4 | 15.01 | 10.46 | 7.83 | 6.48 | 61.7 | 57.5 | 38.3 | 42.5 |
| **49** | 39.5 | 60.5 | 15.83 | 10.76 | 8.02 | 6.69 | 56.3 | 51.2 | 43.7 | 48.8 |
| **50** | 32.1 | 67.9 | 17.91 | 11.14 | 7.88 | 6.95 | 51.9 | 43.2 | 48.1 | 56.8 |
| **55** | 25.7 | 74.3 | 21.97 | 13.17 | 7.35 | 6.61 | 50.8 | 40.8 | 49.2 | 59.2 |
| **56** | 20.2 | 79.8 | 20.62 | 13.03 | 8.69 | 7.10 | 37.6 | 31.8 | 62.4 | 68.2 |
| **60** | 8.4 | 91.6 | 25.34 | 14.70 | 9.81 | 7.71 | 19.1 | 14.8 | 80.9 | 85.2 |
| **Calculated Head Grade: 11.10% Pb and 8.30% Zn** | | | | | | | | | | |

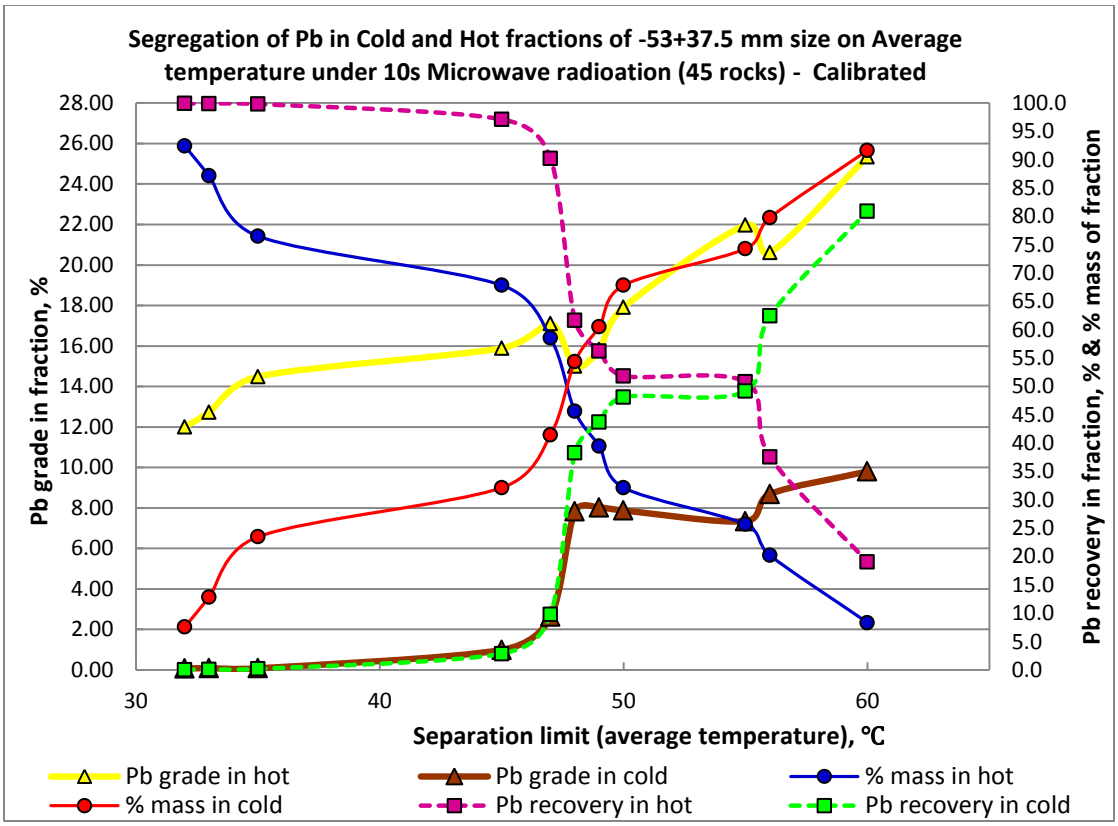
Segregation of Pb in Cold and Hot fractions of -53+37.5 mm size on Average temperature under 10s Microwave radioation (45 rocks) - Calibrated
Pb grade in fraction, %
Pb recovery in fraction, % & % mass of fraction
Separation limit (average temperature), ℃
Pb grade in hot
Pb grade in cold
% mass in hot
% mass in cold
Pb recovery in hot
Pb recovery in cold

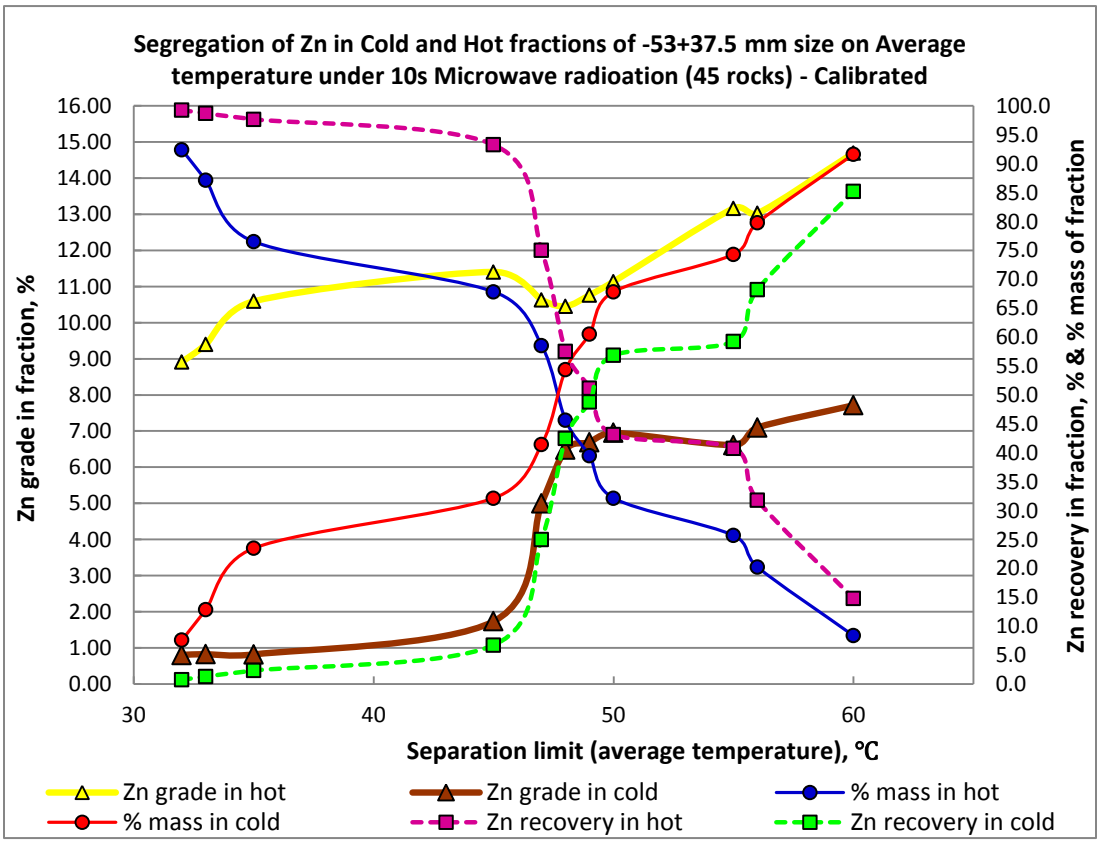
Segregation of Zn in Cold and Hot fractions of -53+37.5 mm size on Average temperature under 10s Microwave radioation (45 rocks) - Calibrated
Zn grade in fraction, %
Zn recovery in fraction, % & % mass of fraction
Separation limit (average temperature), ℃
Zn grade in hot
Zn grade in cold
% mass in hot
% mass in cold
Zn recovery in hot
Zn recovery in cold

**-53+37.5 mm MW/IR Sorting Results –Group in 9 10s for 45 Rocks (Calibrated XRF Surface Reading)**

| Separation Temperature, °C | Hot Fraction | Cold Fraction | Wt. % in Hot Fraction | | Wt. % in Cold Fraction | | % in Hot Fraction | | % in Cold Fraction | |
|---|---|---|---|---|---|---|---|---|---|---|
| | | | Concentrate Grades, % | | Waste Grades, % | | Metal Recovery, % | | Metal Recovery, % | |
| | Conc. % | Waste % | Pb | Zn | Pb | Zn | Pb | Zn | Pb | Zn |
| **24** | 98.1 | 1.9 | 11.32 | 8.44 | 0.01 | 0.82 | 100.0 | 99.8 | 0.0 | 0.2 |
| **25** | 82.9 | 17.1 | 13.38 | 9.84 | 0.08 | 0.81 | 99.9 | 98.3 | 0.1 | 1.7 |
| **26** | **75.6** | **24.4** | **14.66** | **10.70** | **0.08** | **0.85** | **99.8** | **97.5** | **0.2** | **2.5** |
| **28** | 64.6 | 35.4 | 15.99 | 11.34 | 2.18 | 2.73 | 93.0 | 88.4 | 7.0 | 11.6 |
| **29** | 47.7 | 52.3 | 13.90 | 11.60 | 8.55 | 5.28 | 59.8 | 66.7 | 40.2 | 33.3 |
| **30** | 29.9 | 70.1 | 14.57 | 10.78 | 9.62 | 7.23 | 39.3 | 38.9 | 60.7 | 61.1 |
| **31** | 16.2 | 83.8 | 18.50 | 11.55 | 9.67 | 7.67 | 27.0 | 22.6 | 73.0 | 77.4 |
| **32** | 7.9 | 92.1 | 14.40 | 11.36 | 10.82 | 10.57 | 10.2 | 10.8 | 89.8 | 89.2 |
| **Calculated Head Grade: 11.10% Pb and 8.30% Zn** | | | | | | | | | | |

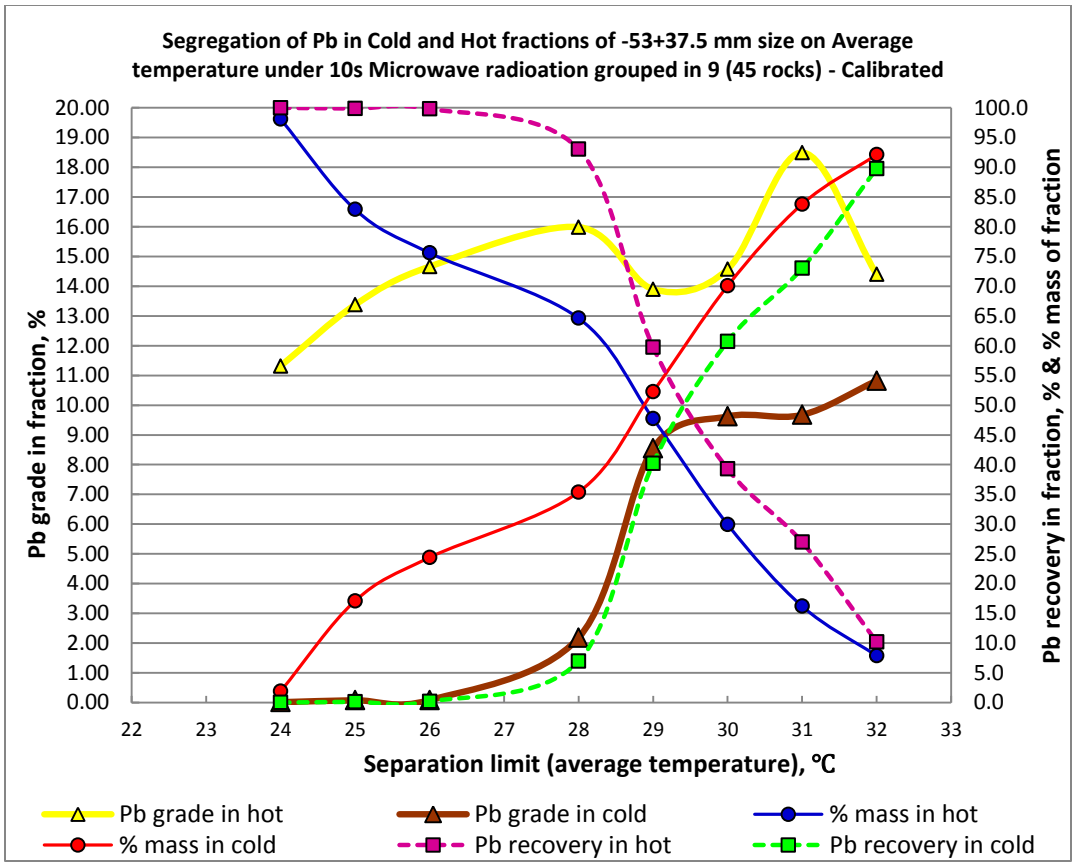
Segregation of Pb in Cold and Hot fractions of -53+37.5 mm size on Average temperature under 10s Microwave radioation grouped in 9 (45 rocks) - Calibrated
Pb grade in fraction, %
Pb recovery in fraction, % & % mass of fraction
Separation limit (average temperature), ℃
Pb grade in hot
Pb grade in cold
% mass in hot
% mass in cold
Pb recovery in hot
Pb recovery in cold

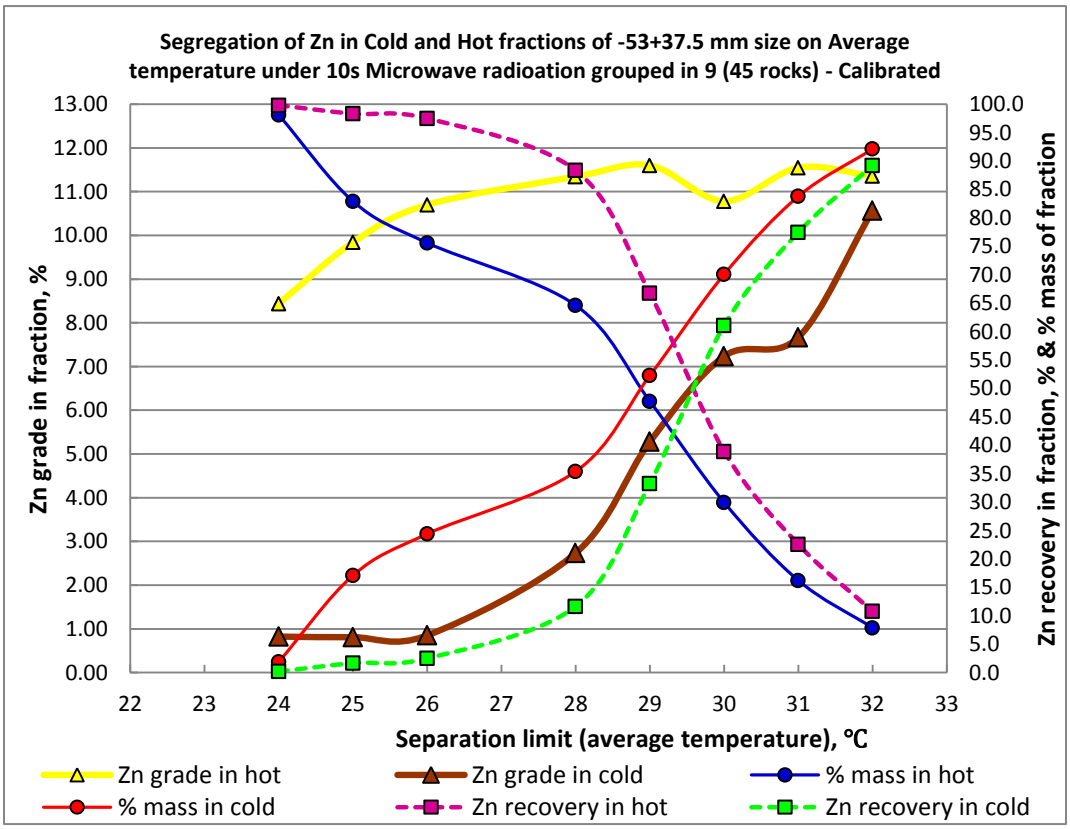
Segregation of Zn in Cold and Hot fractions of -53+37.5 mm size on Average temperature under 10s Microwave radioation grouped in 9 (45 rocks) - Calibrated
Zn grade in fraction, %
Zn recovery in fraction, % & % mass of fraction
Separation limit (average temperature), ℃
Zn grade in hot
Zn grade in cold
% mass in hot
% mass in cold
Zn recovery in hot
Zn recovery in cold

**-53+37.5 mm Size Fraction Sorting Results Summary**

| Test Condition | Separation Limit, °C | Mass % of Cold | Pb in Hot Fraction, % | | Zn in Hot Fraction, % | |
|---|---|---|---|---|---|---|
| | | | Grade | Recovery | Grade | Recovery |
| 10s | 35 | 21.3 | 14.03 | 99.8 | 10.63 | 98.0 |
| 20s | 70 | 28.7 | 15.12 | 97.6 | 11.28 | 94.2 |
| 30s | 90 | 28.7 | 15.12 | 97.6 | 11.28 | 94.2 |
| Calculated Head Grade: 11.06% Pb and 8.54% Zn 50 rocks being tested | | | | | | |
| **Test Condition** | **Separation Limit, °C** | **Mass % of Cold** | **Pb in Hot Fraction, %** | | **Zn in Hot Fraction, %** | |
| | | | **Grade** | **Recovery** | **Grade** | **Recovery** |
| Individual | 35 | 23.5 | 14.49 | 99.8 | 10.59 | 97.7 |
| Group in 9 | 26 | 24.4 | 14.66 | 99.8 | 10.70 | 97.5 |
| Calculated Head Grade: 11.10% Pb and 8.30% Zn 45 rocks being tested | | | | | | |

**-37.5+26.5 mm Size Fraction MW/IR Sorting**

**Initial Data Set**

| Sample ID | Weight, g | Metal Content, % | | | Average Temperature, °C | | | | |
|---|---|---|---|---|---|---|---|---|---|
| | | Pb | Zn | Pb+Zn | 5s | 10s | 15s | G4-10s | G9-10s |
| 1 | 213.2 | 1.47 | 1.57 | 3.04 | 33 | 48 | 67 | 38 | 33 |
| 2 | 146.1 | 1.01 | 1.05 | 2.06 | 35 | 52 | 71 | 41 | 35 |
| 3 | 86.3 | 46.55 | 24.71 | 71.26 | 44 | 83 | 114 | 42 | 37 |
| 4 | 97.6 | 1.11 | 2.10 | 3.21 | 37 | 58 | 82 | 38 | 36 |
| 5 | 75.4 | 0.06 | 0.87 | 0.93 | 29 | 36 | 42 | 32 | 29 |
| 6 | 70.1 | 8.12 | 37.79 | 45.90 | 46 | 88 | 124 | 68 | 44 |
| 7 | 77.2 | 4.03 | 2.30 | 6.33 | 40 | 70 | 94 | 52 | 39 |
| 8 | 64.5 | 0.19 | 4.60 | 4.79 | 32 | 55 | 61 | 31 | 30 |
| 9 | 39.9 | 0.02 | 0.79 | 0.80 | 27 | 36 | 43 | 27 | 26 |
| 10 | 42.1 | 0.04 | 0.80 | 0.84 | 28 | 35 | 37 | 28 | 27 |
| 11 | 143.4 | 0.38 | 7.41 | 7.79 | 35 | 55 | 77 | 45 | 38 |
| 12 | 87.0 | 0.21 | 13.66 | 13.87 | 36 | 60 | 82 | 46 | 39 |
| 13 | 40.2 | 0.41 | 13.41 | 13.82 | 56 | 111 | 162 | 73 | 52 |
| 14 | 31.7 | 0.03 | 0.79 | 0.82 | 28 | 32 | 38 | 26 | 27 |
| 15 | 83.0 | 1.24 | 30.71 | 31.94 | 42 | 73 | 104 | 50 | 42 |
| 16 | 94.0 | 0.08 | 0.81 | 0.89 | 39 | 64 | 88 | 49 | 41 |
| 17 | 40.7 | 0.02 | 0.78 | 0.80 | 27 | 32 | 39 | 27 | 26 |
| 18 | 34.3 | 0.03 | 0.78 | 0.81 | 28 | 42 | 50 | 29 | 27 |
| 19 | 91.1 | 2.11 | 11.94 | 14.05 | 41 | 69 | 98 | 58 | 41 |
| 20 | 49.0 | 0.41 | 2.99 | 3.40 | 50 | 93 | 116 | 68 | 40 |
| 21 | 87.4 | 0.04 | 0.87 | 0.91 | 38 | 64 | 87 | 51 | 38 |
| 22 | 95.9 | 0.12 | 9.08 | 9.19 | 36 | 64 | 79 | 46 | 35 |
| 23 | 68.3 | 60.92 | 14.35 | 75.27 | 45 | 82 | 110 | 44 | 32 |
| 24 | 39.3 | 0.76 | 1.75 | 2.50 | 54 | 106 | 149 | 53 | 40 |
| 25 | 98.7 | 0.85 | 11.89 | 12.74 | 40 | 67 | 93 | 49 | 37 |

| Sample ID | Weight, g | Metal Content, % | | | Average Temperature, °C | | | | |
|---|---|---|---|---|---|---|---|---|---|
| | | Pb | Zn | Pb+Zn | 5S | 10s | 15s | G4-10s | G9-10s |
| 26 | 89.8 | 29.92 | 11.11 | 41.03 | 41 | 69 | 103 | 48 | 37 |
| 27 | 65.1 | 8.86 | 28.08 | 36.94 | 49 | 91 | 128 | 55 | 39 |
| 28 | 64.7 | 0.45 | 16.29 | 16.74 | 46 | 83 | 125 | 51 | 47 |
| 29 | 30.4 | 0.03 | 0.82 | 0.85 | 27 | 33 | 43 | 27 | 27 |
| 30 | 37.5 | 0.01 | 0.88 | 0.89 | 27 | 32 | 38 | 27 | 27 |
| 31 | 134.0 | 0.60 | 0.95 | 1.54 | 39 | 60 | 75 | 51 | 39 |
| 32 | 35.7 | 0.18 | 8.10 | 8.28 | 51 | 93 | 145 | 62 | 43 |
| 33 | 41.2 | 0.02 | 0.80 | 0.81 | 26 | 27 | 29 | 26 | 27 |
| 34 | 62.0 | 0.83 | 23.03 | 23.87 | 46 | 81 | 116 | 64 | 42 |
| 35 | 98.1 | 0.64 | 9.05 | 9.69 | 38 | 61 | 84 | 45 | 36 |
| 36 | 59.8 | 0.28 | 5.52 | 5.80 | 48 | 88 | 125 | 62 | 44 |
| 37 | 40.4 | 24.25 | 42.71 | 66.96 | 61 | 135 | 168 | 85 | 51 |
| 38 | 33.0 | 0.04 | 0.81 | 0.85 | 31 | 39 | 49 | 29 | 27 |
| 39 | 31.4 | 0.04 | 0.84 | 0.88 | 34 | 54 | 76 | 37 | 31 |
| 40 | 42.7 | 0.16 | 1.10 | 1.26 | 45 | 74 | 108 | 62 | 40 |
| 41 | 54.4 | 0.04 | 16.45 | 16.50 | 38 | 74 | 79 | 37 | 31 |
| 42 | 63.2 | 22.99 | 40.72 | 63.70 | 49 | 97 | 130 | 57 | 43 |
| 43 | 65.5 | 3.75 | 28.65 | 32.41 | 48 | 86 | 115 | 55 | 47 |
| 44 | 57.3 | 0.19 | 28.18 | 28.37 | 48 | 93 | 127 | 65 | 48 |
| 45 | 107.8 | 0.68 | 17.95 | 18.64 | 41 | 71 | 89 | 66 | 44 |
| 46 | 36.9 | 0.03 | 0.82 | 0.85 | 27 | 32 | 37 | 27 | |
| 47 | 27.1 | 0.02 | 0.87 | 0.90 | 26 | 31 | 32 | 28 | |
| 48 | 62.0 | 0.02 | 9.04 | 9.06 | 28 | 34 | 35 | 28 | |
| 49 | 42.4 | 0.03 | 0.80 | 0.83 | 26 | 29 | 31 | | |
| 50 | 43.7 | 0.02 | 0.75 | 0.76 | 27 | 32 | 35 | | |

## Sortability Graph

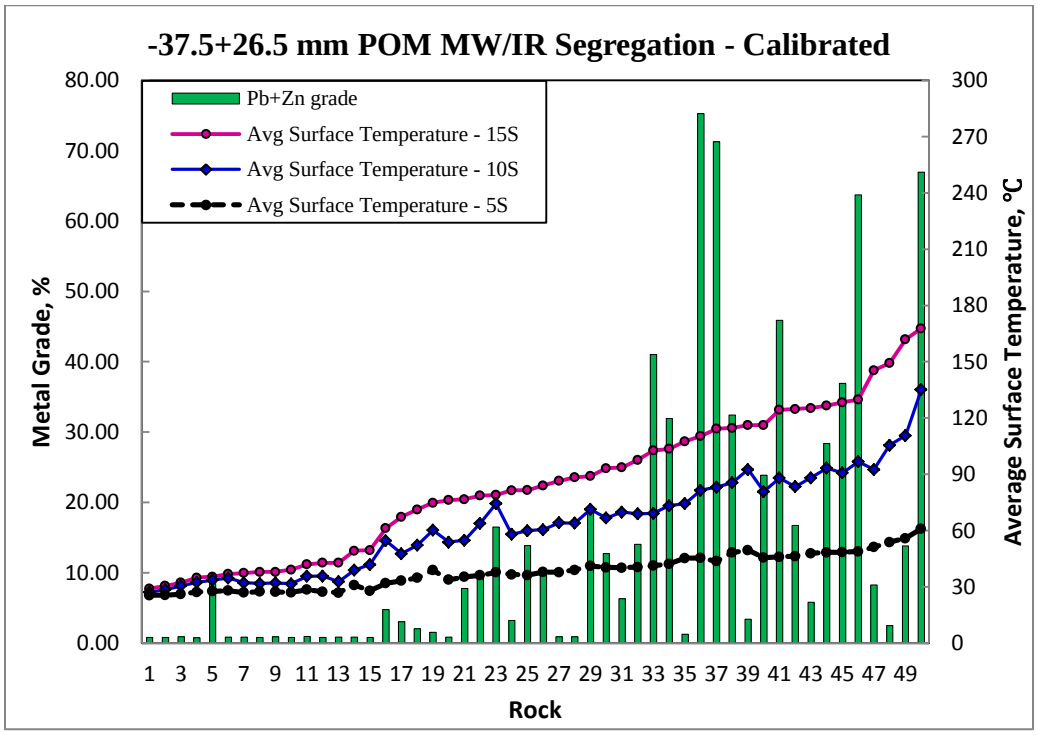


## Individual and Group Tests

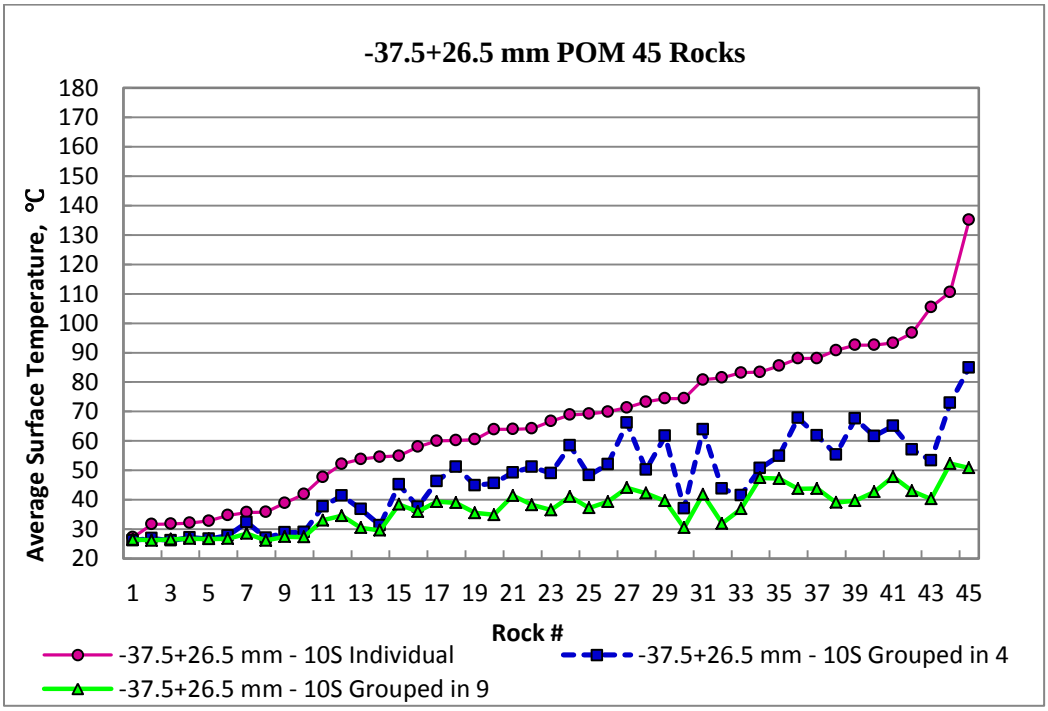

**-37.5+26.5 mm MW/IR Sorting Results –Individual 5s (Calibrated XRF Surface Readings)**

| Separation Temperature, °C | Hot Fraction | Cold Fraction | Wt. % in Hot Fraction | | Wt. % in Cold Fraction | | % in Hot Fraction | | % in Cold Fraction | |
|---|---|---|---|---|---|---|---|---|---|---|
| | | | Concentrate Grades, % | | Waste Grades, % | | Metal Recovery, % | | Metal Recovery, % | |
| | Conc. % | Waste % | Pb | Zn | Pb | Zn | Pb | Zn | Pb | Zn |
| **26** | 96.8 | 3.2 | 4.98 | 10.36 | 0.02 | 0.82 | 100.0 | 99.7 | 0.0 | 0.3 |
| **27** | 90.1 | 9.9 | 5.34 | 11.08 | 0.02 | 0.81 | 100.0 | 99.2 | 0.0 | 0.8 |
| **28** | 85.1 | 14.9 | 5.65 | 11.50 | 0.02 | 1.80 | 99.9 | 97.3 | 0.1 | 2.7 |
| **33** | **73.8** | **26.2** | **6.39** | **12.97** | **0.38** | **1.83** | **97.9** | **95.2** | **2.1** | **4.8** |
| **35** | 64.4 | 35.6 | 7.22 | 14.30 | 0.45 | 2.37 | 96.7 | 91.6 | 3.3 | 8.4 |
| **37** | 56.2 | 43.8 | 8.20 | 15.20 | 0.46 | 3.44 | 95.8 | 85.0 | 4.2 | 15.0 |
| **38** | 49.2 | 50.8 | 9.33 | 16.26 | 0.43 | 4.03 | 95.4 | 79.6 | 4.6 | 20.4 |
| **40** | 37.4 | 62.6 | 11.9 | 20.18 | 0.58 | 4.00 | 92.5 | 75.1 | 7.5 | 24.9 |
| **42** | 26.6 | 73.4 | 13.4 | 21.20 | 1.71 | 6.02 | 74.0 | 56.0 | 26.0 | 44.0 |
| **45** | 20.8 | 79.2 | 5.62 | 22.63 | 4.60 | 6.75 | 24.3 | 46.8 | 75.7 | 53.2 |
| **48** | 9.7 | 90.3 | 9.26 | 21.54 | 4.34 | 8.82 | 18.7 | 20.8 | 81.3 | 79.2 |
| **50** | 4.5 | 95.5 | 6.64 | 16.85 | 4.73 | 9.73 | 6.3 | 7.6 | 93.7 | 92.4 |
| **Calculated Head Grade: 4.82% Pb and 10.06% Zn** | | | | | | | | | | |

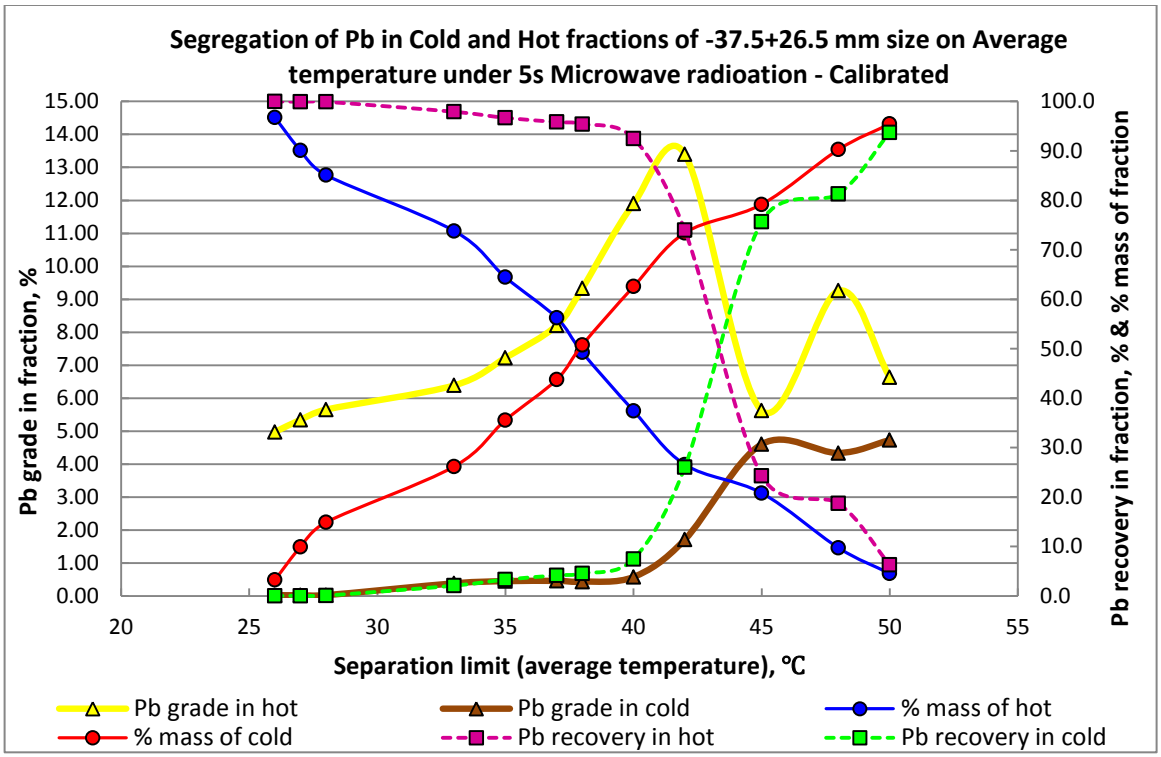
Segregation of Pb in Cold and Hot fractions of -37.5+26.5 mm size on Average temperature under 5s Microwave radioation - Calibrated
Pb grade in fraction, %
Pb recovery in fraction, % & % mass of fraction
Separation limit (average temperature), ℃
Pb grade in hot
Pb grade in cold
% mass of hot
% mass of cold
Pb recovery in hot
Pb recovery in cold

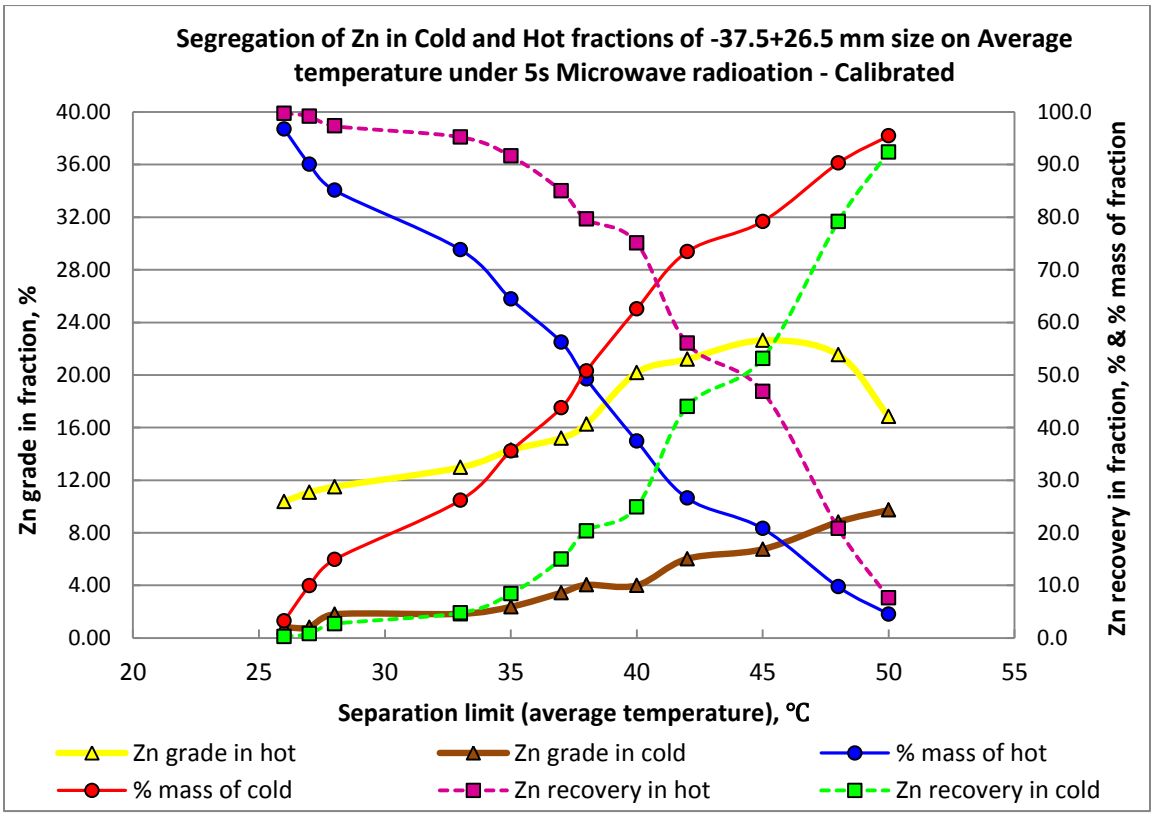
Segregation of Zn in Cold and Hot fractions of -37.5+26.5 mm size on Average temperature under 5s Microwave radioation - Calibrated
Zn grade in fraction, %
Zn recovery in fraction, % & % mass of fraction
Separation limit (average temperature), ℃
Zn grade in hot
Zn grade in cold
% mass of hot
% mass of cold
Zn recovery in hot
Zn recovery in cold

**-37.5+26.5 mm MW/IR Sorting Results –Individual 10s (Calibrated XRF Surface Readings)**

| Separation Temperature, °C | Hot Fraction | Cold Fraction | Wt. % in Hot Fraction | | Wt. % in Cold Fraction | | % in Hot Fraction | | % in Cold Fraction | |
|---|---|---|---|---|---|---|---|---|---|---|
| | | | Concentrate Grades, % | | Waste Grades, % | | Metal Recovery, % | | Metal Recovery, % | |
| | Conc. % | Waste % | Pb | Zn | Pb | Zn | Pb | Zn | Pb | Zn |
| **31** | 96.8 | 3.2 | 4.98 | 10.36 | 0.02 | 0.82 | 100 | 99.7 | 0.0 | 0.3 |
| **32** | 91.2 | 8.8 | 5.28 | 10.95 | 0.02 | 0.81 | 100 | 99.3 | 0.0 | 0.7 |
| **40** | 82.9 | 17.1 | 5.80 | 11.78 | 0.03 | 1.69 | 99.9 | 97.1 | 0.1 | 2.9 |
| **50** | **75.7** | **24.3** | **6.23** | **12.76** | **0.40** | **1.62** | **98.0** | **96.1** | **2.0** | **3.9** |
| **55** | 64.4 | 35.6 | 7.22 | 14.30 | 0.45 | 2.37 | 96.7 | 91.6 | 3.3 | 8.4 |
| **60** | 55.1 | 44.9 | 8.33 | 15.90 | 0.49 | 2.87 | 95.4 | 87.2 | 4.6 | 12.8 |
| **65** | 44.2 | 55.8 | 10.35 | 18.59 | 0.44 | 3.31 | 94.9 | 81.6 | 5.1 | 18.4 |
| **70** | 33.7 | 66.3 | 10.71 | 21.36 | 1.81 | 4.30 | 75.1 | 71.7 | 24.9 | 28.3 |
| **80** | 25.3 | 74.7 | 14.05 | 22.19 | 1.68 | 5.94 | 73.9 | 55.9 | 26.1 | 44.1 |
| **85** | 17.1 | 82.9 | 6.70 | 23.29 | 4.43 | 7.32 | 23.8 | 39.6 | 76.2 | 60.4 |
| **90** | 11.4 | 88.6 | 7.93 | 22.51 | 4.41 | 8.45 | 18.8 | 25.5 | 81.2 | 74.5 |
| **95** | 5.3 | 94.7 | 13.54 | 26.80 | 4.32 | 9.11 | 15.0 | 14.3 | 85.0 | 85.7 |
| **Calculated Head Grade: 4.82% Pb and 10.06% Zn** | | | | | | | | | | |

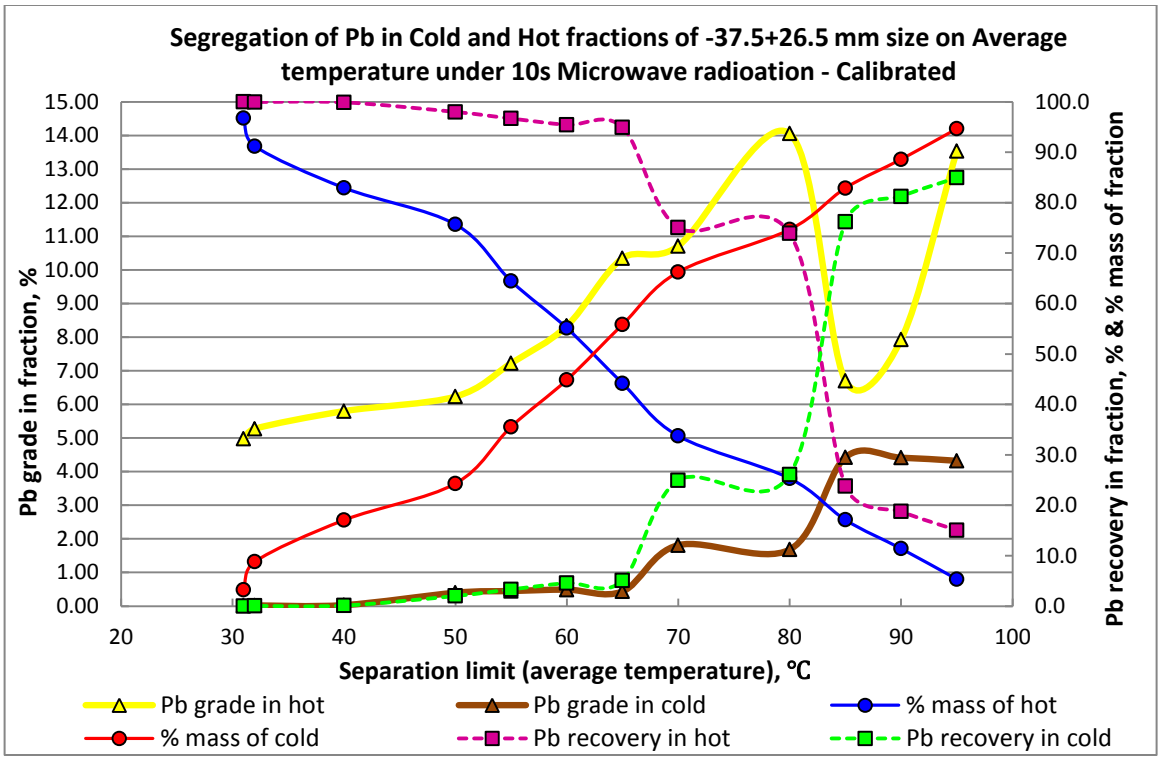
Segregation of Pb in Cold and Hot fractions of -37.5+26.5 mm size on Average temperature under 10s Microwave radioation - Calibrated
Pb grade in fraction, %
Pb recovery in fraction, % & % mass of fraction
Separation limit (average temperature), ℃
Pb grade in hot
Pb grade in cold
% mass of hot
% mass of cold
Pb recovery in hot
Pb recovery in cold

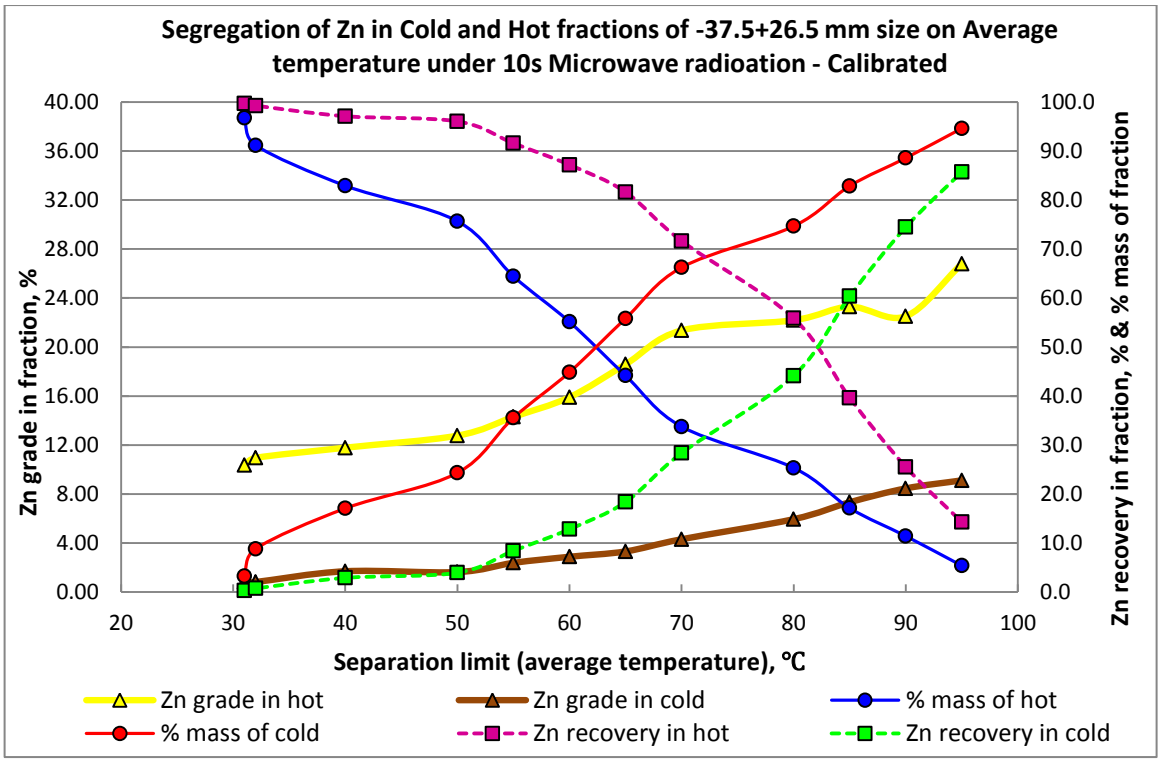
Segregation of Zn in Cold and Hot fractions of -37.5+26.5 mm size on Average temperature under 10s Microwave radioation - Calibrated
Zn grade in fraction, %
Zn recovery in fraction, % & % mass of fraction
Separation limit (average temperature), ℃
Zn grade in hot
Zn grade in cold
% mass of hot
% mass of cold
Zn recovery in hot
Zn recovery in cold

**-37.5+26.5 mm MW/IR Sorting Results –Individual 15s (Calibrated XRF Surface Readings)**

| Separation Temperature, °C | Hot Fraction | Cold Fraction | Wt. % in Hot Fraction | | Wt. % in Cold Fraction | | % in Hot Fraction | | % in Cold Fraction | |
|---|---|---|---|---|---|---|---|---|---|---|
| | | | Concentrate Grades, % | | Waste Grades, % | | Metal Recovery, % | | Metal Recovery, % | |
| | Conc. % | Waste % | Pb | Zn | Pb | Zn | Pb | Zn | Pb | Zn |
| **35** | 93.7 | 6.3 | 5.14 | 10.52 | 0.02 | 3.16 | 100.0 | 98.0 | 0.0 | 2.0 |
| **40** | 88.2 | 11.8 | 5.46 | 11.13 | 0.02 | 2.07 | 99.9 | 97.6 | 0.1 | 2.4 |
| **45** | 83.9 | 16.1 | 5.73 | 11.65 | 0.03 | 1.74 | 99.9 | 97.2 | 0.1 | 2.8 |
| **70** | **73.8** | **26.2** | **6.39** | **12.97** | **0.38** | **1.83** | **97.9** | **95.2** | **2.1** | **4.8** |
| **76** | 64.7 | 35.3 | 7.18 | 14.66 | 0.47 | 1.62 | 96.5 | 94.3 | 3.5 | 5.7 |
| **80** | 56.1 | 43.9 | 8.24 | 15.43 | 0.43 | 3.18 | 96.1 | 86.1 | 3.9 | 13.9 |
| **85** | 47.9 | 52.1 | 9.55 | 16.69 | 0.46 | 3.96 | 95.0 | 79.5 | 5.0 | 20.5 |
| **95** | 34.3 | 65.7 | 12.93 | 20.38 | 0.58 | 4.67 | 92.1 | 69.5 | 7.9 | 30.5 |
| **105** | 26.6 | 73.4 | 13.40 | 21.20 | 1.71 | 6.02 | 74.0 | 56.0 | 26.0 | 44.0 |
| **115** | 18.9 | 81.1 | 5.81 | 22.03 | 4.58 | 7.27 | 22.8 | 41.4 | 77.2 | 58.6 |
| **125** | 10.0 | 90.0 | 9.01 | 25.32 | 4.35 | 8.37 | 18.6 | 25.1 | 81.4 | 74.9 |
| **130** | 4.5 | 95.5 | 6.64 | 16.85 | 4.73 | 9.73 | 6.3 | 7.6 | 93.7 | 92.4 |
| **Calculated Head Grade: 4.82% Pb and 10.06% Zn** | | | | | | | | | | |

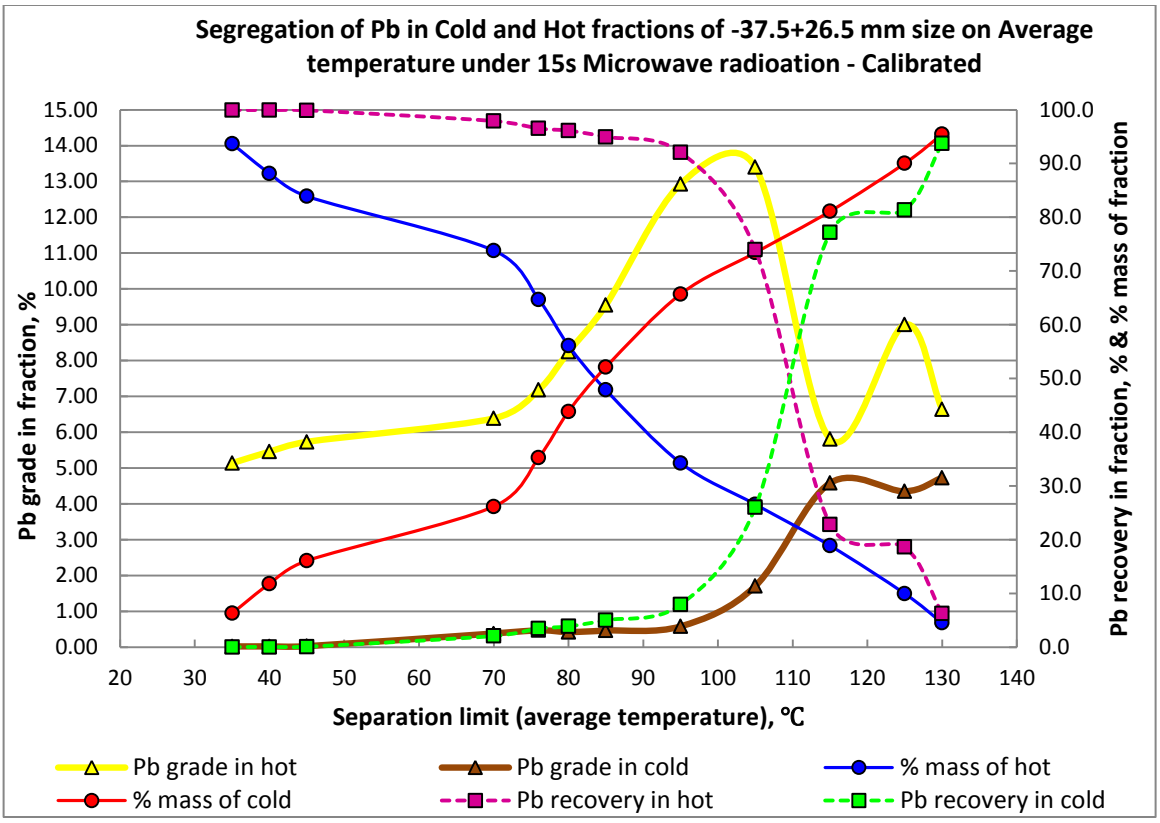
Segregation of Pb in Cold and Hot fractions of -37.5+26.5 mm size on Average temperature under 15s Microwave radioation - Calibrated
Pb grade in fraction, %
Pb recovery in fraction, % & % mass of fraction
Separation limit (average temperature), ℃
Pb grade in hot
Pb grade in cold
% mass of hot
% mass of cold
Pb recovery in hot
Pb recovery in cold

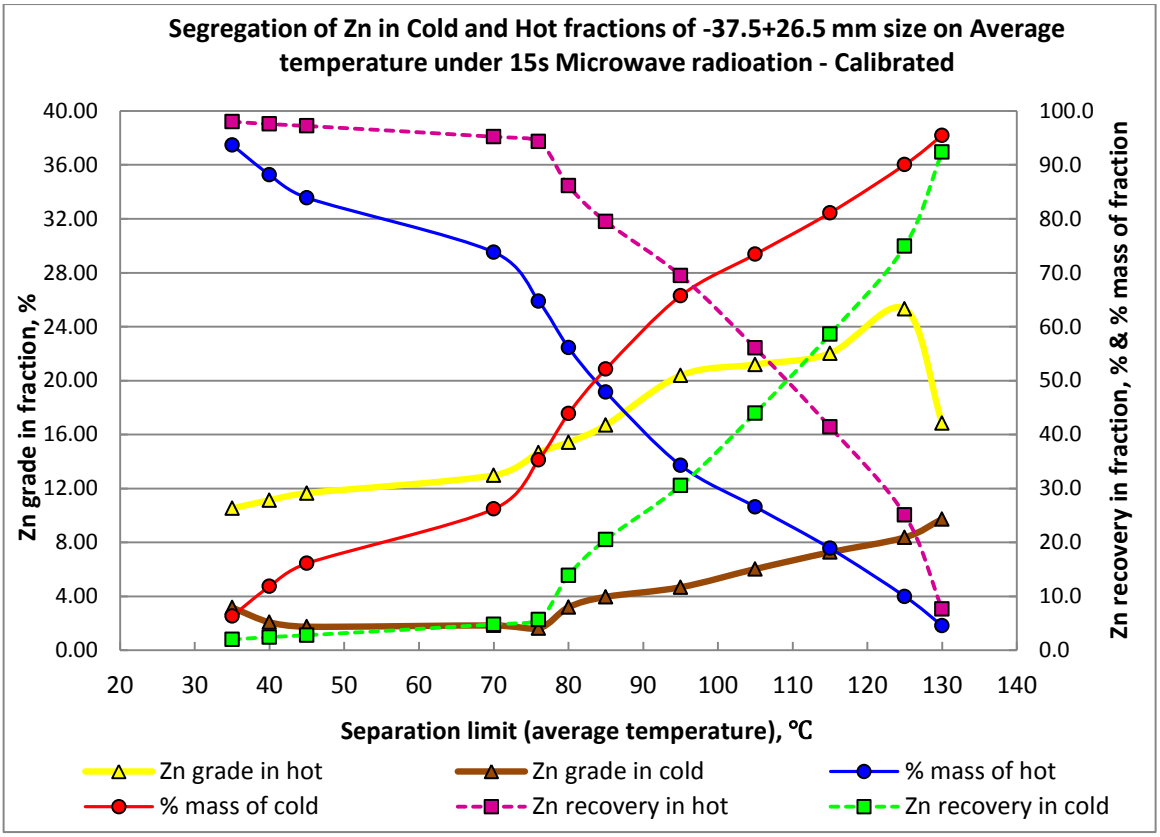
Segregation of Zn in Cold and Hot fractions of -37.5+26.5 mm size on Average temperature under 15s Microwave radioation - Calibrated
Zn grade in fraction, %
Zn recovery in fraction, % & % mass of fraction
Separation limit (average temperature), ℃
Zn grade in hot
Zn grade in cold
% mass of hot
% mass of cold
Zn recovery in hot
Zn recovery in cold

**-37.5+26.5 mm MW/IR Sorting Results –Individual 10s 45 rocks (Calibrated XRF Surface Readings)**

| Separation Temperature, °C | Hot fraction | Cold fraction | Wt. % in Hot Fraction | | Wt. % in Cold Fraction | | % in Hot Fraction | | % in Cold Fraction | |
|---|---|---|---|---|---|---|---|---|---|---|
| | | | Concentrate Grades, % | | Waste Grades, % | | Metal Recovery, % | | Metal Recovery, % | |
| | Conc. % | Waste % | Pb | Zn | Pb | Zn | Pb | Zn | Pb | Zn |
| **32** | 95.3 | 4.7 | 5.38 | 10.99 | 0.02 | 0.81 | 100.0 | 99.6 | 0.0 | 0.4 |
| **40** | 88.4 | 11.6 | 5.80 | 11.78 | 0.03 | 0.82 | 99.9 | 99.1 | 0.1 | 0.9 |
| **52** | **76.2** | **23.8** | **6.54** | **13.87** | **0.62** | **1.07** | **97.1** | **97.6** | **2.9** | **2.4** |
| **55** | 68.7 | 31.3 | 7.22 | 14.30 | 0.54 | 2.19 | 96.7 | 93.5 | 3.3 | 6.5 |
| **60** | 58.8 | 41.2 | 8.33 | 15.90 | 0.57 | 2.82 | 95.5 | 89.0 | 4.5 | 11.0 |
| **65** | 47.1 | 52.9 | 10.35 | 18.59 | 0.49 | 3.32 | 94.9 | 83.3 | 5.1 | 16.7 |
| **70** | 36.0 | 64.0 | 10.71 | 21.36 | 2.00 | 4.41 | 75.1 | 73.1 | 24.9 | 26.9 |
| **80** | 27.0 | 73.0 | 14.05 | 22.19 | 1.83 | 6.19 | 74.0 | 57.0 | 26.0 | 43.0 |
| **85** | 18.2 | 81.8 | 6.70 | 23.29 | 4.78 | 7.66 | 23.8 | 40.4 | 76.2 | 59.6 |
| **90** | 12.2 | 87.8 | 7.93 | 22.51 | 4.74 | 8.85 | 18.8 | 26.0 | 81.2 | 74.0 |
| **95** | 5.7 | 94.3 | 13.54 | 26.80 | 4.62 | 9.52 | 15.0 | 14.5 | 85.0 | 85.5 |
| **100** | 3.7 | 96.3 | 8.56 | 19.46 | 5.00 | 10.16 | 6.2 | 6.9 | 93.8 | 93.1 |
| **Calculated Head Grade: 5.13% Pb and 10.51% Zn** | | | | | | | | | | |

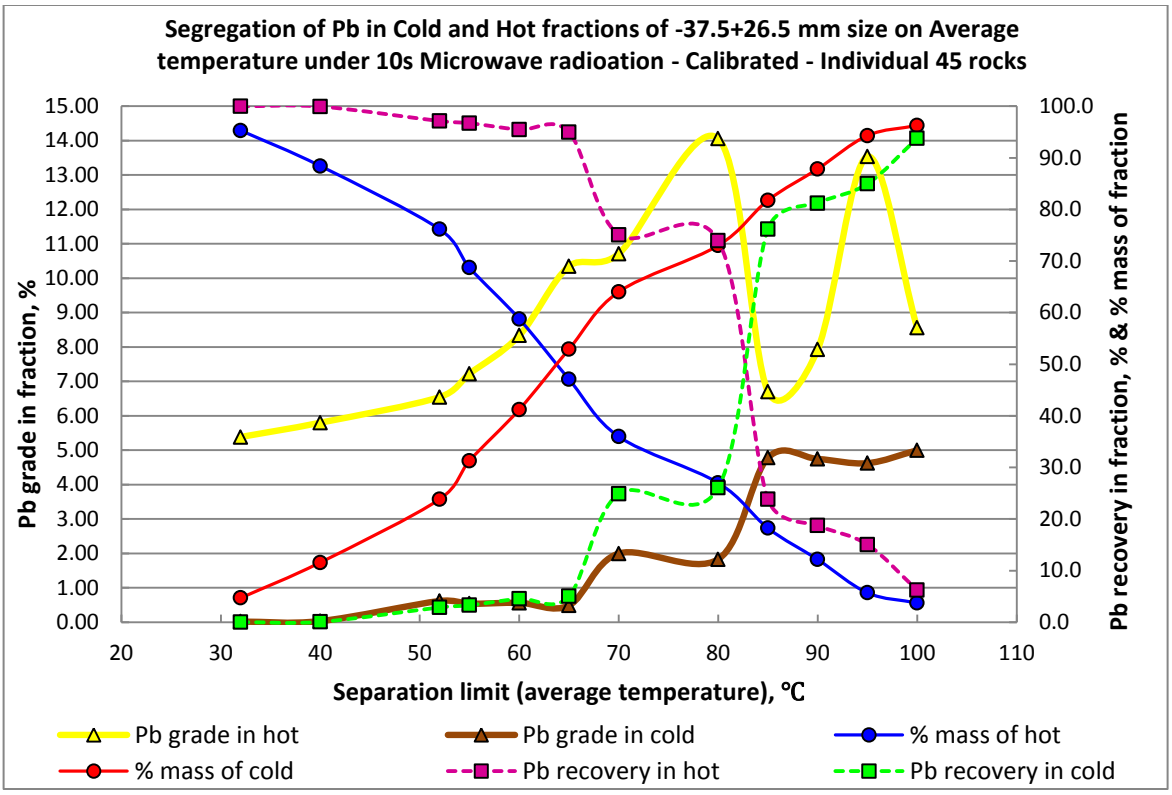
Segregation of Pb in Cold and Hot fractions of -37.5+26.5 mm size on Average temperature under 10s Microwave radioation - Calibrated - Individual 45 rocks
Pb grade in fraction, %
Pb recovery in fraction, % & % mass of fraction
Separation limit (average temperature), ℃
Pb grade in hot
Pb grade in cold
% mass of hot
% mass of cold
Pb recovery in hot
Pb recovery in cold

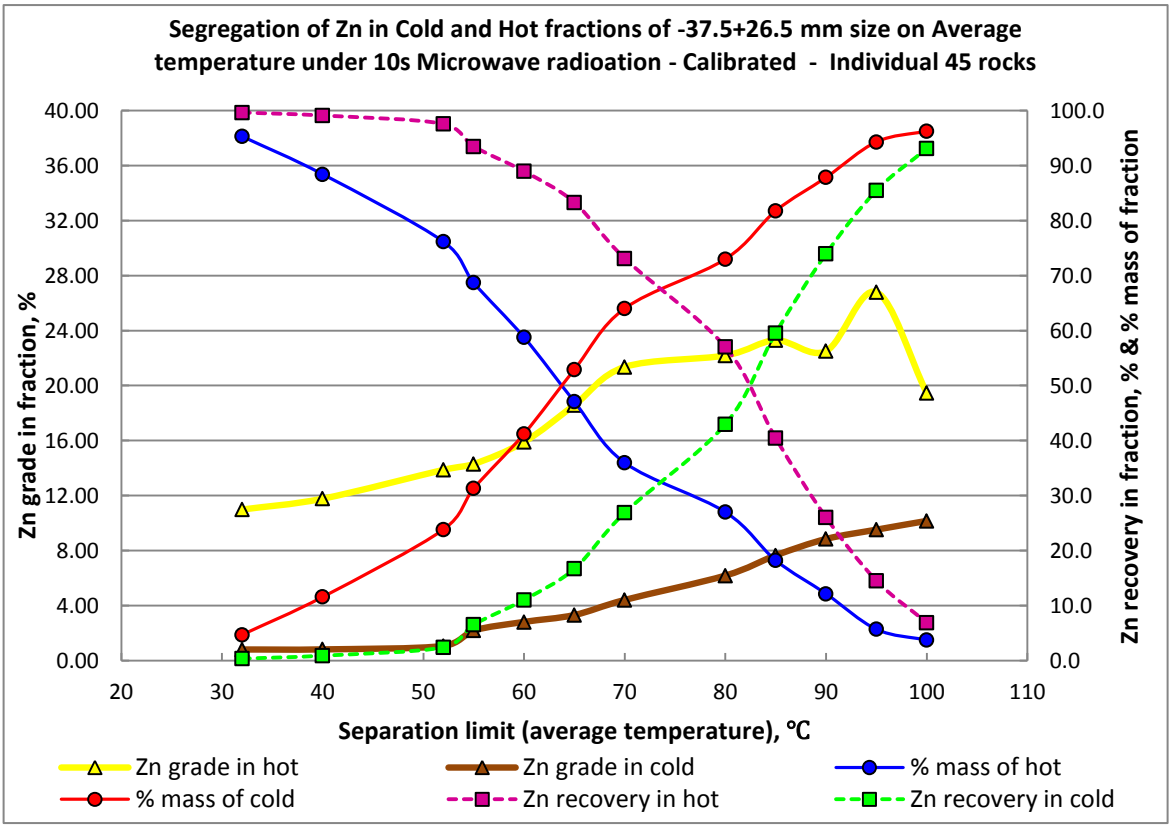
Segregation of Zn in Cold and Hot fractions of -37.5+26.5 mm size on Average temperature under 10s Microwave radioation - Calibrated - Individual 45 rocks
Zn grade in fraction, %
Zn recovery in fraction, % & % mass of fraction
Separation limit (average temperature), ℃
Zn grade in hot
Zn grade in cold
% mass of hot
% mass of cold
Zn recovery in hot
Zn recovery in cold

**-37.5+26.5 mm MW/IR Sorting Results – Group in 4 – 10s 45 rocks (Calibrated XRF Surface Readings)**

| Separation Temperature, °C | Hot Fraction | Cold Fraction | Wt. % in Hot Fraction | | Wt. % in Cold Fraction | | % in Hot Fraction | | % in Cold Fraction | |
|---|---|---|---|---|---|---|---|---|---|---|
| | | | Concentrate Grades, % | | Waste Grades, % | | Metal Recovery, % | | Metal Recovery, % | |
| | Conc. % | Waste % | Pb | Zn | Pb | Zn | Pb | Zn | Pb | Zn |
| 27 | 93.1 | 6.9 | 5.51 | 11.23 | 0.02 | 0.81 | 100.0 | 99.5 | 0.0 | 0.5 |
| 30 | 89.7 | 10.3 | 5.72 | 11.62 | 0.03 | 0.80 | 99.9 | 99.2 | 0.1 | 0.8 |
| **37** | **82.7** | **17.3** | **6.20** | **12.13** | **0.05** | **2.78** | **99.8** | **95.4** | **0.2** | **4.6** |
| 40 | 73.0 | 27.0 | 6.84 | 13.51 | 0.52 | 2.41 | 97.3 | 93.8 | 2.7 | 6.2 |
| 42 | 65.7 | 34.3 | 5.62 | 13.91 | 4.20 | 3.98 | 72.0 | 87.0 | 28.0 | 13.0 |
| 45 | 56.1 | 43.9 | 4.21 | 14.68 | 6.31 | 5.18 | 46.0 | 78.3 | 54.0 | 21.7 |
| 50 | 39.0 | 61.0 | 3.73 | 15.63 | 6.03 | 7.23 | 28.4 | 58.0 | 71.6 | 42.0 |
| 52 | 27.7 | 72.3 | 4.78 | 20.40 | 5.27 | 6.72 | 25.8 | 53.8 | 74.2 | 46.2 |
| 55 | 22.4 | 77.6 | 4.72 | 19.97 | 5.25 | 7.78 | 20.6 | 42.6 | 79.4 | 57.4 |
| 60 | 17.6 | 82.4 | 3.10 | 18.95 | 5.57 | 8.71 | 10.6 | 31.7 | 89.4 | 68.3 |
| 65 | 9.6 | 90.4 | 5.40 | 22.75 | 5.10 | 9.21 | 10.1 | 20.7 | 89.9 | 79.3 |
| **Calculated Head Grade: 5.13% Pb and 10.51% Zn** | | | | | | | | | | |

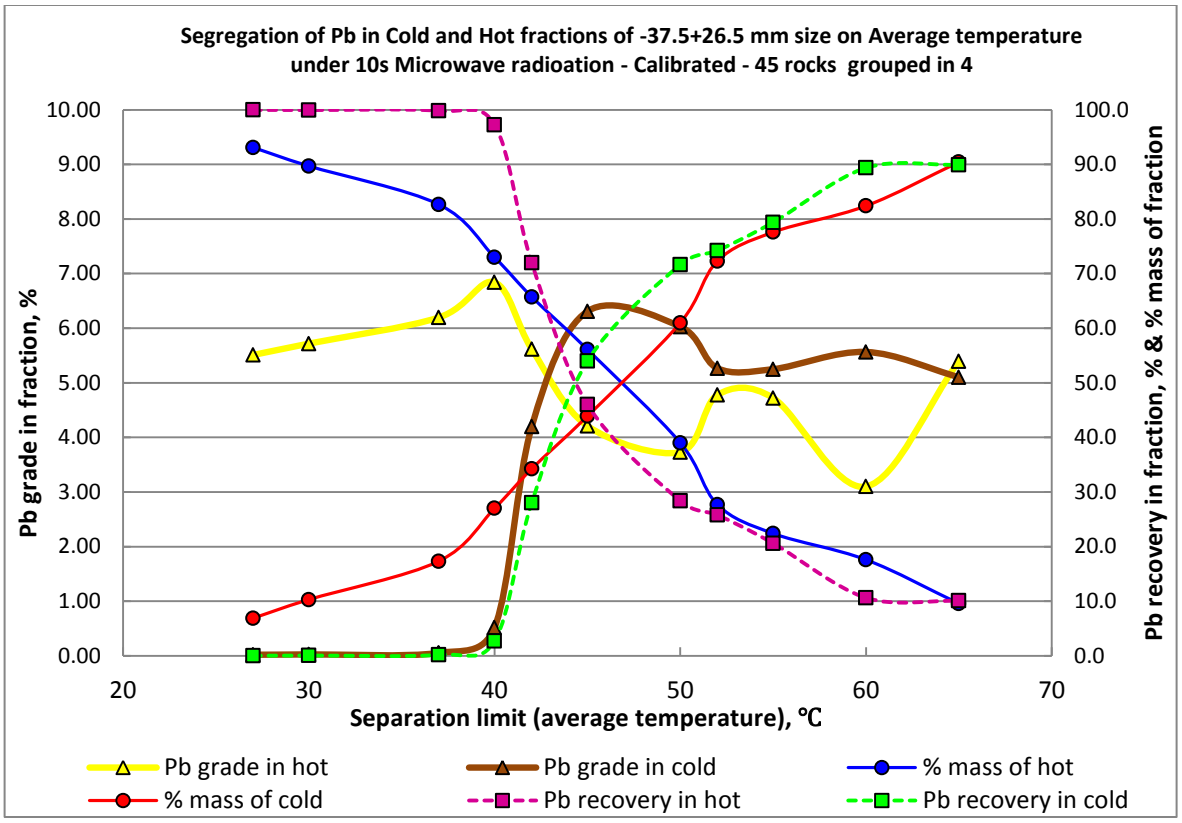
Segregation of Pb in Cold and Hot fractions of -37.5+26.5 mm size on Average temperature under 10s Microwave radioation - Calibrated - 45 rocks grouped in 4
Pb grade in fraction, %
Pb recovery in fraction, % & % mass of fraction
Separation limit (average temperature), ℃
Pb grade in hot
Pb grade in cold
% mass of hot
% mass of cold
Pb recovery in hot
Pb recovery in cold

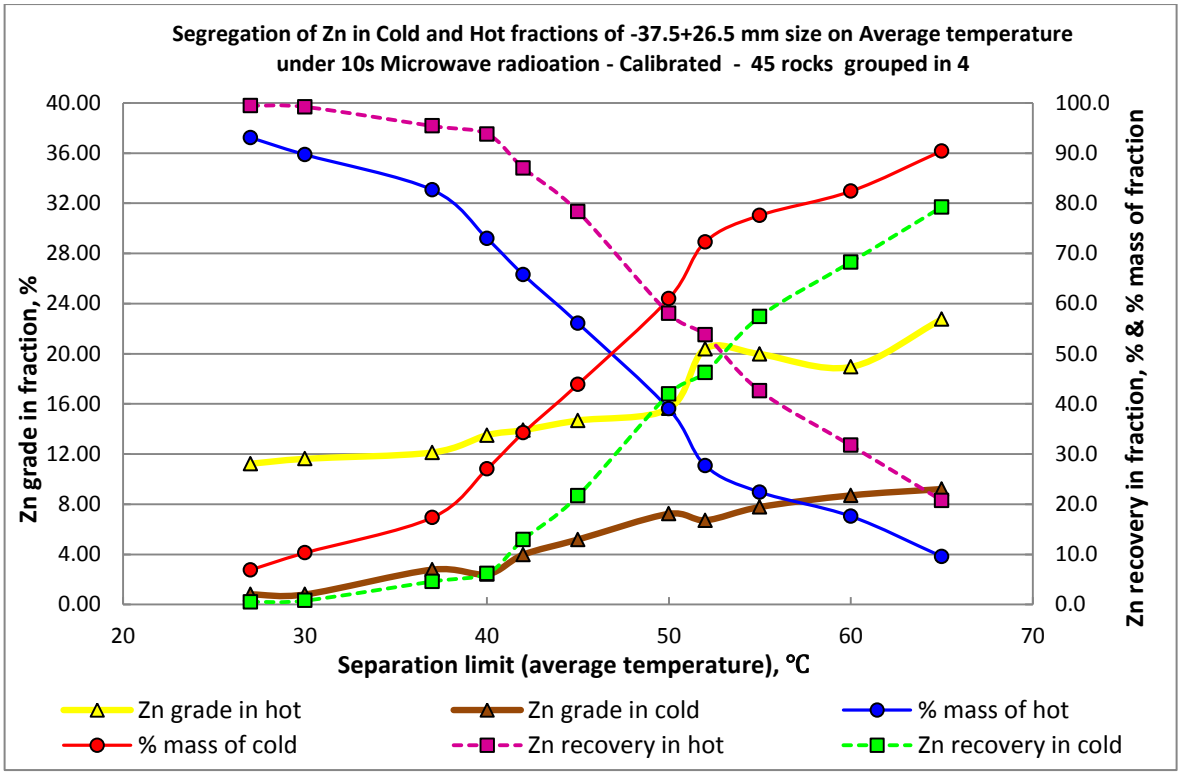
Segregation of Zn in Cold and Hot fractions of -37.5+26.5 mm size on Average temperature under 10s Microwave radioation - Calibrated - 45 rocks grouped in 4
Zn grade in fraction, %
Zn recovery in fraction, % & % mass of fraction
Separation limit (average temperature), ℃
Zn grade in hot
Zn grade in cold
% mass of hot
% mass of cold
Zn recovery in hot
Zn recovery in cold

**-37.5+26.5 mm MW/IR Sorting Results – Group in 9 – 10s 45 rocks (Calibrated XRF Surface Readings)**

| Separation Temperature, °C | Hot Fraction | Cold Fraction | Wt. % in Hot Fraction | | Wt. % in Cold Fraction | | % in Hot Fraction | | % in Cold Fraction | |
|---|---|---|---|---|---|---|---|---|---|---|
| | | | Concentrate Grades, % | | Waste Grades, % | | Metal Recovery, % | | Metal Recovery, % | |
| | Conc. % | Waste % | Pb | Zn | Pb | Zn | Pb | Zn | Pb | Zn |
| 26 | 97.5 | 2.5 | 5.26 | 10.76 | 0.02 | 0.78 | 100.0 | 99.8 | 0.0 | 0.2 |
| 27 | 89.7 | 10.3 | 5.72 | 11.62 | 0.03 | 0.80 | 99.9 | 99.2 | 0.1 | 0.8 |
| **31** | **82.7** | **17.3** | **6.20** | **12.13** | **0.05** | **2.78** | **99.8** | **95.4** | **0.2** | **4.6** |
| 33 | 73.9 | 26.1 | 5.05 | 13.01 | 5.37 | 3.42 | 72.7 | 91.5 | 27.3 | 8.5 |
| 35 | 66.4 | 33.6 | 5.54 | 14.01 | 4.32 | 3.60 | 71.7 | 88.5 | 28.3 | 11.5 |
| 36 | 60.3 | 39.7 | 6.02 | 14.86 | 3.79 | 3.90 | 70.7 | 85.2 | 29.3 | 14.8 |
| 37 | 51.7 | 48.3 | 2.92 | 14.73 | 7.49 | 5.99 | 29.5 | 72.5 | 70.5 | 27.5 |
| 39 | 33.2 | 66.8 | 3.58 | 18.76 | 5.90 | 6.41 | 23.1 | 59.3 | 76.9 | 40.7 |
| 41 | 23.4 | 76.6 | 4.74 | 24.76 | 5.25 | 6.17 | 21.6 | 55.0 | 78.4 | 45.0 |
| 42 | 18.8 | 81.2 | 5.63 | 24.12 | 5.02 | 7.35 | 20.6 | 43.2 | 79.4 | 56.8 |
| 45 | 8.4 | 91.6 | 4.78 | 25.40 | 5.16 | 9.15 | 7.8 | 20.2 | 92.2 | 79.8 |
| 50 | 2.5 | 97.5 | 12.36 | 28.10 | 4.95 | 10.05 | 6.0 | 6.7 | 94.0 | 93.3 |
| **Calculated Head Grade: 5.13% Pb and 10.51% Zn** | | | | | | | | | | |

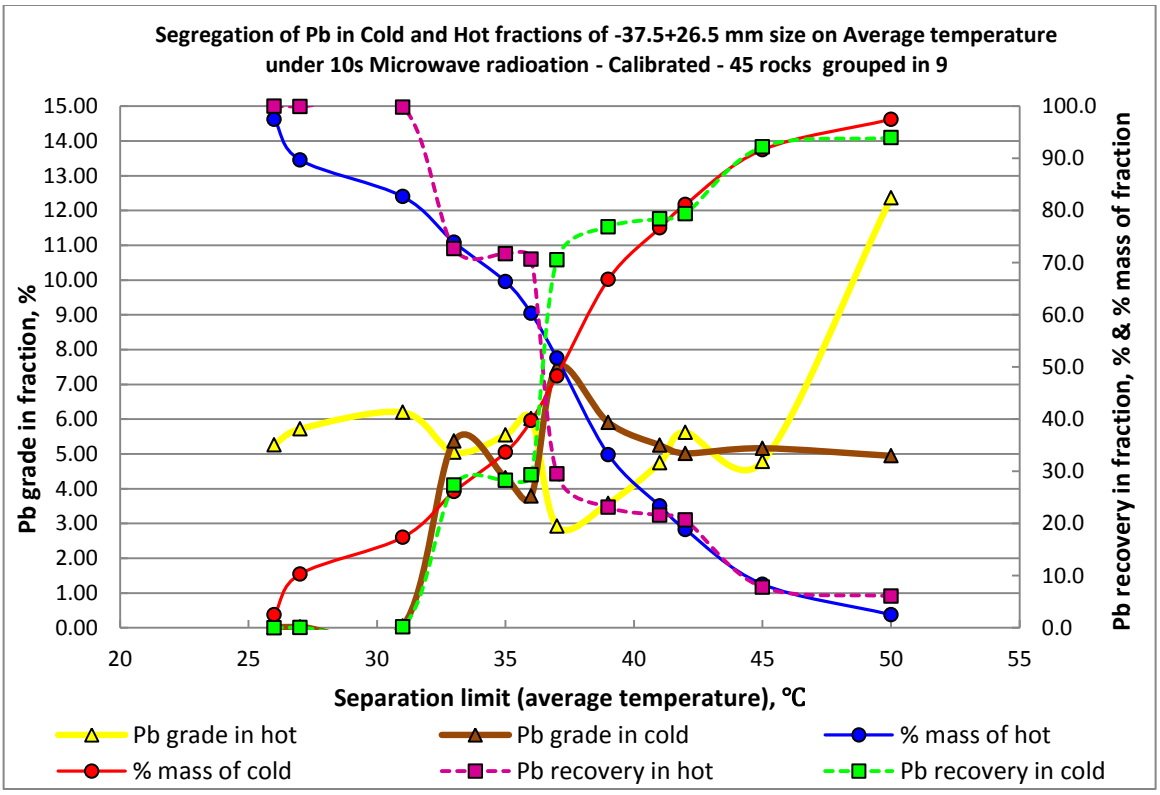
Segregation of Pb in Cold and Hot fractions of -37.5+26.5 mm size on Average temperature under 10s Microwave radioation - Calibrated - 45 rocks grouped in 9
Pb grade in fraction, %
Pb recovery in fraction, % & % mass of fraction
Separation limit (average temperature), ℃
Pb grade in hot
Pb grade in cold
% mass of hot
% mass of cold
Pb recovery in hot
Pb recovery in cold

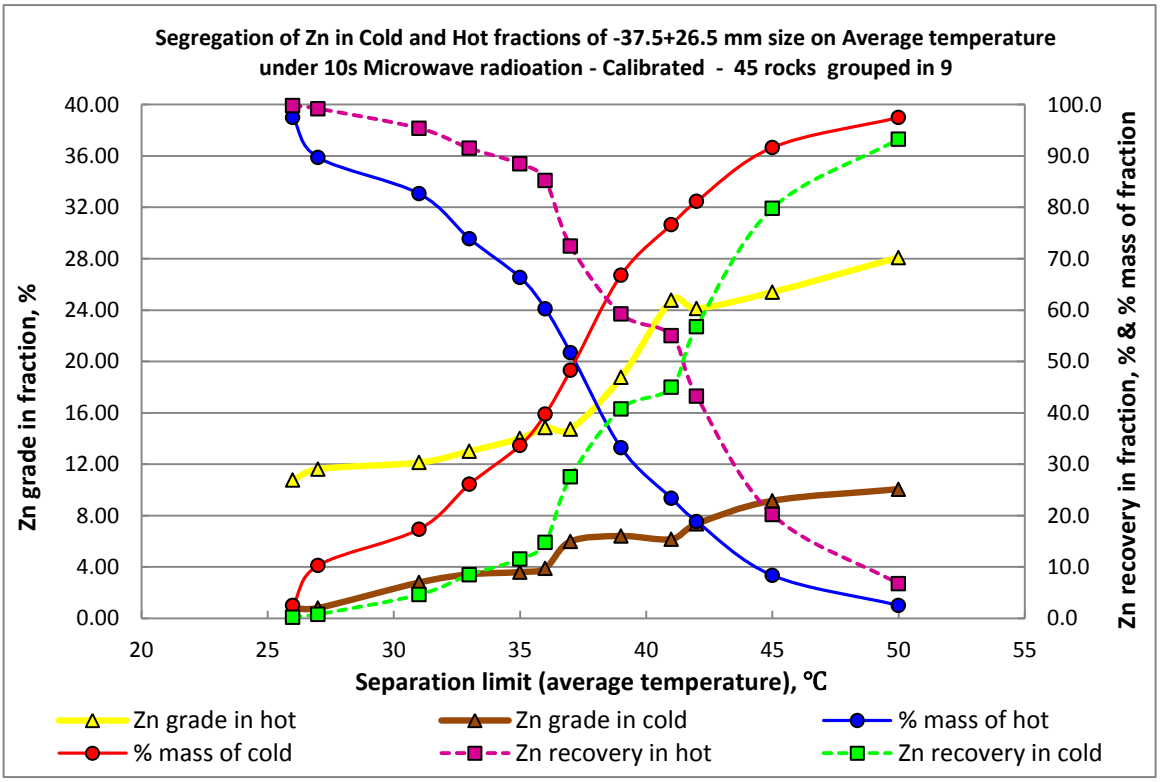
Segregation of Zn in Cold and Hot fractions of -37.5+26.5 mm size on Average temperature under 10s Microwave radioation - Calibrated - 45 rocks grouped in 9
Zn grade in fraction, %
Zn recovery in fraction, % & % mass of fraction
Separation limit (average temperature), ℃
Zn grade in hot
Zn grade in cold
% mass of hot
% mass of cold
Zn recovery in hot
Zn recovery in cold

**-37.5+26.5 mm Size Fraction Soring Results Summary**

| Test Condition | Separation Limit, °C | Mass % of Cold | Pb in Hot Fraction, % | | Zn in Hot Fraction, % | |
|---|---|---|---|---|---|---|
| | | | Grade | Recovery | Grade | Recovery |
| 5s | 33 | 26.2 | 6.39 | 97.9 | 12.97 | 95.2 |
| 10s | 50 | 24.3 | 6.23 | 98.0 | 12.76 | 96.1 |
| 15s | 70 | 26.2 | 6.39 | 97.9 | 12.97 | 95.2 |
| Calculated Head Grade : 4.82% Pb and 10.06% Zn 50 rocks being tested | | | | | | |
| **Test Condition** | **Separation Limit, °C** | **Mass % of Cold** | **Pb in Hot Fraction, %** | | **Zn in Hot Fraction, %** | |
| | | | **Grade** | **Recovery** | **Grade** | **Recovery** |
| Individual | 52 | 23.8 | 6.54 | 97.1 | 13.87 | 97.6 |
| Group in 4 | 37 | 17.3 | 6.20 | 99.8 | 12.13 | 95.4 |
| Group in 9 | 31 | 17.3 | 6.20 | 99.8 | 12.13 | 95.4 |
| Calculated Head Grade : 5.13% Pb and 10.51% Zn 45 rocks being tested | | | | | | |

**-26.5+19 mm Size Fraction MW/IR Sorting**

**Initial Data Set**

| Sample ID | Weight, g | Metal Content, % | | | Average Temperature, °C | | | |
|---|---|---|---|---|---|---|---|---|
| | | Pb | Zn | Pb+Zn | 5s | 10s | 15s | G9-10s |
| 1 | 66.1 | 36.10 | 13.03 | 49.13 | 40 | 65 | 90 | 49 |
| 2 | 32.2 | 0.54 | 12.10 | 12.65 | 60 | 108 | 152 | 58 |
| 3 | 36.1 | 42.82 | 17.04 | 59.85 | 57 | 112 | 173 | 46 |
| 4 | 34.5 | 0.17 | 3.60 | 3.77 | 46 | 98 | 146 | 48 |
| 5 | 25.2 | 0.02 | 0.77 | 0.78 | 25 | 30 | 33 | 24 |
| 6 | 22.1 | 0.03 | 0.79 | 0.82 | 29 | 41 | 51 | 25 |
| 7 | 21.7 | 2.37 | 3.17 | 5.54 | 66 | 135 | 186 | 62 |
| 8 | 22.7 | 22.25 | 15.04 | 37.29 | 67 | 128 | 183 | 53 |
| 9 | 45.6 | 31.86 | 17.57 | 49.43 | 48 | 89 | 122 | 46 |
| 10 | 32.2 | 4.47 | 22.62 | 27.10 | 62 | 129 | 187 | 52 |
| 11 | 52.2 | 0.43 | 15.46 | 15.89 | 48 | 91 | 114 | 58 |
| 12 | 27.7 | 6.46 | 15.13 | 21.59 | 51 | 115 | 138 | 52 |
| 13 | 50.3 | 0.36 | 33.88 | 34.24 | 47 | 95 | 120 | 52 |
| 14 | 18.7 | 0.03 | 0.80 | 0.83 | 34 | 58 | 76 | 27 |
| 15 | 11.5 | 0.05 | 0.86 | 0.90 | 27 | 32 | 38 | 25 |
| 16 | 43.3 | 20.17 | 23.91 | 44.08 | 49 | 100 | 129 | 55 |
| 17 | 23.3 | 0.04 | 0.81 | 0.86 | 27 | 36 | 42 | 26 |
| 18 | 36.6 | 0.16 | 0.83 | 0.99 | 50 | 102 | 143 | 55 |
| 19 | 37.0 | 1.09 | 1.06 | 2.15 | 48 | 95 | 135 | 55 |
| 20 | 31.8 | 37.17 | 21.13 | 58.30 | 57 | 110 | 159 | 54 |
| 21 | 31.7 | 0.02 | 0.75 | 0.77 | 27 | 34 | 40 | 26 |
| 22 | 33.4 | 0.11 | 21.53 | 21.63 | 34 | 45 | 60 | 30 |
| 23 | 25.3 | 0.05 | 17.85 | 17.90 | 56 | 110 | 146 | 49 |
| 24 | 18.5 | 0.05 | 0.94 | 0.99 | 26 | 33 | 36 | 26 |
| 25 | 28.1 | 0.08 | 1.20 | 1.28 | 29 | 43 | 50 | 28 |

| Sample ID | Weight, g | Metal Content, % | | | Average Temperature, °C | | | |
|---|---|---|---|---|---|---|---|---|
| | | Pb | Zn | Pb+Zn | 5s | 10s | 15s | G9-10s |
| 26 | 48.0 | 5.02 | 17.60 | 22.62 | 49 | 94 | 121 | 57 |
| 27 | 53.2 | 4.93 | 34.27 | 39.20 | 53 | 96 | 159 | 56 |
| 28 | 27.4 | 5.34 | 24.60 | 29.94 | 62 | 133 | 170 | 66 |
| 29 | 12.6 | 0.04 | 0.81 | 0.85 | 26 | 32 | 36 | 26 |
| 30 | 16.4 | 0.02 | 0.75 | 0.77 | 28 | 33 | 42 | 26 |
| 31 | 45.3 | 17.16 | 24.13 | 41.28 | 52 | 101 | 136 | 54 |
| 32 | 45.8 | 20.96 | 17.99 | 38.95 | 50 | 100 | 128 | 47 |
| 33 | 40.0 | 22.36 | 15.77 | 38.12 | 54 | 107 | 145 | 66 |
| 34 | 37.3 | 2.23 | 11.51 | 13.74 | 52 | 100 | 144 | 58 |
| 35 | 35.2 | 24.50 | 20.40 | 44.90 | 54 | 111 | 152 | 61 |
| 36 | 23.3 | 0.03 | 0.79 | 0.82 | 26 | 32 | 36 | 26 |
| 37 | 15.8 | 0.49 | 3.85 | 4.34 | 33 | 51 | 64 | 29 |
| 38 | 23.8 | 17.55 | 13.32 | 30.87 | 65 | 129 | 172 | 76 |
| 39 | 28.1 | 0.04 | 0.86 | 0.90 | 27 | 33 | 38 | 26 |
| 40 | 22.2 | 0.00 | 0.84 | 0.84 | 28 | 32 | 38 | 26 |
| 41 | 41.6 | 0.25 | 19.79 | 20.04 | 46 | 96 | 112 | 44 |
| 42 | 23.7 | 27.70 | 19.19 | 46.89 | 76 | 150 | 191 | 80 |
| 43 | 29.3 | 0.64 | 5.52 | 6.16 | 61 | 114 | 164 | 67 |
| 44 | 14.7 | 0.54 | 3.13 | 3.67 | 34 | 55 | 77 | 33 |
| 45 | 24.4 | 20.40 | 23.97 | 44.36 | 58 | 123 | 183 | 65 |
| 46 | 24.2 | 0.01 | 0.82 | 0.83 | 27 | 32 | 42 | |
| 47 | 35.7 | 0.36 | 3.44 | 3.80 | 50 | 99 | 135 | |
| 48 | 17.8 | 0.03 | 0.88 | 0.91 | 27 | 32 | 37 | |
| 49 | 21.4 | 0.04 | 0.85 | 0.89 | 26 | 32 | 37 | |
| 50 | 41.9 | 2.79 | 6.08 | 8.86 | 51 | 103 | 129 | |

## Sortability Graph

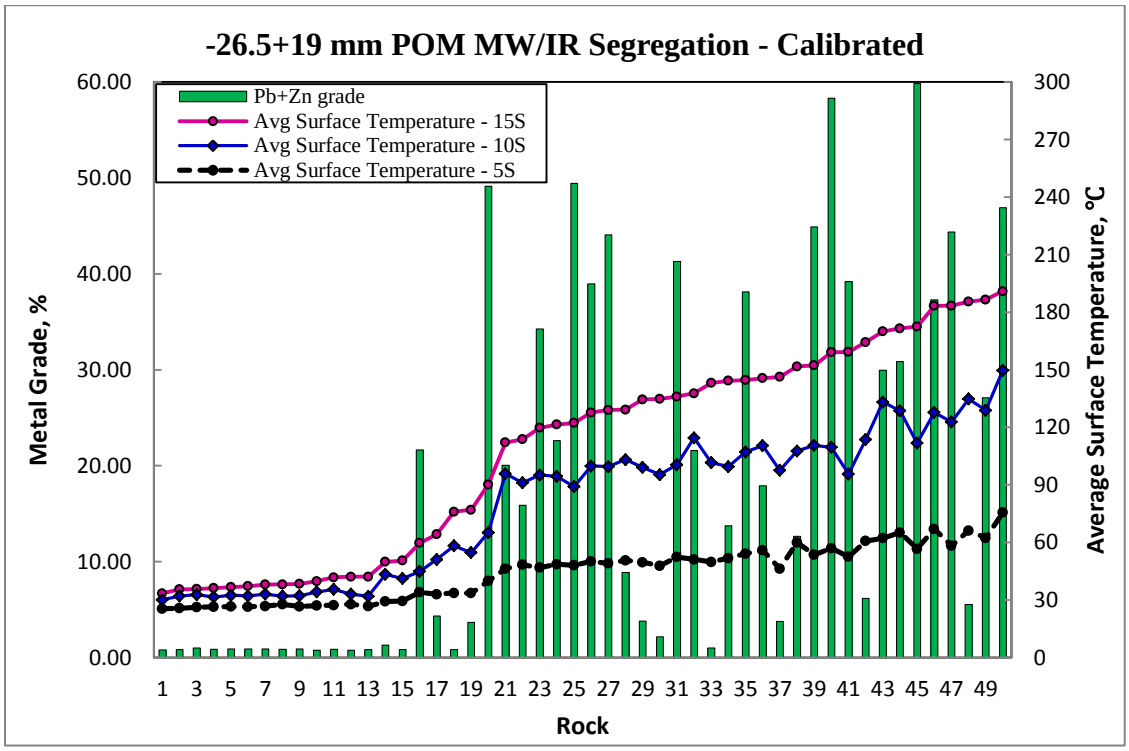


## Individual and Group Tests

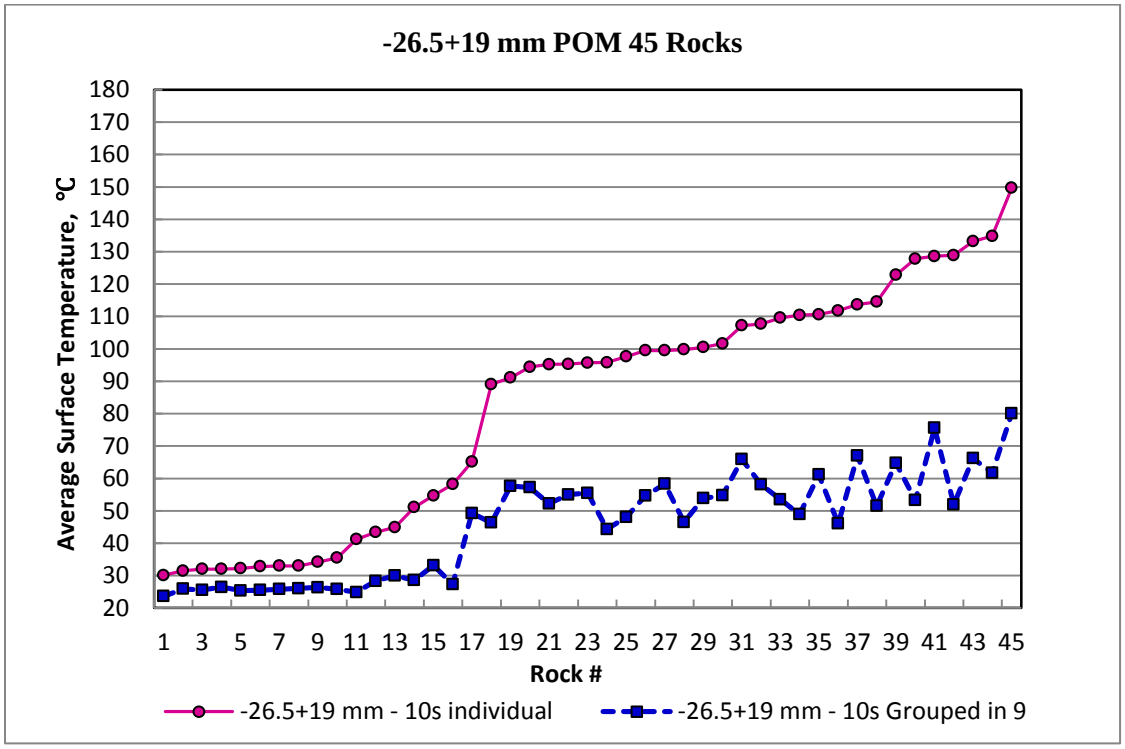

**-26.5+19 mm MW/IR Sorting Results – Individual 5s (Calibrated XRF Surface Readings)**

| Separation Temperature, °C | Hot Fraction | Cold Fraction | Wt. % in Hot Fraction | | Wt. % in Cold Fraction | | % in Hot Fraction | | % in Cold Fraction | |
|---|---|---|---|---|---|---|---|---|---|---|
| | | | Concentrate Grades, % | | Waste Grades, % | | Metal Recovery, % | | Metal Recovery, % | |
| | Conc. % | Waste % | Pb | Zn | Pb | Zn | Pb | Zn | Pb | Zn |
| **26** | 93.5 | 6.5 | 9.90 | 13.65 | 0.04 | 0.82 | 100.0 | 99.6 | 0.0 | 0.4 |
| **27** | 84.7 | 15.3 | 10.92 | 14.98 | 0.03 | 0.82 | 99.9 | 99.0 | 0.1 | 1.0 |
| **30** | **79.0** | **21.0** | **11.71** | **16.00** | **0.03** | **0.85** | **99.9** | **98.6** | **0.1** | **1.4** |
| **35** | **73.7** | **26.3** | **12.53** | **16.42** | **0.08** | **2.73** | **99.8** | **94.4** | **0.2** | **5.6** |
| **40** | 69.5 | 30.5 | 11.09 | 16.62 | 5.09 | 4.17 | 83.2 | 90.1 | 16.8 | 9.9 |
| **47** | 61.4 | 38.6 | 12.53 | 16.05 | 4.08 | 7.70 | 83.0 | 76.8 | 17.0 | 23.2 |
| **48** | 52.7 | 47.3 | 12.74 | 16.68 | 5.39 | 8.53 | 72.5 | 68.5 | 27.5 | 31.5 |
| **50** | 39.3 | 60.7 | 13.68 | 17.71 | 6.41 | 9.66 | 58.0 | 54.2 | 42.0 | 45.8 |
| **55** | 21.2 | 78.8 | 15.68 | 16.51 | 7.53 | 11.83 | 36.0 | 27.3 | 64.0 | 72.7 |
| **60** | 11.6 | 88.4 | 10.73 | 15.19 | 9.07 | 12.51 | 13.5 | 13.8 | 86.5 | 86.2 |
| **65** | 4.4 | 95.6 | 17.81 | 12.70 | 8.87 | 12.83 | 8.4 | 4.3 | 91.6 | 95.7 |
| **Calculated Head Grade : 9.26% Pb and 12.82% Zn** | | | | | | | | | | |

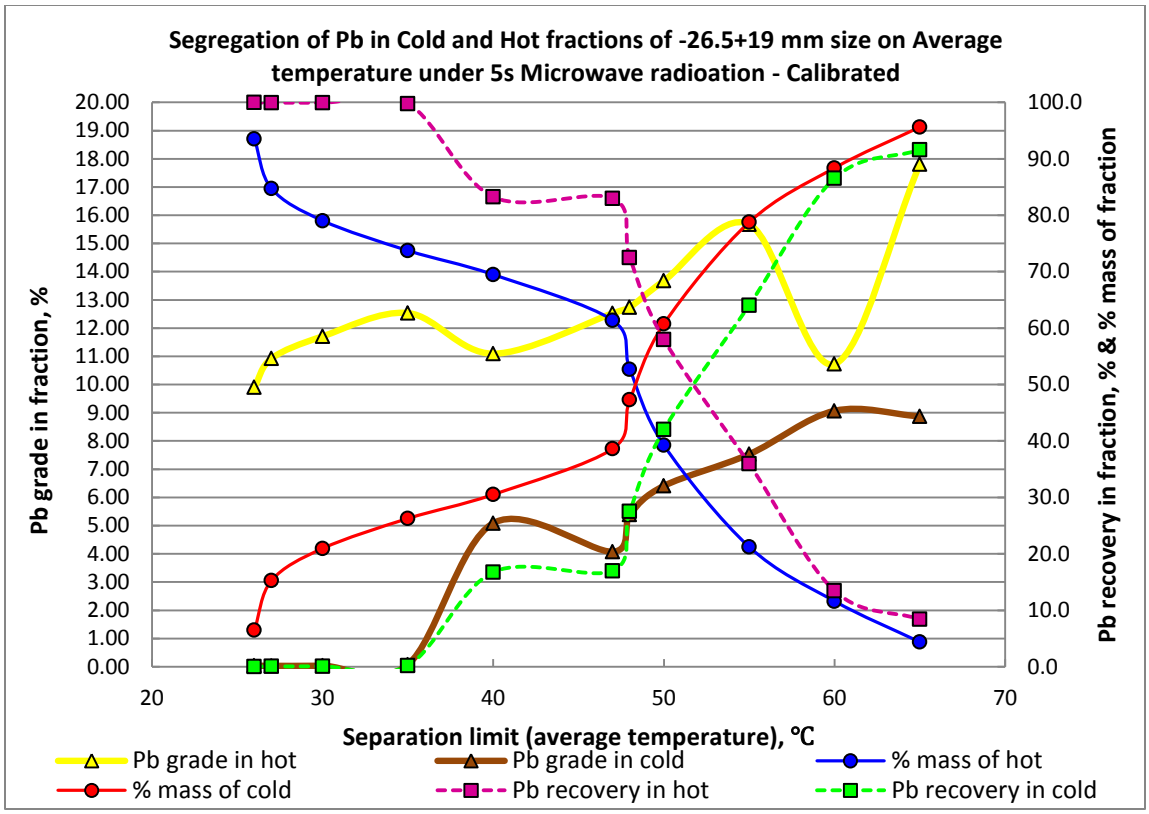
Segregation of Pb in Cold and Hot fractions of -26.5+19 mm size on Average temperature under 5s Microwave radioation - Calibrated
Pb grade in fraction, %
Pb recovery in fraction, % & % mass of fraction
Separation limit (average temperature), ℃
Pb grade in hot
Pb grade in cold
% mass of hot
% mass of cold
Pb recovery in hot
Pb recovery in cold

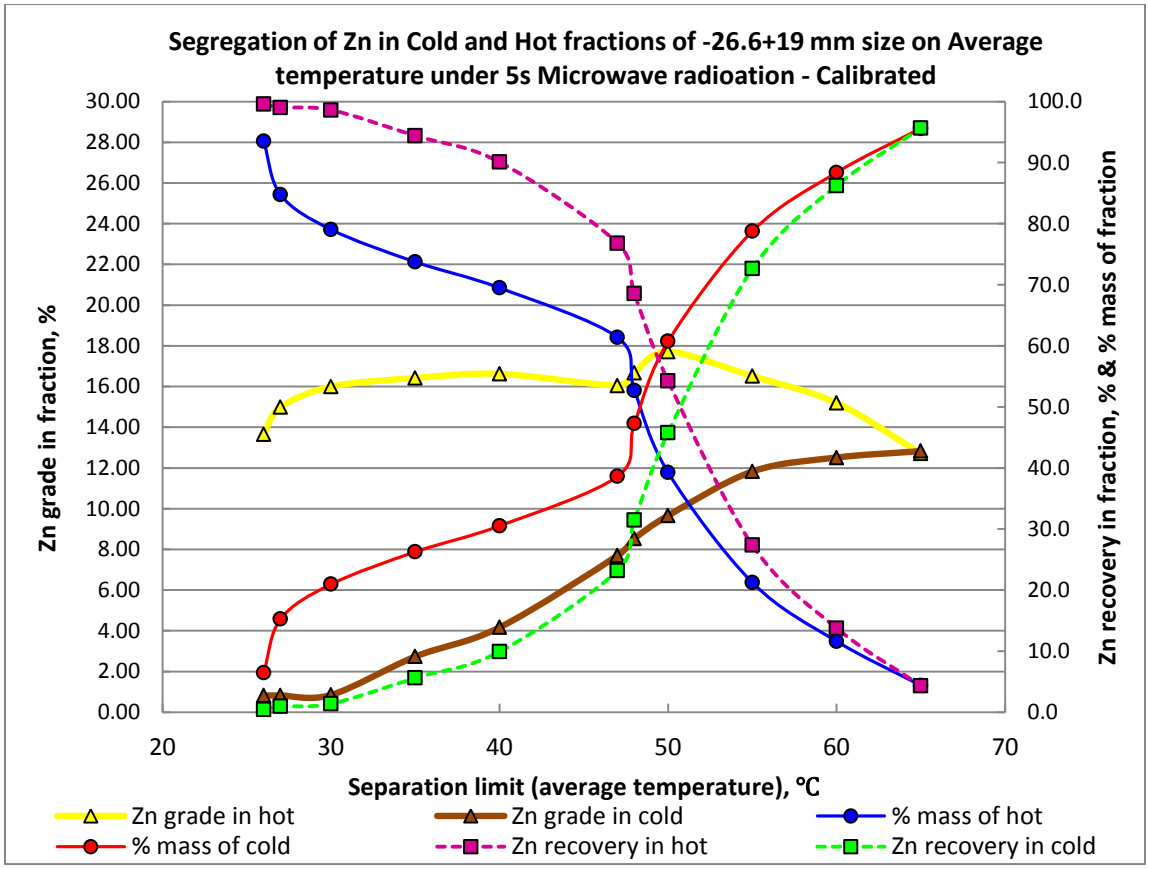
Segregation of Zn in Cold and Hot fractions of -26.6+19 mm size on Average temperature under 5s Microwave radioation - Calibrated
Zn grade in fraction, %
Zn recovery in fraction, % & % mass of fraction
Separation limit (average temperature), ℃
Zn grade in hot
Zn grade in cold
% mass of hot
% mass of cold
Zn recovery in hot
Zn recovery in cold

**-26.5+19 mm MW/IR Sorting Results – Individual 10s (Calibrated XRF Surface Readings)**

| Separation Temperature, °C | Hot fraction | Cold Fraction | Wt. % in Hot Fraction | | Wt. % in Cold Fraction | | % in Hot Fraction | | % in Cold Fraction | |
|---|---|---|---|---|---|---|---|---|---|---|
| | | | Concentrate Grades, % | | Waste Grades, % | | Metal Recovery, % | | Metal Recovery, % | |
| | Conc., % | Waste, % | Pb | Zn | Pb | Zn | Pb | Zn | Pb | Zn |
| **32** | 89.8 | 10.2 | 10.31 | 14.18 | 0.03 | 0.82 | 100.0 | 99.3 | 0.0 | 0.7 |
| **33** | 85.8 | 14.2 | 10.79 | 14.81 | 0.03 | 0.83 | 100.0 | 99.1 | 0.0 | 0.9 |
| **45** | **76.9** | **23.1** | **12.03** | **15.84** | **0.04** | **2.77** | **99.9** | **95.0** | **0.1** | **5.0** |
| **60** | 73.7 | 26.3 | 12.53 | 16.42 | 0.08 | 2.73 | 99.8 | 94.4 | 0.2 | 5.6 |
| **80** | 69.5 | 30.5 | 11.09 | 16.62 | 5.09 | 4.17 | 83.2 | 90.1 | 16.8 | 9.9 |
| **95** | 54.5 | 45.5 | 12.05 | 16.25 | 5.92 | 8.72 | 70.9 | 69.1 | 29.1 | 30.9 |
| **100** | 35.8 | 64.2 | 14.39 | 15.44 | 6.40 | 11.36 | 55.6 | 43.1 | 44.4 | 56.9 |
| **105** | 27.8 | 72.2 | 16.42 | 16.67 | 6.50 | 11.34 | 49.4 | 36.2 | 50.6 | 63.8 |
| **110** | 19.5 | 80.5 | 16.52 | 16.71 | 7.50 | 11.88 | 34.8 | 25.5 | 65.2 | 74.5 |
| **120** | 11.3 | 88.7 | 13.75 | 18.02 | 8.69 | 12.16 | 16.8 | 15.9 | 83.2 | 84.1 |
| **130** | 4.7 | 95.3 | 11.73 | 16.45 | 9.14 | 12.64 | 5.9 | 6.0 | 94.1 | 94.0 |
| **Calculated Head Grade : 9.26% Pb and 12.82% Zn** | | | | | | | | | | |

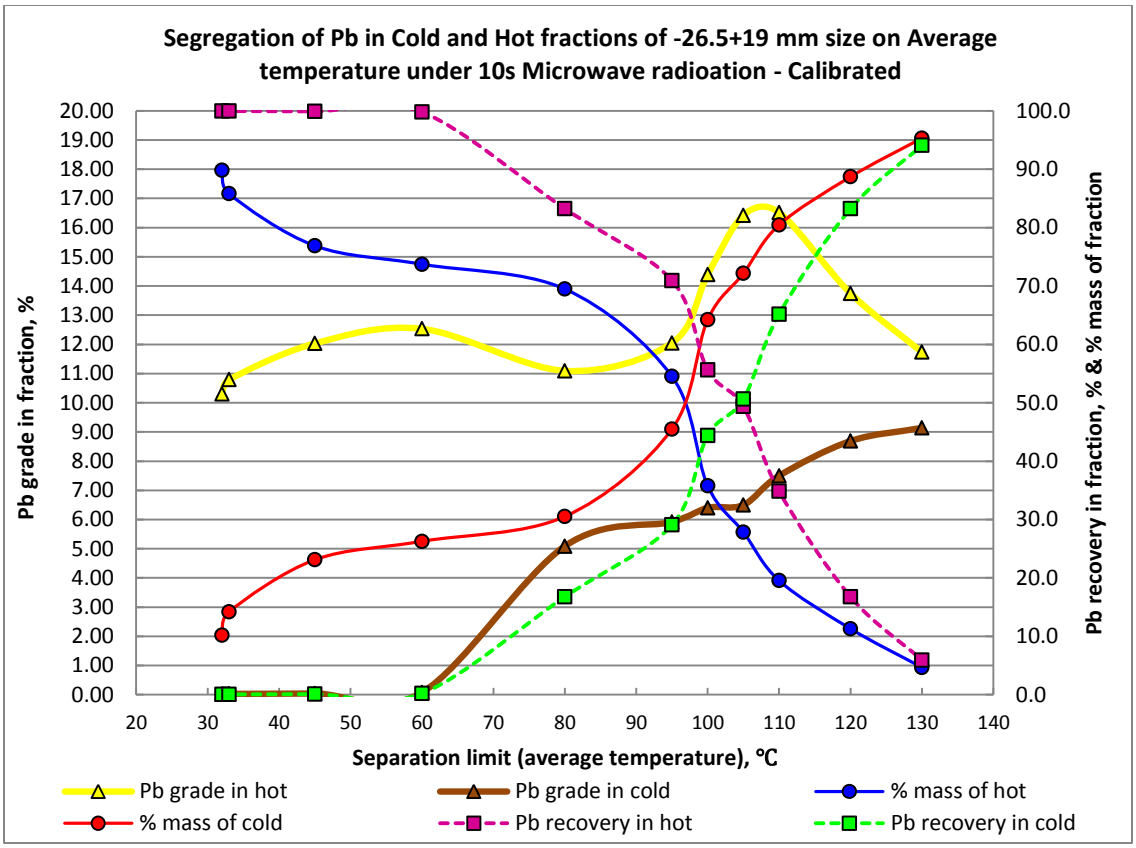
Segregation of Pb in Cold and Hot fractions of -26.5+19 mm size on Average temperature under 10s Microwave radioation - Calibrated
Pb grade in fraction, %
Pb recovery in fraction, % & % mass of fraction
Separation limit (average temperature), ℃
Pb grade in hot
Pb grade in cold
% mass of hot
% mass of cold
Pb recovery in hot
Pb recovery in cold

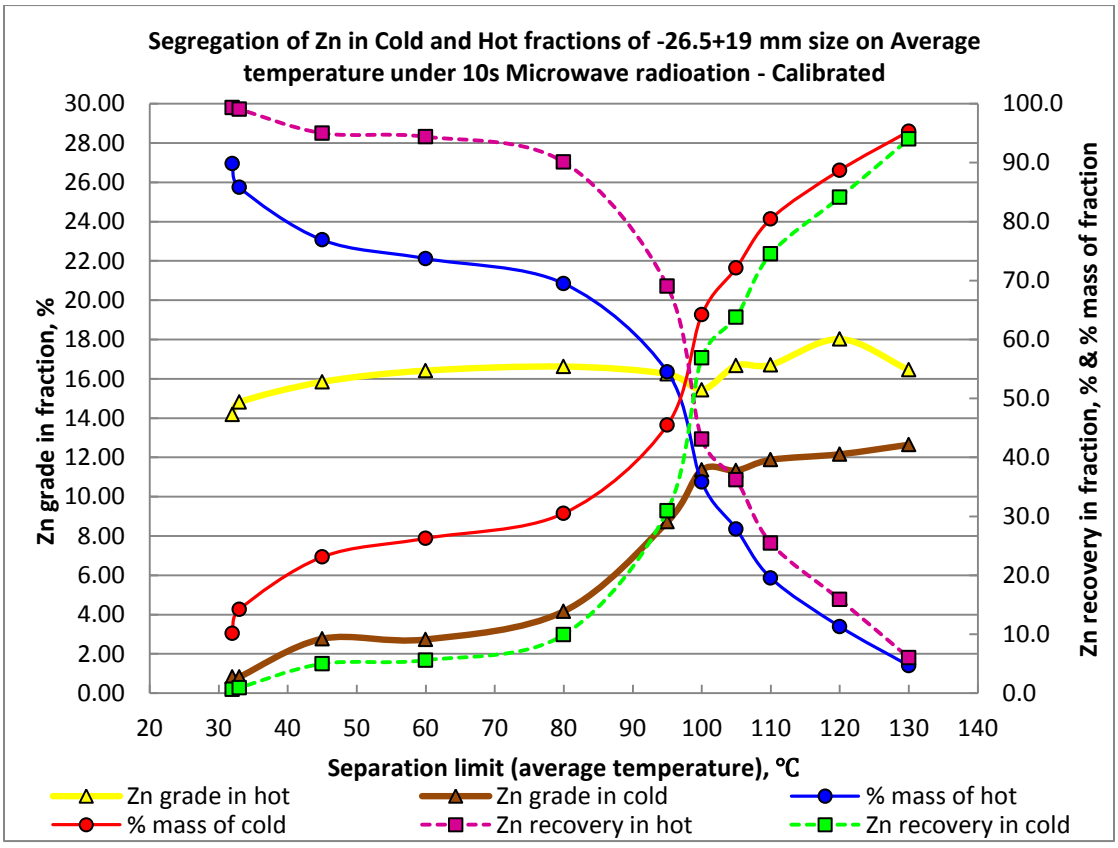
Segregation of Zn in Cold and Hot fractions of -26.5+19 mm size on Average temperature under 10s Microwave radioation - Calibrated
Zn grade in fraction, %
Zn recovery in fraction, % & % mass of fraction
Separation limit (average temperature), ℃
Zn grade in hot
Zn grade in cold
% mass of hot
% mass of cold
Zn recovery in hot
Zn recovery in cold

**-26.5+19 mm MW/IR Sorting Results – Individual 15s (Calibrated XRF Surface Readings)**

| Separation Temperature, °C | Hot Fraction | Cold Fraction | Wt. % in Hot Fraction | | Wt. % in Cold Fraction | | % in Hot Fraction | | % in Cold Fraction | |
|---|---|---|---|---|---|---|---|---|---|---|
| | | | Concentrate Grades,% | | Waste Grades, % | | Metal Recovery, % | | Metal Recovery, % | |
| | Conc. % | Waste % | Pb | Zn | Pb | Zn | Pb | Zn | Pb | Zn |
| **36** | 94.9 | 5.1 | 9.76 | 13.47 | 0.03 | 0.82 | 100.0 | 99.7 | 0.0 | 0.3 |
| **40** | 86.4 | 13.6 | 10.72 | 14.72 | 0.03 | 0.83 | 100.0 | 99.1 | 0.0 | 0.9 |
| **60** | **76.9** | **23.1** | **12.03** | **15.84** | **0.04** | **2.77** | **99.9** | **95.0** | **0.1** | **5.0** |
| **80** | **73.7** | **26.3** | **12.53** | **16.42** | **0.08** | **2.73** | **99.8** | **94.4** | **0.2** | **5.6** |
| **90** | 69.5 | 30.5 | 11.09 | 16.62 | 5.09 | 4.17 | 83.2 | 90.1 | 16.8 | 9.9 |
| **120** | 60.2 | 39.8 | 12.74 | 15.62 | 3.99 | 8.58 | 82.9 | 73.4 | 17.1 | 26.6 |
| **125** | 54.2 | 45.8 | 12.15 | 15.40 | 5.84 | 9.76 | 71.1 | 65.1 | 28.9 | 34.9 |
| **135** | 41.1 | 58.9 | 12.89 | 16.75 | 6.73 | 10.08 | 57.2 | 53.7 | 42.8 | 46.3 |
| **145** | 29.1 | 70.9 | 13.92 | 17.92 | 7.34 | 10.73 | 43.8 | 40.7 | 56.2 | 59.3 |
| **155** | 21.0 | 79.0 | 16.63 | 19.74 | 7.31 | 10.99 | 37.6 | 32.3 | 62.4 | 67.7 |
| **170** | 11.9 | 88.1 | 20.68 | 16.85 | 7.72 | 12.28 | 26.5 | 15.6 | 73.5 | 84.4 |
| **185** | 5.0 | 95.0 | 10.98 | 16.14 | 9.17 | 12.65 | 5.9 | 6.3 | 94.1 | 93.7 |
| **Calculated Head Grade : 9.26% Pb and 12.82% Zn** | | | | | | | | | | |

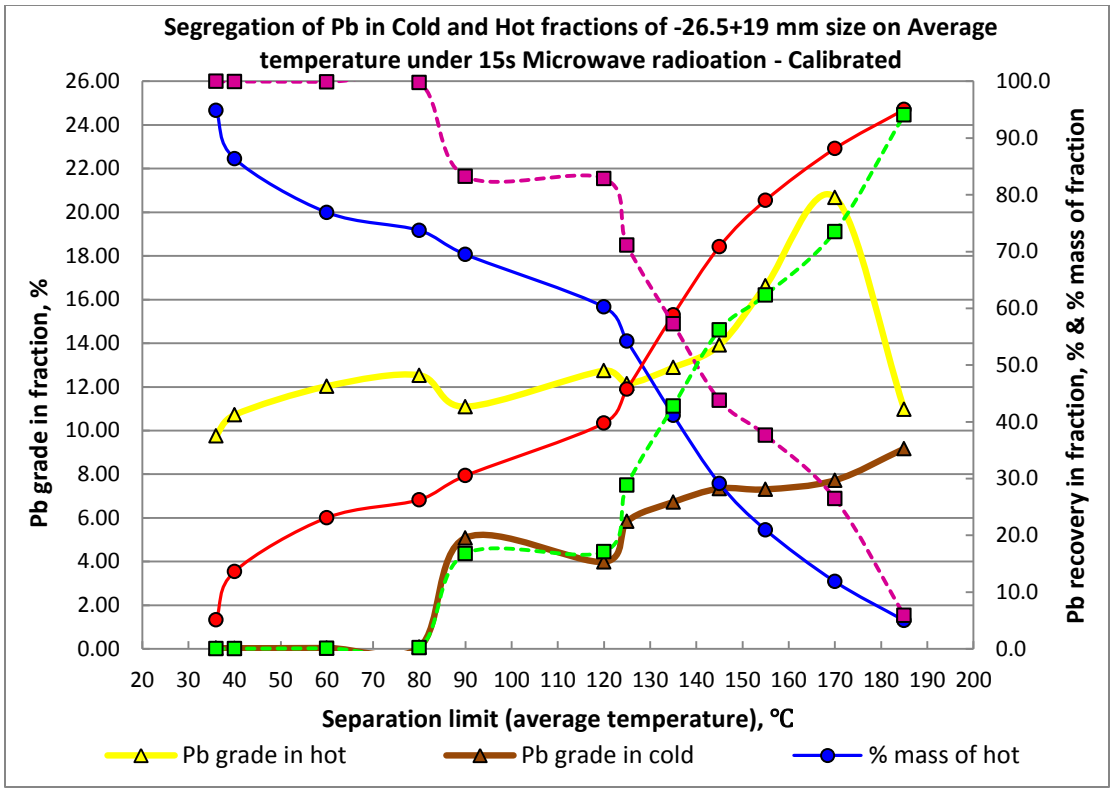
Segregation of Pb in Cold and Hot fractions of -26.5+19 mm size on Average temperature under 15s Microwave radioation - Calibrated
Pb grade in fraction, %
Pb recovery in fraction, % & % mass of fraction
Separation limit (average temperature), ℃
Pb grade in hot
Pb grade in cold
% mass of hot

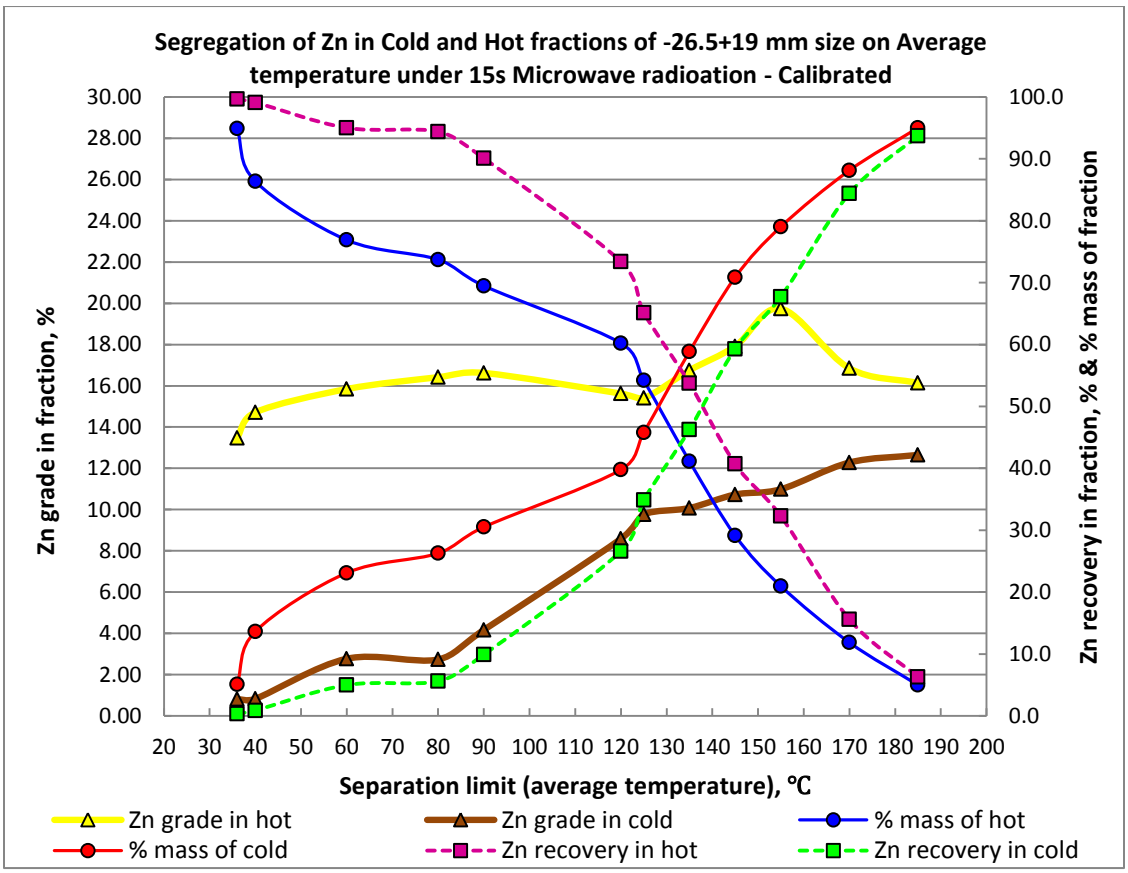
Segregation of Zn in Cold and Hot fractions of -26.5+19 mm size on Average temperature under 15s Microwave radioation - Calibrated
Zn grade in fraction, %
Zn recovery in fraction, % & % mass of fraction
Separation limit (average temperature), ℃
Zn grade in hot
Zn grade in cold
% mass of hot
% mass of cold
Zn recovery in hot
Zn recovery in cold

**-26.5+19 mm MW/IR Sorting Results – Individual 10s 45 rocks (Calibrated XRF Surface Readings)**

| Separation Temperature, °C | Hot Fraction | Cold Fraction | Wt. % in Hot Fraction | | Wt. % in Cold Fraction | | % in Hot Fraction | | % in Cold Fraction | |
|---|---|---|---|---|---|---|---|---|---|---|
| | | | Concentrate Grades, % | | Waste Grades, % | | Metal Recovery, % | | Metal Recovery, % | |
| | Conc. % | Waste % | Pb | Zn | Pb | Zn | Pb | Zn | Pb | Zn |
| **32** | 93.3 | 6.7 | 10.81 | 14.73 | 0.02 | 0.81 | 100.0 | 99.6 | 0.0 | 0.4 |
| **35** | 86.6 | 13.4 | 11.65 | 15.80 | 0.03 | 0.81 | 100.0 | 99.2 | 0.0 | 0.8 |
| **45** | **79.1** | **20.9** | **12.75** | **16.60** | **0.04** | **3.18** | **99.9** | **95.2** | **0.1** | **4.8** |
| **65** | 70.9 | 29.1 | 11.82 | 17.53 | 5.87 | 4.68 | 83.1 | 90.1 | 16.9 | 9.9 |
| **95** | 54.5 | 45.5 | 13.09 | 17.39 | 6.50 | 9.49 | 70.7 | 68.7 | 29.3 | 31.3 |
| **98** | 45.3 | 54.7 | 15.30 | 16.58 | 5.77 | 11.49 | 68.7 | 54.5 | 31.3 | 45.5 |
| **100** | 36.4 | 63.6 | 15.33 | 16.20 | 7.09 | 12.42 | 55.3 | 42.8 | 44.7 | 57.2 |
| **110** | 21.5 | 78.5 | 16.52 | 16.71 | 8.33 | 13.00 | 35.2 | 26.0 | 64.8 | 74.0 |
| **120** | 12.4 | 87.6 | 13.75 | 18.02 | 9.57 | 13.20 | 16.9 | 16.2 | 83.1 | 83.8 |
| **130** | 5.1 | 94.9 | 11.73 | 16.45 | 10.00 | 13.65 | 6.0 | 6.1 | 94.0 | 93.9 |
| **Calculated Head Grade: 10.09% Pb and 13.79% Zn** | | | | | | | | | | |

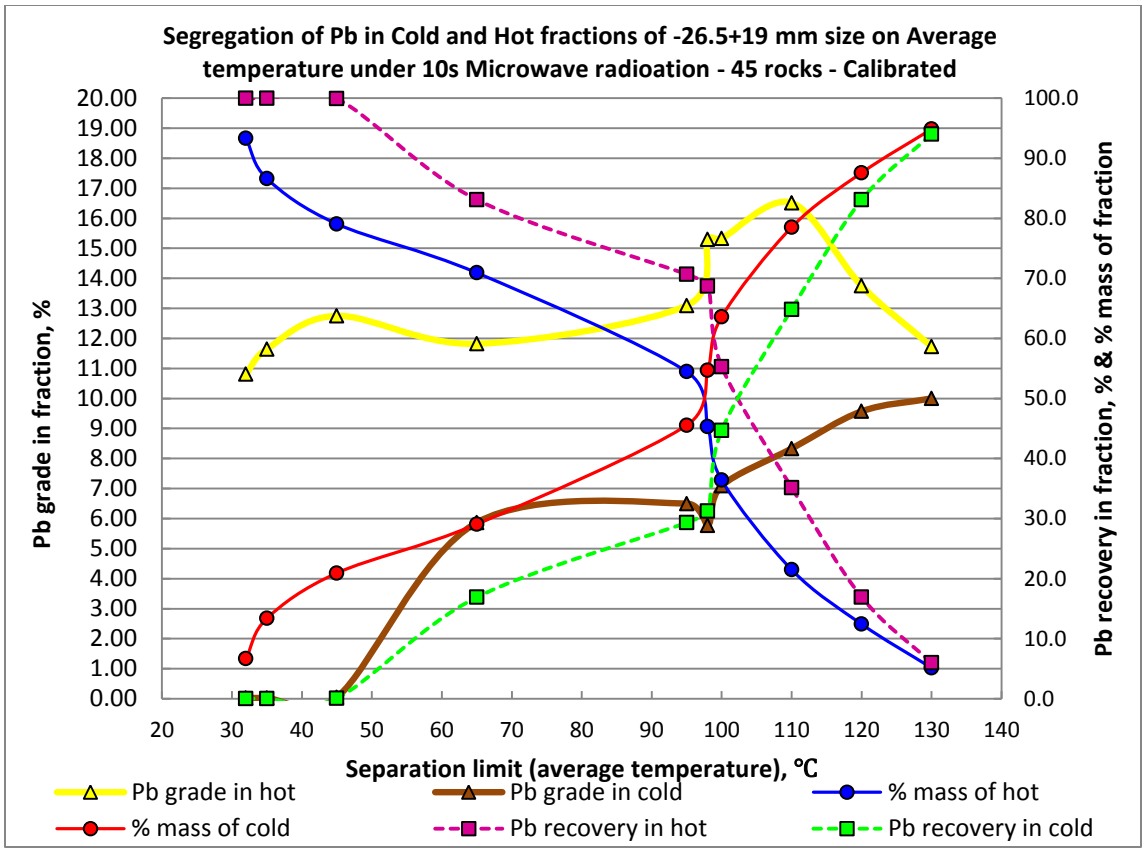
Segregation of Pb in Cold and Hot fractions of -26.5+19 mm size on Average temperature under 10s Microwave radioation - 45 rocks - Calibrated
Pb grade in fraction, %
Pb recovery in fraction, % & % mass of fraction
Separation limit (average temperature), ℃
Pb grade in hot
Pb grade in cold
% mass of hot
% mass of cold
Pb recovery in hot
Pb recovery in cold

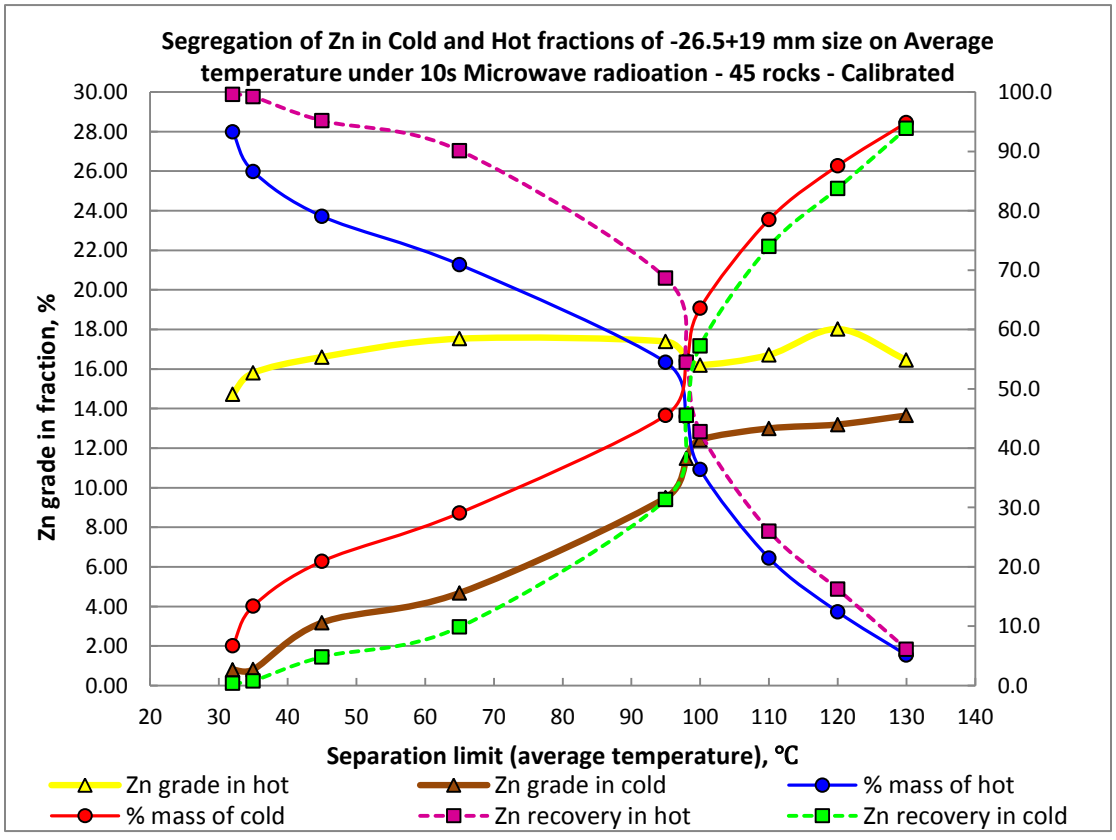
Segregation of Zn in Cold and Hot fractions of -26.5+19 mm size on Average temperature under 10s Microwave radioation - 45 rocks - Calibrated
Zn grade in fraction, %
Separation limit (average temperature), ℃
Zn grade in hot
Zn grade in cold
% mass of hot
% mass of cold
Zn recovery in hot
Zn recovery in cold

**-26.5+19 mm MW/IR Sorting Results – Group in 9- 10s 45 rocks (Calibrated XRF Surface Readings)**

| Separation Temperature, °C | Hot Fraction | Cold Fraction | Wt. % in Hot Fraction | | Wt. % in Cold Fraction | | % in Hot Fraction | | % in Cold Fraction | |
|---|---|---|---|---|---|---|---|---|---|---|
| | | | Concentrate Grades, % | | Waste Grades, % | | Metal Recovery, % | | Metal Recovery, % | |
| | Conc. % | Waste % | Pb | Zn | Pb | Zn | Pb | Zn | Pb | Zn |
| **25** | 95.8 | 4.2 | 10.53 | 14.36 | 0.03 | 0.79 | 100.0 | 99.8 | 0.0 | 0.2 |
| **26** | **83.4** | **16.6** | **12.09** | **16.38** | **0.03** | **0.81** | **100.0** | **99.0** | **0.0** | **1.0** |
| **30** | **76.6** | **23.4** | **13.15** | **17.06** | **0.06** | **3.08** | **99.8** | **94.8** | **0.2** | **5.2** |
| **45** | 72.7 | 27.3 | 13.85 | 17.15 | 0.10 | 4.88 | 99.7 | 90.3 | 0.3 | 9.7 |
| **50** | 54.8 | 45.2 | 10.18 | 18.01 | 9.98 | 8.69 | 55.3 | 71.5 | 44.7 | 28.5 |
| **53** | 45.4 | 54.6 | 10.97 | 16.77 | 9.36 | 11.32 | 49.3 | 55.2 | 50.7 | 44.8 |
| **55** | 31.7 | 68.3 | 9.30 | 17.63 | 10.46 | 12.02 | 29.2 | 40.5 | 70.8 | 59.5 |
| **60** | 15.9 | 84.1 | 15.72 | 16.01 | 9.02 | 13.38 | 24.8 | 18.5 | 75.2 | 81.5 |
| **65** | 10.2 | 89.8 | 14.79 | 15.52 | 9.56 | 13.60 | 14.9 | 11.5 | 85.1 | 88.5 |
| **70** | 3.4 | 96.6 | 22.61 | 16.25 | 9.66 | 13.71 | 7.5 | 4.0 | 92.5 | 96.0 |
| **Calculated Head Grade: 10.09% Pb and 13.79% Zn** | | | | | | | | | | |

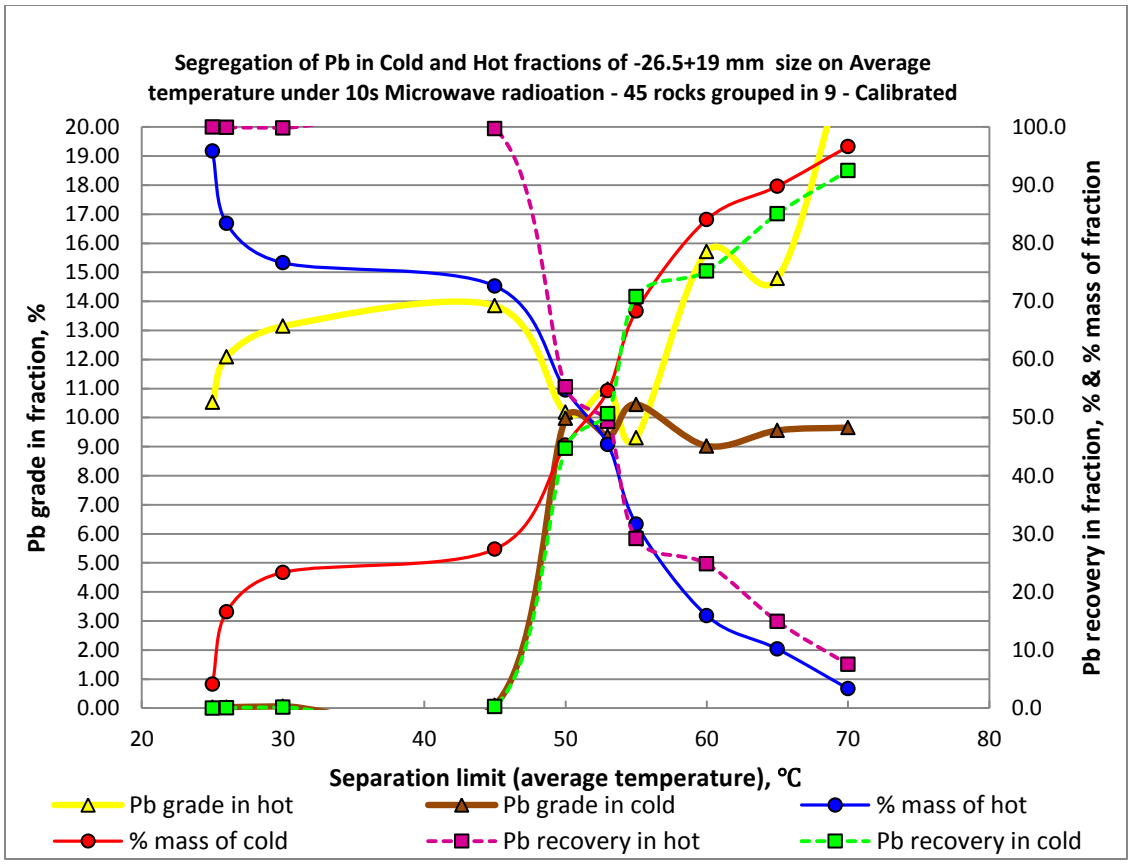
Segregation of Pb in Cold and Hot fractions of -26.5+19 mm size on Average temperature under 10s Microwave radioation - 45 rocks grouped in 9 - Calibrated
Pb grade in fraction, %
Pb recovery in fraction, % & % mass of fraction
Separation limit (average temperature), ℃
Pb grade in hot
Pb grade in cold
% mass of hot
% mass of cold
Pb recovery in hot
Pb recovery in cold

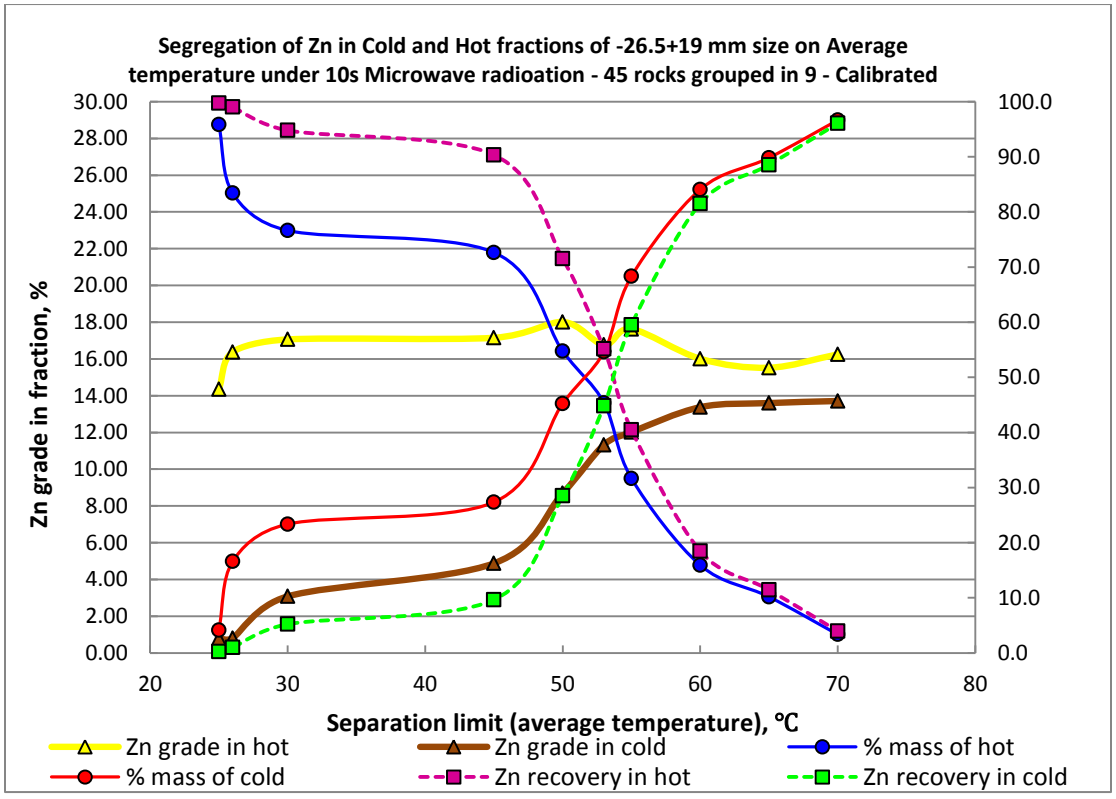
Segregation of Zn in Cold and Hot fractions of -26.5+19 mm size on Average temperature under 10s Microwave radioation - 45 rocks grouped in 9 - Calibrated
Zn grade in fraction, %
Separation limit (average temperature), ℃
Zn grade in hot
Zn grade in cold
% mass of hot
% mass of cold
Zn recovery in hot
Zn recovery in cold

**-26.5+19 mm Size Fraction Sorting Results Summary**

| Test Condition | Separation Limit, °C | Mass % of Cold | Pb in Hot Fraction, % | | Zn in Hot Fraction, % | |
|---|---|---|---|---|---|---|
| | | | Grade | Recovery | Grade | Recovery |
| 5s | 30 | 21.0 | 11.71 | 99.9 | 16.00 | 98.6 |
| 10s | 45 | 23.1 | 12.03 | 99.9 | 15.84 | 95.0 |
| 15s | 60 | 23.1 | 12.03 | 99.9 | 15.84 | 95.0 |
| Calculated Head Grade:9.26% Pb and 12.86% of Zn 50 rocks being tested | | | | | | |
| **Test Condition** | **Separation Limit, °C** | **Mass % of Cold** | **Pb in Hot Fraction, %** | | **Zn in Hot Fraction, %** | |
| | | | **Grade** | **Recovery** | **Grade** | **Recovery** |
| Individual | 45 | 20.9 | 12.75 | 99.9 | 16.60 | 95.2 |
| Group in 9 | 26 | 16.6 | 12.09 | 100.0 | 16.38 | 99.0 |
| Calculated Head Grade: 10.09% Pb and 13.79% Zn 45 rocks being tested | | | | | | |

**-19+13.2 mm Size Fraction MW/IR Sorting Results**

**Initial Data Set**

| Sample ID | Weight, g | Metal Content, % | | Average Temperature, °C | | | | |
|---|---|---|---|---|---|---|---|---|
| | | Pb | Zn | 5s | 10s | 15s | G9-10s | G25-10s |
| 1 | 7.6 | 29.79 | 2.92 | 49 | 105 | 156 | 75 | 48 |
| 2 | 5.2 | 11.17 | 6.30 | 66 | 150 | 194 | 90 | 70 |
| 3 | 8.2 | 0.35 | 1.07 | 62 | 165 | 223 | 82 | 56 |
| 4 | 4.6 | 0.01 | 1.53 | 26 | 28 | 31 | 26 | 25 |
| 5 | 5.3 | 0.02 | 0.86 | 28 | 34 | 39 | 27 | 26 |
| 6 | 5.8 | 4.88 | 29.45 | 97 | 187 | 280 | 140 | 82 |
| 7 | 13.0 | 0.24 | 13.92 | 45 | 101 | 122 | 84 | 48 |
| 8 | 6.8 | 0.04 | 0.77 | 26 | 29 | 33 | 26 | 25 |
| 9 | 4.9 | 0.19 | 1.28 | 26 | 29 | 32 | 26 | 25 |
| 10 | 5.7 | 15.63 | 9.76 | 70 | 115 | 173 | 105 | 47 |
| 11 | 7.1 | 0.05 | 1.04 | 26 | 31 | 32 | 27 | 26 |
| 12 | 4.6 | 1.33 | 0.90 | 76 | 155 | 244 | 116 | 85 |
| 13 | 7.5 | 0.04 | 0.84 | 27 | 32 | 33 | 27 | 26 |
| 14 | 8.7 | 0.04 | 3.63 | 28 | 31 | 35 | 26 | 25 |
| 15 | 7.7 | 0.05 | 0.89 | 27 | 30 | 35 | 28 | 26 |
| 16 | 8.2 | 17.99 | 30.70 | 64 | 130 | 194 | 97 | 60 |
| 17 | 12.1 | 6.35 | 2.21 | 65 | 132 | 181 | 84 | 55 |
| 18 | 9.5 | 1.54 | 1.26 | 49 | 105 | 146 | 65 | 47 |
| 19 | 6.4 | 0.23 | 0.80 | 46 | 88 | 121 | 50 | 45 |
| 20 | 10.1 | 1.13 | 1.41 | 48 | 122 | 127 | 73 | 55 |
| 21 | 7.1 | 8.18 | 7.95 | 85 | 194 | 299 | 177 | 74 |
| 22 | 10.4 | 0.03 | 0.77 | 26 | 28 | 31 | 27 | 26 |
| 23 | 13.2 | 1.00 | 8.97 | 58 | 115 | 166 | 76 | 64 |
| 24 | 10.0 | 0.04 | 0.76 | 26 | 29 | 32 | 28 | 26 |
| 25 | 4.5 | 0.03 | 0.79 | 29 | 30 | 37 | 30 | 27 |

| Sample ID | Weight, g | Metal Content, % | | Average Temperature, °C | | | | |
|---|---|---|---|---|---|---|---|---|
| | | Pb | Zn | 5s | 10s | 15s | G9-10s | G25–10s |
| 26 | 7.0 | 0.02 | 0.75 | 28 | 28 | 33 | 27 | 25 |
| 27 | 4.4 | 9.33 | 4.15 | 59 | 128 | 203 | 89 | 69 |
| 28 | 8.2 | 7.45 | 31.30 | 53 | 113 | 148 | 92 | 75 |
| 29 | 5.2 | 24.86 | 25.51 | 115 | 239 | 271 | 162 | 113 |
| 30 | 4.9 | 0.04 | 15.77 | 37 | 61 | 86 | 46 | 34 |
| 31 | 4.5 | 42.06 | 28.24 | 70 | 164 | 197 | 116 | 92 |
| 32 | 5.8 | 0.01 | 1.22 | 27 | 39 | 32 | 28 | 26 |
| 33 | 6.1 | 0.03 | 1.01 | 28 | 30 | 34 | 28 | 26 |
| 34 | 4.6 | 0.04 | 0.81 | 28 | 29 | 33 | 28 | 26 |
| 35 | 7.4 | 10.89 | 28.38 | 49 | 105 | 149 | 63 | 47 |
| 36 | 7.6 | 3.11 | 26.65 | 64 | 134 | 202 | 95 | 81 |
| 37 | 11.1 | 0.62 | 1.97 | 63 | 127 | 186 | 95 | 64 |
| 38 | 9.0 | 0.12 | 13.03 | 47 | 88 | 153 | 64 | 61 |
| 39 | 9.4 | 21.58 | 1.77 | 68 | 124 | 190 | 89 | 52 |
| 40 | 7.6 | 0.03 | 0.75 | 27 | 31 | 37 | 29 | 26 |
| 41 | 6.8 | 0.02 | 0.75 | 28 | 28 | 28 | 27 | 26 |
| 42 | 5.6 | 0.02 | 0.76 | 28 | 30 | 32 | 29 | 26 |
| 43 | 8.8 | 0.01 | 0.89 | 34 | 42 | 55 | 34 | 31 |
| 44 | 3.7 | 0.02 | 0.76 | 36 | 56 | 102 | 42 | 33 |
| 45 | 10.1 | 0.16 | 7.99 | 70 | 122 | 225 | 99 | 73 |
| 46 | 7.7 | 2.09 | 3.94 | 67 | 123 | 191 | | 65 |
| 47 | 5.9 | 0.82 | 17.52 | 50 | 97 | 159 | | 48 |
| 48 | 4.7 | 1.98 | 30.00 | 41 | 70 | 105 | | 32 |
| 49 | 7.3 | 0.04 | 0.97 | 28 | 32 | 36 | | 27 |
| 50 | 5.2 | 0.03 | 0.77 | 27 | 31 | 37 | | 27 |

## Sortability Graph

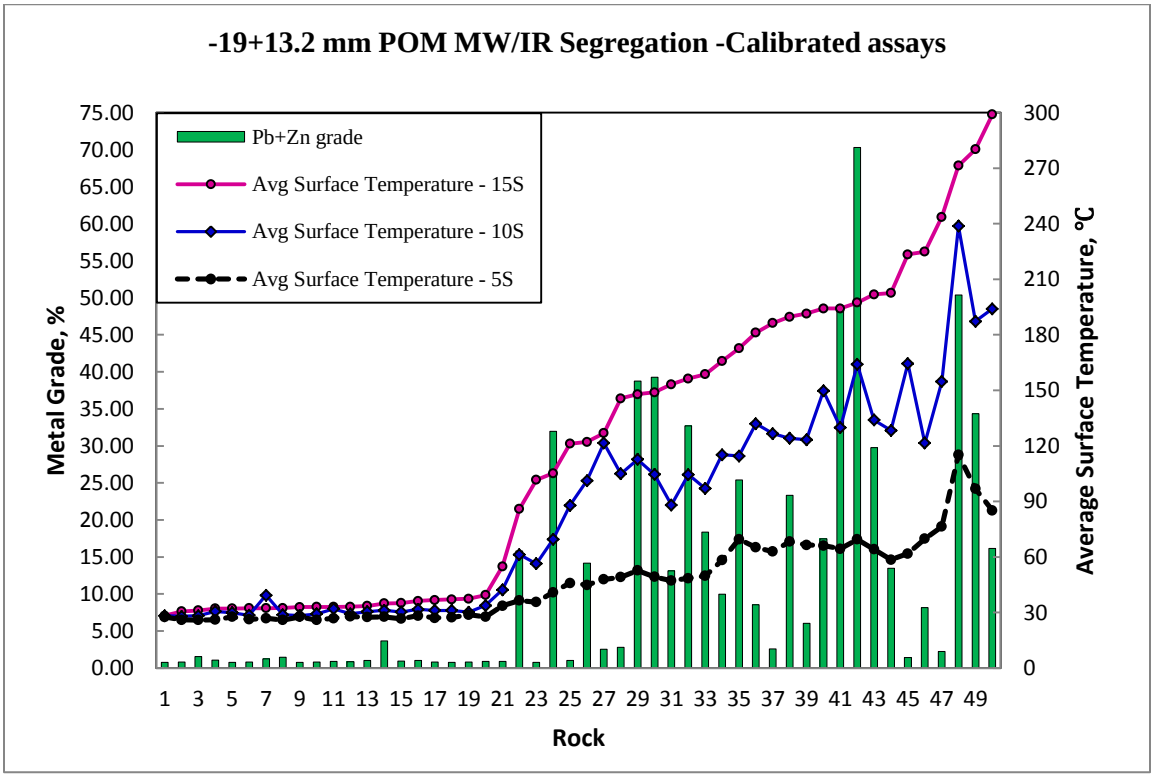


## Individual and Group Tests

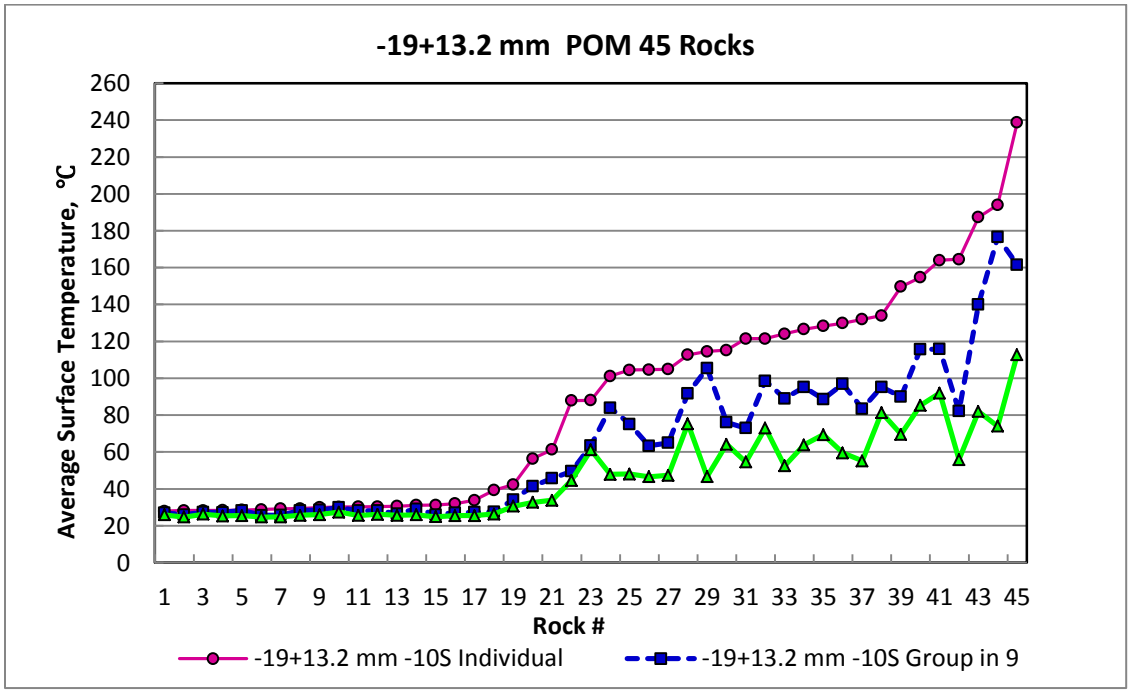

**-19+13.2 mm MW/IR Sorting Results – Individual- 5s (Calibrated XRF Surface Readings)**

| Separation Temperature, °C | Hot Fraction | Cold Fraction | Wt. % in Hot Fraction | | Wt. % in Cold Fraction | | % in Hot Fraction | | % in Cold Fraction | |
|---|---|---|---|---|---|---|---|---|---|---|
| | | | Concentrate Grades, % | | Waste Grades, % | | Metal Recovery, % | | Metal Recovery, % | |
| | Conc. % | Waste % | Pb | Zn | Pb | Zn | Pb | Zn | Pb | Zn |
| **26** | 87.9 | 12.1 | 4.73 | 8.17 | 0.05 | 0.95 | 99.8 | 98.4 | 0.2 | 1.6 |
| **27** | 78.6 | 21.4 | 5.28 | 9.04 | 0.05 | 0.92 | 99.8 | 97.3 | 0.2 | 2.7 |
| **28** | **64.4** | **35.6** | **6.44** | **10.73** | **0.04** | **1.08** | **99.7** | **94.7** | **0.3** | **5.3** |
| **40** | 58.4 | 41.6 | 7.10 | 11.41 | 0.04 | 1.53 | 99.6 | 91.3 | 0.4 | 8.7 |
| **45** | 53.5 | 46.5 | 7.68 | 10.79 | 0.11 | 3.28 | 98.8 | 79.1 | 1.2 | 20.9 |
| **47** | 49.3 | 50.7 | 8.33 | 11.04 | 0.11 | 3.67 | 98.7 | 74.5 | 1.4 | 25.5 |
| **50** | 38.1 | 61.9 | 8.33 | 11.66 | 1.60 | 4.62 | 76.3 | 60.9 | 23.7 | 39.1 |
| **60** | 31.0 | 69.0 | 9.21 | 10.83 | 1.89 | 5.71 | 68.6 | 46.0 | 31.4 | 54.0 |
| **65** | 18.0 | 82.0 | 11.93 | 10.83 | 2.46 | 6.53 | 51.6 | 26.7 | 48.4 | 73.3 |
| **70** | 6.3 | 93.7 | 9.77 | 16.04 | 3.79 | 6.72 | 14.7 | 13.7 | 85.3 | 86.3 |
| **Calculated Heat Grade : 4.16% Pb and 7.30% Zn** | | | | | | | | | | |

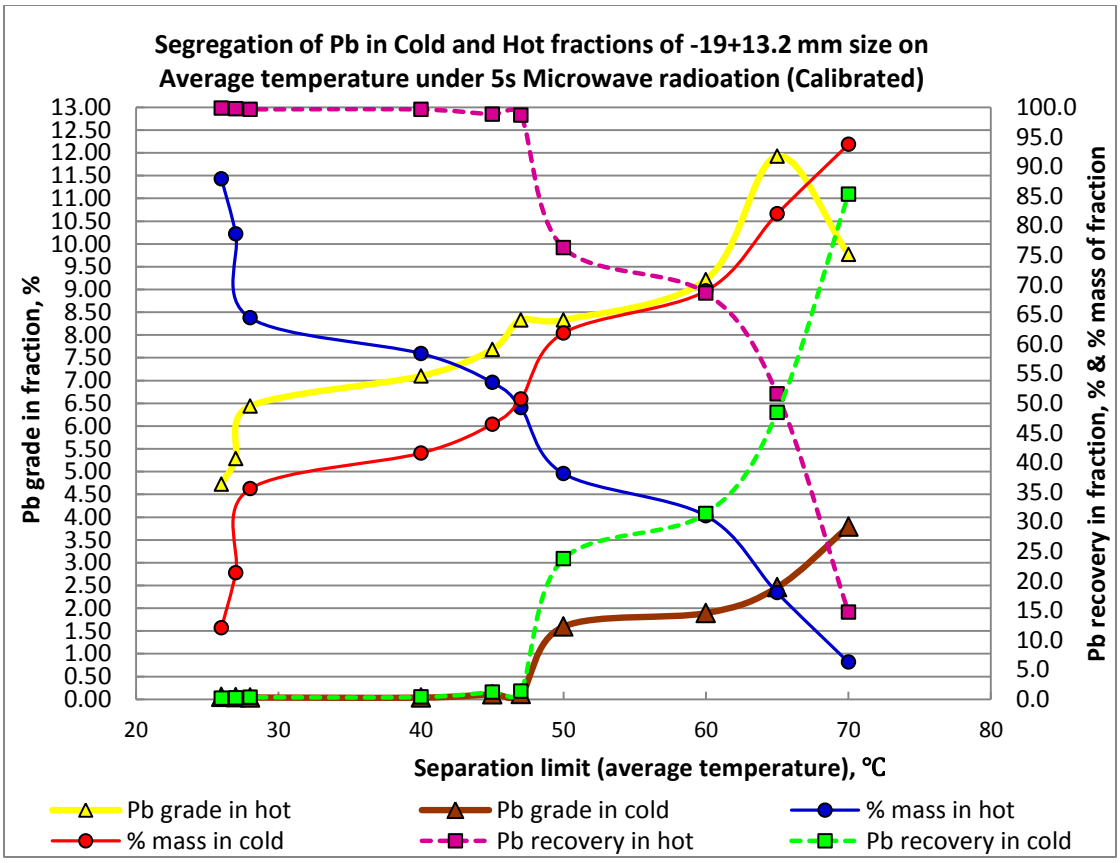
Segregation of Pb in Cold and Hot fractions of -19+13.2 mm size on Average temperature under 5s Microwave radioation (Calibrated)
Pb grade in fraction, %
Pb recovery in fraction, % & % mass of fraction
Separation limit (average temperature), ℃
Pb grade in hot
Pb grade in cold
% mass in hot
% mass in cold
Pb recovery in hot
Pb recovery in cold

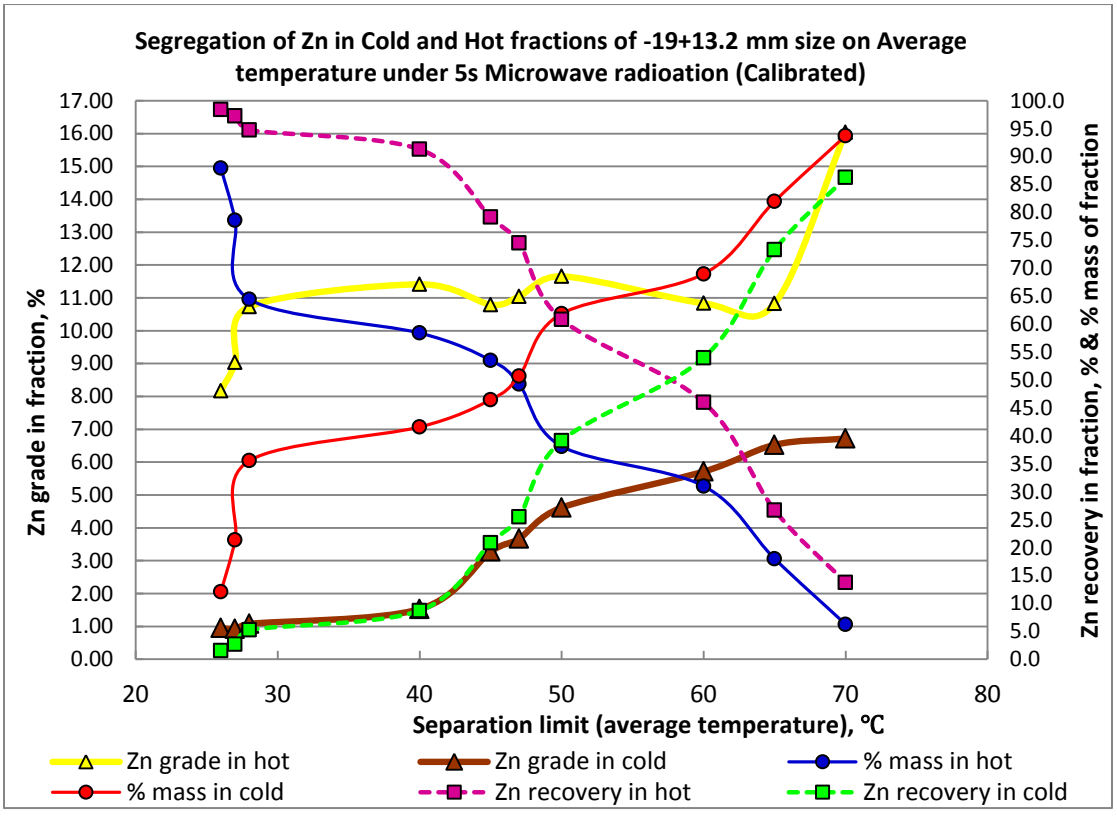
Segregation of Zn in Cold and Hot fractions of -19+13.2 mm size on Average temperature under 5s Microwave radioation (Calibrated)
Zn grade in fraction, %
Zn recovery in fraction, % & % mass of fraction
Separation limit (average temperature), ℃
Zn grade in hot
Zn grade in cold
% mass in hot
% mass in cold
Zn recovery in hot
Zn recovery in cold

**-19+13.2 mm MW/IR Sorting Results – Individual- 10s (Calibrated XRF Surface Readings)**

| Separation Temperature, °C | Hot Fraction | Cold Fraction | Wt. % in Hot Fraction | | Wt. % in Cold Fraction | | % in Hot Fraction | | % in Cold Fraction | |
|---|---|---|---|---|---|---|---|---|---|---|
| | | | Concentrate Grades, % | | Waste Grades, % | | Metal Recovery, % | | Metal Recovery, % | |
| | Conc. % | Waste % | Pb | Zn | Pb | Zn | Pb | Zn | Pb | Zn |
| **28** | 92.1 | 7.9 | 4.52 | 7.85 | 0.02 | 0.88 | 100.0 | 99.0 | 0.0 | 1.0 |
| **29** | 84.8 | 15.2 | 4.90 | 8.45 | 0.04 | 0.88 | 99.8 | 98.2 | 0.2 | 1.8 |
| **30** | 78.2 | 21.8 | 5.31 | 9.09 | 0.04 | 0.87 | 99.8 | 97.4 | 0.2 | 2.6 |
| **31** | **70.3** | **29.7** | **5.90** | **9.92** | **0.04** | **1.09** | **99.7** | **95.6** | **0.3** | **4.4** |
| **40** | **63.2** | **36.8** | **6.56** | **10.93** | **0.04** | **1.07** | **99.7** | **94.6** | **0.3** | **5.4** |
| **60** | 61.5 | 38.5 | 6.94 | 11.51 | 0.04 | 1.05 | 99.6 | 94.2 | 0.4 | 5.8 |
| **70** | 57.1 | 42.9 | 7.22 | 10.99 | 0.10 | 2.39 | 99.0 | 86.0 | 1.0 | 14.0 |
| **100** | 51.2 | 48.8 | 8.00 | 11.03 | 0.13 | 3.38 | 98.5 | 77.4 | 1.5 | 22.6 |
| **105** | 40.9 | 59.1 | 7.84 | 10.96 | 1.62 | 4.77 | 77.0 | 61.4 | 23.0 | 38.6 |
| **125** | 23.2 | 76.8 | 9.14 | 12.55 | 2.66 | 5.72 | 50.8 | 39.8 | 49.2 | 60.2 |
| **130** | 16.6 | 83.4 | 9.49 | 12.64 | 3.10 | 6.24 | 37.9 | 28.8 | 62.1 | 71.2 |
| **155** | 8.5 | 91.5 | 13.24 | 16.10 | 3.32 | 6.48 | 27.0 | 18.7 | 73.0 | 81.3 |
| **Calculated Heat Grade : 4.16% Pb and 7.30% Zn** | | | | | | | | | | |

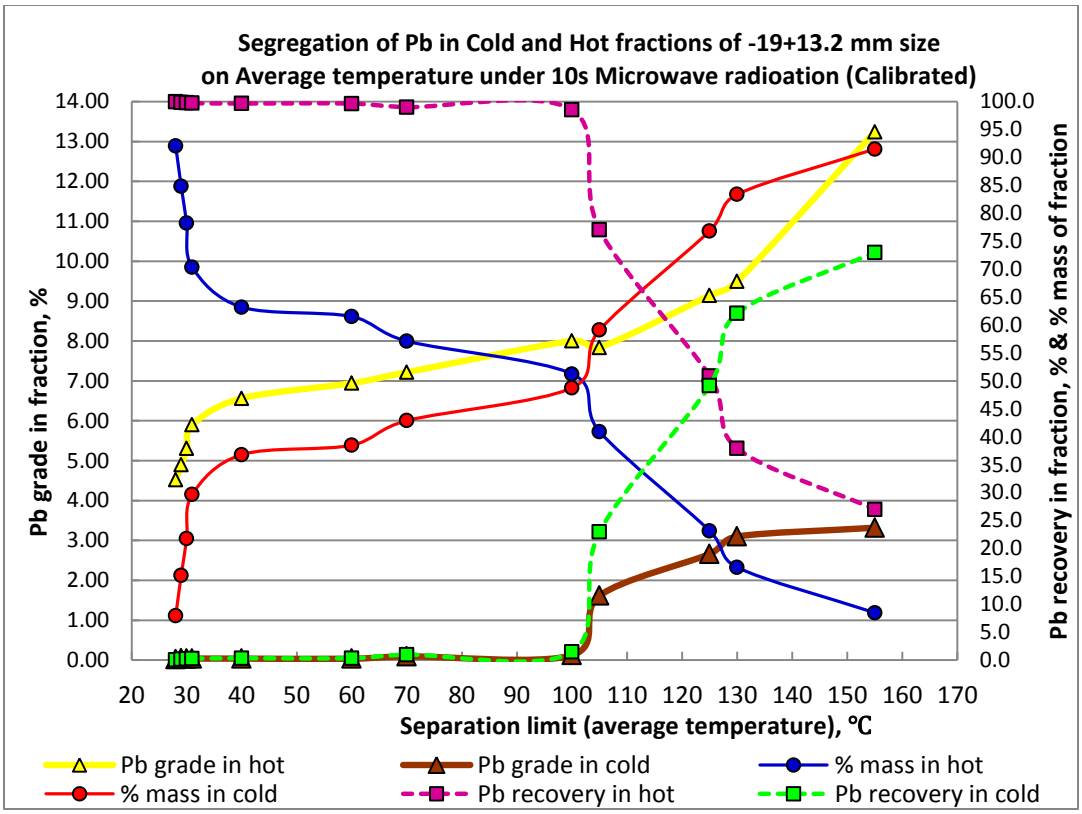
Segregation of Pb in Cold and Hot fractions of -19+13.2 mm size
on Average temperature under 10s Microwave radioation (Calibrated)
Pb grade in fraction, %
Pb recovery in fraction, % & % mass of fraction
Separation limit (average temperature), ℃
Pb grade in hot
Pb grade in cold
% mass in hot
% mass in cold
Pb recovery in hot
Pb recovery in cold

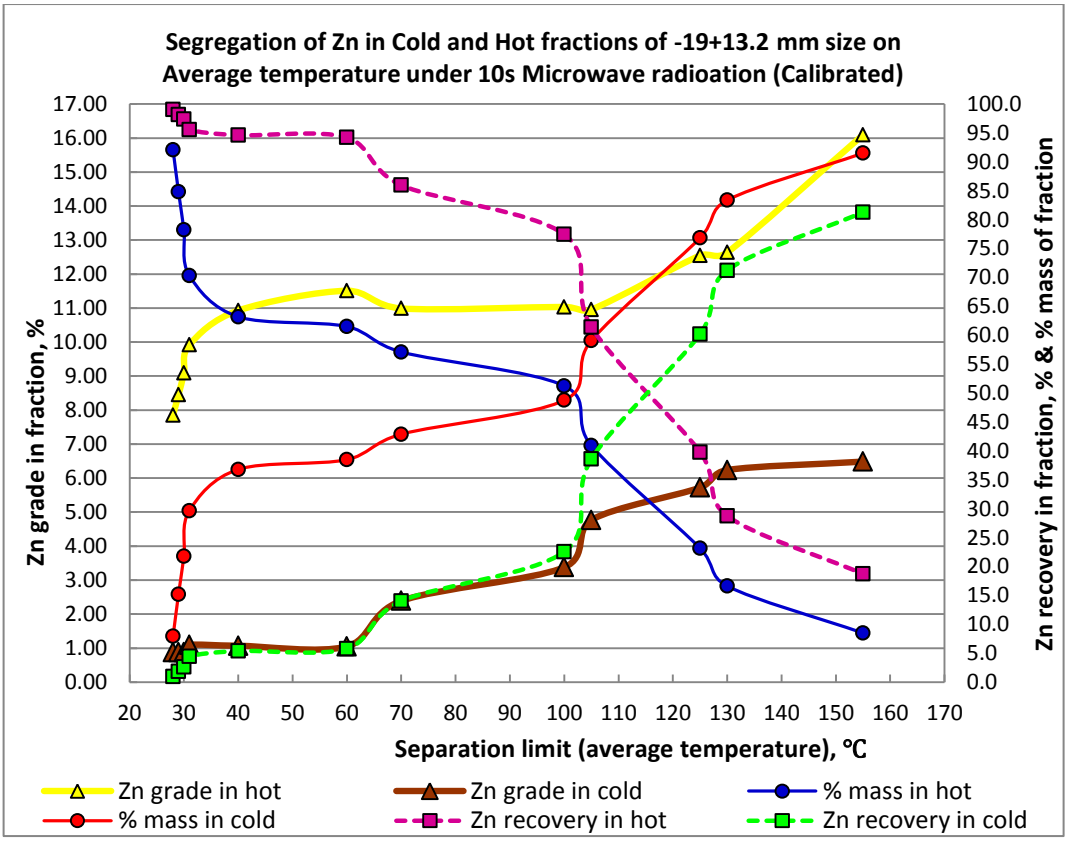
Segregation of Zn in Cold and Hot fractions of -19+13.2 mm size on
Average temperature under 10s Microwave radioation (Calibrated)
Zn grade in fraction, %
Zn recovery in fraction, % & % mass of fraction
Separation limit (average temperature), ℃
Zn grade in hot
Zn grade in cold
% mass in hot
% mass in cold
Zn recovery in hot
Zn recovery in cold

**-19+13.2 mm MW/IR Sorting Results – Individual- 15s (Calibrated XRF Surface Readings)**

| Separation Temperature, °C | Hot Fraction | Cold Fraction | Wt. % in Hot Fraction | | Wt. % in Cold Fraction | | % in Hot Fraction | | % in Cold Fraction | |
|---|---|---|---|---|---|---|---|---|---|---|
| | | | Concentrate Grades, % | | Waste Grades, % | | Metal Recovery, % | | Metal Recovery, % | |
| | Conc. % | Waste % | Pb | Zn | Pb | Zn | Pb | Zn | Pb | Zn |
| **31** | 94.0 | 6.0 | 4.43 | 7.71 | 0.02 | 0.92 | 100.0 | 99.2 | 0.0 | 0.8 |
| **32** | 84.8 | 15.2 | 4.90 | 8.44 | 0.04 | 0.96 | 99.8 | 98.0 | 0.2 | 2.0 |
| **33** | 77.6 | 22.4 | 5.35 | 9.14 | 0.04 | 0.90 | 99.8 | 97.2 | 0.2 | 2.8 |
| **36** | **69.4** | **30.6** | **5.98** | **10.02** | **0.04** | **1.13** | **99.7** | **95.3** | **0.3** | **4.7** |
| **50** | **63.2** | **36.8** | **6.56** | **10.93** | **0.04** | **1.07** | **99.7** | **94.6** | **0.3** | **5.4** |
| **100** | 60.6 | 39.4 | 6.98 | 11.23 | 0.04 | 1.55 | 99.6 | 91.4 | 0.4 | 8.6 |
| **120** | 57.1 | 42.9 | 7.22 | 10.99 | 0.10 | 2.39 | 99.0 | 86.0 | 1.0 | 14.0 |
| **150** | 42.1 | 57.9 | 8.67 | 10.47 | 0.89 | 5.00 | 87.6 | 60.3 | 12.4 | 39.7 |
| **170** | 32.2 | 67.8 | 9.22 | 10.58 | 1.97 | 6.44 | 71.4 | 46.7 | 28.6 | 53.3 |
| **190** | 21.7 | 78.3 | 8.93 | 14.20 | 2.84 | 5.39 | 46.5 | 42.1 | 53.5 | 57.9 |
| **200** | 14.6 | 85.4 | 5.49 | 12.72 | 3.94 | 6.37 | 19.3 | 25.5 | 80.7 | 74.5 |
| **250** | 5.0 | 95.0 | 11.92 | 19.88 | 3.76 | 6.64 | 14.3 | 13.6 | 85.7 | 86.4 |
| **Calculated Heat Grade : 4.16% Pb and 7.30% Zn** | | | | | | | | | | |

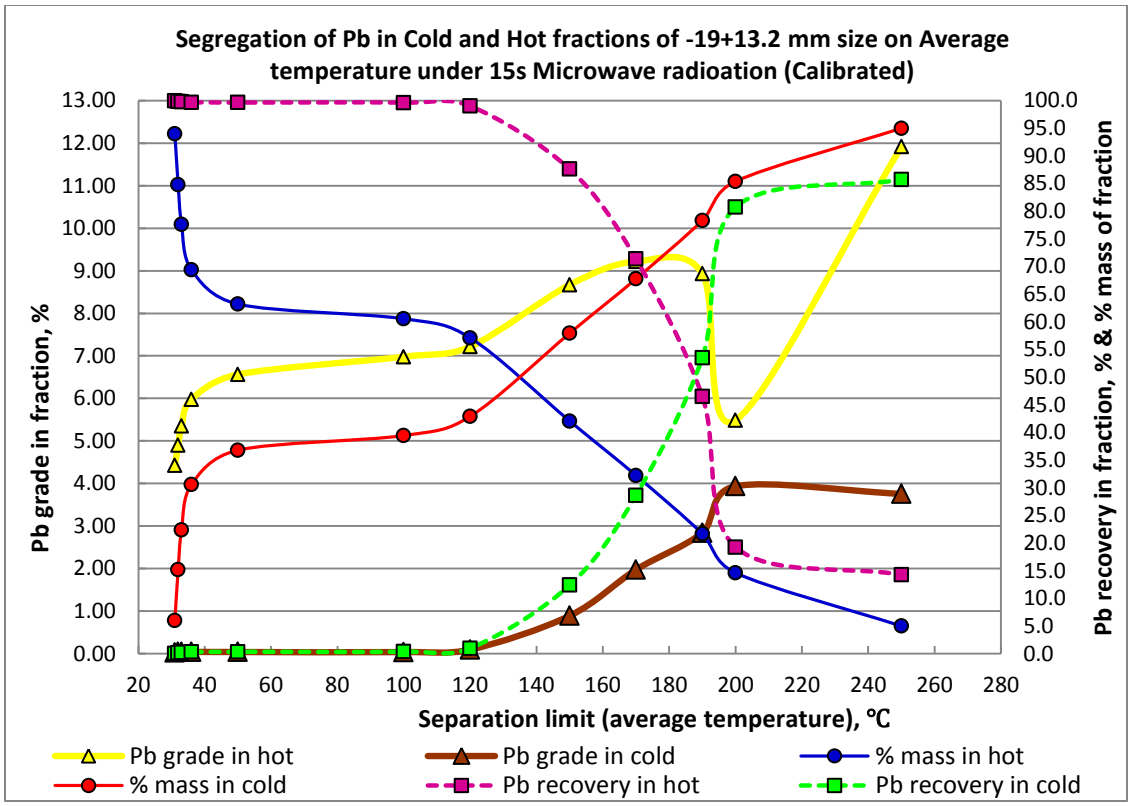
Segregation of Pb in Cold and Hot fractions of -19+13.2 mm size on Average temperature under 15s Microwave radioation (Calibrated)
Pb grade in fraction, %
Pb recovery in fraction, % & % mass of fraction
Separation limit (average temperature), ℃
Pb grade in hot
Pb grade in cold
% mass in hot
% mass in cold
Pb recovery in hot
Pb recovery in cold

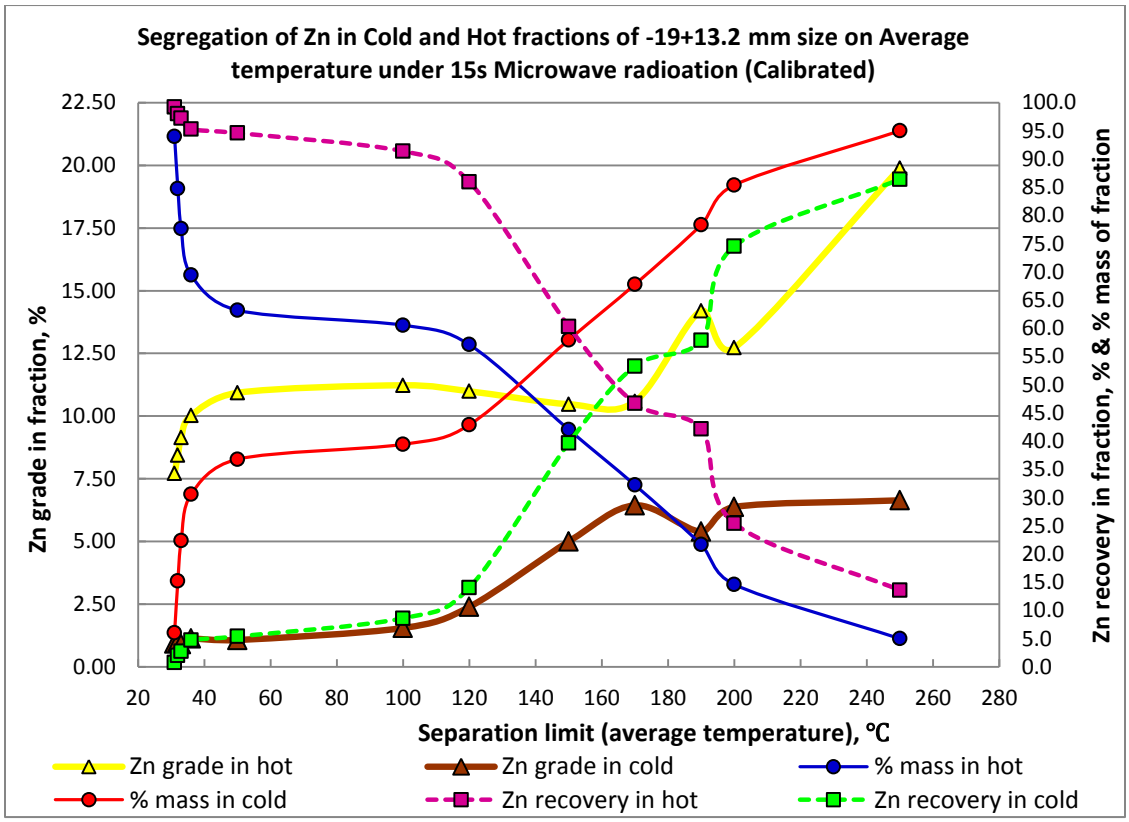
Segregation of Zn in Cold and Hot fractions of -19+13.2 mm size on Average temperature under 15s Microwave radioation (Calibrated)
Zn grade in fraction, %
Zn recovery in fraction, % & % mass of fraction
Separation limit (average temperature), ℃
Zn grade in hot
Zn grade in cold
% mass in hot
% mass in cold
Zn recovery in hot
Zn recovery in cold

**-19+13.2 mm MW/IR Sorting Results – Individual- 10s -45 rocks (Calibrated XRF Surface Readings)**

| Separation Temperature, °C | Hot Fraction | Cold Fraction | Wt. % in Hot Fraction | | Wt. % in Cold Fraction | | % in Hot Fraction | | % in Cold Fraction | |
|---|---|---|---|---|---|---|---|---|---|---|
| | | | Concentrate Grades, % | | Waste Grades, % | | Metal Recovery, % | | Metal Recovery, % | |
| | Conc. % | Waste % | Pb | Zn | Pb | Zn | Pb | Zn | Pb | Zn |
| **28** | 91.3 | 8.7 | 4.88 | 7.71 | 0.02 | 0.88 | 100.0 | 98.9 | 0.0 | 1.1 |
| **29** | 83.4 | 16.6 | 5.33 | 8.36 | 0.04 | 0.88 | 99.8 | 98.0 | 0.2 | 2.0 |
| **30** | 76.2 | 23.8 | 5.83 | 9.07 | 0.04 | 0.87 | 99.8 | 97.1 | 0.2 | 2.9 |
| **31** | 69.2 | 30.8 | 6.43 | 9.80 | 0.04 | 1.11 | 99.7 | 95.2 | 0.3 | 4.8 |
| **40** | **63.6** | **36.4** | **6.99** | **10.58** | **0.04** | **1.09** | **99.7** | **94.4** | **0.3** | **5.6** |
| **60** | **61.7** | **38.3** | **7.43** | **11.19** | **0.04** | **1.07** | **99.7** | **94.0** | **0.3** | **6.0** |
| **70** | 58.3 | 41.7 | 7.62 | 11.07 | 0.04 | 1.59 | 99.7 | 90.7 | 0.3 | 9.3 |
| **100** | 53.7 | 46.3 | 8.26 | 11.34 | 0.05 | 2.22 | 99.5 | 85.5 | 0.5 | 14.5 |
| **105** | 42.4 | 57.6 | 8.15 | 11.34 | 1.74 | 4.01 | 77.5 | 67.5 | 22.5 | 32.5 |
| **125** | 25.3 | 74.7 | 9.14 | 12.55 | 2.87 | 5.28 | 51.9 | 44.6 | 48.1 | 55.4 |
| **130** | 18.2 | 81.8 | 9.49 | 12.64 | 3.34 | 5.89 | 38.7 | 32.2 | 61.3 | 67.8 |
| **155** | 9.3 | 90.7 | 13.24 | 16.10 | 3.56 | 6.20 | 27.6 | 21.0 | 72.4 | 79.0 |
| **Calculated Heat Grade : 4.46% Pb and 7.12% Zn** | | | | | | | | | | |

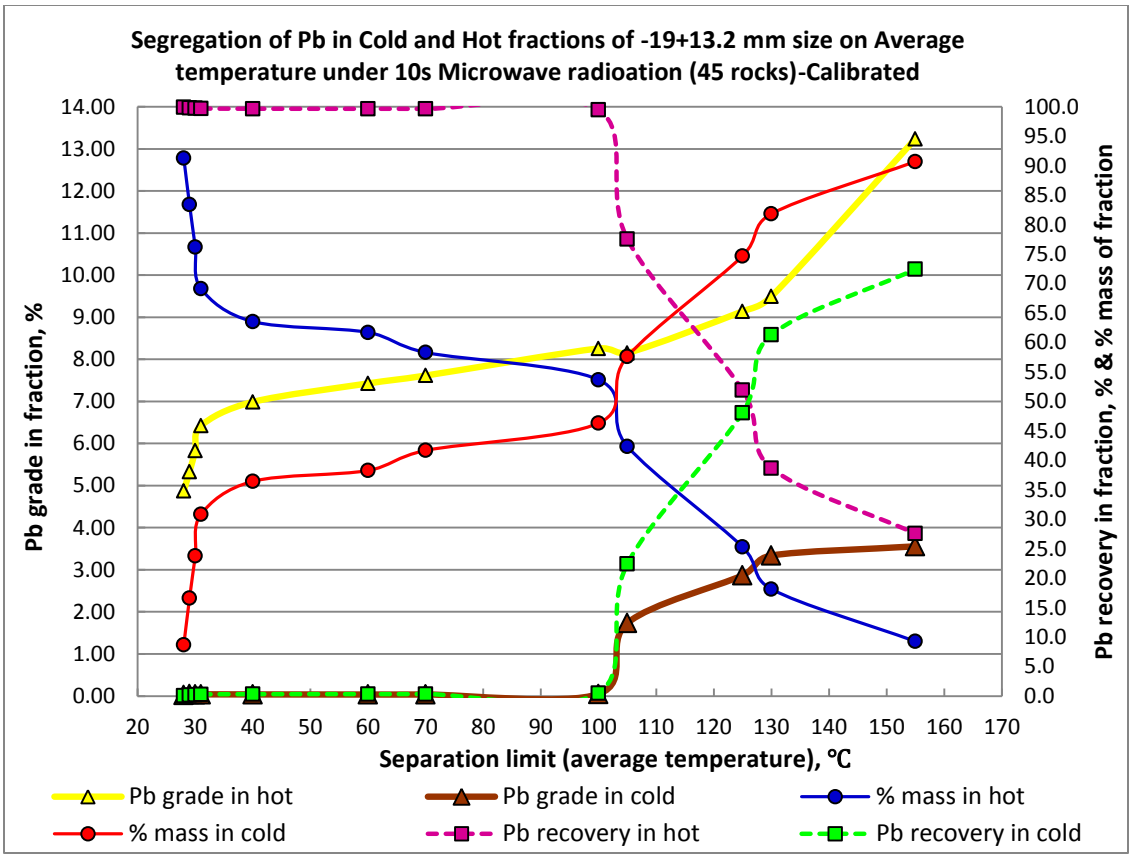
Segregation of Pb in Cold and Hot fractions of -19+13.2 mm size on Average temperature under 10s Microwave radioation (45 rocks)-Calibrated
Pb grade in fraction, %
Pb recovery in fraction, % & % mass of fraction
Separation limit (average temperature), ℃
Pb grade in hot
Pb grade in cold
% mass in hot
% mass in cold
Pb recovery in hot
Pb recovery in cold

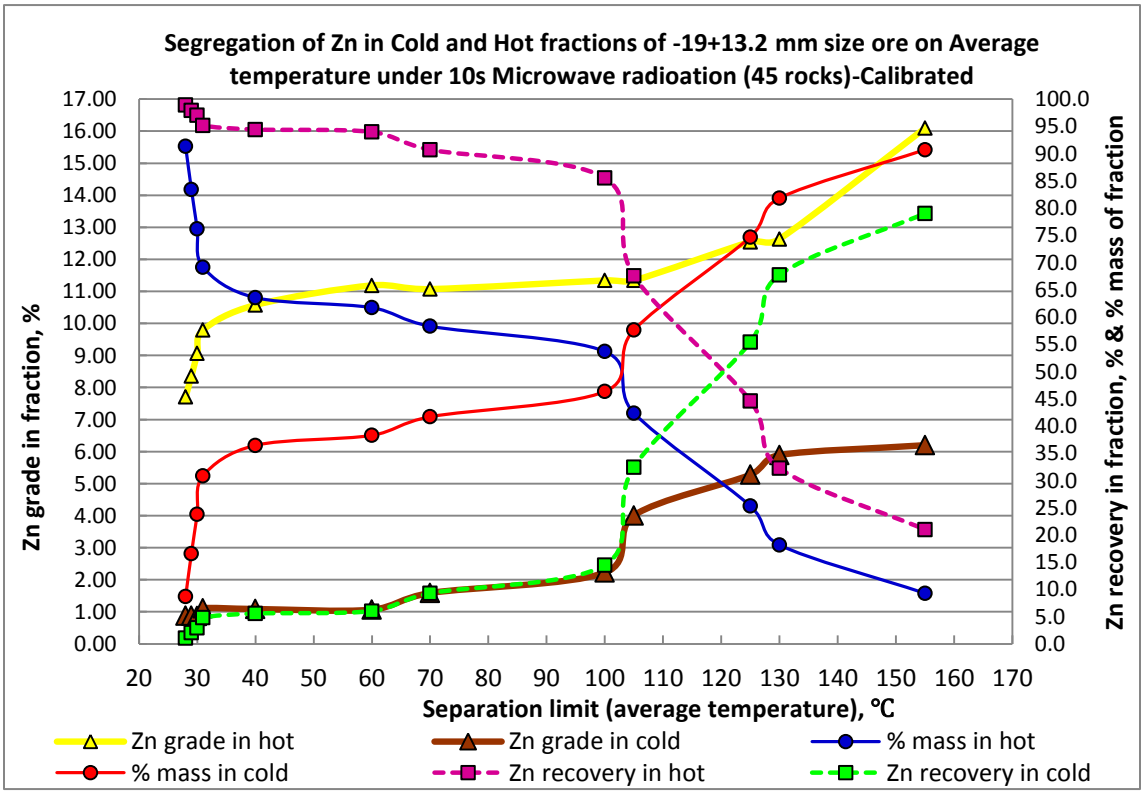
Segregation of Zn in Cold and Hot fractions of -19+13.2 mm size ore on Average temperature under 10s Microwave radioation (45 rocks)-Calibrated
Zn grade in fraction, %
Zn recovery in fraction, % & % mass of fraction
Separation limit (average temperature), ℃
Zn grade in hot
Zn grade in cold
% mass in hot
% mass in cold
Zn recovery in hot
Zn recovery in cold

**-19+13.2 mm MW/IR Sorting Results – Group in 9- 10s -45 rocks (Calibrated XRF Surface Readings)**

| Separation Temperature, °C | Hot Fraction | Cold Fraction | Wt. % in Hot Fraction | | Wt. % in Cold Fraction | | % in Hot Fraction | | % in Cold Fraction | |
|---|---|---|---|---|---|---|---|---|---|---|
| | | | Concentrate Grades, % | | Waste Grades, % | | Metal Recovery, % | | Metal Recovery, % | |
| | Conc. % | Waste % | Pb | Zn | Pb | Zn | Pb | Zn | Pb | Zn |
| **26** | 92.5 | 7.5 | 4.81 | 7.53 | 0.06 | 2.01 | 99.9 | 97.9 | 0.1 | 2.1 |
| **27** | 79.2 | 20.8 | 5.62 | 8.66 | 0.04 | 1.26 | 99.8 | 96.3 | 0.2 | 3.7 |
| **28** | **68.9** | **31.1** | **6.45** | **9.82** | **0.04** | **1.14** | **99.7** | **95.0** | **0.3** | **5.0** |
| **30** | **63.6** | **36.4** | **6.99** | **10.58** | **0.04** | **1.09** | **99.7** | **94.4** | **0.3** | **5.6** |
| **50** | 57.2 | 42.8 | 7.87 | 11.42 | 0.04 | 1.55 | 99.6 | 90.5 | 0.4 | 9.5 |
| **70** | 48.6 | 51.4 | 8.54 | 11.15 | 0.60 | 3.30 | 93.1 | 76.1 | 6.9 | 23.9 |
| **80** | 39.3 | 60.7 | 8.63 | 12.61 | 1.75 | 3.56 | 76.1 | 69.6 | 23.9 | 30.4 |
| **85** | 29.2 | 70.8 | 10.74 | 14.71 | 1.86 | 3.98 | 70.5 | 60.4 | 29.5 | 39.6 |
| **90** | 23.5 | 76.5 | 9.49 | 17.42 | 2.91 | 3.95 | 50.1 | 57.6 | 49.9 | 42.4 |
| **100** | 9.9 | 90.1 | 15.20 | 16.62 | 3.27 | 6.07 | 33.8 | 23.1 | 66.2 | 76.9 |
| **120** | 5.5 | 94.5 | 11.92 | 19.88 | 4.03 | 6.38 | 14.6 | 15.2 | 85.4 | 84.8 |
| **Calculated Heat Grade : 4.46% Pb and 7.12% Zn** | | | | | | | | | | |

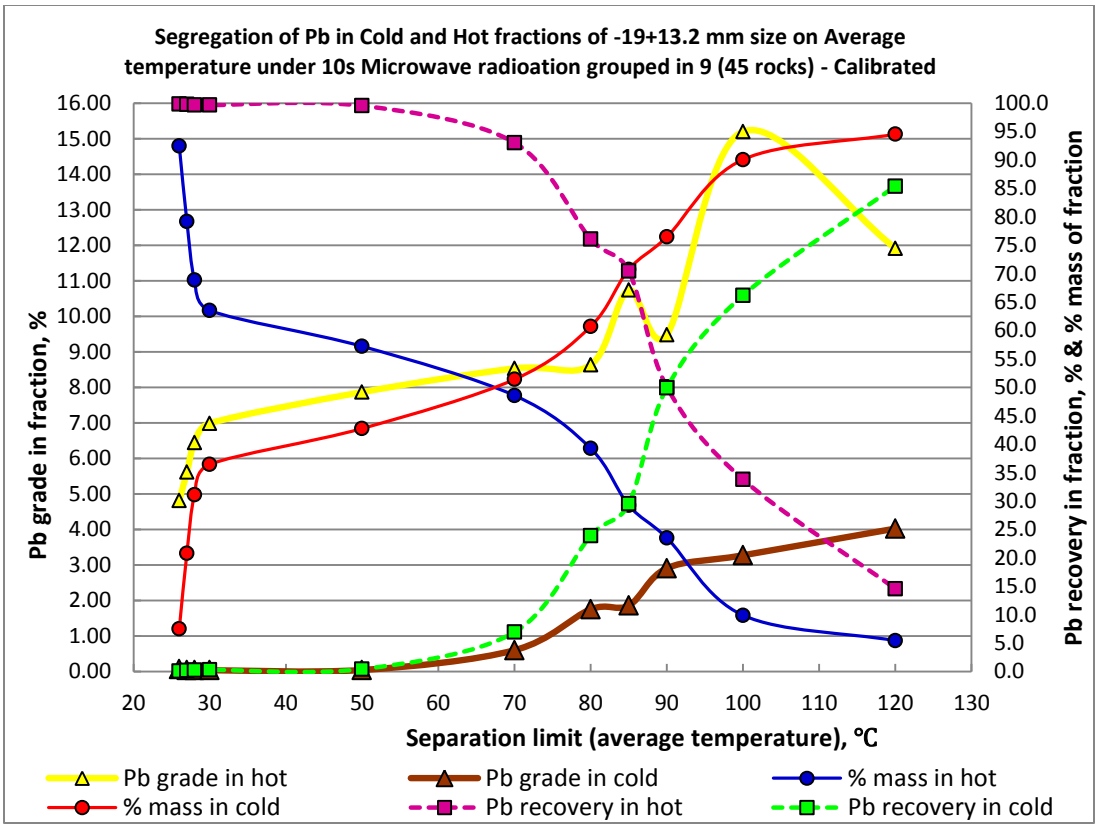
Segregation of Pb in Cold and Hot fractions of -19+13.2 mm size on Average temperature under 10s Microwave radioation grouped in 9 (45 rocks) - Calibrated
Pb grade in fraction, %
Pb recovery in fraction, % & % mass of fraction
Separation limit (average temperature), ℃
Pb grade in hot
Pb grade in cold
% mass in hot
% mass in cold
Pb recovery in hot
Pb recovery in cold

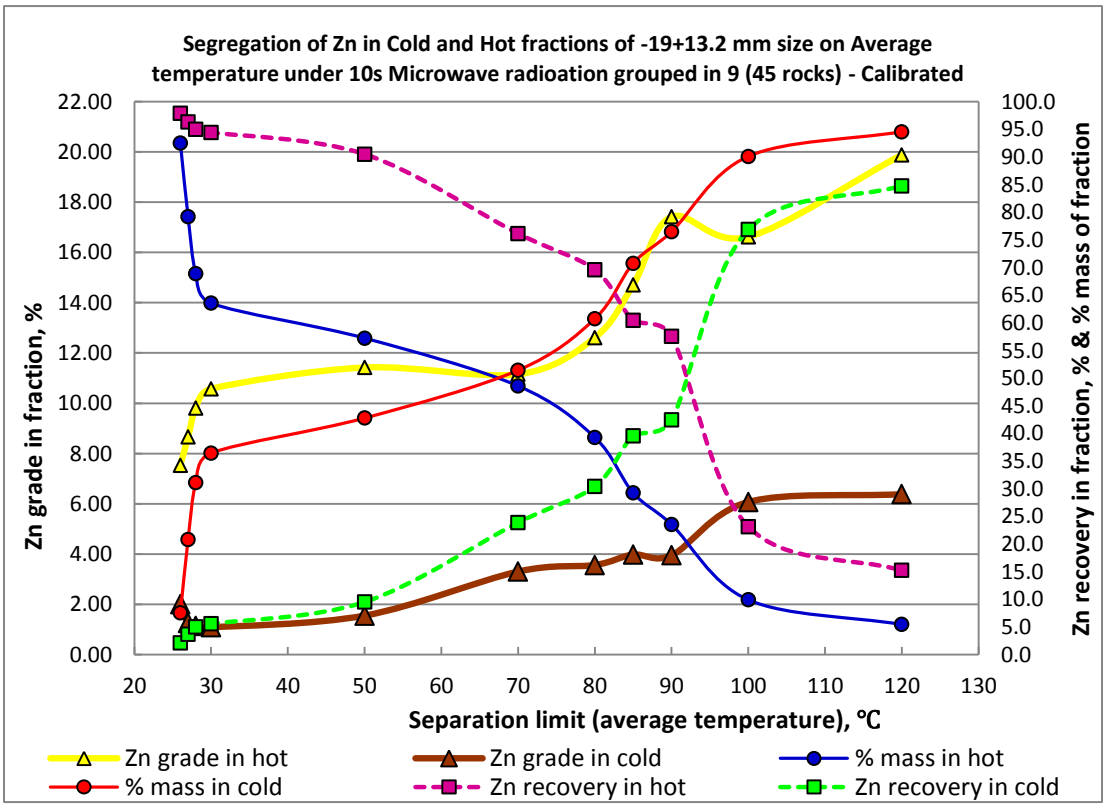
Segregation of Zn in Cold and Hot fractions of -19+13.2 mm size on Average temperature under 10s Microwave radioation grouped in 9 (45 rocks) - Calibrated
Zn grade in fraction, %
Zn recovery in fraction, % & % mass of fraction
Separation limit (average temperature), ℃
Zn grade in hot
Zn grade in cold
% mass in hot
% mass in cold
Zn recovery in hot
Zn recovery in cold

**-19+13.2 mm MW/IR Sorting Results – Group in 25- 10s -45 rocks (Calibrated XRF Surface Readings)**

| Separation Temperature, °C | Hot Fraction | Cold Fraction | Wt. % in Hot Fraction | | Wt. % in Cold Fraction | | % in Hot Fraction | | % in Cold Fraction | |
|---|---|---|---|---|---|---|---|---|---|---|
| | | | Concentrate Grades, % | | Waste Grades,% | | Metal Recovery, % | | Metal Recovery, % | |
| | Conc. % | Waste % | Pb | Zn | Pb | Zn | Pb | Zn | Pb | Zn |
| **25** | 90.4 | 9.6 | 4.93 | 7.69 | 0.05 | 1.73 | 99.9 | 97.7 | 0.1 | 2.3 |
| **26** | **64.9** | **35.1** | **6.84** | **10.37** | **0.04** | **1.10** | **99.7** | **94.6** | **0.3** | **5.4** |
| **35** | 58.3 | 41.7 | 7.62 | 11.07 | 0.04 | 1.59 | 99.7 | 90.7 | 0.3 | 9.3 |
| **50** | 43.4 | 56.6 | 7.36 | 11.51 | 2.24 | 3.75 | 71.3 | 73.0 | 28.7 | 27.0 |
| **60** | 28.9 | 71.1 | 6.43 | 13.95 | 3.65 | 4.34 | 41.7 | 56.7 | 58.3 | 43.3 |
| **70** | 16.0 | 84.0 | 9.37 | 19.42 | 3.52 | 4.78 | 33.6 | 43.6 | 66.4 | 56.4 |
| **80** | 8.3 | 91.7 | 13.60 | 23.01 | 3.62 | 5.67 | 25.2 | 29.0 | 74.8 | 71.0 |
| **90** | 2.9 | 97.1 | 32.84 | 26.78 | 3.60 | 6.53 | 21.5 | 11.0 | 78.5 | 89.0 |
| **Calculated Heat Grade : 4.46% Pb and 7.12% Zn** | | | | | | | | | | |

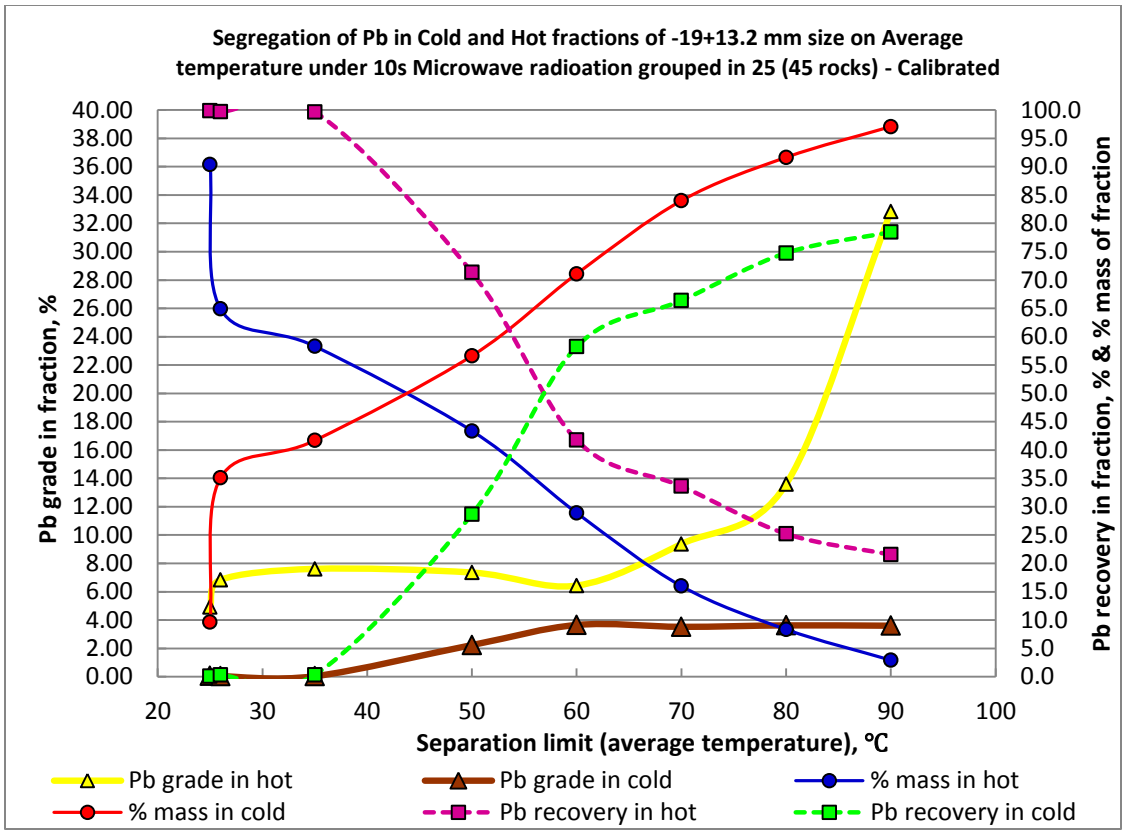
Segregation of Pb in Cold and Hot fractions of -19+13.2 mm size on Average temperature under 10s Microwave radioation grouped in 25 (45 rocks) - Calibrated
Pb grade in fraction, %
Pb recovery in fraction, % & % mass of fraction
Separation limit (average temperature), ℃
Pb grade in hot
Pb grade in cold
% mass in hot
% mass in cold
Pb recovery in hot
Pb recovery in cold

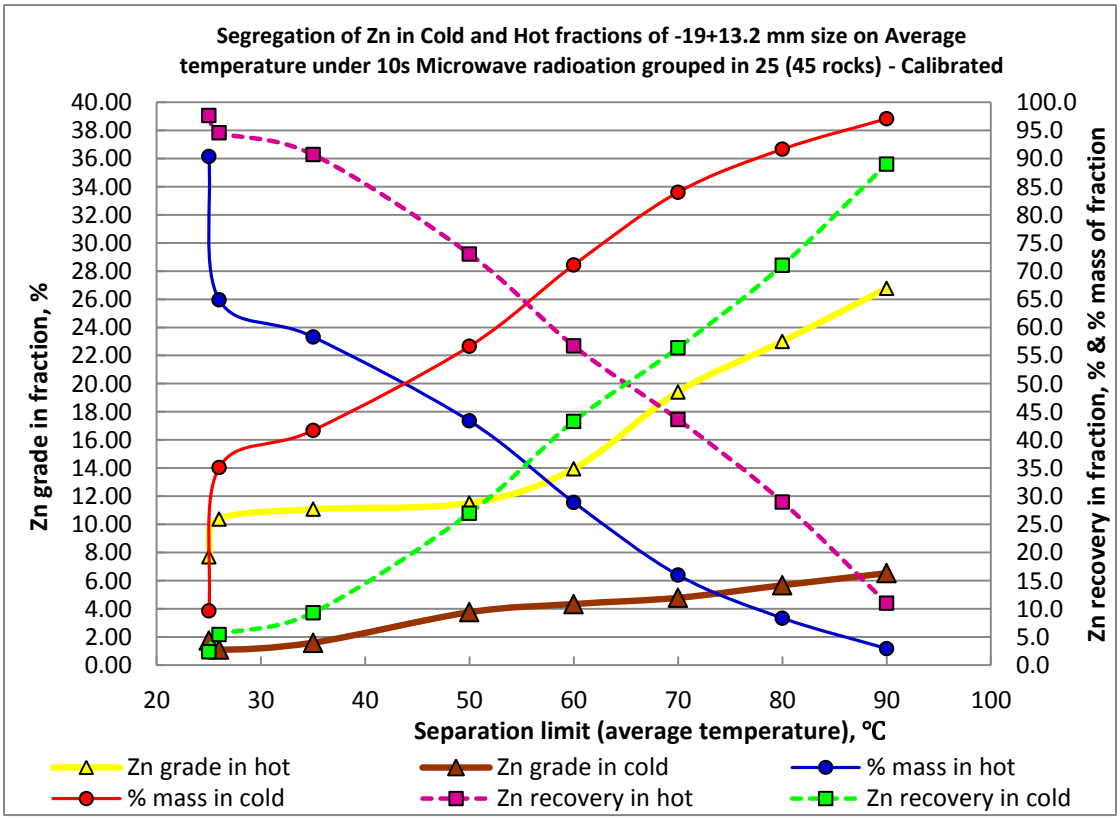
Segregation of Zn in Cold and Hot fractions of -19+13.2 mm size on Average temperature under 10s Microwave radioation grouped in 25 (45 rocks) - Calibrated
Zn grade in fraction, %
Zn recovery in fraction, % & % mass of fraction
Separation limit (average temperature), ℃
Zn grade in hot
Zn grade in cold
% mass in hot
% mass in cold
Zn recovery in hot
Zn recovery in cold

**-19+13.2 mm Size Fraction Sorting Results Summary**

| Test Condition | Separation Limit, °C | Mass % of Cold | Pb in Hot Fraction, % | | Zn in Hot Fraction, % | |
|---|---|---|---|---|---|---|
| | | | Grade | Recovery | Grade | Recovery |
| 5s | 27 | 21.4 | 5.28 | 99.8 | 9.04 | 97.3 |
| 5s | 28 | 35.6 | 6.44 | 99.7 | 10.73 | 94.7 |
| 10s | 31 | 29.7 | 5.90 | 99.7 | 9.92 | 95.6 |
| 10s | 40 | 36.8 | 6.56 | 99.7 | 10.93 | 94.6 |
| 15s | 36 | 30.6 | 5.98 | 99.7 | 10.02 | 95.3 |
| 15s | 50(40) | 36.8 | 6.56 | 99.7 | 10.93 | 94.6 |
| Calculated Heat Grade : 4.16% Pb and 7.30% Zn 50 rocks being tested | | | | | | |
| **Test Condition** | **Separation Limit, °C** | **Mass % of Cold** | **Pb in Hot Fraction, %** | | **Zn in Hot Fraction, %** | |
| | | | **Grade** | **Recovery** | **Grade** | **Recovery** |
| Individual | 31 | 30.8 | 6.43 | 99.7 | 9.80 | 95.2 |
| Individual | 40 | 36.4 | 6.99 | 99.7 | 10.58 | 94.4 |
| Group in 9 | 28 | 31.1 | 6.45 | 99.7 | 9.82 | 95.0 |
| Group in 9 | 30 | 36.4 | 6.99 | 99.7 | 10.58 | 94.4 |
| Group in 25 | 26 | 35.1 | 6.84 | 99.7 | 10.37 | 94.6 |
| Calculated Heat Grade : 4.46% Pb and 7.12% Zn 45 rocks being tested | | | | | | |

## APPENDIX E IMPACT EVALUATION DATA

### Full Bond Ball Mill Work Index Test

| | | | | |
|---|---|---|---|---|
| Bond Test #: | **POM BW** | Aperture Test Sieve: | **180** | microns |
| Project: | MASc Research Thesis | Test Feed Density: | **3.60** | g/cc |
| Date: | 2-Mar-12 | Undersize in the Test Feed: | **12.70** | % |
| Performed by: | Yan Tong | Mill Solid Load: | **1524.7** | g |
| Ore Type | Lead-Zinc massive sulfide | Ideal Potential Product: | **435.6** | g |
| Sample Source: | Pend Oreille Mine | Ideal Circulating Load: | **1089.1** | g |

| Cycle | Test Feed Added | Number of Revs. | Weight of Oversize | Weight of Undersize | | | | |
|---|---|---|---|---|---|---|---|---|
| | | | | Feed | Discharge | Net Product | Net / Rec | Circulating Load Ratio |
| 1 | 1524.7 | 100 | 907.0 | 193.6 | 617.7 | 424.1 | 4.24 | 147 |
| 2 | 617.7 | 84 | 1161.6 | 78.4 | 363.1 | 284.7 | 3.38 | 320 |
| 3 | 363.1 | 115 | 1073.3 | 46.1 | 451.4 | 405.3 | 3.52 | 238 |
| 4 | 451.4 | 108 | 1099.3 | 57.3 | 425.4 | 368.1 | 3.42 | 258 |
| 5 | 425.4 | 112 | 1090.0 | 54.0 | 434.7 | 380.7 | 3.41 | 251 |
| 6 | 434.7 | 111 | 1089.0 | 55.2 | 435.7 | 380.5 | 3.41 | 250 |
| 7 | 435.7 | 111 | 1089.0 | 55.3 | 435.7 | 380.4 | 3.41 | 250 |

**BOND'S WORK INDEX FORMULA**

$$Wi = 44.5 / (Pi^{.23} \times Gpb^{.82} \times (10/\sqrt{P} - 10/\sqrt{F}))$$

| | | | | |
|---|---|---|---|---|
| Pi = Sieve size tested | 180 | microns | WORK INDEX (Wi) | |
| Gpb = Net Undersize produced per revolution of mill | 3.41 | grams | **7.57** | kw-hr/ton |
| P = 80% passing size of test prodcut | 136 | microns | **8.33** | kw-hr/tonne |
| F = 80% passing size of test feed | 2338 | microns | | |

NB: Gbp = Average of last 3 Net/Rev Cycles

## Bond Ball Mill Grindability Test Size Analysis

| | | Feed | | Product | |
|---|---|---|---|---|---|
| Sieve [mesh] | Size [microns] | Weight [g] | Cum. Passing [%] | Weight [g] | Cum. Passing [%] |
| 7 | 2800 | 0.0 | 100.0 | | |
| 10 | 2000 | 76.6 | 65.4 | | |
| 14 | 1400 | 41.3 | 46.7 | | |
| 18 | 1000 | 22.7 | 36.4 | | |
| 25 | 710 | 16.5 | 29.0 | | |
| 35 | 500 | 12.5 | 23.3 | | |
| 45 | 355 | 9.3 | 19.1 | | |
| 60 | 250 | 8.0 | 15.5 | | |
| 80 | 180 | 6.2 | 12.7 | 0.0 | 100.0 |
| 120 | 125 | 6.1 | 9.9 | 212.8 | 75.0 |
| 170 | 90 | 5.0 | 7.7 | 175.5 | 54.4 |
| 230 | 63 | 4.9 | 5.5 | 121.3 | 40.1 |
| 325 | 45 | 3.8 | 3.8 | 118.0 | 26.3 |
| | -45 | 8.3 | 0.0 | 223.8 | 0.0 |
| Total mass | | 221.2 | | 851.4 | |

**Interpolations**

| | | Feed | | Product | |
|---|---|---|---|---|---|
| Linear | 50 | P50= | 1506.1 | F50= | 81.7 |
| Linear | 80 | P80= | **2338.0** | F80= | **136.0** |
| Semi-log | 50 | P50= | 1491.1 | P50= | 80.6 |
| Semi-log | 80 | P80= | **2305.5** | P80= | **134.4** |
| Log-log | 50 | P50= | 1505.1 | P50= | 81.5 |
| Log-log | 80 | P80= | **2346.7** | P80= | **135.6** |

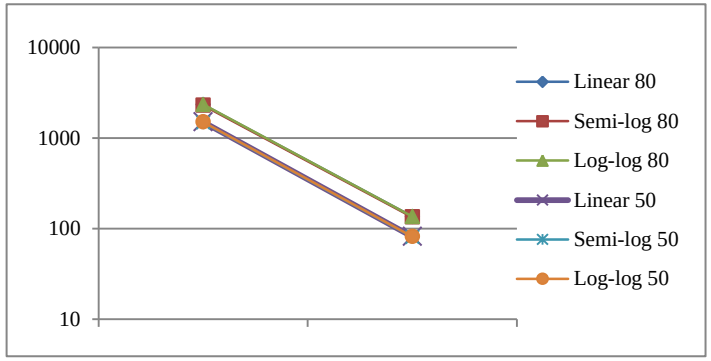


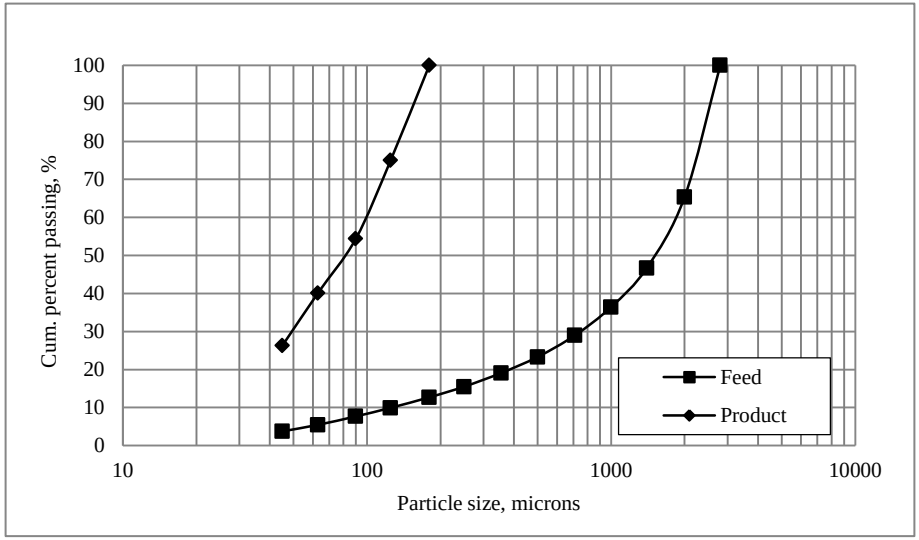

## Feed size analysis of XRF Feed, XRF Concentrates and XRF Waste

**Bond Ball Mill Grindability Test Size Analysis**

| | | XRF Feed | | XRF Conc. | | XRF Conc.-2 | | XRF Waste | |
|---|---|---|---|---|---|---|---|---|---|
| Sieve | Size | Weight | Cum. Passing | Weight | Cum. Passing | Weight | Cum. Passing | Weight | Cum. Passing |
| [mesh] | [microns] | [g] | [%] | [g] | [%] | [g] | [%] | [g] | [%] |
| 7 | 2800 | 0.0 | 100.0 | 0.0 | 100.0 | 0.0 | 100.0 | 0.0 | 100.0 |
| 10 | 2000 | 76.6 | 65.4 | 62.2 | 71.9 | 52.1 | 63.5 | 59.5 | 63.2 |
| 14 | 1400 | 41.3 | 46.7 | 38.1 | 54.7 | 25.0 | 45.9 | 31.0 | 44.0 |
| 18 | 1000 | 22.7 | 36.4 | 24.1 | 43.8 | 13.6 | 36.4 | 16.1 | 34.0 |
| 25 | 710 | 16.5 | 29.0 | 18.3 | 35.5 | 10.4 | 29.1 | 11.9 | 26.7 |
| 35 | 500 | 12.5 | 23.3 | 13.9 | 29.3 | 7.7 | 23.7 | 8.5 | 21.4 |
| 45 | 355 | 9.3 | 19.1 | 10.5 | 24.5 | 6.0 | 19.5 | 6.5 | 17.4 |
| 60 | 250 | 8.0 | 15.5 | 8.9 | 20.5 | 4.8 | 16.1 | 5.5 | 14.0 |
| 80 | 180 | 6.2 | 12.7 | 6.8 | 17.4 | 5.6 | 12.2 | 4.3 | 11.3 |
| 120 | 125 | 6.1 | 9.9 | 7.1 | 14.2 | 3.4 | 9.8 | 4.1 | 8.8 |
| 170 | 90 | 5.0 | 7.7 | 5.4 | 11.8 | 2.5 | 8.0 | 3.1 | 6.9 |
| 230 | 63 | 4.9 | 5.5 | 6.5 | 8.9 | 1.8 | 6.8 | 3.0 | 5.0 |
| 325 | 45 | 3.8 | 3.8 | 5.6 | 6.3 | 2.8 | 4.8 | 2.1 | 3.7 |
| | -45 | 8.3 | 0.0 | 14.0 | 0.0 | 6.9 | 0.0 | 6.0 | 0.0 |
| Total mass | | 221.2 | | 221.4 | | 142.6 | | 161.6 | |

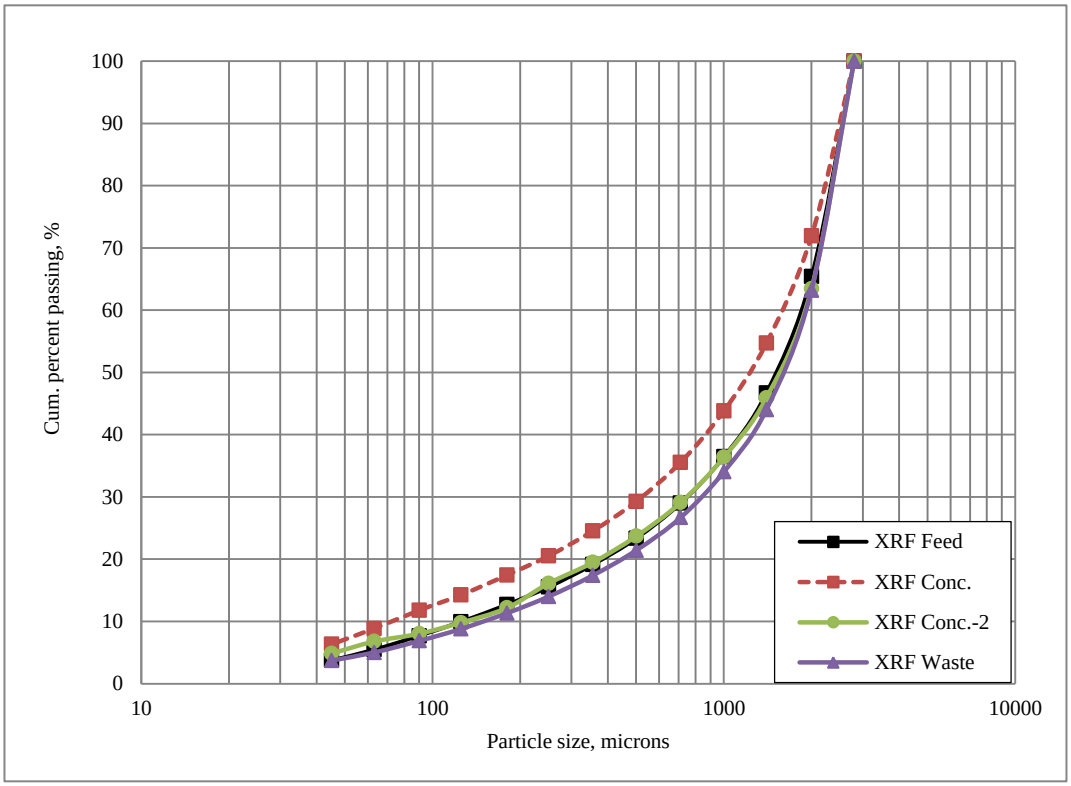

## Product size analysis of XRF Feed, XRF Concentrates and XRF Waste

**Bond Ball Mill Grindability Test Product Size Analysis**

| | | XRF Feed | | XRF Conc. | | XRF Conc.-2 | | XRF Waste | |
|---|---|---|---|---|---|---|---|---|---|
| Sieve | Size | Weight | Cum. Passing | Weight | Cum. Passing | Weight | Cum. Passing | Weight | Cum. Passing |
| [mesh] | [microns] | [g] | [%] | [g] | [%] | [g] | [%] | [g] | [%] |
| 7 | 2800 | 0.0 | 100.0 | 0.0 | 100.0 | 0.0 | 100.0 | 0.0 | 100.0 |
| 14 | 1400 | 10.2 | 97.6 | 8.0 | 98.1 | 10.7 | 97.5 | 10.5 | 97.5 |
| 25 | 710 | 7.4 | 95.9 | 7.3 | 96.4 | 8.7 | 95.4 | 8.6 | 95.5 |
| 45 | 355 | 8.0 | 94.0 | 8.0 | 94.5 | 8.9 | 93.3 | 9.8 | 93.2 |
| 80 | 180 | 15.8 | 90.3 | 10.3 | 92.1 | 9.5 | 91.0 | 12.6 | 90.3 |
| 120 | 125 | 22.7 | 84.9 | 8.0 | 90.2 | 10.7 | 88.5 | 23.2 | 84.8 |
| 170 | 90 | 27.9 | 78.3 | 26.5 | 84.0 | 24.8 | 82.6 | 29.5 | 77.9 |
| 230 | 63 | 35.8 | 69.9 | 36.5 | 75.4 | 35.8 | 74.0 | 47.2 | 66.8 |
| 325 | 45 | 71.4 | 53.1 | 84.0 | 55.7 | 80.2 | 55.0 | 84.2 | 47.1 |
| | -45 | 225.5 | 0.0 | 237.0 | 0.0 | 231.1 | 0.0 | 200.6 | 0.0 |
| Total mass | | 424.7 | | 425.6 | | 420.4 | | 426.2 | |

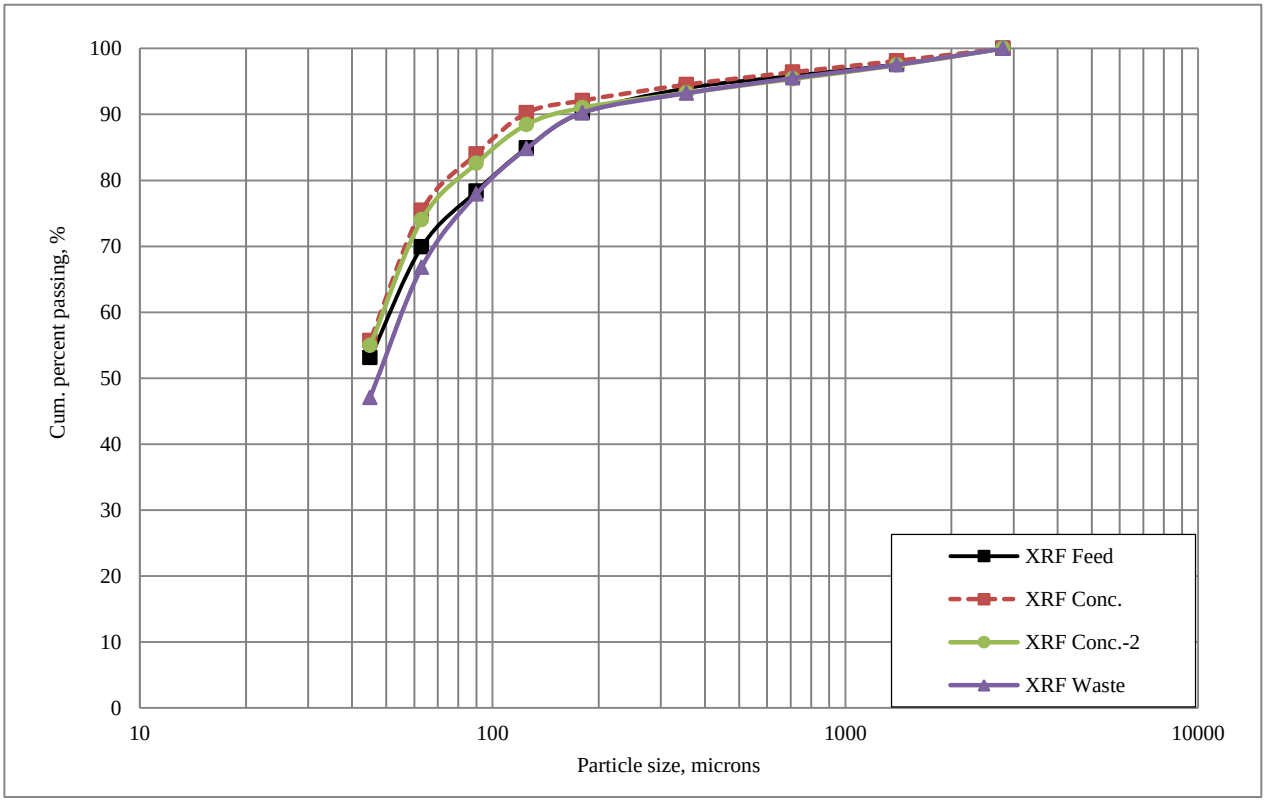

## Grindability Test Results

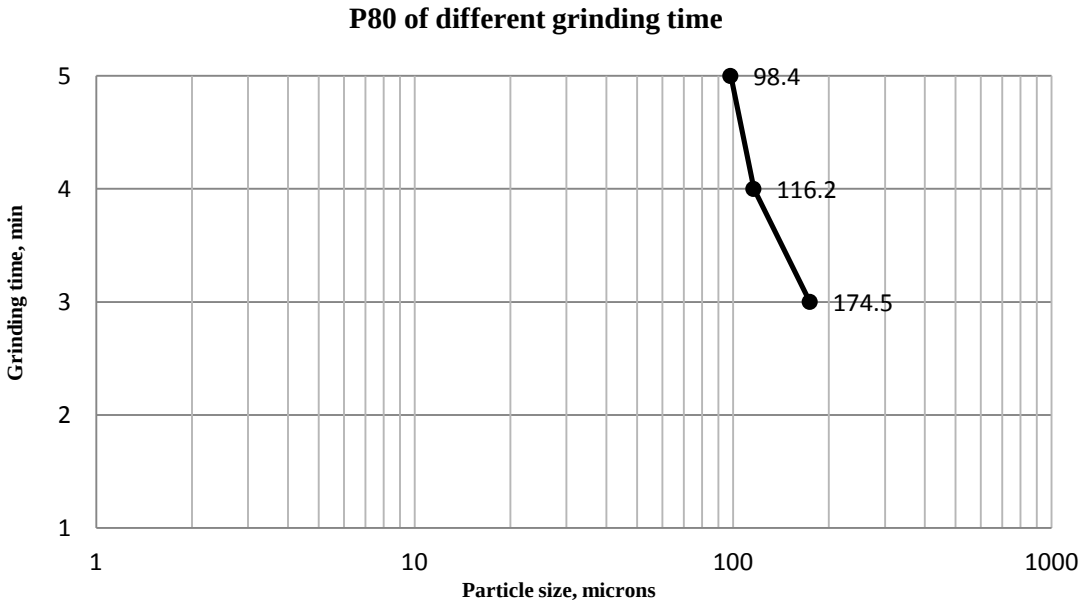


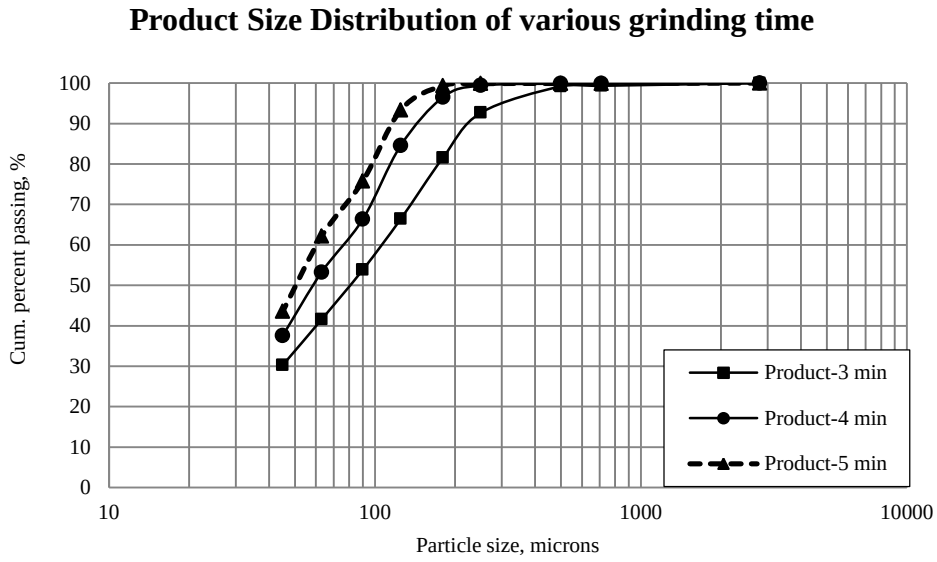

## Rod Mill Grindability Test Size Analysis- 3 minutes

| | | Feed | | Product | |
|---|---|---|---|---|---|
| Sieve | Size | Weight | Cum. Passing | Weight | Cum. Passing |
| [mesh] | [microns] | [g] | [%] | [g] | [%] |
| | 12000 | | 100.0 | | |
| 1/2 inch | 8000 | 10.3 | 98.9 | | |
| 5 | 4000 | 485.5 | 44.7 | | |
| 7 | 2800 | 400.1 | 0.0 | | 100.0 |
| 25 | 710 | | | 3.3 | 99.3 |
| 35 | 500 | | | 0.7 | 99.2 |
| 60 | 250 | | | 32.7 | 92.7 |
| 80 | 180 | | | 55.7 | 81.5 |
| 120 | 125 | | | 75.6 | 66.4 |
| 170 | 90 | | | 62.8 | 53.8 |
| 230 | 63 | | | 61.4 | 41.6 |
| 325 | 45 | | | 56.4 | 30.3 |
| | -45 | | | 151.4 | 0.0 |
| Total mass | | 895.9 | | 500 | |

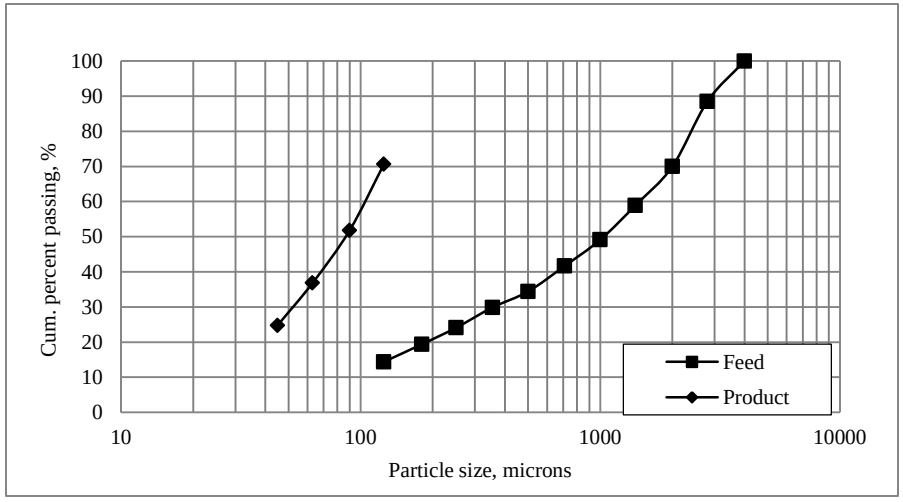


### Interpolations

| | | Feed | | Product | |
|---|---|---|---|---|---|
| Linear | 50 | P50= | 4394.2 | F50= | 81.6 |
| Linear | 80 | P80= | **6608.6** | F80= | **174.5** |
| Semi-log | 50 | P50= | 4282.8 | P50= | 80.5 |
| Semi-log | 80 | P80= | **6286.0** | P80= | **173.5** |
| Log-log | 50 | P50= | 4414.3 | P50= | 81.3 |
| Log-log | 80 | P80= | **6651.6** | P80= | **174.1** |

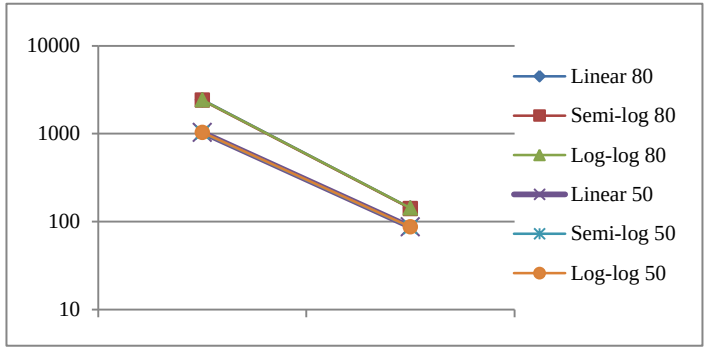

## Rod Mill Grindability Test Size Analysis – 4 minutes

| | | Feed | | Product | |
|---|---|---|---|---|---|
| Sieve | Size | Weight | Cum. Passing | Weight | Cum. Passing |
| [mesh] | [microns] | [g] | [%] | [g] | [%] |
| | 12000 | | 100.0 | | |
| 1/2 inch | 8000 | 10.3 | 98.9 | | |
| 5 | 4000 | 485.5 | 44.7 | | |
| 7 | 2800 | 400.1 | 0.0 | | 100.0 |
| 25 | 710 | | | 0.6 | 99.9 |
| 35 | 500 | | | 0.1 | 99.9 |
| 60 | 250 | | | 2.3 | 99.4 |
| 80 | 180 | | | 14.6 | 96.5 |
| 120 | 125 | | | 59.5 | 84.6 |
| 170 | 90 | | | 91.2 | 66.3 |
| 230 | 63 | | | 65.5 | 53.2 |
| 325 | 45 | | | 78.3 | 37.6 |
| | -45 | | | 187.9 | 0.0 |
| Total mass | | 895.9 | | 500 | |

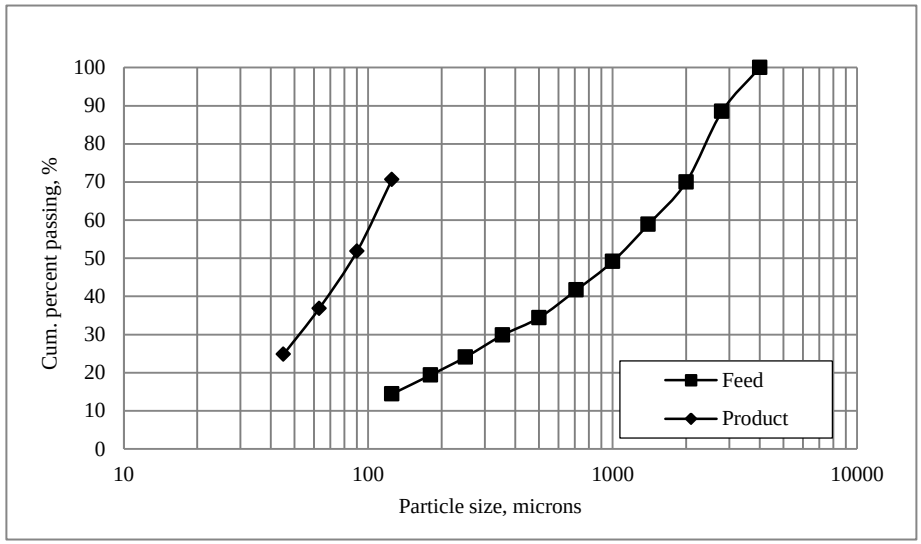


**Interpolations**

| | | Feed | | Product | |
|---|---|---|---|---|---|
| Linear | 50 | P50= | 4394.2 | F50= | 59.3 |
| Linear | 80 | P80= | **6608.6** | F80= | **116.2** |
| Semi-log | 50 | P50= | 4282.8 | P50= | 58.8 |
| Semi-log | 80 | P80= | **6286.0** | P80= | **115.1** |
| Log-log | 50 | P50= | 4414.3 | P50= | 59.3 |
| Log-log | 80 | P80= | **6651.6** | P80= | **115.9** |

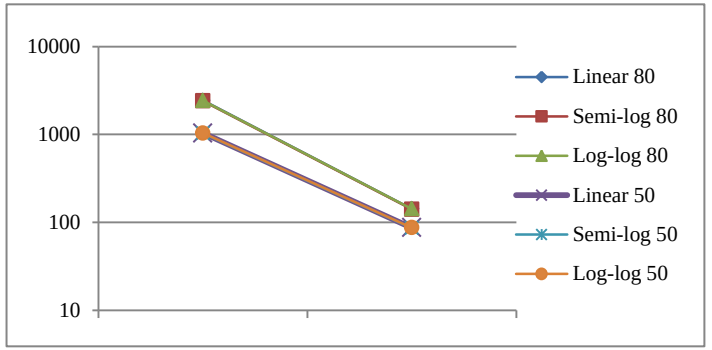

## Rod Mill Grindability Test Size Analysis – 5 minutes

| | | Feed | | Product | |
|---|---|---|---|---|---|
| Sieve [mesh] | Size [microns] | Weight [g] | Cum. Passing [%] | Weight [g] | Cum. Passing [%] |
| | 12000 | | 100.0 | | |
| 1/2 inch | 8000 | 10.3 | 98.9 | | |
| 5 | 4000 | 485.5 | 44.7 | | |
| 7 | 2800 | 400.1 | 0.0 | | 100.0 |
| 25 | 710 | | | 0.4 | 99.9 |
| 35 | 500 | | | 0.1 | 99.9 |
| 60 | 250 | | | 0.2 | 99.9 |
| 80 | 180 | | | 2.6 | 99.3 |
| 120 | 125 | | | 30.0 | 93.3 |
| 170 | 90 | | | 87.8 | 75.8 |
| 230 | 63 | | | 68.3 | 62.1 |
| 325 | 45 | | | 92.8 | 43.6 |
| | -45 | | | 217.8 | 0.0 |
| Total mass | | 895.9 | | 500 | |

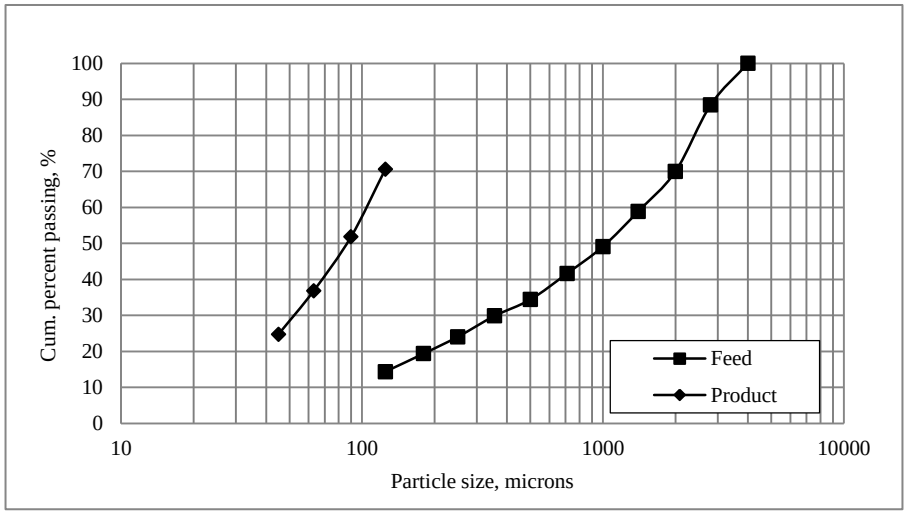


### Interpolations
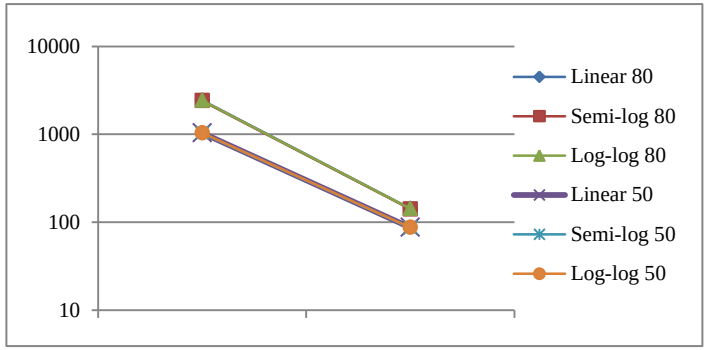
| | | Feed | | Product | |
|---|---|---|---|---|---|
| Linear | 50 | P50= | 4394.2 | F50= | 51.2 |
| Linear | 80 | P80= | **6608.6** | F80= | **98.4** |
| Semi-log | 50 | P50= | 4282.8 | P50= | 50.6 |
| Semi-log | 80 | P80= | **6286.0** | P80= | **97.4** |
| Log-log | 50 | P50= | 4414.3 | P50= | 51.3 |
| Log-log | 80 | P80= | **6651.6** | P80= | **98.0** |